Durham E-Theses

Applications of Modern Methods for Scattering Amplitudes

FRANCESCO BUCIUNI

How to cite:

Use policy

Applications of Modern Methods for Scattering Amplitudes

Francesco Buciuni

A Thesis presented for the degree of

Doctor of Philosophy

Durham University

Applications of Modern Methods for Scattering Amplitudes

Francesco Buciuni

Submitted for the degree of Doctor of Philosophy

April 2018

Abstract

The large amount of new high energy data being collected by the LHC experiments has the potential to provide new information about the nature of the fundamental forces through precision comparisons with the Standard Model. These precision measurements require intensive perturbative scattering amplitude computations with large multiplicity final states. In this thesis we develop new on-shell methods for the analytic computation of scattering amplitudes in QCD which offer improved evaluation speed and numerical stability over currently available techniques and also allow us to explore the structure of amplitudes in gauge theories. We apply these techniques to extract compact analytic expression for the triple collinear splitting functions at one-loop in QCD and supersymmetric gauge theories which contribute to the universal factorisation at N^3LO. We also investigate improvements to dimensionally regulated one-loop amplitude computations by combining the six-dimensional spinor helicity formalism and a momentum twistor parameterisation with the integrand reduction and generalised unitarity methods. This allowed the development of a completely algebraic approach to the computation of dimensionally regulated amplitudes in QCD including massive fermions. We present applications to Higgs plus five-gluon scattering in the large top mass limit and top pair production with up to three partons. In the case of massive one-loop amplitudes we present a new approach to the problem of wave-function renormalisation which only requires gauge invariant, on-shell building blocks. Massive one-loop amplitudes contain information that cannot be extracted from unregulated cuts, the new approach

instead constrains the amplitudes using the universal poles in $6 - 2\epsilon$ dimensions which can be computed from an effective Lagrangian on dimension six operators.

Declaration

The work in this thesis is based on research carried out at the Institute of Particle Physics Phenomenology, Department of Physics, Durham University, England, UK and at the Higgs Centre for Theoretical Physics, School of Physics and Astronomy, The University of Edinburgh, Scotland, UK.

The research described in this thesis was carried out in collaboration with Dr Simon Badger, Christian Brønnum-Hansen, Dr Donal O'Connell and Dr Tiziano Peraro. Aspects of chapters 4, 5 and 7 are based on the following published works:

- S. Badger, F. Buciuni and T. Peraro, *One-loop triple collinear splitting amplitudes in QCD*, *JHEP* **09** (2015) 188, [1507.05070]

- S. Badger, C. Brønnum-Hansen, F. Buciuni and D. O'Connell, *A unitarity compatible approach to one-loop amplitudes with massive fermions*, *JHEP* **06** (2017) 141, [1703.05734]

No part of this thesis has been submitted elsewhere for any other degree or qualification and it is all my own work unless referenced to the contrary in the text.

Acknowledgements

Contents

Chapter 1

Introduction

In the last century, the scientific community has made incredible progress towards understanding the fundamental laws that describe nature. Quantum Mechanics and Relativity have played the most import role in the interpretation of experimental observations. Furthermore, Quantum Mechanics and Special Relativity have been successfully combined together in the framework of Quantum Field Theory (QFT), which represents particles as excited quantum states of physical fields. In particular, gauge theories, a special class of QFT, succeeded in providing the most accurate picture of the fundamental interactions at high-energy, where both quantum and relativistic effects are very important. The formulation of gauge theories is based on the description of the symmetries of nature, which is theoretically achieved using the mathematical tool of symmetry groups.

The theory of the Standard Model of particle physics (SM) [3, 4] currently provides the most accurate description of the fundamental particles and their interactions. The SM is a gauge theory based on (special) unitary groups, which give the representation of Electromagnetic, Weak and Strong interactions. It also contains a scalar field, the Higgs, which is responsible for the symmetry breaking and for all the masses of the particles of the SM.

The validation of the SM has been the main topic among particle physicists since the latter half of the 20th century. This effort led to the realisation of many advanced experiments based on particle collisions. Remarkable particle colliders such as the Large Electron-Positron Collider (LEP) and Large Hadron Collider (LHC) at CERN,

Tevatron at FermiLab, DESY, SLAC and Belle produced a large number of detailed tests which validated the SM. The last notable support arrived in 2012 with the discovery of a scalar particle [5, 6] which, after a continued collection of data, is still consistent with the Higgs boson predicted by the SM.

However, the SM cannot be considered a complete theory of nature, since it does not provide explanations for many observed phenomena. Firstly it does not include Gravity, which is instead described by General Relativity. Moreover, it fails in the interpretation of the cosmological evidence of Dark Matter and Dark Energy, and does not explain the observations of neutrino oscillations and matter-antimatter asymmetry. For this reason, a lot of effort has been put into the development of theories, classified as Beyond Standard Model theories (BSM), that try to extend the SM to include these phenomena. A huge effort is also devoted to improving the accuracy of the experimental measurements to enable a deeper analysis of particles interactions.

The search for signals of new physics requires that theoretical uncertainties be kept in line with experimental errors. The need for precise prediction has become particularly important since the advent of the LHC, which has produced a large amount of high energy data. Indeed the high center-of-mass energy in LHC collisions makes it capable of probing physics at high energy scales and thus at a more fundamental level. However, LHC events are also characterised by a large background of known physics which could hide signals of deviations from the SM. Therefore, in order to make the best use of the data from the LHC and other high-energy experiments, one needs to understand the physics of the SM as accurately as possible.

The task of performing precise prediction in QFT is not trivial and has stimulated theoretical studies since the early development of the SM. The exact computation of observables in QFT for realistic models is not possible at the moment. The most practical method available so far relies on the use of perturbation theory, which allows us to approximate the results as a power expansion in the coupling constant of the theory. The calculation of each term of the perturbative expansion is in principle possible at every order. However, it is very well known that the degree of

complexity of the calculations grows extremely fast when increasing the number of external states and the order of the expansion, such that traditional approaches are ineffective other than for simple cases.

A key ingredient in obtaining precise theoretical predictions is the calculation of scattering amplitudes. The perturbative scattering amplitudes are related to the probability that particular final states are produced in a collision. In perturbation theory, scattering amplitudes can be computed in terms of the well known Feynman diagrams, which allow us to visualise all the possible interactions between particles predicted by the theory. Amplitudes contributing at higher order in the perturbative expansion, for a certain process, can be classified in terms of the number of loops of virtual particles appearing in the diagrams. Considering the high energy in the centre of mass available at LHC, many particles are often produced in the final state of a collision. This requires the computation of amplitudes with many external particles. Moreover, accurate descriptions of high energy collisions often require higher order quantum corrections. However, such calculations are plagued by a high degree of complexity and cannot be achieved by traditional approaches to Feynman diagrams. For these reasons, new methods, algorithms and automated tools for the computation of scattering amplitudes have been developed and used for numeric, semi-numeric and analytic computations.

At tree-level, modern methods such as Berends-Giele [7] and BCFW [8] recursion relations, have significantly boosted the computation of high-multiplicity amplitudes. In the context of the computation of one-loop amplitudes, it has been known for a long time, thanks to techniques such as tensor reduction [9], that any amplitude can be decomposed as a linear combinations of scalar Feynman integrals. However, the methods inspired by unitarity represented a revolutionary step for these calculations. In the unitarity-based approaches [10, 11], which originate from the optical theorem, a loop amplitude can be rewritten as a sum over multiple residues, or cuts, each of which factorise in the products of on-shell tree-level amplitudes. As a result, one can project out the coefficients of the integral basis just by looking at all possible cuts. An important contribution has been given by the idea of integrand reduction algorithms, such as OPP reduction [12], which are based on the univer-

sal decomposition of loop integrands. The implementation of these methods within several automated frameworks [13, 14, 15, 16, 17, 18, 19] has considerably enhanced our ability to make precise phenomenological predictions.

At two and higher loops, the situation is more complicated. The basis of integrals is not known a priori and it is identified only after the reduction of the amplitudes. The most successful reduction method for higher-loop amplitudes so far is Integration by Parts (IBP) [20], especially using the Laporta algorithm [21]. The calculation of the integral basis is addressed using a wide variety of techniques such as differential equations [22, 23], asymptotic expansions [24], sector decomposition, contour deformation [25] and many others. Also, generalised unitarity and integrand reduction have been extended at higher loops, opening the advantages of on-shell frameworks.

Despite years of improvements in the technology for scattering amplitude computations, many important processes still remain unknown, resulting in theoretical predictions lying behind experimental precision. The current frontier for theoretical predictions consists of many $2 \to 2$ processes established at next-to-next-to-leading order (NNLO) accuracy and a $2 \to 1$ process established at N^{3}LO [26, 27]. A schematic overview of the state of art of the calculations relevant for physics of hadron collider is shown in Fig. 1.1. The difficulties on pushing forward the status of Fig. 1.1 relies mainly on the fact that no QCD scattering amplitudes are known beyond four points at two loops and three points at three loops. This situation stimulates the research of new approaches in order to bypass the bottlenecks that, at the moment, forbid such calculations. Therefore more formal studies about the mathematical structure of QFT may reveal a new simplicity in scattering amplitudes theory and inspire more effective frameworks.

In this thesis, we will explore new methods for the calculation of scattering amplitudes and we will show some of their applications in QCD at one-loop. Our first aim is to provide a framework which is suitable for obtaining analytic results. The analytic expressions present several advantages in comparison with the numerical implementations. Firstly they enable us to understand the structure and the properties of scattering amplitudes and thus to make progress in computational methods.
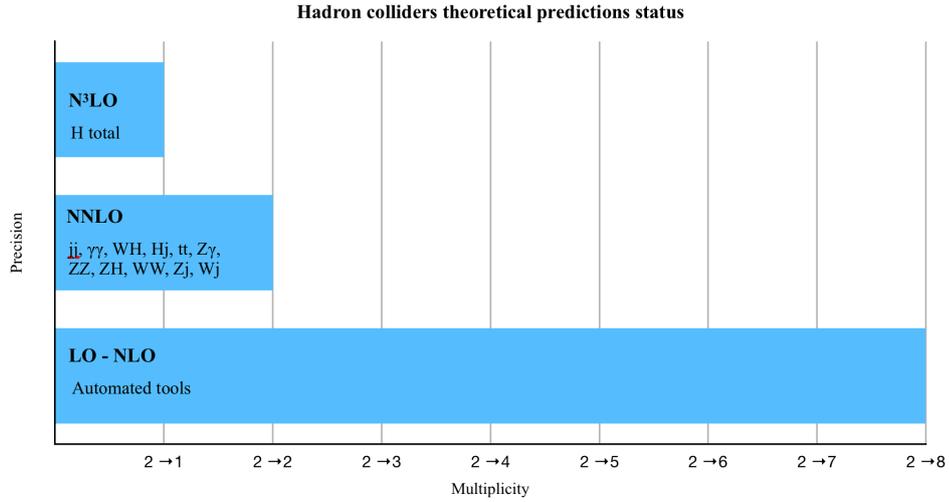
Figure 1.1: Current status of theoretical predictions for processes relevant at hadron colliders.

Moreover, analytic expressions can avoid the appearance of spurious poles, which at the level of numerical integration can lead to numerical instabilities. This aspect turns out to be particularly important in higher order applications, where integrations over complicated phase-space regions are required. For example NNLO predictions for $2 \to 3$ or N^{3}LO prediction for $2 \to 2$ processes require $2 \to 4$ one-loop amplitudes. In these calculations high multiplicity one-loop amplitudes must have fast and stable evaluations, since the integration of unresolved radiation is involved.

An on-shell approach is based on the key idea that, working with physical degree of freedoms, is more efficient than traditional computation of Feynman diagrams. We make use of dedicated techniques such as spinor-helicity formalism, momentum-twistor parametrisation [28], generalised unitarity and integrand reduction, providing a complete algebraic framework where only rational functions appear into intermediate steps. We compute the universal one-loop triple collinear splitting functions for QCD [1], obtaining compact analytic expressions by introducing a new parametrisation of the kinematics in the collinear limit based on spinor-helicity. This result can be used to establish the N^{3}LO subtraction terms for differential observables. We explore how higher dimensional representations of the one-loop

amplitudes are capable to produce results in dimensional regularisation. In particular, a six dimensional spacetime is enough for one-loop applications. Therefore the on-shell building-blocks of generalised unitarity are represented by making use of the six dimensional spinor-helicity formalism [29]. We present the computation of the one-loop Higgs plus five-gluon scattering amplitudes in the large top mass limit as an example of this approach. We provide a benchmark for a rational phase-space point and show that the method is suitable for a finite field fitting reconstruction [30]. Computation of amplitudes with massive fermions via unitarity methods are relatively few tough some prescriptions have been available for some time [31, 32]. We develop a new approach for the computation of one-loop amplitudes with massive fermions that uses only on-shell ingredients, bypassing the traditional conflict with wavefunction renormalization. Finally we apply this method to the computation of the one-loop $t\bar{t}$ plus three partons helicity amplitudes, also showing how the introduction of a spin basis reduces the degree of complexity of the calculation.

The thesis is organised as follows. In Chapter 2 we review some well known concepts about the Standard Model, focusing in particular on perturbative QCD. In Chapter 3 we introduced the properties of QCD scattering amplitudes and the frameworks of spinor-helicity and momentum twistors for the representation of the kinematic information. In Chapter 4 we discuss some of the modern methods for scattering amplitude calculations such as generalised unitarity and integrand reduction, also in combination with the six-dimensional spinor-helicity formalism. In Chapter 5 we compute the universal one-loop triple collinear splitting functions in QCD. In Chapter 6 we discuss the calculation of the one-loop amplitudes for Higgs plus five-gluon scattering in the large mass top limit. In Chapter 7 we propose a unitarity compatible approach to one-loop amplitudes with massive fermions. In Chapter 8 we show the calculation of the one-loop amplitudes for the $t\bar{t}$ plus three partons scattering, based on the new method of Chapter 7.

Chapter 2

Standard Model

In this chapter we review some fundamentals concepts about the Standard Model. We focus in particular on QCD, discussing the computation of physical observables in perturbation theory. This chapter is meant to be an introduction to the theoretical and phenomenological topics which will be used and developed in the rest of the thesis. We do not attempt to make a comprehensive treatment on these subjects, most of which are well known. A complete review of these topics can be found in many textbooks and manuals such as [33, 34].

2.1 The theory of the Standard Model

The Standard Model provides an accurate picture of nature at small scales, however it is unable to describe many other phenomena such as dark matter, dark energy, neutrino masses and it does not include gravity. In more detail, the Standard Model is a gauge theory based on the symmetry group $SU(3)_C \times SU(2)_L \times U(1)_Y$. It is made of three main ingredients: Quantum Chromodynamics (QCD), the theory of the strong interaction between coloured quarks and gluons, described by a gauge group with a local $SU(3)_C$ symmetry; the Electroweak (EW) theory, which unifies the electromagnetic and weak interactions of quarks and leptons under the gauge group $SU(2)_L \times U(1)_Y$; and the Higgs mechanism, which spontaneously breaks the electroweak symmetry into a $U(1)$ group describing QED and is responsible for giving mass to the quarks and charged leptons through a Yukawa-type interaction.

Electroweak theory

The symmetry group of the EW interaction is the direct product $SU(2)_L \times U(1)_Y$. The former describes the weak interaction and defines a non-abelian chiral symmetry which only affects the left-handed components of the fermion fields. The $U(1)_Y$ is the abelian symmetry group of the electromagnetic interaction. The Lagrangian of the EW gauge bosons is

$$\mathcal{L} = -\frac{1}{4} W_i^{\mu\nu} W_{\mu\nu}^i - \frac{1}{4} B^{\mu\nu} B_{\mu\nu} \tag{2.1.1}$$

with the field tensors $W_i^{\mu\nu}$ ($i = 1, 2, 3$) and $B^{\mu\nu}$ defined in terms of the vector boson fields

$$W_i^{\mu\nu} = \partial^\mu W_i^\nu - \partial^\nu W_i^\mu + g_W \epsilon_{ijk} W_j^\mu W_k^\nu$$
$$B^{\mu\nu} = \partial^\mu B^\nu - \partial^\nu B^\mu \tag{2.1.2}$$

where g_W is the gauge coupling of $SU(2)_L$ and ϵ_{ijk} is the Levi-Civita tensor representing the structure constants of $SU(2)$.

The EW theory describes the interactions of two kinds of fermions: quarks and leptons. The left-handed components of the fermions are organised into $SU(2)_L$ doublets, while the right-handed components are all singlet with respect to $SU(2)_L$

$$Q_1 = P_L \begin{pmatrix} u \\ d \end{pmatrix}, \quad u_{R_1} = P_R(u), \quad d_{R_1} = P_R(d), \quad L_1 = P_L \begin{pmatrix} \nu_e \\ e^- \end{pmatrix}, \quad e_{R_1} = P_R(e^-)$$

$$Q_2 = P_L \begin{pmatrix} c \\ s \end{pmatrix}, \quad u_{R_2} = P_R(c), \quad d_{R_2} = P_R(s), \quad L_2 = P_L \begin{pmatrix} \nu_\mu \\ \mu^- \end{pmatrix}, \quad e_{R_2} = P_R(\mu^-)$$

$$\tag{2.1.3}$$

$$Q_3 = P_L \begin{pmatrix} t \\ b \end{pmatrix}, \quad u_{R_3} = P_R(t), \quad d_{R_3} = P_R(b), \quad L_3 = P_L \begin{pmatrix} \nu_\tau \\ \tau^- \end{pmatrix}, \quad e_{R_3} = P_R(\tau^-)$$

where $P_{L,R}$ are the chiral state projection operators,

$$P_L = \frac{1}{2}(1 - \gamma_5), \qquad P_R = \frac{1}{2}(1 + \gamma_5). \tag{2.1.4}$$

The Lagrangian for massless fermions is

$$\mathcal{L}_{\text{fermions}} = i\bar{L}_i \not{D} L_i + i\bar{e}_{R_i} \not{D} e_{R_i} + i\bar{Q}_i \not{D} Q_i + i\bar{u}_{R_i} \not{D} u_{R_i} + i\bar{d}_{R_i} \not{D} d_{R_i} \tag{2.1.5}$$

The W_i^μ and B^μ fields define the covariant derivative

$$D^\mu = \partial^\mu - ig_W t^i W_i^\mu - ig'_W Y B^\mu \tag{2.1.6}$$

where t^i are the generators of SU(2), g'_W is the coupling of U(1)$_\text{Y}$ and Y is a diagonal matrix whose elements are the charges (known as hypercharge) of the particles with respect to the interaction of the symmetry group U(1)$_\text{Y}$. We see that the SU(2)$_\text{L}$ singlets R are trivially SU(2)$_\text{L}$ invariant and therefore do not couple to the corresponding gauge fields W_i^μ. The neutrinos ν_i only interact with the W_i^μ field bosons. They are very light and, although their actual mass is not known, in high-energy computations they can be assumed to be massless. Notice that, with this assumption, the right-handed component of the neutrinos does not take part in any interaction in the SM and therefore it can be omitted from the Lagrangian altogether. Given the covariant derivative (2.1.6), one can consider the physical boson fields defined as

$$W^{\pm\mu} = \frac{1}{\sqrt{2}}(W_1^\mu \pm iW_2^\mu) \tag{2.1.7}$$

$$\begin{pmatrix} Z^{0\mu} \\ A^\mu \end{pmatrix} = \begin{pmatrix} \cos\theta_W & -\sin\theta_W \\ \sin\theta_W & \cos\theta_W \end{pmatrix} \begin{pmatrix} W_3^\mu \\ B^\mu \end{pmatrix} \tag{2.1.8}$$

where the Weinberg angle θ_W is given by

$$sin^2\theta_W = \frac{g'^2_W}{g'^2_W + g^2_W}. \tag{2.1.9}$$

	Q	t^3	Y
$(u, c, t)_L$	2/3	1/2	1/3
$(d, s, b)_L$	-1/3	-1/2	1/3
$(\nu_e, \nu_\mu, \nu_\tau)_L$	0	1/2	-1
$(e^-, \mu^-, \tau^-)_L$	-1	-1/2	-1
$(u, c, t)_R$	2/3	0	4/3
$(d, s, b)_R$	-1/3	0	-2/3
$(\nu_e, \nu_\mu, \nu_\tau)_R$	-	-	-
$(e^-, \mu^-, \tau^-)_R$	-1	0	-2

Table 2.1: Quantum numbers of the fermions in the electroweak theory of the Standard Model

In the SM the vector field A is identified with the massless electro-magnetic field, the photon, of Quantum electrodynamics (QED), while the W^+, W^- and Z^0 are massive gauge bosons of the weak interaction. Such identification implies the following relations between the electric charge Q, the isospin t^3, the hypercharge Y and θ_W,

$$Q = t^3 + \frac{Y}{2} \tag{2.1.10}$$

$$g_W \sin \theta_W = g'_W \cos \theta_W = e \tag{2.1.11}$$

The quantum numbers of the electroweak sector for the all fermions are listed in Table 2.1. According to experimental observations, the vector bosons of the electroweak interactions are massive. However, adding mass terms to the Lagrangian in Eq. (2.1.1) is well known to yield a non-renormalizable theory, which cannot be used to make perturbative predictions. In order to give mass to vector bosons, one can introduce a spontaneous symmetry breaking mechanism, the Higgs mechanism. Within this procedure, the mass of a vector boson is not an intrinsic property of the particle but a dynamic effect which preserves the renormalizability of the theory.

Higgs mechanism

The Higgs field is a doublet of scalar fields $\phi = (\phi^+, \phi^0)$, whose Lagrangian is

$$\mathcal{L} = (D^\mu \phi)^\dagger (D_\mu \phi) - V(\phi), \quad V(\phi) = \lambda |\phi|^4 - \mu^2 |\phi|^2 \tag{2.1.12}$$

The spontaneous symmetry breaking is due to the negative mass term in the potential $V(\phi)$, which has a classical minimum at

$$|\phi| = \sqrt{\frac{\mu^2}{2\lambda}} \equiv \frac{v}{\sqrt{2}}. \tag{2.1.13}$$

Up to a gauge choice, we can choose a particular direction for the minimum and parametrise ϕ as

$$\phi = \frac{1}{\sqrt{2}} \begin{pmatrix} 0 \\ v + H \end{pmatrix} \tag{2.1.14}$$

where H is the physical Higgs field. By inserting this expression into the Higgs Lagrangian of Eq. (2.1.12) one obtains a sum of interaction terms, including self-interactions of the Higgs field H as well as interactions between the Higgs and the vector bosons, and quadratic terms in the vector bosons which represent mass terms. With an explicit calculation, one can check that in the final Lagrangian the bosons W^+, W^- and Z^0 acquire the masses m_W and m_Z respectively, given by

$$m_W = \frac{1}{2} v g_W \qquad m_Z = \frac{1}{2} v \sqrt{g_W^2 + g_W'^2} = \frac{m_W}{\cos \theta_W}. \tag{2.1.15}$$

The Higgs boson also acquires a physical mass given by

$$m_H = \sqrt{2} \mu = \sqrt{2\lambda} v. \tag{2.1.16}$$

In the SM the Higgs mechanism is also needed to give masses to quarks and leptons. Indeed a Dirac mass term in the Lagrangian for a fermion ψ would, after

splitting it into the right- and left-handed components, look like

$$m\bar{\psi}\psi = m(\bar{\psi}_L\psi_R + \bar{\psi}_R\psi_L), \tag{2.1.17}$$

which is not $\text{SU}(2)_\text{L}$ invariant. We can however introduce a new contribution to the Lagrangian which contains Yukawa couplings between the unbroken Higgs field ϕ and the fermions of the form

$$\mathcal{L}_{\text{Yukawa}} = -\lambda_e(\bar{L}\cdot\phi)e_R - \lambda_d(\bar{Q}\cdot\phi)d_R - \lambda_u(\bar{Q}\cdot\tilde{\phi})u_R + h.c. + \dots \tag{2.1.18}$$

with $\tilde{\phi} = \epsilon^{ij}\phi_{ij}^*$, where ϵ^{ij} is the Levi-Civita tensor in two dimensions. After symmetry breaking, this will become

$$\mathcal{L}_{\text{Yukawa}} = -m_e\bar{e}e\left(1 + \frac{H}{v}\right) + m_d\bar{d}d\left(1 + \frac{H}{v}\right) + m_u\bar{u}u\left(1 + \frac{H}{v}\right) + \dots \tag{2.1.19}$$

and the fermions acquire the masses

$$m_i = \frac{\lambda_i}{\sqrt{2}}v. \tag{2.1.20}$$

In the most general case, the couplings λ_i will thus become generic complex matrices. By diagonalizing the mass sector, one can introduce mixing between the quarks (but not the leptons, if the neutrinos are taken as massless) of different generations, proportional to the elements of the so-called Cabibbo-Kobayashi-Maskawa (CKM) matrix. This also gives a theoretical explanation for the observed CP violation in electroweak interactions. At very high energies, where the masses of the two lightest generations of quarks can be neglected, one can often assume the CKM matrix to be diagonal and thus no mixing between different generations of quarks is present.

2.2 QCD

Quantum Chromodynamics (QCD) is a non-abelian gauge theory with symmetry group $\text{SU}(N_c)$, with $N_c = 3$. It describes the strong interaction between n_f flavours

of quarks and the gluons. The quarks are spin-1/2 fermions and the gluons are the vector bosons which mediate the interaction. For perturbative QCD the Lagrangian is

$$\mathcal{L} = -\frac{1}{4}G_a^{\mu\nu}G_{\mu\nu}^a + \sum_{f=1}^{n_f} \bar{\psi}_f(i\not{D} - m_f)\psi_f + \mathcal{L}_{\text{gf}} + \mathcal{L}_{\text{ghost}} \qquad (2.2.21)$$

where the field tensor $G_a^{\mu\nu}$ can be written in terms of the gluon vector field A_a^μ as

$$G_a^{\mu\nu} \equiv \partial^\mu A_a^\nu - \partial^\nu A_a^\mu + g_s f_{abc} A_b^\mu A_c^\nu \qquad (2.2.22)$$

The vector field defines the covariant derivative as

$$D^\mu \equiv \partial^\mu - i g_s t^a A_a^\mu \qquad (2.2.23)$$

and the ψ_f are the quark fields. In nature, $n_f = 6$ different flavours of quarks have been observed, denoted down, up, strange, charm, bottom, and top. In computations relevant for high-energy processes at colliders such as LHC, the masses of the lightest flavours, namely all but the top and in some cases the bottom quark, are usually neglected. The matrices t^a are the generators of the gauge group $\text{SU}(N_c)$, which are related to the structure constants f_{abc} of the group by the commutation relation

$$[t^a, t^b] = i f^{abc} t^c, \qquad \text{tr}(t^a t^a) = \frac{1}{2}\delta^{ab} \qquad (2.2.24)$$

The charge of strongly interacting particles is called colour. Each flavour of quark lives in the fundamental representation of the group $\text{SU}(N_c)$, with colour index running from 1 to N_c. The gluons, which are the gauge bosons and thus live in the adjoint representation of the symmetry group, can have $N_c^2 - 1$ different colours. Due to confinement, coloured particles have never been observed as free states, but only bound into composite objects called hadrons (such as protons and neutrons) whose total colour charge is zero.

The contribution $\mathcal{L}_{gf}$ is the gauge fixing term which, in the class of axial gauges

[1] , has the form

$$\mathcal{L}_{\text{gf}} = -\frac{1}{2\xi}(n^\nu A_\nu^a)^2, \tag{2.2.25}$$

where n^μ is a constant vector and ξ is a parameter. Common choices are made imposing $n^2 < 0$ (space-like gauge), $n^2 = 0$ (light-cone gauge) or $n^2 < 0$ (temporal gauge), considering the limit $\xi \to 0$.

We also recall that the quantisation of a non-abelian gauge theory such as QCD requires the introduction of unphysical fields known as ghosts described by the term $\mathcal{L}_{\text{ghost}}$ in eq. (2.2.21),

$$\mathcal{L}_{\text{ghost}} = \partial_\mu \eta^{a\dagger}(D^\mu_{ab}\eta^b). \tag{2.2.26}$$

The ghost field η^a is a complex scalar field which obeys the Fermi statistics and, in the computation of scattering amplitudes and physical observables, cancels out the contributions from unphysical polarisations of the gauge bosons.

In the Lagrangian (2.2.21), g_s is the coupling constant of the strong interaction. Since there are no exact analytical solutions for the eigenstates of QCD, one can consider approximate solutions in perturbation theory, considering the full theory as a perturbation around the free state defined at $g_s = 0$. A computation in perturbative QCD is typically organised by expanding the result in powers of the coupling α_s defined as

$$\alpha_s = \frac{g_s^2}{4\pi}. \tag{2.2.27}$$

The physical value of α_s is dependent on the characteristic energy scale for the process μ through the renormalization group equation

$$\frac{\partial \alpha_s(\mu^2)}{\partial \log(\mu^2)} = \beta\left(\alpha_s(\mu^2)\right). \tag{2.2.28}$$

---

[1]Another widely used class of gauges is the covariant gauge $L_{\text{gf}} = -\frac{1}{2\xi}(\partial_\mu A^\mu)^2$, where common choices of ξ are the Feynman-t'Hooft gauge $\xi = 1$ and Landau gauge $\xi \to 0$.

The beta function of QCD $\beta\left(\alpha_s\right)$ can be computed perturbatively and the expansion at first order (one-loop order) is

$$\beta\left(\alpha_s(\mu^2)\right) = -\frac{1}{3}\left(11N_c - 2n_f\right)\frac{\alpha_s^2}{2\pi} + \mathcal{O}(\alpha_s^3) \tag{2.2.29}$$

which allows us to relate α_s at two energy scales μ and Q

$$\alpha_s(Q^2) = \frac{\alpha_s(\mu^2)}{1 - \frac{1}{3}\left(11N_c - 2n_f\right)\frac{\alpha_s^2(\mu^2)}{2\pi}\log\left(\frac{Q^2}{\mu^2}\right)}. \tag{2.2.30}$$

For $N_c = 3$ and $n_f = 6$ the beta function is negative and the solution (2.2.30) shows that α_s is a decreasing function that asymptotically goes to zero as the energy scale goes to infinity. This phenomenon, known as asymptotic freedom, is particularly important because it allows us to use perturbation theory at high energy, where the coupling is $\alpha_s \ll 1$. On the other hand, the critical energy scale below which the perturbative approach no longer yields useful results, is that for which $\alpha_s(\mu^2) \approx 1$. That value is denoted Λ_{QCD} and has the value of approximately 250 MeV. In the regime where $\mu \ll \Lambda_{QCD}$ we find that the free quarks and gluons picture is not a good approximation, and it is also here we find the quarks and gluons bound inside hadrons like protons, neutrons, and pions. This behaviour of the coloured particles, to bind together to form colourless states, is known as confinement.

The value of α_s at the LHC energy scale (TeV) is $\alpha_s \approx 0.1$, hence, the strong force dominates the other interactions and quantum corrections in perturbation theory are required to make precise predictions. At hadron colliders observables are therefore dominated by strong interacting radiation which is measured as large numbers of collimated bound-state hadrons in the detector. In particular, given the high center-of-mass energy available at LHC, many external particles are produced in the final state, which makes the prediction of processes with many final states very important in order to predict background relevant for new physical phenomena.
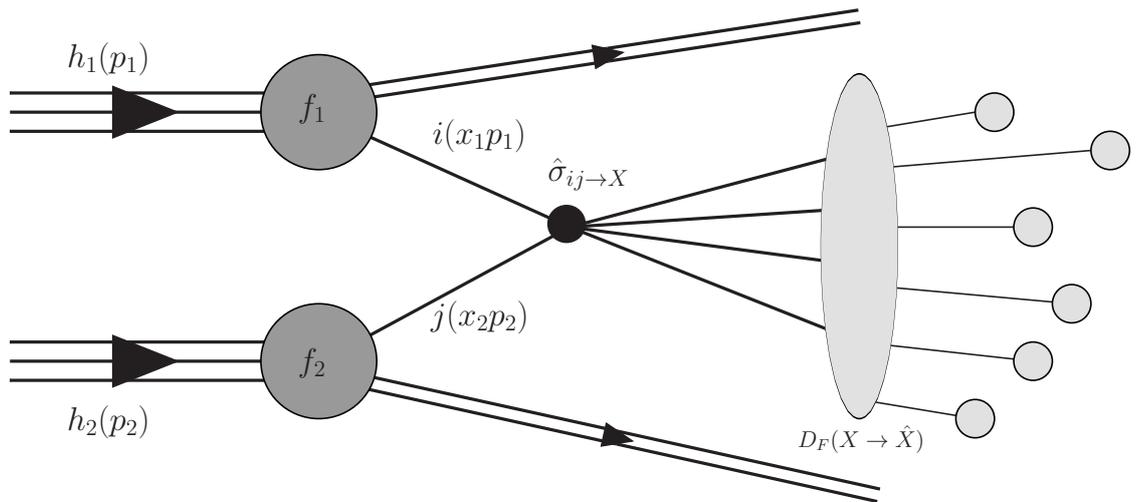
Figure 2.1: Schematic diagram for the process $h_1 h_2 \to \hat{X}$, where the two hadrons h_1 and h_2 collide producing $\hat{X}$ final states. Here the $f_{1,2}$ are the PDFs and D_F is the fragmentation function. The function $\hat{\sigma}_{ij \to X}$ denotes the hard cross section, which represents the perturbative and process-dependent term of the diagram.

2.3   Observables in QCD

The main physical observables computed in particle physics are cross sections and decay rates. In the relativistic regime at hadron colliders, the properties of elementary particles are investigated through scattering experiments, where two beams of particles collide and the outgoing products are measured. The probability of a particular final state can be expressed in terms of the cross section. In this section we briefly recall some concepts about the calculation of cross sections and the role of scattering amplitudes.

In order to make a theoretical prediction for a realistic scattering process, such as the ones measured at colliders, several steps are necessary. A schematic picture of such hadronic scattering is illustrated in Fig. 2.1. The first step is to consider the information about the initial state of the process. When comprises elementary particles, its theoretical description is particularly easy, being identified by the incoming momenta (and helicities, if the incoming beam is polarized). If in the initial state we

have composite objects, such as hadrons, we instead need information about their structure. The composition of hadrons (such as protons and neutrons) in terms of partons is encoded in the parton distribution functions (PDFs). These cannot be computed perturbatively and need to be measured experimentally. However, since the structure of the hadrons does not depend on the considered process or experiment, the PDFs are assumed to be universal, i.e. PDFs measured using data from a set of processes (or experiments) can be used in order to make predictions for other processes (or experiments). The next step consists of a description of the fundamental interactions between the elementary particles involved in the process. These hard interactions are described by the scattering amplitudes which can be computed in perturbation theory and represent the main process-dependent part of a process. The final step regards the knowledge of how the final state of this elementary interaction further evolves, from high to low energy, into a physical final state which can be measured in a detector. This final state evolution is in turn the combination of several ingredients, such as the soft and collinear emission of extra radiation, use of measurement functions to reconstruct the final state signatures of quarks and gluons produced in the hard scattering, and hadronization (how final state partons combine together into hadrons). Similarly to the PDFs, these final-state ingredients are assumed to be universal and can usually be implemented in process-independent algorithms.

We consider a $2 \to n$ process with 2 incoming elementary particles and n outgoing particles, with kinematic $p_1 p_1 \to p_1 \ldots p_{n+2}$. If the initial (in) and the final (out) states are constructed independently, the probability that such a process occurs is given by

$$\mathcal{P} = |_{\text{out}}\langle p_3 \ldots p_{n+2} | p_1 p_2 \rangle_{\text{in}}|^2 = \lim_{T \to \infty} |\langle p_1 \ldots p_{n+2} | e^{-i2HT} | p_1 p_2 \rangle|^2 \equiv |\langle p_1 \ldots p_{n+2} | \mathcal{S} | p_1 p_2 \rangle|^2,$$

(2.3.31)

where H is the Hamiltonian and T the time, which define the unitary scattering operator $\mathcal{S}$. Usually the $\mathcal{S}$ matrix is written in a such a way that all the information

about the interaction is contained in the transition matrix $\mathcal{T}$,

$$\mathcal{S} = \mathbf{1} - i\mathcal{T}. \tag{2.3.32}$$

The scattering amplitude $\mathcal{A}$ is then defined from $\mathcal{T}$ by the momentum conservation condition,

$$\langle p_3 \dots p_{n+2} | \mathcal{T} | p_1 p_2 \rangle = i(2\pi)^4 \delta^{(4)}\Big(p_1 + p_2 - \sum_{i=3}^{n+2} p_i\Big)\mathcal{A} \tag{2.3.33}$$

The amplitude $\mathcal{A}$ can be computed in perturbation theory using Feynman diagrams and the Feynman rules listed in Appendix A. The cross section can then be calculated by integrating the squared scattering amplitude over the phase space of the final state, and dividing by the incoming flux,

$$d\sigma = \frac{1}{2E_1 E_2 |v_1 - v_2|} \prod_{j=3}^{n} \frac{d^3 p_j}{(2\pi)^2 2E_j} \delta^{(4)}\Big(p_1 + p_2 - \sum_{i=3}^{n+2} p_i\Big)|\mathcal{A}|^2 \tag{2.3.34}$$

where the difference $|v_1 - v_2|$ is the relative velocity of the beam as viewed from the laboratory frame.

If the initial states are bound states such as hadrons, one should instead compute a partonic cross section between the initial partons and the other elementary particles involved, convoluting the cross section for the hard process (2.3.34) with the PDFs. This organisation of the calculation is valid under the assumption that short-distance and long-distance effects factorise. Factorisation allows us to break up such a complex problem, which it is unclear how to approach in a single framework, into different pieces, treated as approximately independent, that we are able to compute. For a process with two hadrons in the initial states $h_1 h_2 \to X$, with kinematics $p_1 p_2 \to p_3 \dots p_{n+2}$, the total cross section is a sum of all the possible

partonic channels

$$d\boldsymbol{\sigma}(h_1(p_1)h_2(p_2) \to X) = \sum_{ij} \int_0^1 dx_1 dx_2 f_{i,h_1}(x_1, \mu_F^2) f_{j,h_2}(x_2, \mu_F^2) \times \qquad (2.3.35)$$

$$d\hat{\sigma}_{ij}\Big(i(x_1p_1)j(x_2p_2) \to \hat{X}, \mu_F^2, \mu_R^2, Q^2\Big) D_F(\hat{X} \to X) + \mathcal{O}(\Lambda_{QCD}/Q)$$

where $f_{i,h}$ denotes the distribution of the parton i in the hadron h and the integration variables x represent the fraction of the momentum of the hadrons carried by the respective parton involved in the interaction. The fragmentation functions D_F parametrise the transition from partonic final state $\hat{X}$ to the hadronic observable Xs. Finally we have the dependence on three different scales: the hard scattering scale Q^2, the factorisation scale μ_F, which can be thought as the scale separating the long and short-distance physics, and the renormalization scale μ_R in which the coupling constant α_s evolves.

The PDFs $f_{i,h}(x, \mu_F)$ are non-perturbative functions which are not a priori calculable, but a perturbative differential equation governing their evolution with μ_F can be obtained by requiring that physical scattering cross sections be independent of such an un-physical scale. The resulting renormalization group equation is called the DGLAP equation[35, 36, 37] and can be used to run the PDFs between different scales. The DGLAP equation can be written as, [2]

$$\frac{\partial}{\partial \log(\mu_F^2)} f_i(x, \mu_F^2) = P_{ij}\left(x, \mu_F^2\right) \otimes f_j(x, \mu_F^2), \qquad (2.3.36)$$

where the splitting functions P_{ij}, which can be computed in perturbation theory, are the evolution kernel of the PDFs and contain the collinear divergences which are absorbed into the PDFs.

The partonic cross section is then calculable in perturbation theory, and does not depend on the type of incoming hadron. We expand the partonic cross section

---

[2]We make use of the Mellin convolution $P \otimes f \equiv \int_x^1 \frac{dy}{y} P(\frac{x}{y}) f(y, \mu_F^2)$

$d\hat{\sigma}_{ij}$ in power of $\alpha_s(\mu^2)$ as

$$d\hat{\sigma}_{ij} = d\hat{\sigma}_{ij,LO} + \frac{\alpha_s(\mu^2)}{2\pi}d\hat{\sigma}_{ij,NLO} + \left(\frac{\alpha_s(\mu^2)}{2\pi}\right)^2 d\hat{\sigma}_{ij,NNLO} + \mathcal{O}(\alpha_s^3) \qquad (2.3.37)$$

where leading order (LO), next-to-leading order (NLO) and next-to-next-to-leading order (NNLO) corrections are identified. At LO, the cross section is obtained by evaluating the tree-level cross section for the processes and integrating over the n-parton final state $d\Phi_n$,

$$d\hat{\sigma}_{ij,LO} = \int_{\Phi_n} d\hat{\sigma}_{ij,LO}^B. \qquad (2.3.38)$$

The $d\hat{\sigma}_{ij,LO}^B$ is called Born-level partonic cross section and is related to the lowest-order matrix element squared $\mathcal{A}_n^{(0)}$,

$$d\hat{\sigma}_{ij,LO}^B = \frac{1}{2Q^2}\prod_{j=3}^{n}\frac{d^3p_j}{(2\pi)^2 2E_j}\delta^{(4)}\big(x_1p_1 + x_2p_2 - \sum_{i=3}^{n+2}p_i\big)|\mathcal{A}_n^{(0)}|^2. \qquad (2.3.39)$$

This coefficient is finite and hence can be integrated over all of phase space. Moving to the next terms in the perturbative expansion, divergences appear and the integration cannot be performed straightforwardly. These divergences need to be regularised and they typically cancel out only at the end of the computation of physical observables. In such terms the origin of the divergences are the integrals in the loop (virtual) momenta associated with diagrams which contain loops and the integration of un-resolved emission of real particles in the final states. The former typically generate ultraviolet (UV) and infrared (IR) divergences. These divergences can be regularised by a procedure called dimensional regularisation [38] [3], which consists of performing the loop integration in a generic number of dimensions

---

[3]Other regularisation schemes also exist. The most famous is the dimensional cut-off, in which one introduces an upper limit Λ for the integral.

d,

$$\int_0^\infty \prod_i d^4 k_i \rightarrow \int_0^\infty \prod_i d^d k_i. \qquad (2.3.40)$$

Then the ultraviolet divergences are removed from the scattering amplitudes by UV renormalization, after a proper choice of renormalization scheme, which requires the introduction of a unphysical scale μ_R. On the other hand, infrared divergences only cancel after summing, order by order in perturbation theory, the contributions from virtual correction terms and those with emission of extra radiation in the final state (Kinoshita-Lee-Nauenberg theorem [39, 40]). After performing renormalization to absorb the UV divergences, the NLO contribution to the cross section can be written as

$$d\hat{\sigma}_{ij,NLO} = \int_{\Phi_n} d\hat{\sigma}^V_{ij,NLO} + \int_{\Phi_{n+1}} d\hat{\sigma}^R_{ij,NLO} \qquad (2.3.41)$$

where the two pieces on the right-hand side are respectively the virtual and the real terms. The former is the integration over the NLO contributions to the squared matrix element, given by the one-loop amplitude $\mathcal{A}^{(1)}_m$,

$$d\hat{\sigma}^V_{ij,NLO} = 2\Re[\mathcal{A}^{(1)}_m \mathcal{A}^{(0)*}_m] \qquad (2.3.42)$$

and the latter involves a process with the emission of an additional external particle in the final state

$$d\hat{\sigma}^R_{ij,NLO} = |\mathcal{A}^{(0)}_{m+1}|^2. \qquad (2.3.43)$$

Diagrammatic representation of these contributions is showed in Fig. 2.2. However, since the two integrations are performed on different phase spaces, a direct application of the formula above in a numerical phase-space integration is not possible. The most common trick to deal with this problem relies on rewriting Eq. (2.3.41)

(a) virtual   (b) real
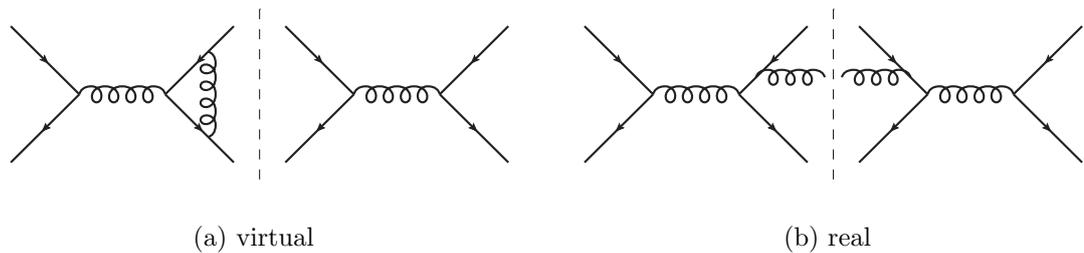
Figure 2.2: Diagrammatic representation of the matrix element squared of a $2 \to 2$ process, contributing to the same order of the perturbative expansion of the cross section in the strong coupling.

as

$$d\hat{\sigma}_{ij,NLO} = \int_{\Phi_n} \left(d\hat{\sigma}_{ij,NLO}^V + \int_{\Phi_1} d\hat{\sigma}_{ij,NLO}^S \right) + \int_{\Phi_{n+1}} \left(d\hat{\sigma}_{ij,NLO}^R - d\hat{\sigma}_{ij,NLO}^S \right) \quad (2.3.44)$$

where we introduced a new term $d\hat{\sigma}_{ij,NLO}^S$, called a subtraction term. The subtraction term clearly doesn't change the final result of the expression and it makes the two terms on the right-hand side finite, such that the integrals can be performed numerically. The choice of $d\hat{\sigma}_{ij,NLO}^S$ is not unique and different subtraction schemes have been proposed, such as Catani-Seymour dipole subtraction [41], FKS subtraction [42, 43] and the phace-space slicing method [44] [4].

The general idea behind these methods is to construct a suitable form for the subtraction term $d\hat{\sigma}^S$ such that, in Eq. (2.3.44), the integrand over Φ_1 can be performed numerically after the expansion in the dimensional regulation parameter ϵ. Then the divergences are cancelled and the two finite terms can be integrated numerically. The generation of the appropriate subtraction terms requires one to combine the soft and collinear limits into one universal set of functions that achieve the correct limiting behaviour for both soft and collinear radiation. Because the IR limits are universal, they can be classified using a set of process-independent functions that only has to be worked out once and for all. Indeed in gauge theory, scattering amplitudes factorise in the soft and collinear limit, where the singularities

---

[4]In recent years many other methods have been proposed for NNLO applications.

are incapsulated in the universal soft eikonal factor and in the collinear splitting function respectively [45], which can be computed in perturbation theory.

Similar approaches have been applied successfully at NNLO, where Eq. (2.3.41) and (2.3.44) turn into more complicated expressions due to the appearance of multi-loop amplitudes and the real emission of multiple unresolved final states. Also the numbers of subtraction terms required to remove IR singularities for higher orders in the perturbative expansion grows extremely fast and predictions require highly intensive simulations. Figure 2.3 shows the real and virtual contributions to a cross
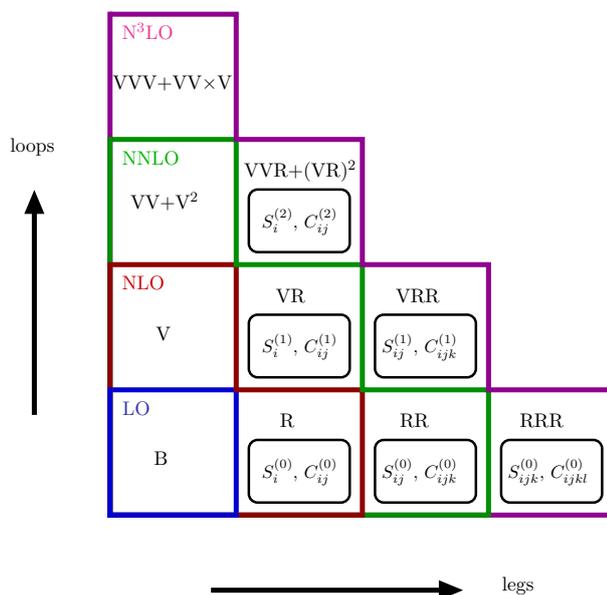
Figure 2.3: The contributions to perturbative cross sections up to N^{3}LO. This consists of virtual (V) corrections up to three loops and real radiation (R) corrections with up to 3 additional unresolved legs. In the real radiation contributions the primary infrared limits of soft (S) and collinear (C) should be removed from the matrix elements and re-combined with the virtual corrections to obtain an infrared finite result.

section up to N^{3}LO and the primary singular limits which are either multiple soft, $S^{(l)}_{i_1 \dots i_n}$, or multiple collinear, $C^{(l)}_{i_1 \dots i_n}$, where the superscript (l) indicates the loop order and the subscript $i_1 \dots i_n$ indicates the set of particles involved in the singular limit.

The final states of the hard process described above can be partons, i.e. quarks

and gluons. However, as we briefly mentioned introducing Eq. (2.3.37), partons are never observed as free states in detectors because, after the interaction, they combine into hadrons. For this reason, theory and experimental results are often presented in terms of jet cross sections, where a jet is a collimated cone of hadrons and can be regarded as the footprint of a parton in the final state of the hard scattering process. Several jet algorithms have been proposed in order to identify them from the signals of an event. Nowadays the most used jet algorithms are based on clustering, which consist in defining a distance d_{ij} between any two particles i and j, as well as a distance d_{iB} between a particle i and the beam (B). The definition of the algorithm is given by the functional form of the distances and the most popolar ones are: the k_T algorithm [46], the Cambridge-Aachen algorithm [47], SIScone [48] and the anti-k_t algorithm [49]. Then the algorithm is implemented recursively by computing these distances for the set of all measured momenta p_i and then removing i from the list if d_{iB} is the minimum or replacing p_i and p_j with their sum if d_{ij} is the minimum. Iterating the algorithm for all the particles in the list, the final object is called a jet.

To conclude, we briefly discuss two unphysical scales we introduced so far, namely the factorisation scale μ_F and the renormalization scale μ_R. In QFT the dependence on these scales would cancel out if we were able to sum all orders in perturbation theory and obtain an exact result. However, in a fixed-order perturbative computation, this cancellation doesn't happen because of neglected higher-order terms. The most important terms of these contributions have a logarithmic form like $\ln^k Q_i^2/\mu_{R,F}^2$ where Q_i are the physical scales of the process. In general there isn't an unique prescription to get rid of these terms, but one can try to minimise their effects by choosing values for μ_F and μ_R that are close to the physical scales. Also, since the unphysical dependence on the renormalization and factorisation scales is an effect of the neglected higher-order terms, it can also be exploited in order to determine the theoretical uncertainty of perturbative results, which can be obtained by varying μ_F and μ_R on a given range. A common practice is to choose a central value$\mu_F = \mu_R = \mu_0$ and then vary them between $\mu_0/2$ and 2μ.

A complete discussion of all elements of the latest precision simulations for

hadron colliders is beyond the scope of this thesis. However it's important to remark that all these techniques and their implementation have led, in the last decades, to a very precise theoretical description of the Standard Model [50]. The current frontier of this research is to test the SM at the LHC using at least theoretical predictions at NNLO, which will be required to match projected experimental uncertainties.

Chapter 3

Scattering amplitudes in QCD

In quantum field theory, after an appropriate quantisation of the fields appearing in the Lagrangian, the perturbative expansion of the correlation function in the coupling leads to a series whose terms can be computed order by order. As a result, scattering amplitudes can be written as a sum of objects called Feynman diagrams, which allow us to visualise the effects of the interactions to arbitrary high order.

For the theory of QCD, whose Lagrangian is given in Eq. (2.2.21), a general amplitude is given by a sum of connected Feynman diagrams joining the initial and the final states,

$$\mathcal{A}(p_1, \ldots, p_n) = \sum \text{diagram}\,(g_s, \text{colour}, \text{kinematics}) \qquad (3.0.1)$$

which are functions of the strong coupling constant, the momenta through kinematics invariants and the SU(3) colour factors. The Feynman diagrams are obtained by combining the Feynman rules derived from the Lagrangian. The set of Feynman rules of QCD is given in Appendix A. In perturbation theory, scattering amplitudes are usually categorised according with the number of loops of the diagrams. Amplitudes with zero loops are called tree-level, then there are one-loop amplitudes, two-loop amplitudes and so on.

The traditional calculation of scattering amplitudes at a given loop order involves several steps. Firstly, some operations are required, such as considering all Feynman diagrams and performing colour, Lorentz and Clifford algebra. The next step

involves the integration of the loop momenta, which also requires a regularisation procedure. Finally, the loop amplitudes must be renormalized in order to compute physical observables.

In this Chapter we introduce some well known properties of scattering amplitudes which have been used to obtain the results of this thesis. In particular, we discuss the colour decomposition in QCD and the frameworks of spinor helicity formalism and momentum twistor parametrisation for the representation of the kinematics. An exhaustive introduction on scattering amplitudes can be found in many textbooks and manuals, e.g. [33, 51].

3.1   Colour decomposition

A useful method to organise the calculation of scattering amplitudes in QCD is the colour decomposition [7, 52], which allows us to disentangle the colour from the kinematics.

A general QCD amplitude can be decomposed into a basis of $\mathrm{SU}(N_c)$ colour factors and ordered partial amplitudes which depend only on momenta and helicities of the external states. For an n-point L-loop amplitude this can be represented as,

$$\mathcal{A}_n^{(L)}(\{a_i\}, \{p_i^{\lambda_i}\}) = \sum_c C_c(\{a_i\}) A_{n;c}^{(L)}(\{p_i^{\lambda_i}\}) \qquad (3.1.2)$$

where a_i, λ_i and p_i are colour indices (adjoint or fundamental), helicity and momenta of the ith leg. Unless explicitly indicated otherwise, we understand that the index i runs from 1 to n, e.g.

$$\{p_i^{\lambda_i}\} \equiv \{p_i^{\lambda_i}\}_{i=1}^n = \{p_1^{\lambda_1}, \ldots, p_n^{\lambda_n}\}. \qquad (3.1.3)$$

For cross-section computations we are required to square these amplitudes and sum

over the colour indices. This sum can be represented as,

$$\mathcal{M}_n^{(L,L')}(\{p_i^{\lambda_i}\}) = \sum_{a_i} \left(\mathcal{A}_n^{(L)}(\{a_i\}, \{p_i^{\lambda_i}\})\right)^\dagger \mathcal{A}_n^{(L')}(\{a_i\}, \{p_i^{\lambda_i}\})$$

$$= \left(\vec{A}_n^{(L)}(\{p_i^{\lambda_i}\})\right)^\dagger \cdot \mathcal{C}_n^{(L,L')} \cdot \vec{A}_n^{(L')}(\{p_i^{\lambda_i}\}), \qquad (3.1.4)$$

where the matrix $\mathcal{C}_n^{(L,L')}$ is a function of N_c defined by

$$\left(\mathcal{C}_n^{(L,L')}\right)_{cc'} = \sum_{a_i} \left(C_c(\{a_i\})\right)^\dagger C_{c'}(\{a_i\}), \qquad (3.1.5)$$

while $\vec{A}^{(L)}$ is a vector of partial amplitudes $A_{n;c}^{(L)}$

$$\vec{A}^{(L)} = \{A_{n;1}^{(L)}, A_{n;2}^{(L)}, \ldots\}. \qquad (3.1.6)$$

Partial amplitudes may in turn be written in terms of primitive amplitudes $A_p^{[X]}$ which further decompose colour and flavour structure due to the internal loops,

$$A_{n;c}^{(L)} = \sum_{p,X} R_{c,p,X}(N_c, N_f) A_{n,p}^{[L,X]}, \qquad (3.1.7)$$

where X runs over the independent primitive topologies at L loops and p runs over permutations of the n external legs. Eq. (3.1.4) can thus be equivalently written as

$$\mathcal{M}_n^{(L,L')}(\{p_i^{\lambda_i}\}) = \left(\vec{A}_n^{[L]}(\{p_i^{\lambda_i}\})\right)^\dagger \cdot \mathcal{C}_n^{[L,L']} \cdot \vec{A}_n^{[L']}(\{p_i^{\lambda_i}\}) \qquad (3.1.8)$$

where $\vec{A}_n^{[L]}$ is a vector of primitive amplitudes $A_{n,p}^{[L,X]}$ and the matrix $\mathcal{C}_n^{[L,L']}$ can be related to $\mathcal{C}_n^{(L,L')}$ defined in Eq. (3.1.5) by the change of basis in Eq. (3.1.7).

To determine the colour decomposition and compute the colour factors we consider the generators T^a which can be obtained from the standard ones t^a introduced in Eq. (2.2.24) by a change of normalisation,

$$T^a \equiv \frac{1}{\sqrt{2}} t^a, \qquad [T^a, T^b] = i\sqrt{2} f^{abc} T^c, \qquad \mathrm{tr}(T^a T^b) = \delta^{ab}, \qquad (3.1.9)$$

such that the additional factors $\sqrt{2}$ that appear in the intermediate steps and the Feynman rules cancel out with the ones which would appear in the total results for the colour-ordered amplitudes if we used the standard normalization instead. Using the following relations for the generators T^a and the structure constants f^{abc},

$$\sum_{a=1}^{N_c^2-1} (T^a)_i^{\bar{j}} (T^a)_k^{\bar{l}} = \delta_i^{\bar{l}} \delta_k^{\bar{j}} - \frac{1}{N_c} \delta_i^{\bar{j}} \delta_k^{\bar{l}}, \tag{3.1.10}$$

$$f^{abc} = \frac{-i}{\sqrt{2}} \left(\text{tr}(T^a T^b T^c) - \text{tr}(T^b T^a T^c) \right), \tag{3.1.11}$$

the colour dependence may be written in terms of T^a only.

Different colour decompositions have been proposed, e.g. based on the structure constant [53], however we will usually refer to the basis of fundamental generators.

3.2 Spinor-helicity formalism

The spinor-helicity formalism manifestly encodes the massless condition of particles and therefore it turns out to be particularly useful to represent scattering amplitudes. First introduced in the context of amplitudes involving massless four dimensional particles, it has been proved to be suitable for describing also massive particles and has been extended to represent momenta living in higher dimensions. For the purpose of this thesis, the spinor-helicity formalism in four and six dimensions will be described. An exhaustive and pedagogical review of the spinor helicity formalism can be found in [51, 54].

Spinor-helicity formalism in four dimensions

The basic idea of the spinor-helicity formalism is to represent massless four dimensional momenta p^μ in terms of a pair of two dimensional spinors $\{\lambda(p), \tilde{\lambda}(p)\}$. Such spinors can be constructed as follows. We consider the Lorentz contraction of a massless momentum p^μ,

$$p^\mu \equiv (p_0, p_1, p_2, p_3), \qquad p^2 = 0, \tag{3.2.12}$$

with the Pauli matrices σ^μ,

$$\sigma^\mu \equiv \left(I_2, \sigma^1, \sigma^2, \sigma^3\right), \tag{3.2.13}$$

whose definition in the Weyl representation is

$$I_2 = \begin{pmatrix} 1 & 0 \\ 0 & 1 \end{pmatrix}, \quad \sigma^1 = \begin{pmatrix} 0 & 1 \\ 1 & 0 \end{pmatrix}, \quad \sigma^2 = \begin{pmatrix} 0 & -i \\ i & 0 \end{pmatrix}, \quad \sigma^3 = \begin{pmatrix} 1 & 0 \\ 0 & -1 \end{pmatrix}. \tag{3.2.14}$$

The metric tensor is defined as $\eta^{\mu\nu} = \mathrm{diag}(1, -1, -1, -1)$. The two dimensional matrix $p_{\alpha\dot\beta} \equiv \sigma \cdot p$, which has the explicit form

$$p_{\alpha\dot\beta} = \begin{pmatrix} p_- & -p_-^\perp \\ -p_+^\perp & p_+ \end{pmatrix}, \qquad \begin{aligned} p_\pm &= p_0 \pm p_3, \\ p_\pm^\perp &= p_1 \pm i p_2 \end{aligned} \tag{3.2.15}$$

is rank-1, since $\det(p_{\alpha\dot\beta}) = 0$, and therefore it can be written as the outer product of two dimensional vectors

$$p_{\alpha\dot\beta} = \lambda_\alpha(p)\tilde\lambda_{\dot\beta}(p) \tag{3.2.16}$$

The vectors λ and $\tilde\lambda$ (we will omit the argument p when it is understood) are respectively the holomorphic and anti-holomorphic Weyl-spinors associated to the momentum p^μ and can be parametrised as follows,

$$\lambda_\alpha = t \left(\frac{p_-^\perp}{\sqrt{p_+}}, -\sqrt{p_+} \right)^T, \qquad \tilde\lambda_{\dot\beta} = t^{-1} \left(\frac{p_+^\perp}{\sqrt{p_+}}, -\sqrt{p_+} \right). \tag{3.2.17}$$

These are the fundamental objects of the spinor-helicity formalism. The rescaling parameter t is related to the little group symmetry, which is the group of transformations that leaves the momentum of a massless particle invariant; it represents the rotations in the xy plane and therefore is characterised by $SO(2) \simeq U(1)$. We raise

and lower the holomorphic and anti-holomorphic spinor indices with

$$\varepsilon^{\alpha\beta} = \varepsilon^{\dot\alpha\dot\beta} \equiv \begin{pmatrix} 0 & 1 \\ -1 & 0 \end{pmatrix}, \qquad \varepsilon_{\alpha\beta} = \varepsilon_{\dot\alpha\dot\beta} \equiv \begin{pmatrix} 0 & -1 \\ 1 & 0 \end{pmatrix} \tag{3.2.18}$$

as

$$\lambda^\alpha = \varepsilon^{\alpha\beta}\lambda_\beta, \qquad \tilde\lambda_{\dot\alpha} = \varepsilon_{\dot\alpha\dot\beta}\tilde\lambda^{\dot\beta}. \tag{3.2.19}$$

Also, we introduce the compact braket notation for the spinors,

$$\langle i| \equiv \lambda^\alpha(p_i), \quad |i\rangle \equiv \lambda_\alpha(p_i), \quad [i| \equiv \tilde\lambda_{\dot\alpha}(p_i), \quad |i] \equiv \tilde\lambda^{\dot\alpha}(p_i). \tag{3.2.20}$$

The Lorentz invariant product is constructed contracting the spinor indices,

$$\langle ij\rangle = \lambda(p_i)_\alpha \lambda(p_j)_\beta \varepsilon^{\alpha\beta},$$
$$[ij] = \tilde\lambda(p_i)_{\dot\alpha} \tilde\lambda(p_j)_{\dot\beta} \varepsilon^{\dot\alpha\dot\beta} \tag{3.2.21}$$
$$\langle ij\rangle[ji] = 2p_i p_j \equiv s_{ij}$$

The spinor object described so far have the following useful properties:

- for real momenta $\tilde\lambda = \lambda^\dagger$

- $\langle ij\rangle = -\langle ji\rangle$, $[ij] = -[ji]$, $\langle ii\rangle = 0$, $[ii] = 0$ and $\langle i\sigma^\mu j] = [j\sigma^\mu i\rangle$

- Fiertz identity $\langle i\sigma^\mu j][k\sigma_\mu l] = 2\langle ik\rangle[lj]$

- Schouten identity $\langle ij\rangle\langle kl\rangle + \langle ik\rangle\langle lj\rangle + \langle il\rangle\langle jk\rangle = 0$

- we adopt the analytic continuation $|-k\rangle = i|k\rangle$, $|-k] = i|k]$

Clearly the bi-spinors introduced above are related to the massless fermion and anti-fermion external states. Indeed considering the massless Dirac equation

$$\gamma_\mu p^\mu \psi(p) = 0, \tag{3.2.22}$$

where γ^μ are defined as,

$$\gamma^\mu = \begin{pmatrix} 0 & \sigma^\mu \\ \tilde{\sigma}^\mu & 0 \end{pmatrix}, \qquad \gamma^5 = \begin{pmatrix} -I_2 & 0 \\ 0 & I_2 \end{pmatrix}, \qquad (3.2.23)$$

with $\tilde{\sigma}^\mu = (I_2, -\sigma^i)$, we obtain the Weyl equations,

$$\begin{pmatrix} 0 & p_{\alpha\dot{\beta}} \\ p^{\dot{\alpha}\beta} & 0 \end{pmatrix} \begin{pmatrix} \tilde{\lambda}_{\dot{\beta}} \\ \lambda^\alpha \end{pmatrix} = 0. \qquad (3.2.24)$$

Therefore, we can establish the following relations for the helicity states of the (anti)fermions,

$$u_+ = v_- = \begin{pmatrix} 0 \\ \lambda^\alpha \end{pmatrix}, \qquad u_- = v_+ = \begin{pmatrix} \tilde{\lambda}_{\dot{\alpha}} \\ 0 \end{pmatrix}, \qquad (3.2.25)$$

$$\bar{u}_+ = \bar{v}_- = \left(\tilde{\lambda}^{\dot{\alpha}}, 0 \right), \qquad \bar{u}_- = \bar{v}_+ = \left(0, \lambda_\alpha \right). \qquad (3.2.26)$$

Finally, the polarisation vectors can be written using this formalism,

$$\epsilon_-^\mu(p, q) = \frac{\langle p\sigma^\mu q]}{\sqrt{2}[pq]}, \qquad \epsilon_+^\mu(p, q) = \frac{\langle q\sigma^\mu p]}{\sqrt{2}\langle pq \rangle}, \qquad (3.2.27)$$

where q is an arbitrary reference spinors such that $p \neq q$, which corresponds to working in a light-like gauge. The polarisation vectors satisfy the expected relations,

$$p \cdot \epsilon_\pm(p, q) = 0, \qquad \epsilon_\pm(p, q) \cdot \epsilon_\mp(p, q) = 0, \qquad \epsilon_\pm(p, q) \cdot \epsilon_\pm(p, q) = -1, \qquad (3.2.28)$$

and the completeness relation,

$$\sum_{s=\pm} \epsilon_s^{*\mu}(p, q)\epsilon_s^\nu(p, q) = -\eta^{\mu\nu} + \frac{p^\mu q^\nu + q^\mu p^\nu}{p \cdot q}. \qquad (3.2.29)$$

Spinor-helicity formalism in six dimensions

The spinor algebra can be constructed in all even dimensions. In particular, we will present a parametrisation of the spinor-helicity in six dimension, following [29]. Let consider a massless momentum p^μ living in a 6 dimensional space with metric tensor signature,

$$\eta^{\mu\nu} = \text{diag}(1, -1, -1, -1, -1, -1). \tag{3.2.30}$$

The Σ and $\tilde{\Sigma}$ Pauli matrices are six 4×4 matrices respectively, which are defined as

$$
\begin{aligned}
\Sigma^0 &= i\sigma^1 \otimes \sigma^2 & \tilde{\Sigma}^0 &= -i\sigma^1 \otimes \sigma^2 \\
\Sigma^1 &= i\sigma^2 \otimes \sigma^3 & \tilde{\Sigma}^1 &= i\sigma^2 \otimes \sigma^3 \\
\Sigma^2 &= \sigma^2 \otimes \sigma^0 & \tilde{\Sigma}^2 &= -\sigma^2 \otimes \sigma^0 \\
\Sigma^3 &= -i\sigma^2 \otimes \sigma^1 & \tilde{\Sigma}^3 &= -i\sigma^2 \otimes \sigma^1 \\
\Sigma^4 &= -\sigma^3 \otimes \sigma^2 & \tilde{\Sigma}^4 &= \sigma^3 \otimes \sigma^2 \\
\Sigma^5 &= -i\sigma^0 \otimes \sigma^2 & \tilde{\Sigma}^5 &= -i\sigma^0 \otimes \sigma^2,
\end{aligned} \tag{3.2.31}
$$

and obey the Clifford algebra,

$$\Sigma^\mu \tilde{\Sigma}^\nu + \Sigma^\nu \tilde{\Sigma}^\mu = 2\eta^{\mu\nu}. \tag{3.2.32}$$

The Dirac equations for the holomorphic and anti-holomorphic spinors are,

$$p_\mu \Sigma^\mu_{AB} \lambda^A_\alpha = 0, \qquad p_\mu \tilde{\Sigma}^\mu_{AB} \tilde{\lambda}^{A\dot{\alpha}} = 0, \tag{3.2.33}$$

where the indices A, B belong to fundamental group $SU(4)$ and the $\alpha, \dot{\alpha}$ belong to the little group $SU(2) \times SU(2)$. The 4×4 matrices $p \cdot \Sigma$ and $p \cdot \tilde{\Sigma}$ take the explicit

form,

$$
p^\mu \Sigma_{\mu AB} = \begin{pmatrix} 0 & -p_+^6 & -p_+^\perp & p_+ \\ -p_+^6 & 0 & -p_- & p_-^\perp \\ p_+^\perp & p_- & 0 & -p_-^6 \\ -p_+ & -p_-^\perp & -p_-^6 & 0 \end{pmatrix}, \; p^\mu \tilde{\Sigma}_{\mu AB} = \begin{pmatrix} 0 & -p_+^6 & -p_-^\perp & -p_- \\ -p_-^6 & 0 & p_+ & p_+^\perp \\ p_-^\perp & -p_+ & 0 & -p_+^6 \\ p_- & -p_+^\perp & -p_+^6 & 0 \end{pmatrix},
$$

$$(3.2.34)$$

where $p_\pm = p^0 \pm p^3$, $p_\pm^\perp = p^1 \pm ip^2$ and $p_\pm^6 = p^4 \pm ip^5$. The solutions to the Dirac equations (3.2.33) can be found in terms of the components of these matrices. In particular, we present a useful class of solutions that is free of square roots,

$$
\lambda(p)_\alpha^A = \begin{bmatrix} 0 & -\frac{p_+^6 p_+}{p_-^\perp} & p_+ & \frac{p_+ p_+}{p_-^\perp} \\ \frac{p_-^\perp}{p_+} & 1 & 0 & \frac{p_-^6}{p_+} \end{bmatrix}_{\alpha A}, \qquad \tilde{\lambda}(p)_{A\dot\alpha} = \begin{bmatrix} \frac{p_-^6}{p_-^\perp} & p_+ \\ 0 & p_-^\perp \\ -\frac{p_-}{p_-^\perp} & p_+^6 \\ 1 & 0 \end{bmatrix}_{A\dot\alpha}. \qquad (3.2.35)
$$

As in the four dimensional case, momenta and invariants can be constructed from the spinors by contracting the appropriate fundamental and little group indices,

- momenta:

$$
p_{AB} = p_\mu \Sigma^\mu_{AB} = \varepsilon^{\dot\alpha\dot\beta}\tilde{\lambda}_{A\dot\alpha}\tilde{\lambda}_{B\dot\beta}, \qquad p^{AB} = p^\mu \tilde{\Sigma}^{AB}_\mu = \varepsilon_{\alpha\beta}\lambda^{A\alpha}\lambda^{B\beta} \qquad (3.2.36)
$$

$$
p^\mu = -\frac{1}{4}\langle p^\alpha \Sigma^\mu p^\beta \rangle \varepsilon_{\alpha\beta} = -\frac{1}{4}[p_{\dot\alpha}\tilde{\Sigma}^\mu p_{\dot\beta}]\varepsilon^{\dot\alpha\dot\beta} \qquad (3.2.37)
$$

- polarisation vectors:

$$
\epsilon^\mu_{\alpha\dot\beta} = -\frac{\langle p_\alpha \Sigma^\mu q^\gamma \rangle \langle q_\gamma | p_{\dot\beta}]}{2\sqrt{2}p \cdot q} = \frac{\langle p_\alpha | q_{\dot\gamma}][q^{\dot\gamma}\tilde{\Sigma}^\mu p_{\dot\beta}]}{2\sqrt{2}p \cdot q} \qquad (3.2.38)
$$

- Lorentz invariants:

$$\langle i^\alpha | j_{\dot\beta}] = [j_{\dot\beta} | i^\alpha\rangle = \lambda^{A\alpha}(p_i)\tilde\lambda_{A\dot\beta}(p_j), \tag{3.2.39}$$

$$s_{ij} = -\det([j_{\dot\beta}|i^\alpha\rangle), \tag{3.2.40}$$

$$\langle i^\alpha j^\beta k^\gamma l^\delta\rangle = \varepsilon_{ABCD}\lambda^{A\alpha}(p_i)\lambda^{B\beta}(p_j)\lambda^{C\gamma}(p_k)\lambda^{D\delta}(p_l), \tag{3.2.41}$$

$$[i_{\dot\alpha}j_{\dot\beta}k_{\dot\gamma}l_{\dot\delta}] = \varepsilon^{ABCD}\tilde\lambda_{A\dot\alpha}(p_i)\tilde\lambda_{B\dot\beta}(p_j)\tilde\lambda_{C\dot\gamma}(p_k)\tilde\lambda_{D\dot\delta}(p_l), \tag{3.2.42}$$

where ε_{ABCD} is the 4 Levi-Civita tensor,

- properties and identities:

$$\langle i_\alpha \Sigma^\mu j_\beta\rangle[k_{\dot\gamma}\tilde\Sigma_\mu l_{\dot\delta}] = 2\Big(\langle i_\alpha|l_{\dot\delta}]\langle j_\beta|k_{\dot\gamma}] + \langle i_\alpha|k_{\dot\gamma}]\langle j_\beta|l_{\dot\delta}]\Big) \tag{3.2.43}$$

$$\langle ijkl\rangle\langle m| + \langle jklm\rangle\langle i| + \langle klmi\rangle\langle j| + \langle lmij\rangle\langle k| + \langle mijk\rangle\langle l| = 0 \tag{3.2.44}$$

where in the Schouten identity (3.2.44) the little group indices are understood.

Spinor-helicity formalism for massive momenta

As shown in the previous sections, the spinor-helicity formalism seems to be the natural representation of amplitudes involving massless particles. Moreover, it can be used to represent massive particles as well. In this section we will describe the parametrisation of four dimensional massive momenta using the spinor-helicity formalism in four and six dimensions. First of all, we can notice that, in the case of a massive particle of mass m, the eq. (3.2.15) gives,

$$\det(p_{\alpha\dot\beta}) = m^2, \tag{3.2.45}$$

therefore the matrix $\det(p_{\alpha\dot\beta})$ has rank two and can be written as a sum of two matrices of rank one

$$p_{\alpha\dot\beta} = \lambda^I_\alpha \tilde\lambda_{\dot\beta I}, \qquad I = 1, 2, \tag{3.2.46}$$

which can be related to two massless momenta. The formalism to represent massive momenta using spinor variables has been studied extensively in [55, 56, 57, 58, 59]. In this section we follow the notation of [60].

The general strategy is to define a massless projection with respect to a light-like reference vector η,

$$(p^\flat)^\mu = p^\mu - \frac{m^2}{2p \cdot \eta}\eta^\mu, \tag{3.2.47}$$

such that $(p^\flat)^2 = 0$. A complete set of solutions of the Dirac equation for the massive momentum p can then be constructed from the Weyl spinors of $p^\flat$ and η:

$$\bar{u}_+(p, m; p^\flat, \eta) = \frac{\langle\eta|(\not{p} + m)}{\langle\eta p^\flat\rangle}, \qquad \bar{u}_-(p, m; p^\flat, \eta) = \frac{[\eta|(\not{p} + m)}{[\eta p^\flat]},$$

$$v_+(p, m; p^\flat, \eta) = \frac{(\not{p} - m)|\eta\rangle}{\langle p^\flat\eta\rangle}, \qquad v_-(p, m; p^\flat, \eta) = \frac{(\not{p} - m)|\eta]}{[p^\flat\eta]}, \tag{3.2.48}$$

with the following relations between helicity states,

$$u_-(p, m; p^\flat, \eta) = -\frac{\langle p^\flat\eta\rangle}{m}u_+(p, m; \eta, p^\flat), \tag{3.2.49}$$

$$v_-(p, m; p^\flat, \eta) = \frac{\langle p^\flat\eta\rangle}{m}v_+(p, m; \eta, p^\flat). \tag{3.2.50}$$

An alternative representation of massive four momenta can be constructed using the six dimensional spinor-helicity formalism. We follow the description given in [2]. In this case, the key consideration is to map the massive 4-momenta into massless 6-momenta. To make clear the distinction between four and six dimensional momenta we use $\bar{p}$ for 4-momenta and p for 6-momenta. We begin our discussion by looking at the Dirac equation for massive fermion in four dimensions,

$$(\gamma \cdot \bar{p} - m)u_s(\bar{p}) = 0 \text{ and } \bar{u}_s(p)(\gamma \cdot \bar{p} - m) = 0, \tag{3.2.51}$$

We embed the massive four dimensional momentum $\bar{p}$ into a six dimensional massless

momentum by declaring that

$$p = (\bar{p}, 0, m), \text{ so } p^2 = \bar{p}^2 - m^2 = 0. \tag{3.2.52}$$

and then we can write the six dimensional Dirac equation for p

$$(\Sigma \cdot p)_{AB} \lambda_a^B(p) = 0, \qquad (\tilde{\Sigma} \cdot p)^{AB} \tilde{\lambda}_{B\dot{a}}(p) = 0 \tag{3.2.53}$$

The representation of the Σ matrices is simply related to the four dimensional γ-matrices. The relation for the first four Σ matrices is

$$-\tilde{\Sigma}^{5,AX} \Sigma^\mu_{XB} = (\gamma^\mu)^A_{\ B} = \tilde{\Sigma}^{\mu,AX} \Sigma^5_{XB}, \tag{3.2.54}$$

For the remaining two Σ matrices we have

$$-\tilde{\Sigma}^{5,AX} \Sigma^4_{XB} = (-\gamma^0 \gamma^1 \gamma^2 \gamma^3)^A_{\ B} = i(\gamma^5)^A_{\ B}, \tag{3.2.55}$$

$$-\tilde{\Sigma}^{5,AX} \Sigma^5_{XB} = \mathbf{1}^A_{\ B}. \tag{3.2.56}$$

Having embedded our massive four-dimensional momentum into six dimensions, we are interested in showing in detail how massless six-dimensional spinors relate to the usual massive four-dimensional Dirac spinors. We begin by writing the massless six-dimensional Dirac equation (3.2.53) in detail as

$$(\Sigma \cdot p)_{AB} \lambda_a^B(p) = \left(\Sigma^\mu p_\mu - \Sigma^5 p^{(5)}\right)_{AB} \lambda_a^B(p) = 0. \tag{3.2.57}$$

Multiplying from the left by $-\tilde{\Sigma}^{5,XA}$ we obtain

$$(\gamma \cdot \bar{p} - p_1^{(5)})^X_{\ B} \lambda^B(p) = 0. \tag{3.2.58}$$

Notice how the sign on the sixth component of momentum determines whether $\lambda(p)$ should be associated with the four-dimensional spinor for a fermion $u(p)$ or an

anti-fermion $v(p)$:

$$\lambda(p) = \begin{cases} u(\bar{p}) & , \ p^{(5)} = m \\ v(\bar{p}) & , \ p^{(5)} = -m \end{cases}. \tag{3.2.59}$$

A similar calculation shows how to identify massless six-dimensional spinors with the conjugate four-dimensional Dirac spinors:

$$
\begin{aligned}
0 &= \lambda^A(p)(\Sigma^\mu p_\mu - \Sigma^5 p^{(5)})_{AB} \\
&= \lambda^A(p)(-\Sigma^5 \tilde{\Sigma}^5)_A^{\ X}(\Sigma^\mu p_\mu - \Sigma^5 p^{(5)})_{XB} \\
&= \lambda^A(p)\Sigma^5_{AX}(\gamma \cdot \bar{p} - p^{(5)})^X_{\ B}.
\end{aligned}
\tag{3.2.60}
$$

Again the sixth momentum component determines whether $\lambda(p)\Sigma^5$ should be identified with $\bar{u}(p)$ or $\bar{v}(p)$:

$$\lambda(p)\Sigma^5 = \begin{cases} \bar{u}(\bar{p}) & , \ p^{(5)} = m \\ \bar{v}(\bar{p}) & , \ p^{(5)} = -m \end{cases}. \tag{3.2.61}$$

In the following, we find it useful to write an explicit representation for $\lambda^A(p)$ that allows us to make direct connection with the specific four-dimensional Dirac spinors given in (3.2.48). We use a massless (in the four dimensional sense) reference vector η, as introduced in (3.2.47), with Weyl spinors $\kappa_\alpha(\eta), \tilde{\kappa}^{\dot{\alpha}}(\eta)$ and define the six dimensional spinors:

$$\lambda^{Aa}(\eta, \bar{p}^\flat) = \begin{pmatrix} 0 & \frac{\tilde{\kappa}^{\dot{\alpha}}(\eta)}{[p^\flat \eta]} \\ \frac{\kappa_\alpha(\eta)}{\langle p^\flat \eta \rangle} & 0 \end{pmatrix}, \ \tilde{\lambda}_{A\dot{a}}(\eta, \bar{p}^\flat) = \begin{pmatrix} 0 & \frac{\tilde{\kappa}_{\dot{\alpha}}(\eta)}{[p^\flat \eta]} \\ \frac{\kappa^\alpha(\eta)}{\langle p^\flat \eta \rangle} & 0 \end{pmatrix}. \tag{3.2.62}$$

Using $(\Sigma \cdot p)_{AB}(\tilde{\Sigma} \cdot p)^{BC} = 0$ we see that the Dirac equation (3.2.53) is solved by setting

$$\lambda^A(p) = (\tilde{\Sigma} \cdot p)^{AB}\tilde{\lambda}_B(\eta, \bar{p}^\flat). \tag{3.2.63}$$

The anti-chiral case is completely analogous:

$$\tilde{\lambda}_A(p) = (\Sigma \cdot p)_{AB} \lambda^B(\eta, \vec{p}^{\flat}). \tag{3.2.64}$$

The discussion following (3.2.57) showed how these six dimensional spinors solve the massive Dirac equation in four dimensions with the appropriate choice of sign for $p^{(5)}$.

3.3 Momentum twistor parametrisation

Momenta entering in scattering amplitudes satisfy momentum conservation. Clearly, would be convenient to represent amplitudes in term of variables which encode this constraint by construction. As seen in the previous sections, we introduced the spinor-helicity formalism as the natural language to describe the massless condition of particles. In this section we discuss another formalism, called momentum twistors. It, introduced by Hodges [28], makes both massless condition,$p^2 = 0$, and momentum conservation,$\sum p = 0$, manifest.

We begin by defining the dual momentum coordinates, x_i^{μ},

$$p_i^{\mu} = x_i^{\mu} - x_{i-1}^{\mu} \tag{3.3.65}$$

with the boundary condition $x_0 = x_{n+1}$, which automatically satisfy the momentum conservation condition $\sum_{i=1}^{n} p_i^{\mu} = 0$. The momentum twistor for a particle i is a 4-component object Z_{iA},

$$Z_{iA} = \left(\lambda_{\alpha}(i), \mu^{\dot{\alpha}}(i) \right) \tag{3.3.66}$$

where $\lambda_{\alpha}(i)$ are holomorphic Weyl spinors of momenta p_i as introduced in section 3.2 and $\mu^{\dot{\alpha}}(i)$ are anti-holomorphic spinors defined using the dual momentum coor-

dinates,

$$\mu^{\dot{\alpha}}(i) = (\sigma \cdot x_i)^{\alpha\dot{\alpha}} \lambda_\alpha(i). \tag{3.3.67}$$

The dual spinor W is defined as,

$$W_i^A = \left(\tilde{\mu}_\alpha(i), \tilde{\lambda}^{\dot{\alpha}}(i) \right) = \frac{\varepsilon^{ABCD} Z_{(i-1)B} Z_{iC} Z_{(i+1)D}}{\langle (i-1)i \rangle \langle i(i+1) \rangle} \tag{3.3.68}$$

from which it follows that the anti-holomorphic spinor is,

$$\tilde{\lambda}^{\dot{\alpha}}(i) = \frac{\langle (i-1)i \rangle \mu^{\dot{\alpha}}(i+1) + \langle (i+1)(i-1) \rangle \mu^{\dot{\alpha}}(i) + \langle i(i+1) \rangle \mu^{\dot{\alpha}}(i-1)}{\langle (i-1)i \rangle \langle i(i+1) \rangle}. \tag{3.3.69}$$

The kinematics for a n-particle system is defined by using the spinors $\mu_{\dot{\alpha}}(i)$ instead of $\tilde{\lambda}_{\dot{\alpha}}(i)$. The full set of momentum twistors can be represented as a $4 \times n$ matrix, where the number of independent parameters can be reduced to $3n - 10$ using the Poincarè and U(1) symmetries of the $Z_i(\lambda_i, \mu_i)$. The explicit representation of this matrix is not unique and the ideal choice, in term of simplicity of the final expression of the amplitudes, can be space-dependent. To clarify the construction of the momentum twistor parametrisation, we give a four-point example, where a useful parametrisation is,

$$Z_4 = \begin{pmatrix} \lambda_1 & \lambda_2 & \lambda_3 & \lambda_4 \\ \mu_1 & \mu_2 & \mu_3 & \mu_4 \end{pmatrix} = \begin{pmatrix} 1 & 0 & \frac{1}{z_1} & \frac{1+z_2}{z_1 z_2} \\ 0 & 1 & 1 & 1 \\ 0 & 0 & 1 & 0 \\ 0 & 0 & 0 & 1 \end{pmatrix}, \tag{3.3.70}$$

with z_1 and z_2 being two free parameters. We can then find the corresponding anti-holomorphic spinors $\tilde{\lambda}_i$ by using Eq. (3.3.69),

$$\tilde{\lambda}_1 = \begin{pmatrix} -1 \\ 1 \end{pmatrix}, \quad \tilde{\lambda}_2 = \begin{pmatrix} -z_1 \\ 0 \end{pmatrix}, \quad \tilde{\lambda}_3 = \begin{pmatrix} z_1 \\ z_2 \end{pmatrix}, \quad \tilde{\lambda}_4 = \begin{pmatrix} 0 \\ -z_2 \end{pmatrix}. \tag{3.3.71}$$

As expected for a four-point kinematic, the two momentum twistor variables can be

related to the Mandelstam invariants,

$$s_{12} = z_1 \equiv s, \qquad s_{23} = z_2 \equiv t, \qquad s_{13} = -z_1 - z_2 \equiv u, \qquad (3.3.72)$$

where the last relation tell us that momentum conservation is automatically imposed. For the five-point case we have a more complicated matrix with five variables,

$$Z_5 = \begin{pmatrix} 1 & 0 & \frac{1}{z_1} & \frac{1+z_2}{z_1 z_2} & \frac{1+z_3+z_2 z_3}{z_1 z_2 z_3} \\ 0 & 1 & 1 & 1 & 1 \\ 0 & 0 & 0 & \frac{z_4}{z_2} & 1 \\ 0 & 0 & 1 & 1 & \frac{z_4 - z_5}{z_4} \end{pmatrix} \qquad (3.3.73)$$

which leads to the anti-holomorphic spinors,

$$\tilde{\lambda}_1 = \begin{pmatrix} -\frac{z_4 - z_5}{z_4} \\ 1 \end{pmatrix}, \tilde{\lambda}_2 = \begin{pmatrix} -z_1 \\ 0 \end{pmatrix}, \tilde{\lambda}_3 = \begin{pmatrix} z_1 \\ z_1 z_4 \end{pmatrix}, \qquad (3.3.74)$$

$$\tilde{\lambda}_4 = \begin{pmatrix} \frac{z_1 z_2 z_3 z_5}{z_4} \\ z_1 \left(z_2 z_3 - z_4 z_3 - z_4\right) \end{pmatrix}, \tilde{\lambda}_5 = \begin{pmatrix} -\frac{z_1 z_2 z_3 z_5}{z_4} \\ -z_1 z_3 \left(z_2 - z_4\right) \end{pmatrix}.$$

The cyclic Mandelstam invariants are then related to the momentum twistor variables by

$$s_{12} = z_1,$$

$$s_{23} = z_1 z_4,$$

$$s_{34} = \frac{z_1 \left(-z_2 z_3 + z_4 z_3 + z_2 z_5 z_3 + z_4\right)}{z_2}, \qquad (3.3.75)$$

$$s_{45} = z_1 z_5,$$

$$s_{51} = z_1 z_3 \left(z_2 - z_4 + z_5\right).$$

For a n-point kinematics, a parametrisation can be written as,

$$Z_n = \begin{pmatrix} 1 & 0 & q_1 & q_2 & q_3 & \cdots & q_{n-1} & q_{n-2} \\ 0 & 1 & 1 & 1 & 1 & \cdots & 1 & 1 \\ 0 & 0 & 0 & \frac{z_{n-1}}{z_2} & z_n & \cdots & z_{2n-6} & 1 \\ 0 & 0 & 1 & 1 & z_{2n-5} & \cdots & z_{3n-11} & 1 - \frac{z_{3n-10}}{z_{n-1}} \end{pmatrix}, \tag{3.3.76}$$

where $q_k = \sum_{i=1}^{k} \left(\Pi_{j=1}^{i} z_j \right)^{-1}$, and the z_i can be written in terms of the external momenta as,

$$
\begin{aligned}
z_1 &= s_{12}, \\
z_{n-1} &= \frac{s_{23}}{s_{12}}, \\
z_{3n-10} &= \frac{s_{123}}{s_{12}}, \\
z_i &= -\frac{\langle i(i-1)\rangle\langle (i+2)1\rangle}{\langle 1i\rangle\langle (i+1)i+2\rangle}, \quad i \in \{2, n-2\}, \\
z_i &= -\frac{[2(2+\cdots+i-n+4)i-n+5\rangle}{\langle 1(i-n+5)\rangle[21]}, \quad i \in \{n, 2n-6\}, \\
z_i &= \frac{\langle 1(2+3)(2+\cdots+i-2n+9)(i-2n+10)\rangle}{s_{23}\langle 1(i-2n+10)\rangle}, \quad i \in \{2n-5, 3n-11\}.
\end{aligned}
\tag{3.3.77}
$$

It is important to remark that such representations give a parametrisation of the phase space in terms of rational functions, which turns to be particularly useful to investigate properties of scattering amplitudes such as factorisation and pole structures. Also, one can obtain exact numerical phase space points just by filling the Z matrix with rational numbers.

Furthermore, we notice that the use of this parametrisation cancels the phase information related to parity invariance. However, the phase information can be restored as a prefactor,

$$\mathcal{A}(1,\ldots,n) = \Phi_{\text{phase}}\tilde{\mathcal{A}}(z_1,\ldots,z_{3n-10}), \tag{3.3.78}$$

after the simplification of the rational function $\tilde{\mathcal{A}}$.

Chapter 4

Modern methods for scattering amplitudes

In this chapter we explore some methods for scattering amplitude computations, which allow us to bypass the traditional approach of Feynman diagrams. Among these methods, the ones inspired by unitarity have been studied since the 1960s, when Cutkosky established how discontinuities of loop diagrams can be computed by considering the Optical Theorem [61]. More recently, Witten's interpretation of perturbative gauge theory as a string theory in twistor space [62] inspired the development of new frameworks for the calculation of scattering amplitudes such as on-shell recursion relations and generalised unitarity.

In particular, we discuss the on-shell techniques of BCFW recursion relation [8] for tree-level amplitudes and unitarity-based methods at one-loop [11]. We review integrand reduction [12, 63] as an algebraic reduction algorithm for one-loop amplitudes calculations. We also show how amplitudes in dimensional regularisation can be computed by combining unitarity cuts and integrand reduction within the framework of the six dimensional spinor-helicity formalism.

4.1 BCFW recursion relations

The calculation of tree-level scattering amplitudes is traditionally approached by computing all Feynman diagrams associated to the process. However, the number

of Feynman diagrams grows very fast with the number of external legs and the expressions generated in this way are known not to be the most compact. Therefore, in the last decades, alternatives approaches based on recursion relations have been used extensively in order to perform such calculations more efficiently. The main principle is to re-use calculations for lower multiplicity amplitudes to construct higher multiplicity amplitudes. The most used recursion relation at tree-level are the Berends-Giele [64] and the Britto-Cachazo-Feng-Witten (BCFW) [8, 65] recursion relations.

While Berends-Giele recursion builds amplitudes from lower point off-shell objects, BCFW recursion only uses on-shell gauge-invariant quantities. The idea behind the derivation of the BCFW recursion relation is that tree-level amplitudes can be reconstructed by looking at their residues. We will prove that, in these singular regions, amplitudes factorise into two on-shell amplitudes with lower multiplicity.

The BCFW recursion relation

We begin by considering a tree-level colour ordered amplitude $A(p_1, \ldots, p_n)$ of n gluons. We choose two external legs i and j and introduce a complex variable z. We define the new momenta $\hat{p}_i$ and $\hat{p}_j$ via the following shift,

$$p_i^\mu = \frac{1}{2}\langle i\sigma^\mu i] \quad \rightarrow \quad \hat{p}_i^\mu(z) = p_i^\mu + \frac{z}{2}\langle i\sigma^\mu j] \tag{4.1.1}$$

$$p_j^\mu = \frac{1}{2}\langle j\sigma^\mu j] \quad \rightarrow \quad \hat{p}_j^\mu(z) = p_j^\mu - \frac{z}{2}\langle i\sigma^\mu j] \tag{4.1.2}$$

which for the corresponding two-components Weyl spinors can be written as,

$$|i\rangle \rightarrow |\hat{i}\rangle = |i\rangle + z|j], \qquad |i] = |\hat{i}] \tag{4.1.3}$$

$$|j] \rightarrow |\hat{j}] = |j] - z|i\rangle, \qquad |j\rangle = |\hat{j}\rangle \tag{4.1.4}$$

It easy to check that this shift preserves the on-shell conditions,

$$p_i + p_j = \hat{p}_i + \hat{p}_j, \qquad \hat{p}_i^2 = \hat{p}_j^2 = 0. \tag{4.1.5}$$

Therefore, the amplitude is a complex function of z, $A(z) = A(p_1, \ldots, \hat{p}_i, \ldots, \hat{p}_j, \ldots, n)$, with some poles coming from the propagators. Then we can consider the new function $A(z)/z$, such that its pole in $z = 0$ is related to the physical amplitude $A(0)$. If we assume that $\lim_{z \to +\infty} A(z) = 0$, then

$$\lim_{R \to \infty} \frac{1}{2\pi i} \oint_{C_R} dz \frac{iA(z)}{z} = 0, \tag{4.1.6}$$

where C_R is a contour of very large R. Alternatively Cauchy's theorem states that,

$$\frac{1}{2\pi i} \oint_{C_R} dz \frac{A(z)}{z} = A(0) + \sum_{i=1}^{n} Res_{z=z_i} \frac{A(z)}{z}, \tag{4.1.7}$$

thus the physical amplitude can be written in terms of the residues in z,

$$A(0) = -\sum_{i=1}^{n} Res_{z=z_i} \frac{A(z)}{z}. \tag{4.1.8}$$

The residues at each pole can be computed using the fact that any on-shell tree-level amplitude factorises into a product of lower multiplicity amplitudes. In fact, shifting p_i and p_j as in Eq. (4.1.2), the propagators which separate the legs i and j develop a dependence on z,

$$\hat{P}(z)^2 \equiv \hat{P}_{1l}(z)^2 = \left(p_1^\mu + \cdots + \hat{p}_i^\mu(z) + \cdots + p_l^\mu \right)^2 =$$
$$= \left(p_1^\mu + \cdots + p_i^\mu + \cdots + p_l^\mu + \frac{z}{2} \langle p_i \sigma^\mu p_j] \right)^2 = \tag{4.1.9}$$
$$= \left(P^\mu + \frac{z}{2} \langle p_i \sigma^\mu p_j] \right)^2 = P^2 + z \langle p_i P p_j],$$

where $P^\mu \equiv P_{1l}^\mu = p_1^\mu + \cdots + p_i^\mu + \cdots + p_l^\mu$. As a result, new poles appear in the amplitude $A(z)$. In this case the pole is generated at $\hat{P}(z_0)^2 = 0$, which has solution,

$$z_0 = -\frac{P^2}{\langle p_i P p_j]}. \tag{4.1.10}$$
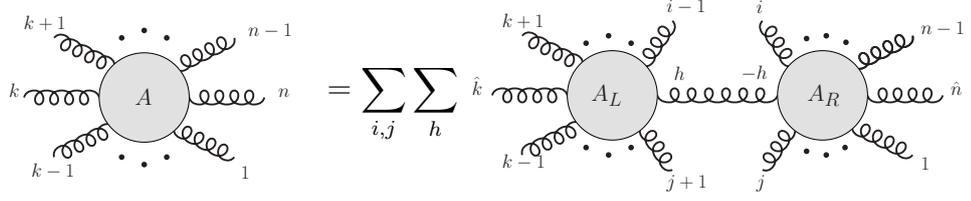
Figure 4.1: Diagrammatic representation of the BCFW recursion relation under the shift $k \to \hat{k}$ and $n \to \hat{n}$. h are the gluon helicity states.

Evaluating the residue of $\frac{A(z)}{z}$ on the right hand-side of Eq. (4.1.8), one gets,

$$
\begin{aligned}
\mathrm{Res}_{z=z_0} \frac{A(z)}{z} &= \lim_{z \to z_0} (z - z_0) \frac{A(z)}{z} = \\
&= \lim_{z \to z_0} \frac{P^2 + z \langle p_i P p_j]}{\langle p_i P p_j]} \frac{1}{z} A^*_{l,\mu}(z) \frac{-i \Sigma_{r,s} \epsilon^\mu_r(z) \epsilon^\nu_s(z)}{P^2 + z \langle p_i P p_j]} A^*_{n-l,\nu}(z) \\
&= \sum_{h=\pm} A^h_l(z_0) \frac{-i}{P^2} A^{-h}_{n-l}(z_0),
\end{aligned}
\tag{4.1.11}
$$

where we have used the completeness relation for the gluon propagator and A^* is an off-shell current. The residue in Eq. (4.1.11) is the product of two simpler tree-level amplitudes $A_l(z)$ and $A_{n-l}(z)$, analytically continued in the complex plane. Finally considering all the residues of Eq. (4.1.8) we find the amplitude can be written as,

$$
\begin{aligned}
A(p_1, \cdots, p_n) = \sum_{r \in \mathrm{partitions}} \sum_{h=\pm} &A_L(p_{a_r}, \ldots, \hat{p}_i, \ldots, p_{b_r}, -\hat{P}^h_{a_r b_r}(z_r)) \frac{-i}{P^2_{a_r b_r}} \\
&A_R(\hat{P}^{-h}_{a_r b_r}(z_r), p_{b_r+1}, \ldots, \hat{p}_j, \ldots, p_{a_r-1})
\end{aligned}
\tag{4.1.12}
$$

where A_L and A_R are lower-point amplitudes which are defined by all the partitions r separating the particles i and j and are evaluated on the corresponding pole z_r. This is the BCFW recursion formula, diagrammatically represented in Fig. 4.1.

The BCFW recursion is remarkable for several reasons. It only involves on-shell amplitudes with a lower number of external legs. One can thus start from 3-point amplitudes, which can be easily worked out from 3-point vertexes, and from these build all higher point amplitudes. In particular, in theories like QCD, the presence of

4- or higher-point vertexes is irrelevant and all the information is already contained in the 3-point interactions [1].

Now we discuss a prescription that one must consider in order to satisfy the behaviour $A(z) \to 0$ when $z \to \infty$. To ensure this behaviour we have to shift gluons with different helicities. In fact, considering the shift Eq. (4.1.3) and Eq. (3.2.27) for the gluon i and j having positive and negative helicity respectively, we obtain the following polarisation vectors,

$$\epsilon^{\mu}_{+}(i(z), a) = \frac{1}{\sqrt{2}(\langle aq \rangle + z\langle ak \rangle)} \langle q\sigma^{\mu} a], \tag{4.1.13}$$

$$\epsilon^{\mu}_{-}(j(z), b) = \frac{1}{\sqrt{2}([bq] - z[bk])} \langle k\sigma^{\mu} b], \tag{4.1.14}$$

that give a contribution of order $\mathcal{O}(z^{-2})$ as $z \to \infty$. In addition, the vertices are of order $\mathcal{O}(z)$ and the propagator of order $\mathcal{O}(z^{-1})$. As a result, the overall amplitude $A(z)/z$ goes to zero faster than $1/z$ at infinity in the complex plane. More systematic studies of this property of scattering amplitudes in the complex plane are given in [66].

One can easily extend the BCFW recursion relation to amplitudes with quarks, though there is an additional requirement that two external quarks i and j cannot be chosen if they are on the same fermion line to satisfy the boundary condition at inifinty.

To show how BCFW works we compute explicitly a 4-gluon amplitude $A(1^-, 2^-, 3^+, 4^+)$. We choose to shift the legs 2 and 3,

$$p^{\mu}_2(z) = p^{\mu}_2 - \frac{z}{2}[3\sigma^{\mu}2\rangle, \qquad p^{\mu}_3(z) = p^{\mu}_3 + \frac{z}{2}[3\sigma^{\mu}2\rangle, \tag{4.1.15}$$

---

[1]Note that 3-point on-shell amplitudes are defined for complex kinematics only, which was a crucial point for the development of this technique [8, 62].

and, using Eq. (4.1.12), we obtain,

$$A(0) = A(1^-, 2^-, -P^+(z_0))\frac{-i}{P^2}A(P^-(z_0), 3^+(z), 4^+) +$$
$$+ A(1^-, 2^-, -P^-(z_0))\frac{-i}{P^2}A(P^+(z_0), 3^+(z), 4^+). \tag{4.1.16}$$

where $P = p_1 + p_2$ is the momentum flowing through the shifted propagator. The pole z_0 is found by solving $P^2(z_0) = 0$,

$$P^2(z_0) = P^2 + z_0[3P2\rangle = 0, \tag{4.1.17}$$

$$z_0 = -\frac{P^2}{[3P2\rangle} = -\frac{\langle 21\rangle[12]}{[3(1+2)2\rangle} = -\frac{[21]}{[31]}. \tag{4.1.18}$$

Now we plug in the expressions for the three-point amplitudes,

$$A(1^-, 2^-, 3^+) = ig\frac{\langle 12\rangle^4}{\langle 12\rangle\langle 23\rangle\langle 31\rangle}, \quad A(1^+, 2^+, 3^-) = -ig\frac{[12]^4}{[12][23][31]}, \tag{4.1.19}$$

$$A(1^+, 2^+, 3^+) = A(1^-, 2^-, 3^-) = 0, \tag{4.1.20}$$

getting the following expression for $A(0)$,

$$A(0) = -ig^2\frac{\langle 12(z_0)\rangle^4}{\langle 12(z_0)\rangle\langle 2(z_0)P(z_0)\rangle\langle P(z_0)1\rangle}\frac{1}{[34]\langle 43\rangle}\frac{[3(z_0)4]^4}{[3(z_0)4][4P(z_0)][P(z_0)3(z_0)]} \tag{4.1.21}$$

which can be simplified to,

$$A(0) = -ig^2\frac{\langle 12\rangle^3}{\langle 2P(z_0)\rangle\langle P(z_0)1\rangle}\frac{1}{\langle 43\rangle}\frac{[3(z_0)4]^2}{[34][4P(z_0)][P(z_0)3]}. \tag{4.1.22}$$

Therefore, performing the spinor algebra for terms involving $P(z_0)$,

$$\langle 2P(z_0)\rangle[P(z_0)4] = \langle 2(3+4)4] + \frac{1}{2}\left(-\frac{[21]}{[31]}\right)\langle 2\sigma^\mu 4][3\sigma_\mu 2\rangle = \langle 23\rangle[34]$$
$$\langle 1P(z_0)\rangle[P(z_0)3] = \langle 14\rangle[43], \tag{4.1.23}$$

we finally find the known compact expression for the 4-gluon amplitude [67],

$$A(0) = ig^2 \frac{\langle 12 \rangle^4}{\langle 12 \rangle \langle 23 \rangle \langle 34 \rangle \langle 41 \rangle}. \qquad (4.1.24)$$

BCFW in six dimensions

The BCFW recursion relation can be generalised for a theory with arbitrary space-time dimensions. In this section we will give some details about the formulation of BCFW in six dimensions, which has been explicitly introduced in [29, 68].

We start shifting two momenta p_i and p_j by a vector proportional to a parameter z, satisfying the same conditions as described in the previous case. Such a vector can be picked to be the polarisation vector of the momentum i with reference vector j as introduced in Eq. (3.2.38), which can be considered as the six dimensional analogue of the vector $\langle i\sigma^\mu j]$,

$$\langle i\sigma^\mu j] \;\rightarrow\; \epsilon^\mu_{i\alpha\dot\beta} = -\frac{\langle p_\alpha \Sigma^\mu q^\sigma \rangle \langle q_\sigma | p_{\dot\beta}]}{2\sqrt{2} p \cdot q}. \qquad (4.1.25)$$

We can deal with the SU(2) little group indices $\alpha, \dot\beta$ by introducing a matrix $X^{\alpha\dot\beta}$ in the definition of the shifted momenta,

$$p_i^\mu \rightarrow \hat p_i^\mu = p_i^\mu + z X^{\alpha\dot\beta} \epsilon^\mu_{i\alpha\dot\beta} \qquad (4.1.26)$$

$$p_j^\mu \rightarrow \hat p_j^\mu = p_j^\mu - z X^{\alpha\dot\beta} \epsilon^\mu_{i\alpha\dot\beta}. \qquad (4.1.27)$$

The massless condition for $\hat p_i$ and $\hat p_j$ requires that the determinant of X must vanish, namely $\det X = 0$, which leads to the following decomposition for X,

$$X^{\alpha\dot\beta} = x^\alpha \tilde x^{\dot\beta}, \qquad (4.1.28)$$

and thus one can define the two spinors,

$$y^\alpha = \tilde x^{\dot\beta} \langle j_\alpha | i^{\dot\beta}]^{-1}, \qquad \tilde y^{\dot\beta} = x^\alpha \langle i^\alpha | i_{\dot\beta}]^{-1}. \qquad (4.1.29)$$

Finally one can implement the shifts for the spinors of $\hat{p}_i$ and $\hat{p}_j$ by using these objects,

$$|\hat{i}_\alpha\rangle = |\hat{i}_\alpha\rangle + zx_\alpha|y\rangle \tag{4.1.30}$$

$$|\hat{j}_\alpha\rangle = |\hat{j}_\alpha\rangle + zy_\alpha|x\rangle \tag{4.1.31}$$

$$|\hat{i}_{\dot{\alpha}}] = |\hat{i}_{\dot{\alpha}}] - z\tilde{x}_{\dot{\alpha}}|\tilde{y}] \tag{4.1.32}$$

$$|\hat{j}_{\dot{\alpha}}] = |\hat{j}_{\dot{\alpha}}] - z\tilde{y}_{\dot{\alpha}}|\tilde{x}] \tag{4.1.33}$$

where $|x\rangle \equiv x^\alpha|x_\alpha\rangle$ and $|\tilde{x}] \equiv x^{\dot{\alpha}}|x_{\dot{\alpha}}]$. Then the BCFW recursion relation for an all-gluon amplitude reads as

$$x^\alpha \tilde{x}^{\dot{\alpha}} A_{\alpha\dot{\alpha}\beta\dot{\beta}...} = \sum_{r\in\text{partitions}} \sum_{\sigma\dot{\sigma}} x^\alpha \tilde{x}^{\dot{\alpha}} A_L(p_{a_r}, \ldots, \hat{p}_i, \ldots, p_{b_r}, -\hat{P}_{a_r b_r}(z_r))_{\alpha\dot{\alpha}\sigma\dot{\sigma}} \tag{4.1.34}$$

$$\frac{-i}{P^2} A_R(\hat{P}_{a_r b_r}(z_r), p_{b_r+1}, \ldots, \hat{p}_j, \ldots, p_{a_r-1})_{\beta\dot{\beta}}^{\sigma\dot{\sigma}}$$

where P are the momentum and $\sigma, \dot{\sigma}$ the polarisation states of the intermediate particles. Clearly this formula is valid for fermion field as well, considering the appropriate modification for the helicities of the intermediate states. We notice that such a formulation of BCFW maintains the little group covariance since the direction of the deformation is not specified, which allows us to obtain an expression valid for all the helicity configurations.

4.2 Unitarity methods

Unitarity-based methods for loop calculations were suggested first in 1960s, when by means of the Cutkosky rules [61], a relation between the imaginary part of a loop amplitude and direct products of on-shell tree-level amplitudes was established. In 1990s [10] it was argued that, for gauge theories, these methods lead to higher computational efficiency than traditional techniques. These methods are based on the key operation of cutting a diagram, where a cut is defined as 'replacing loop propagators with the corresponding δ-functions'. In this way, we cut the diagrams

into two tree-level diagrams, while the loop integral is replaced by an integral over the phase space of the particles crossing the cut. This is much easier than a complete one-loop diagrammatic expansion, due the simplifications arising from working with physical degrees of freedom only. Unitarity cuts can be generalised [11] in the sense of putting a different number of propagators on-shell simultaneously, allowing us to select different kinds of singularities of the amplitude with a more efficient approach than ordinary cuts.

4.2.1 Optical Theorem

We have already introduced the scattering matrix $\mathcal{S}$ in Section 2.3, as the operator which transforms incoming into outgoing states, and the transition matrix $\mathcal{T}$, where the interacting part of the $\mathcal{S}$-matrix is contained. From the unitarity of the $\mathcal{S}$-matrix, $\mathcal{S}^\dagger \mathcal{S} = 1$, we obtain the well known Optical Theorem,

$$-i(\mathcal{T} - \mathcal{T}^\dagger) = \mathcal{T}^\dagger \mathcal{T}. \tag{4.2.35}$$

In perturbation theory, $\mathcal{T}$ can be computed as a sum of Feynman diagrams. The product $\mathcal{T}^\dagger \mathcal{T}$ implies a sum of contributions from all possible intermediate states f. In terms of matrix elements $\mathcal{A}$ for the general process $a \to b$ we have [33],

$$2\Im\mathcal{A}(a \to b) = \sum_f \int d\Pi_f \mathcal{A}^*(b \to \{q_i\}))\mathcal{A}(\{q_i\} \to a)(2\pi)^4\delta^{(4)}(a - \sum_{i=1}^f q_i) \tag{4.2.36}$$

where $\Im$ is the imaginary part and in addition to summing over all possible sets $\{q_i\}$ containing f intermediate particle states, we are also integrating over the complete phase space of these states, as described by the measure,

$$d\Pi_f \equiv \prod_{i=1}^f \int \frac{d^3 q_i}{(2\pi)^3} \frac{1}{2E_i}, \tag{4.2.37}$$

Figure 4.2: Diagrammatic representation of the Optical Theorem. The imaginary part of a scattering amplitude with initial states a and final states b arises from a sum of contributions from all possible set of intermediate states f.

To obtain this result we use the completeness relation for the intermediate states,

$$\int d\Pi_f |\{q_i\}\rangle\langle\{q_i\}| = 1. \tag{4.2.38}$$

In practice, we see that, in perturbation theory, the unitarity of the scattering matrix $\mathcal{S}$ allows us to relate the imaginary part of the one-loop amplitude to a sum a product of two tree-level amplitudes.

A pictorial representation of the Optical Theorem is shown in Figure 4.2.

4.2.2 Cutkosky rules

The imaginary part discussed in Eq. (4.2.36) is also related to discontinuities of scattering amplitudes. In fact, one can prove that the appearance of an imaginary part of the amplitude always requires a branch cut singularity. Such consideration establishes that a discontinuity across the branch cut for the kinematic invariant s is

$$\text{Disc}\mathcal{A}(s) = \lim_{\epsilon \to 0} \left(\mathcal{A}(s + i\epsilon) - \mathcal{A}(s - i\epsilon)\right). \tag{4.2.39}$$

The Cutkosky rules [61] allow us to compute the physical discontinuity of a specified diagram by defining an operation which we will refer to as a unitarity cut,

$$\frac{i}{k^2 - m^2 + i\epsilon} \to -2\pi i \delta^{(+)}(k^2 - m^2), \tag{4.2.40}$$

which puts a propagator on-shell[2]. Therefore, one has to consider the simultaneous cuts of the two propagators (called double cut) identified by all the different channels and then, after integration, the discontinuity of the diagram is given by the sum of all these cuts. Moreover, we can apply the Cutkosky rules at the amplitude level rather than diagram level [10], which has the advantage of involving gauge invariant tree-level building-blocks. For example, in the case of a one-loop amplitude $\mathcal{A}^{(1)}$, the Cutkosky rules give the following expression for a discontinuity in a channel $s_{i,j} = p_{i,j}^2 = (p_i + \cdots + p_j)^2$,

$$\text{Disc}\mathcal{A}^{(1)}|_{s_{i,j}} = \sum_{\text{hel}} \int \frac{d^d k}{(2\pi)^d} \mathcal{A}^{(0)}(k, p_i, \ldots, p_j, -k - p_{i,j}) \mathcal{A}^{(0)}(k + p_{i,j}, p_{j+1}, \ldots, p_{i-1}, -k) \times$$
$$2\pi i \delta^{(+)}(k^2 - m_1^2) 2\pi i \delta^{(+)}((k + p_{i,j})^2 - m_2^2), \qquad (4.2.41)$$

where the sum runs over all the internal helicity states. The key idea for the application of this method is that, after integral reduction (e.g. Passarino-Veltman reduction), a one-loop amplitude in dimensional regularisation can be written in the general form [10, 69] [3],

$$\mathcal{A}^{(1)} = \sum_{i \in \text{topologies}} c_i I_i^{4-2\epsilon}(\epsilon) + \mathcal{R} + \mathcal{O}(\epsilon) \qquad (4.2.42)$$

where I_i are scalar Feynman integrals, c_i are rational coefficients in the kinematic variables, the index i runs over all the possible topologies related to the corresponding process and $\mathcal{R}$ is a rational function of the spinor variables. Since the discontinuities are generated by the integrals, one can use the Cutkosky rules to project out the coefficients c_i by considering the set of all double cuts,

$$\text{Disc}\mathcal{A}^{(1)} = \sum_{i \in t} c_i \text{Disc} I_i^{4-2\epsilon}(\epsilon). \qquad (4.2.43)$$

---

[2]The superscript $(+)$ on the delta functions denotes the choice of a positive-energy solution

[3]Such representation comes from the expansion in ϵ of the general form $\mathcal{A}^{(L)} = \sum_{i \in t} c_i(\epsilon) I_i^{4-2\epsilon}(\epsilon)$

Therefore, the unitarity cuts allow us to compute such coefficients by solving the system of equations given by the double cuts in all the possible channels.

It is important to remark that, with this approach, the calculation of the rational term requires dedicated techniques such as the extension of the cut in arbitrary d dimensions (we will discuss this aspect in the next sections).

4.2.3   Generalised Unitarity

The success obtained by the definition of the scattering amplitudes for complex kinematics [62], led to the idea of generalising the unitarity method beyond the double cut [11] appearing in Eq. (4.2.41).

In fact, one can generalise the procedure by putting a different number of propagators on-shell simultaneously, which allows us to distinguish different kind of singularities. Using this method, the coefficients can be obtained by solving a triangular system, where one can employ a top-down approach starting from topologies with the most propagators.

When a multiple number of propagators is put on-shell, namely a multiple cut is performed, the amplitude factorises in a product of the tree-level amplitudes identified by the cut. A generalisation of the Eq. (4.2.41), for a n-particle one-loop amplitude, can be written as

$$
\mathcal{A}^{(1)}\big|_{\{i_1\ldots i_m\}\text{-cut}} = \sum_{\text{hel}} \int \frac{d^d k}{(2\pi)^d} \tag{4.2.44}
$$
$$
\prod_{j=1}^{m} \mathcal{A}^{(0)}\left(k_{i_j-1}, p_{i_j}, \ldots, p_{i_{j+1}-1}, -k_{i_{j+1}-1}\right) (-2\pi i)\delta(k_{i_j-1}^2 - m_{i_j-1}^2),
$$

where $k_i \equiv k + \sum_{l=1}^{i} p_l$, $k_0 \equiv k$ and $\sum_{l=1}^{i} p_l = 0$. Depending on the cut, multiple on-shell conditions appear in the relation above and, in general, they have complex solutions. This is one of the main differences between the generalised unitarity cuts and the Cutkosky rules, since they have different domains of solutions. Indeed in the case of generalised unitarity, the cut is properly defined as a deformation of the contour integral from the real axis to a circle around the pole of the cut propagator rather than an insertion of the delta function; then the residue theorem allows us

to extract the discontinuities.

For one-loop amplitudes in dimensional regularisation with four dimensional external states, the discontinuities are identified through all the possible single-, double-, triple-, quadruple- and quintuple-cuts, which correspond to putting up to five propagators on-shell respectively. Several techniques have enabled the extraction of the coefficients of the integral basis by performing all these cuts. Generalised unitarity was firstly used in a four dimensional framework in order to compute the coefficients appearing in Eq. (4.2.42), where the cuts were performed considering the loop momentum living in four dimensions and the rational term was obtained with different techniques [70]. Afterwords, this approach has been extended to generalised d-dimensional unitarity [31, 71, 72], which delivers complete one-loop scattering amplitudes in renormalizable quantum field theories within an unique framework. These developments also rely on the combination of generalised unitarity cuts with the integrand reduction of Ossola-Papadopoulos-Pittau (OPP) [12], which allows us to systematically extract each term in the integral basis by using a recursive, algebraic, algorithm. This method will be discussed in detail in the next section.

4.3   Integrand reduction

As discussed in Section 4.2.3, one-loop amplitudes can be expressed as a linear combination of a finite unique set of scalar integrals, which are typically called Master Integrals. Since these integrals are known (see e.g. [73]), the calculation of one-loop amplitudes reduces to the calculation of the coefficients of each scalar integral. The integrand reduction method allows us to rewrite scattering amplitudes as linear combinations of scalar integrals by using the knowledge of the analytic and algebraic structure of loop integrands. Integrand reduction was originally proposed in a four dimensional framework by Ossola, Papadopoulos and Pittau (OPP) [12, 63] for one-loop amplitudes. While traditional unitarity based methods rely on a prior knowledge of the integral basis, integrand reduction does not and can therefore be extended to multi-loop amplitudes in a straightforward way [74, 75, 76, 77].

The integrand reduction method is based on the key observation that the integrand of a loop amplitude is a polynomial numerator in the components of the loop momenta sitting over a set of quadratic loop denominators corresponding to internal propagators. We start the exploration of the integrand reduction method by considering a general (colour ordered) one-loop amplitude $A_n^{(1)}$ with n external legs. In dimensional regularisation the amplitude can be written as

$$A_n^{(1)} = \mu_R^{2\epsilon} \int \frac{d^d k}{(2\pi)^d} \mathcal{I}_n, \qquad \mathcal{I}_n = \frac{\mathcal{N}(k)}{\prod_i D_i} \qquad (4.3.45)$$

The numerator $\mathcal{N}$ and the denominators D_i of the integrand $\mathcal{I}$ are polynomials in the components of the loop momentum k. The d-dimensional loop momentum can be decomposed [78] in the four dimensional component $\bar{k}$ and in the (-2ϵ)-component $\tilde{k}$, which belong to orthogonal subspaces,

$$k^\mu = \bar{k}^{[4]} + \tilde{k}^{[-2\epsilon]}, \qquad k^2 = \bar{k}^2 + \tilde{k}^2 = \bar{k}^2 - \mu^2, \qquad \bar{k} \cdot \tilde{k} = 0, \quad (4.3.46)$$

where $\tilde{k}^2 = -\mu^2$ is the scalar product of the extra dimensional component. The loop denominators are quadratic polynomials in the loop momentum and their general form is

$$D_i = (k + p_i)^2 - m_i^2 = (\bar{k} + p_i)^2 - m_i^2 - \mu^2 \qquad (4.3.47)$$

where p_i is a linear combination of external momenta and m_i are the masses of the particles running in the loop. One can then rewrite some of the scalar products appearing in the numerator as a linear combination of the denominators. These are called reducible scalar products (RSP). The remaining ones are called instead irreducible scalar products (ISP) and allow us to parametrise the numerator. As a result, the numerator of the integrand can be partial fractioned with respect to the denominators [4].

---

[4]Such operations can be done systematically using algebraic geometry and in particular multivariate polynomial division [76, 79]. This tool turns out to be fundamental in the multi-loop case.

Therefore, the integrand can be written in the usual integrand basis of irreducible scalar products including extra dimensional terms following the OPP [12]/EGKM [71, 72] constructions,

$$
\mathcal{I}_n = \sum_{1 \leq i_1 < i_2 < i_3 < i_4 < i_5 \leq n} \frac{\Delta_{\{i_1,i_2,i_3,i_4,i_5\}}}{D_{i_1} D_{i_2} D_{i_3} D_{i_4} D_{i_5}} + \sum_{1 \leq i_1 < i_2 < i_3 < i_4 \leq n} \frac{\Delta_{\{i_1,i_2,i_3,i_4\}}}{D_{i_1} D_{i_2} D_{i_3} D_{i_4}}
$$
$$
+ \sum_{1 \leq i_1 < i_2 < i_3 \leq n} \frac{\Delta_{\{i_1,i_2,i_3\}}}{D_{i_1} D_{i_2} D_{i_3}} + \sum_{1 \leq i_1 < i_2 \leq n} \frac{\Delta_{\{i_1,i_2\}}}{D_{i_1} D_{i_2}} + \sum_{1 \leq i_1 \leq n} \frac{\Delta_{\{i_1\}}}{D_{i_1}}, \qquad (4.3.48)
$$

where δ are polynomials of irreducible scalar products. For renormalizable gauge theories it's known that every one-loop integrand in dimensional regularisation can be decomposed as sum of integrands having five or less loop denominators.

4.3.1   Parametrising the box integrand in 4-dimensions

Before introducing the explicit representation for a complete one-loop amplitude in dimensional regularisation, we show a pedagogical example about the parametrisation of the box integrand in 4-dimensions. We begin by considering a box integrand defined as,

$$
\mathcal{I}_4 = \frac{\Delta_4}{\prod_{i=1}^4 D_i} \qquad (4.3.49)
$$

$$
D_1 = k^2, \qquad D_2 = (k - p_1)^2, \qquad D_3 = (k - p_1 - p_2)^2, \qquad D_4 = (k + p_4)^2,
$$
$$
(4.3.50)
$$

where all the external momenta are massless $p_i^2 = 0$. Since Δ_4 is a scalar quantity, it is a function of k via scalar products with itself or with the momenta $\{p_1, p_2, p_4, w\}$. The momentum w is required in order to parametrise the four dimensional space, since only three of the external momenta are independent. Therefore, the general

---

The mathematical description and the implementation of the multivariate polynomial division will be not discussed in this thesis and we will assume their results.

parametrisation of Δ_4 is,

$$\Delta_4 = \sum_{\{i,j,l,m,n\}} c_{\{i,j,l,m,n\}} (k^2)^i (k \cdot p_1)^j (k \cdot p_2)^l (k \cdot p_4)^m (k \cdot w)^n \qquad (4.3.51)$$

where $\{i, j, l, m, n\}$ is a set of numbers bigger or equal than zero. However, the first four terms in the previous expression can be written as function of propagators and thus are reducible,

$$k^2 = D_1, \quad k \cdot p_1 = \frac{1}{2}(D_1 - D_2), \quad k \cdot p_2 = \frac{1}{2}(D_3 - D_2 - s_{12}), \quad k \cdot p_4 = \frac{1}{2}(D_4 - D_1)$$
$$(4.3.52)$$

As a result, the numerator can be parametrised as

$$\Delta_4 = \sum_i c_i (k \cdot w)^i. \qquad (4.3.53)$$

For renormalisable theories, it is known that the power of k in the numerator cannot be bigger than the power in the denominator and then $i \leq 4$. Now, using the specific expression (see Appendix D),

$$w^\mu = \frac{\langle 231]}{s_{12}} \frac{\langle 1\sigma^\mu 2]}{2} - \frac{\langle 132]}{s_{12}} \frac{\langle 2\sigma^\mu 1]}{2}, \qquad (4.3.54)$$

one can easily prove that $(k \cdot w)^2$ is reducible and thus the upper limit for the exponent in Eq. (4.3.53) is one. Finally we can write the parametrisation of the box numerator in four dimensions as,

$$\Delta_4 = c_0 + c_i (k \cdot w). \qquad (4.3.55)$$

In a similar way one can derive the parametrisation for the other topologies and generalise it in dimensional regularisation.

4.3.2 The complete one-loop integrand

The complete parametrisation of the numerators in dimensional regularisation can be written as,

$$\Delta_{\{i_1,i_2,i_3,i_4,i_5\}} = c^{(0)}_{i_1,i_2,i_3,i_4,i_5}\,\mu^2, \tag{4.3.56a}$$

$$\Delta_{\{i_1,i_2,i_3,i_4\}} = c^{(0)}_{i_1,i_2,i_3,i_4} + c^{(1)}_{i_1,i_2,i_3,i_4}\,(k\cdot w_{1;i_1,i_2,i_3}) + c^{(2)}_{i_1,i_2,i_3,i_4}\,\mu^2$$
$$+ c^{(3)}_{i_1,i_2,i_3,i_4}\,\mu^2(k\cdot w_{1;i_1,i_2,i_3}) + c^{(4)}_{i_1,i_2,i_3,i_4}\,\mu^4, \tag{4.3.56b}$$

$$\Delta_{\{i_1,i_2,i_3\}} = c^{(0)}_{i_1,i_2,i_3} + c^{(1)}_{i_1,i_2,i_3}\,(k\cdot w_{1;i_1,i_2}) + c^{(2)}_{i_1,i_2,i_3}\,(k\cdot w_{2;i_1,i_2})$$
$$+ c^{(3)}_{i_1,i_2,i_3}\,(k\cdot w_{1;i_1,i_2})(k\cdot w_{2;i_1,i_2}) + c^{(4)}_{i_1,i_2,i_3}\,\big((k\cdot w_{1;i_1,i_2})^2 - (k\cdot w_{2;i_1,i_2})^2\big)$$
$$+ c^{(5)}_{i_1,i_2,i_3}\,(k\cdot w_{1;i_1,i_2})^2(k\cdot w_{2;i_1,i_2}) + c^{(6)}_{i_1,i_2,i_3}\,(k\cdot w_{1;i_1,i_2})(k\cdot w_{2;i_1,i_2})^2$$
$$+ c^{(7)}_{i_1,i_2,i_3}\,\mu^2(k\cdot w_{1;i_1,i_2}) + c^{(8)}_{i_1,i_2,i_3}\,\mu^2(k\cdot w_{2;i_1,i_2}) + c^{(9)}_{i_1,i_2,i_3}\,\mu^2, \tag{4.3.56c}$$

$$\Delta_{\{i_1,i_2\}} = c^{(0)}_{i_1,i_2} + c^{(1)}_{i_1,i_2}\,(k\cdot w_{1;i_1}) + c^{(2)}_{i_1,i_2}\,(k\cdot w_{2;i_1}) + c^{(3)}_{i_1,i_2}\,(k\cdot w_{3;i_1})$$
$$+ c^{(4)}_{i_1,i_2}\,(k\cdot w_{1;i_1})(k\cdot w_{2;i_1}) + c^{(5)}_{i_1,i_2}\,(k\cdot w_{1;i_1})(k\cdot w_{3;i_1})$$
$$+ c^{(6)}_{i_1,i_2}\,(k\cdot w_{2;i_1})(k\cdot w_{3;i_1}) + c^{(7)}_{i_1,i_2}\,\big((k\cdot w_{1;i_1})^2 - (k\cdot w_{3;i_1})^2\big)$$
$$+ c^{(8)}_{i_1,i_2}\,\big((k\cdot w_{2;i_1})^2 - (k\cdot w_{3;i_1})^2\big) + c^{(9)}_{i_1,i_2}\,\mu^2 \tag{4.3.56d}$$

$$\Delta_{\{i_1\}} = c^{(0)}_{i_1} + c^{(1)}_{i_1}\,(k\cdot w_1) + c^{(2)}_{i_1}\,(k\cdot w_2) + c^{(3)}_{i_1}\,(k\cdot w_3) + c^{(4)}_{i_1}\,(k\cdot w_4) \tag{4.3.56e}$$

The irreducible numerators $k\cdot w_{x;i_1,\dots,i_s}$ can be constructed using the spurious directions of van Neerven and Vermaseren [80] and vanish after integration. The spurious directions $w_{x;i_1,\dots,i_p}$ are orthogonal to the p dimensional physical space spanned by the momenta entering vertices $i_1,\dots,i_s$ where $x = 1,\dots,s$ with $s + p = 4$. More details about the spurious vectors are given in Appendix D. The extra dimensional scalar product μ^2 gives rise to dimension shifted integrals which in turn lead to rational terms in $d = 4 - 2\epsilon$ dimensions. The coefficients c_i are rational functions of the external kinematics. We call the set of monomials appearing in the parametrisation ISP monomials. After the cancellation of the vanishing integrals over the spurious

directions, the d-dimensional representation of the amplitude is,

$$
\begin{aligned}
A_n^{(1)} =& \sum_{1 \leq i_1 < i_2 < i_3 < i_4 < i_5 \leq n} c_{i_1,i_2,i_3,i_4,i_5}^{(0)} \, I_{i_1,i_2,i_3,i_4,i_5}^d[\mu^2] \\
&+ \sum_{1 \leq i_1 < i_2 < i_3 < i_4 \leq n} c_{i_1,i_2,i_3,i_4}^{(0)} \, I_{i_1,i_2,i_3,i_4}^d[1] + c_{i_1,i_2,i_3,i_4}^{(2)} \, I_{i_1,i_2,i_3,i_4}^d[\mu^2] + c_{i_1,i_2,i_3,i_4}^{(4)} \, I_{i_1,i_2,i_3,i_4}^d[\mu^4] \\
&+ \sum_{1 \leq i_1 < i_2 < i_3 \leq n} c_{i_1,i_2,i_3}^{(0)} \, I_{i_1,i_2,i_3}^d[1] + c_{i_1,i_2,i_3}^{(9)} \, I_{i_1,i_2,i_3}^d[\mu^2] \\
&+ \sum_{1 \leq i_1 < i_2 \leq n} c_{i_1,i_2}^{(0)} \, I_{i_1,i_2}^d[1] + c_{i_1,i_2}^{(9)} \, I_{i_1,i_2}^d[\mu^2] \\
&+ \sum_{1 \leq i_1 \leq n} c_{i_1}^{(0)} \, I_{i_1}^d[1],
\end{aligned} \tag{4.3.57}
$$

where

$$
I_{i_1,i_2,\ldots,i_n}^d[N] = \mu_R^{2\epsilon} \int \frac{d^d k}{(2\pi)^d} \frac{N}{D_{i_1} D_{i_2} \cdots D_{i_n}}. \tag{4.3.58}
$$

Explicitly the dimension shifting relations are [5],

$$
I_{i_1,i_2,\ldots,i_n}^d[\mu^2] = \frac{d-4}{2}(4\pi) I_{i_1,i_2,\ldots,i_n}^{d+2}[1], \tag{4.3.59}
$$

$$
I_{i_1,i_2,\ldots,i_n}^d[\mu^4] = \frac{(d-4)(d-2)}{4}(4\pi)^2 I_{i_1,i_2,\ldots,i_n}^{d+4}[1]. \tag{4.3.60}
$$

In this framework, the reduction of scattering amplitudes into a basis of scalar integrals has been reduced to the problem of performing the integrand decomposition. The coefficients of the integrals can obtained by a polynomial fit of the residues of the decomposition. The traditional way of performing this fit is by evaluating the integrand on multiple cuts, such that some loop denominators vanish.

4.3.3 An integrand reduction algorithm

The idea of extracting the coefficients of the master integrals by performing multiple cuts on the integrand in a four dimensional framework was firstly proposed in [12]

---

[5]A simple derivation of this fact is shown in Appendix A.2 of reference [78]

(OPP). In this section we describe a more general algorithm [71, 72], which allows us to combine the integrand reduction within the d-dimensional generalised unitarity in order to extract the full set of coefficients of a dimensional regularised amplitude.

First of all, using the integrand decomposition in Eq. (4.3.48), we can rewrite the numerator of the amplitude as,

$$\mathcal{N} = \sum_{k=1}^{5} \sum_{1 \leq i_1 < \cdots < i_k \leq n} \Delta_{\{i_1 \ldots i_k\}} \prod_{i \notin \{i_1 \ldots i_k\}} D_i. \tag{4.3.61}$$

By evaluating the numerator on a m-ple cut $D_{i_1} = \cdots = D_{i_m} = 0$, we obtain,

$$\Delta_{\{i_1 \ldots i_m\}}\Big|_{m\text{-cut}} = \left(\frac{\mathcal{N}}{\prod_{i \notin \{i_1 \ldots i_m\}} D_i} - \sum_{k=m+1}^{5} \sum_{1 \leq i_1 < \cdots < i_k \leq n} \frac{\Delta_{\{i_1 \ldots i_k\}}}{\prod_{i \in \{i_1 \ldots i_k\}/\{i_1 \ldots i_m\}} D_i} \right)\Bigg|_{m\text{-cut}}, \tag{4.3.62}$$

where the second sum on the r.h.s. runs over all the partitions of sets of denominators which contain $\{i_1 \ldots i_m\}$.

A top-down approach is taken for the determination of the coefficients of all the residues. One starts from the maximum cuts, which contains only one term, because all the subtraction terms of Eq. (4.3.62) vanish on the cut. In the most general case the numerator is firstly evaluated on the all possible quintuple-cuts, which give the following relation for the residues,

$$\Delta_{\{i_1 \ldots i_5\}}\Big|_{5\text{-cut}} = \left(\frac{\mathcal{N}}{\prod_{i \notin \{i_1 \ldots i_5\}} D_i} \right)\Bigg|_{5\text{-cut}}. \tag{4.3.63}$$

The residues can be parametrised using the parametrisation given in Eq. (4.3.56) in order to fit the coefficients identified by the maximum cuts. The next step consists in the calculation of the residues corresponding to the next-to-maximum cuts, namely all the cuts given by putting on-shell one propagator less than the maximum cut. In this case, by applying Eq. (4.3.56), we need to subtract the non-vanishing terms computed in the previous step and evaluate them on the solutions of this cut. Again, the parametrisation of the residues is used to fit the coefficients. Therefore,
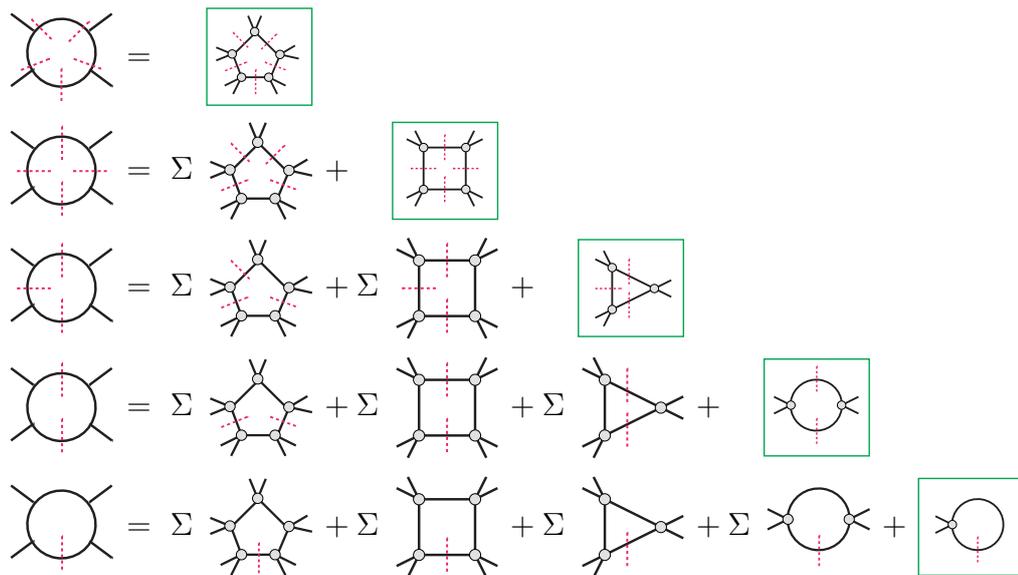
Figure 4.3: Schematic representation of the integrand reduction algorithm at one-loop

the algorithm is repeated recursively up to the lowest topology, delivering the full expression for the amplitude in dimensional regularisation. In Fig. 4.3 is shown a pictorial representation of the algorithm.

The algorithm described in this section can be summarised in the following steps:

1. Consider the numerator $\mathcal{N}$ of the integrand,

2. Evaluate $\mathcal{N}$ on the maximum cuts and solve for the coefficients of the ISP monomials, using the parametrisation of the residue in Eq. (4.3.56),

3. Evaluate the numerator on the cuts with one of the on-shell conditions removed and then solve for the coefficients of the ISP monomials,

4. Repeat the previous step up to the lowest cuts.

The use and variations of the integrand reduction technique within automated frameworks has been particularly successful and produced highly non-trivial phenomenological results.

In this section, we have described a very general procedure which find applications in theories such as QCD and Supersymmetric Yang-Mills. However, some

exceptions may arise, in particular cases where this procedure cannot be used or requires modifications.

4.3.4 Integrand reduction with six dimensional generalised unitarity

In the previous section, we described how integrand reduction combined with generalised unitarity cuts provides a powerful method for loop amplitude calculations. When the numerator is evaluated on the multiple cuts one may try to identify the residue as a product of tree-level amplitudes, as suggested by generalised unitarity. In order to compute the full amplitude in dimensional regularisation, the cuts need to be performed taking into account the loop momentum living in $(4 - 2\epsilon)$-dimensions. However, in this case the tree-level amplitudes for particle living in an arbitrary d-dimension are not so easy to write down.

The solution is to embed the $4 - 2\epsilon$ dimensions in an integer number of dimensions $\mathcal{D}$ bigger than four. Therefore the cuts are performed in $\mathcal{D}$ integer dimensions, where the tree-level can be evaluated. Finally a dimensional reduction procedure removes the extra degrees of freedom introduced by the additional finite dimensions, restoring the result in $4 - 2\epsilon$ [72]. For one-loop applications five dimensions are in principle enough, since one can embed the -2ϵ dimensionality in the fifth component of the loop momentum, satisfying the orthogonality condition required in Eq. (4.3.46).

However, we find it more convenient to embed the loop momentum in six dimensions. This choice has several advantages. First of all, we can use the six dimensional spinor-helicity formalism presented in Section (3.2) to parametrise the tree-level building-blocks of generalised unitarity in six dimensions and multi-leg tree-level can be generated using the BCFW recursion relation described in 4.1. When external massive fermions are involved, a convenient representation of virtual massive propagators can be obtained by allowing the mass to flow in one of the additional components and the (-2ϵ) part in the other (see Section 7). Similar motivations make six dimensions suitable for two-loop applications, since the

(-2ϵ) part of the two loop momenta can live in orthogonal subspaces [6]. Moreover the parametrisation of the six dimensional cuts solutions can be found to be free of square-roots, which traditionally appear in this context, leading to a more efficient reduction algorithm, then suitable to analytic computations and finite field reconstruction[30]. Applications of generalised unitarity in six dimensions can be found in [2, 68, 81, 82].

The general application of integrand reduction within generalised unitarity in six dimensions follows the same steps described in Section 4.3.3. One starts by performing the maximal cuts in six dimensions, thus the amplitude factorises into a product of six dimensional tree-level amplitudes and the coefficients of the ISP monomials can be extracted.

To demonstrate this technique we consider the case of QCD amplitudes with massless loop propagators. We embed the loop momentum in six dimensions as follows,

$$k^{[4-2\epsilon]} \rightarrow k^{[6]} \equiv \ell = \{\bar{\ell}, \ell^{(4)}, \ell^{(5)}\}. \tag{4.3.64}$$

Since we consider the external momenta in four dimensions, the fifth and sixth components only appear squared, so according with (4.3.46) we can write,

$$-\ell^{(4)2} - \ell^{(5)2} = \mu^2. \tag{4.3.65}$$

We span the loop momentum ℓ^μ in the following basis,

$$\beta = \left\{ v^\mu, u^\mu, \langle v^1 \Sigma^\mu u_1 \rangle, \langle v^1 \Sigma^\mu u_2 \rangle, \langle v^2 \Sigma^\mu u_1 \rangle, \langle v^2 \Sigma^\mu u_2 \rangle \right\}, \tag{4.3.66}$$

where v and u are six dimensional massless momenta, and the spinors are defined as in Section 3.2. We introduce a set of parameters τ_i such that,

$$\ell = \beta \cdot \tau, \qquad \tau = \{\tau_0, \tau_1, \tau_2, \tau_3, \tau_4, \tau_5\}, \tag{4.3.67}$$

---

[6]A typical two-loop setup is e.g. $k_1 = (\bar{k}_1, \mu_1, 0)$, $k_1 = (\bar{k}_2, 0, \mu_2)$

where, because the constraint in Eq. (4.3.65), only five of them are independent. With this parametrisation we are turning the integral over the loop momentum components into an integral over the τ_i.

Therefore, when a multiple cut is performed some of these parameters are constrained. For the quintuple-cut, the system of five quadratic equations $D_{i_1} = \cdots = D_{i_5} = 0$ has one solution, so all the parameters are fixed. The quadruple-, triple-, double- and single-cut have instead infinite solutions and one, two, three and four parameters respectively are not frozen by the cut. The free parameters can be sampled to determine a subset of solutions of the cuts, such that one can solve a system of linear independent equations for the coefficients of the integrand parametrisation.

In six dimensions, gluons have $6 - 2 = 4$ polarisation states, so for each extra dimension introduced we get one more state. Therefore working explicitly in six dimensions, the dependence on the spin dimension d_s will be lost but can be recovered through state-sum reduction. The general procedure is described in [72, 81]. Each of these extra states corresponds to the contribution from replacing gluons in the loop by a scalar. By subtracting these scalars the number of polarisation states can be reduced to $d_s - 2$. In the case of amplitudes with massless fermions the state sum reduction can be written as

$$\boldsymbol{c} = \boldsymbol{c}^{6d} - (6 - d_s)\boldsymbol{c}_\phi, \qquad (4.3.68)$$

which is also known as dimensional reduction. Keeping d_s arbitrary we can cover different regularisation schemes, e.g. $d_s = 4$ for the four-dimensional helicity scheme (FDH) or $d_s = 4 - 2\epsilon$ for the conventional dimensional regularization scheme (CDR).

An example of a 4-gluon one-loop scattering amplitude

We consider the example of a colour ordered one-loop scattering amplitude involving four gluons,

$$A_4^{(1)}(1^+, 2^+, 3^-, 4^-) = \int \frac{d^d k}{(2\pi)^d} \frac{\mathcal{N}}{k_0^2 k_1^2 k_2^2 k_3^2}$$

$$k_0 = k, \quad k_1 = k - p_1, \quad k_2 = k - p_1 - p_2, \quad k_3 = k + p_4. \qquad (4.3.69)$$

where all the momenta are assumed to be outgoing.

The numerator can be parametrised following Eq. (4.3.61),

$$
\begin{aligned}
\mathcal{N} = \Delta_{0,1,2,3\}} & \\
& + \Delta_{\{0,1,2\}} k_3^2 + \Delta_{\{0,1,3\}} k_2^2 + \Delta_{\{0,2,3\}} k_1^2 + \Delta_{\{1,2,3\}} k_0^2 \qquad (4.3.70) \\
& + \Delta_{\{0,2\}} k_1^2 k_3^2 + \Delta_{\{1,3\}} k_0^2 k_2^2.
\end{aligned}
$$

The kinematic configuration is the same as that discussed in section 3.3, where we showed that, after pulling out a phase factor, the process can be represented in terms of two momentum twistor variables $s = (p_1 + p_2)^2$ and $t = (p_2 + p_3)^2$.

Now, the integrand reduction algorithm starts by performing multiple cuts in six dimensions. The $4 - 2\epsilon$ loop momentum is replaced with the six dimensional one, $k \to \ell$, in Eq. (4.3.70). The first step is to evaluate the numerator on the maximum-cut, which in this case is the quadruple-cut ($\ell_0^2 = \ell_1^2 = \ell_2^2 = \ell_3^2 = 0$). Because we have a system of four equations for six dimensional momenta and one additional equation from Eq. (4.3.65), one of the parameters in the parametrisation of Eq. (4.3.67) is left unconstrained. The solution for this quadruple-cut can be written as,

$$
\lambda_\alpha^A(\ell_0) = \begin{bmatrix} \frac{s\left(t^2 - \tau_1^2\right)}{4t(s+t)} & 0 & 1 & \frac{s(t-\tau_1)}{2(s+t)} \\ \frac{1}{2}\left(\frac{\tau_1}{t} - 1\right) & 1 & 0 & 1 \end{bmatrix}_{\alpha A} \qquad \tilde{\lambda}_{A\dot\alpha}(\ell_0) = \begin{bmatrix} 0 & 1 \\ -1 & \frac{t-\tau_1}{2t} \\ \frac{s(\tau_1-t)}{2(s+t)} & \frac{s\left(\tau_1^2-t^2\right)}{4t(s+t)} \\ 1 & 0 \end{bmatrix}_{A\dot\alpha}
$$

$$(4.3.71)$$

On the quadruple cut the amplitude factorises into products of four tree-level amplitudes,

$$
\text{Cut}_{0123} = A(-\ell_{0a\dot a}, 1^{2\dot 2}, \ell_1^{b\dot b}) A(-\ell_{1b\dot b}, 2^{2\dot 2}, \ell_2^{c\dot c}) A(-\ell_{2c\dot c}, 3^{1\dot 1}, \ell_3^{d\dot d}) A(-\ell_{3d\dot d}, 4^{1\dot 1}, \ell_0^{a\dot a}),
$$

$$(4.3.72)$$

A pictorial representation of the quadruple-cut is shown in Fig. 4.4. The six dimen-
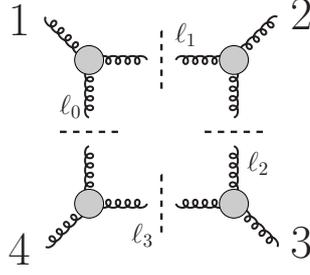
Figure 4.4: Quadruple cut of the four gluon one-loop amplitude.

sional tree-level amplitudes can be evaluated using the standard Feynman rules or the compact expressions in the Appendix B.1. The result for this helicity configuration is

$$\text{Cut}_{0123} = \frac{s^5 t \, (t - \tau_1)^3 \, (t + \tau_1)}{4(s + t)^3}. \tag{4.3.73}$$

Then we need to evaluate the parametrisation of the residue in Eq. (4.3.56) on the cut solutions. In this case the residue is

$$\Delta_{0123} = c_{0123}^{(0)} + c_{0123}^{(1)} \, (\ell \cdot w_{1;123}) + c_{0123}^{(2)} \, \mu^2 + c_{0123}^{(3)} \, \mu^2 (\ell \cdot w_{1;123}) + c_{0123}^{(4)} \, \mu^4, \tag{4.3.74}$$

where the spurious vector w can be chosen to be [7]

$$w^\mu = \frac{\langle 231]}{s} \frac{\langle 1 \sigma^\mu 2]}{2} - \frac{\langle 132]}{s} \frac{\langle 2 \sigma^\mu 1]}{2}. \tag{4.3.75}$$

Therefore, the residue on the six dimensional quadruple-cut takes the form,

$$\Delta_{0123}\big|_{0123} = c_{0123}^{(0)} + c_{0123}^{(1)} \frac{s\tau_1}{s+t} + c_{0123}^{(2)} \frac{s \, (t - \tau_1) \, (t + \tau_1)}{4t(s + t)} + c_{0123}^{(3)} \frac{s^2 \tau_1 \, (t - \tau_1) \, (t + \tau_1)}{4t(s + t)^2}$$

$$\tag{4.3.76}$$

$$+ c_{0123}^{(4)} \frac{s^2 \, (t - \tau_1)^2 \, (t + \tau_1)^2}{16t^2(s + t)^2} + c_{0123}^{(5)} \frac{s^3 \tau_1 \, (t - \tau_1)^2 \, (t + \tau_1)^2}{16t^2(s + t)^3} \tag{4.3.77}$$

---

[7]More details about the spurious vector are given in Appendix D.
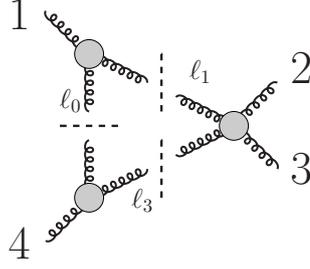
Figure 4.5: Triple-cut involving the ℓ_0, ℓ_1 and ℓ_3 propagators for four gluons amplitudes.

Comparing the results in Eq. (4.3.73) and (4.3.77) term by term in τ_1,

$$\text{Cut}_{0123} = \Delta_{0123}\big|_{0123}, \tag{4.3.78}$$

the coefficients can be obtained by solving a system of linear equations, which has solution

$$c_{0123}^{(0)} = s^2 t^2, \qquad c_{0123}^{(2)} = 4st^2, \qquad c_{0123}^{(4)} = 4t^2, \qquad c_{0123}^{(1)} = c_{0123}^{(3)} = c_{0123}^{(5)} = 0 \tag{4.3.79}$$

Considering the algorithm in Section 4.3.3, we proceed by considering cuts with three on-shell propagators (triple-cut). In this example we show the case of the triple-cut where $\ell_0^2 = \ell_1^2 = \ell_3^2 = 0$. The solution of this system can be written as

$$\lambda_\alpha^A(\ell_0) = \begin{bmatrix} -\tau_2 & \tau_2 & 1 & 0 \\ 0 & \frac{(s+t)\tau_1}{s} & 1 & \frac{st}{s+t} \end{bmatrix}_{\alpha A} \qquad \tilde{\lambda}_{A\dot{\alpha}}(\ell_0) = \begin{bmatrix} -\frac{s^2 t}{(s+t)^2 \tau_1} & \frac{(s+t)\tau_1}{s} \\ -\frac{s^2 t}{(s+t)^2 \tau_1} & 0 \\ 0 & \frac{(s+t)\tau_1\tau_2}{s} \\ 1 & -\frac{(s+t)^2\tau_1\tau_2}{s^2 t} \end{bmatrix}_{A\dot{\alpha}} \tag{4.3.80}$$

where two parameters are not fixed by the cut.

On the triple-cut the amplitudes factorise into products of three tree-level am-

plitudes (see Fig. 4.5),

$$\text{Cut}_{013} = A(-\ell_{0a\dot{a}}, 1^{2\dot{2}}, \ell_1^{b\dot{b}})A(-\ell_{1b\dot{b}}, 2^{2\dot{2}}, 3^{1\dot{1}}, \ell_3^{c\dot{c}})A(-\ell_{3c\dot{c}}, 4^{1\dot{1}}, \ell_0^{a\dot{a}}), \qquad (4.3.81)$$

which, evaluated on the cut, simplifies to,

$$\text{Cut}_{013} = -\frac{s^2t^2\left(-2\tau_2^2 + 2\tau_1\tau_2 - 2\tau_2 - 1\right)^2}{s\tau_1 - s\tau_2 + t\tau_1 - s}. \qquad (4.3.82)$$

Now we need to subtract the contribution from the higher point residue, precisely,

$$\text{Cut}_{013} - \left.\frac{\Delta_{0123}}{\ell_2^2}\right|_{013} = 4t^2\tau_2\left(s + s\tau_2 - s\tau_1\tau_2 + t\tau_1\tau_2 + s\tau_2^2\right) \qquad (4.3.83)$$

where, in the second term of the l.h.s., we have used the coefficients of Eq. (4.3.79). Using Eq. (4.3.56), the residue is parametrised as

$$\begin{aligned}
\Delta_{013} &= c_{013}^{(0)} + c_{013}^{(1)}\left(\ell \cdot w_1\right) + c_{013}^{(2)}\left(\ell \cdot w_2\right) \\
&+ c_{013}^{(3)}\left(\ell \cdot w_1\right)(\ell \cdot w_2) + c_{013}^{(4)}\left(\left(\ell \cdot w_1\right)^2 - (\ell \cdot w_2)^2\right) \\
&+ c_{013}^{(5)}\left(\ell \cdot w_1\right)^2(\ell \cdot w_2) + c_{013}^{(6)}\left(\ell \cdot w_1\right)(\ell \cdot w_2)^2 \\
&+ c_{013}^{(7)}\mu^2(k \cdot w_1) + c_{013}^{(8)}\mu^2(k \cdot w_2) + c_{013}^{(9)}\mu^2, \qquad (4.3.84)
\end{aligned}$$

where the spurious vectors w_1 and w_2 can be chosen to be

$$w_1^\mu = \frac{\langle 1\sigma^\mu 2]}{\langle 132]} + \frac{\langle 2\sigma^\mu 1]}{\langle 231]}, \qquad w_2^\mu = i\left(\frac{\langle 1\sigma^\mu 2]}{\langle 132]} - \frac{\langle 2\sigma^\mu 1]}{\langle 231]}\right). \qquad (4.3.85)$$

Evaluating it on the cut we have,

$$\Delta_{013}\big|_{013} = c^{(0)} + c^{(1)} \left(-\frac{t\tau_1}{s} - \frac{t\tau_2}{s+t} \right) + c^{(2)} \left(\frac{it\tau_1}{s} - \frac{it\tau_2}{s+t} \right) +$$

$$c^{(3)} \left(\frac{it^2\tau_2^2}{(s+t)^2} - \frac{it^2\tau_1^2}{s^2} \right) + c^{(4)} \left(\frac{2t^2\tau_1^2}{s^2} + \frac{2t^2\tau_2^2}{(s+t)^2} \right) +$$

$$c^{(5)} \left(\frac{i\tau_1^3 t^6}{s^3(s+t)^3} + \frac{3i\tau_1^3 t^5}{s^2(s+t)^3} + \frac{i\tau_1^2\tau_2 t^3}{s^2(s+t)} + \frac{3i\tau_1^3 t^4}{s(s+t)^3} + \frac{i\tau_1^3 t^3}{(s+t)^3} - \frac{i\tau_2^3 t^3}{(s+t)^3} - \frac{i\tau_1\tau_2^2 t^3}{s(s+t)^2} \right) +$$

$$c^{(6)} \left(\frac{\tau_1^3 t^6}{s^3(s+t)^3} + \frac{3\tau_1^3 t^5}{s^2(s+t)^3} - \frac{\tau_1^2\tau_2 t^3}{s^2(s+t)} + \frac{3\tau_1^3 t^4}{s(s+t)^3} + \frac{\tau_1^3 t^3}{(s+t)^3} + \frac{\tau_2^3 t^3}{(s+t)^3} - \frac{\tau_1\tau_2^2 t^3}{s(s+t)^2} \right) +$$

$$c^{(7)} \left(\frac{t^2\tau_2\tau_1^2}{s} + \frac{t^2\tau_2^2\tau_1}{s+t} \right) + c^{(8)} \left(\frac{it^2\tau_1\tau_2^2}{s+t} - \frac{it^2\tau_1^2\tau_2}{s} \right) - t\tau_1\tau_2 c^{(9)}. \tag{4.3.86}$$

Again, we can solve for the coefficients by requiring,

$$\text{Cut}_{013} - \frac{\Delta_{0123}}{\ell_2^2}\bigg|_{013} = \Delta_{013}\big|_{013} \tag{4.3.87}$$

which gives us the following result,

$$c_{0123}^{(0)} = 0, \qquad\qquad c_{0123}^{(1)} = 2st(s+t),$$

$$c_{0123}^{(2)} = 2ist(s+t), \qquad\qquad c_{0123}^{(3)} = 2is(s+t)^2,$$

$$c_{0123}^{(4)} = s(s+t)^2, \qquad\qquad c_{0123}^{(5)} = 2i\frac{s}{t}(s+t)^3,$$

$$c_{0123}^{(6)} = -2\frac{s}{t}(s+t)^3, \qquad\qquad c_{0123}^{(7)} = -4t(s+t),$$

$$c_{0123}^{(8)} = 4it(s+t) \qquad\qquad c_{0123}^{(9)} = 0. \tag{4.3.88}$$

With the same procedure one can consider all the remaining triple- and double-cuts and compute the full set of coefficients.

The final step consists of dimensionally reducing the coefficients from 6 to a general dimension d, removing the extra degrees of freedom contained in the six dimensional loop momentum according to eq. (4.3.68). The computation of these extra cuts is done using the same procedure as above, whereas the tree-level amplitudes are different since the gluon internal lines are replaced with scalar lines. For example, the quadruple- and triple-cut computed before lead to the following

(a) Quadruple-cut   (b) Triple-cut
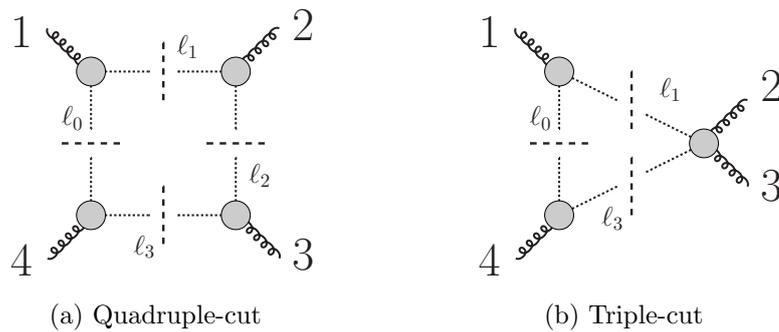
Figure 4.6: Scalar loop contributions to state-sum reduction.

factorisation,

$$\text{Cut}^{\phi}_{0123} = A(-\ell_0, 1^{\alpha\dot{\alpha}}, \ell_1)A(-\ell_1, 2^{\beta\dot{\beta}}, \ell_2)A(-\ell_2, 3^{\gamma\dot{\gamma}}, \ell_3)A(-\ell_3, 4^{\delta\dot{\delta}}, \ell_0) \qquad (4.3.89)$$

$$\text{Cut}^{\phi}_{013} = A(-\ell_0, 1^{\alpha\dot{\alpha}}, \ell_1)A(-\ell_1, 2^{\beta\dot{\beta}}, 3^{\gamma\dot{\gamma}}, \ell_3)A(-\ell_3, 4^{\delta\dot{\delta}}, \ell_0), \qquad (4.3.90)$$

showed also in Fig 4.6. Again the Feynman rules and the compact tree-level amplitudes are given in Appendix A.

One then proceed with the same approach up to the lowest cut, taking into account the appropriate subtraction terms. Further details about the general cut solutions and spurious vectors are given in Appendix D. In the context of this thesis, the same method has been applied to compute the one loop Higgs plus five gluons amplitudes discussed in Section 6 and amplitudes with a massive $t\bar{t}$ discussed in Sections 7 and 8.

Chapter 5

One-loop triple collinear splitting amplitudes in QCD

In this chapter we study the factorisation properties of one-loop scattering amplitudes in the triple collinear limit and extract the universal splitting amplitudes for processes initiated by a gluon. The splitting amplitudes are derived from the analytic Higgs plus four partons amplitudes. We present compact results for primitive helicity splitting amplitudes making use of super-symmetric decompositions. The universality of the collinear factorisation is checked numerically against the full colour six parton squared matrix elements.

5.1 Colour decomposition in the collinear limit

In the limit where m of the external legs become simultaneously collinear, amplitudes factorise into a product of lower multiplicity amplitudes and splitting amplitudes which contain all the infrared divergences:

$$A_n^{(L)}(\{p_i^{\lambda_i}\}) \overset{1\|\dots\|m}{\longrightarrow} \sum_{k=0}^{L} \sum_{\lambda_P} \mathrm{Sp}_m^{(L-k)}(-P^{-\lambda_P}; \{p_i^{\lambda_i}\}_{i=1}^m) A_{n-m+1}^{(k)}(P^{\lambda_P}, \{p_i^{\lambda_i}\}_{i=m+1}^n)$$

$$(5.1.1)$$

where $A_n^{(L)}$ and $\mathrm{Sp}_n^{(L)}$ can either be primitive or partial n-point amplitudes and splitting amplitudes respectively, while $P \equiv p_1 + \cdots + p_m$. A schematic representation
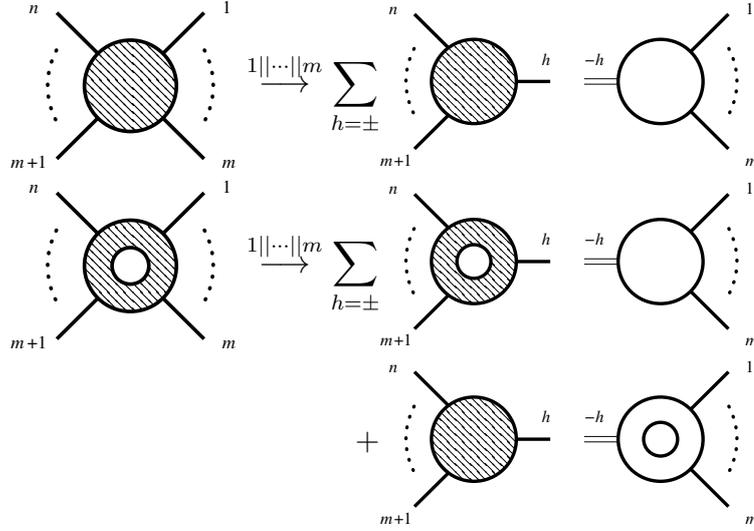
Figure 5.1: Factorisation of tree and one-loop amplitudes in the multi-collinear limit.

of this factorisation is shown in Figure 5.1. The sum of internal helicity states λ_P leads to spin correlations in the factorized squared amplitude $\mathcal{M}^{(L,L')}$,

$$\mathcal{M}_n^{(L,L')}(\{p_i^{\lambda_i}\}) \overset{1\|\cdots\|m}{\to} \sum_{k=0}^{L}\sum_{k'=0}^{L'}\sum_{\lambda_P,\lambda'_P}$$
$$\mathcal{P}_{m;-\lambda_P,-\lambda'_P}^{(L-k,L'-k')}(-P;\{p_i^{\lambda_i}\}_{i=1}^{m})\,\mathcal{M}_{n-m+1;\lambda_P,\lambda'_P}^{(k,k')}(P,\{p_i^{\lambda_i}\}_{i=m+1}^{n}) \qquad (5.1.2)$$

where we can define

$$\mathcal{M}_{n;\lambda_P,\lambda'_P}^{(L,L')}(P,\{p_i^{\lambda_i}\}) = \left(\vec{A}_n^{(L)}(P^{\lambda_P},\{p_i^{\lambda_i}\})\right)^{\dagger}\cdot\mathcal{C}_n^{(L,L')}\cdot\vec{A}_n^{(L')}(P^{\lambda_{P'}},\{p_i^{\lambda_i}\}) \qquad (5.1.3)$$

$$\mathcal{P}_{n;\lambda_P,\lambda'_P}^{(L,L')}(P;\{p_i^{\lambda_i}\}) = \left(\vec{\mathrm{Sp}}_n^{(L)}(P^{\lambda_P};\{p_i^{\lambda_i}\})\right)^{\dagger}\cdot\mathcal{C}_{\mathrm{Sp},n}^{(L,L')}\cdot\vec{\mathrm{Sp}}_n^{(L')}(P^{\lambda_{P'}};\{p_i^{\lambda_i}\}) \qquad (5.1.4)$$

in terms of partial amplitudes or equivalently

$$\mathcal{M}_{n;\lambda_P,\lambda'_P}^{(L,L')}(P,\{p_i^{\lambda_i}\}) = \left(\vec{A}_n^{[L]}(P^{\lambda_P},\{p_i^{\lambda_i}\})\right)^{\dagger}\cdot\mathcal{C}_n^{[L,L']}\cdot\vec{A}_n^{[L']}(P^{\lambda_{P'}},\{p_i^{\lambda_i}\}) \qquad (5.1.5)$$

$$\mathcal{P}_{n;\lambda_P,\lambda'_P}^{(L,L')}(P;\{p_i^{\lambda_i}\}) = \left(\vec{\mathrm{Sp}}_n^{[L]}(P^{\lambda_P};\{p_i^{\lambda_i}\})\right)^{\dagger}\cdot\mathcal{C}_{\mathrm{Sp},n}^{[L,L']}\cdot\vec{\mathrm{Sp}}_n^{[L']}(P^{\lambda_{P'}};\{p_i^{\lambda_i}\}) \qquad (5.1.6)$$

in terms of primitive amplitudes. In the colour matrix $\mathcal{C}_{\mathrm{Sp},n}^{[L,L']}$ we absorbed a prefactor which takes into account colour conservation along the factorized parton, such that

$$\mathcal{C}_{\mathrm{Sp},n}^{[L,L']} = \begin{cases} \dfrac{1}{N_c^2 - 1}\mathcal{C}_n^{[L,L']} & \text{for gluon-initiated Sp} \\ \dfrac{1}{N_c}\mathcal{C}_n^{[L,L']} & \text{for quark-initiated Sp} \end{cases}, \tag{5.1.7}$$

and similar for $\mathcal{C}_{\mathrm{Sp},n}^{(L,L')}$.

5.2 A spinor parametrisation of the multi-collinear limit

We define the multiple collinear limit using a parametrisation of the full kinematics in term of a parameter δ, such that the collinear limit in Eq. (5.1.1) is identified as the leading term as $\delta \to 0$, i.e.

$$\lim_{1||\cdots||m} A_n^{(L)}(\{p_i^{\lambda_i}\}) = \lim_{\delta \to 0} A_n^{(L)}(\{p_i^{\lambda_i}(\delta)\})$$
$$= \sum_{k=0}^{L}\sum_{\lambda_P}\mathrm{Sp}_m^{(L-k)}(-P^{-\lambda_P}, \{p_i^{\lambda_i}\}_{i=1}^m)A_{n-m+1}^{(k)}(P^{\lambda_P}, \{p_i^{\lambda_i}\}_{i=m+1}^n) + \mathcal{O}\left(\frac{1}{\delta^{m-2}}\right). \tag{5.2.8}$$

The parametrisation is defined by,

$$p_i^\mu(\delta) = z_i\tilde{P}^\mu + \delta k_{T,i}^\mu - \delta^2\frac{k_{T,i}^2}{2(P\cdot\eta)z_i}\eta^\mu \qquad i = 1,\ldots,m \tag{5.2.9}$$

$$p_i^\mu(\delta) = K_i^\mu(\delta, \{p\}_{m+1,n}, \eta) \qquad i = m+1,\ldots,n \tag{5.2.10}$$

where $z_i = (p_i\cdot\eta)/(P\cdot\eta)$ are the momentum fractions of the unresolved partons, η is an arbitrary light-like momentum and $\tilde{P}$ is the massless projection of $P = \sum_{i=1}^m p_i$,

$$\tilde{P}^\mu = P^\mu - \frac{P^2}{2P\cdot\eta}\eta^\mu. \tag{5.2.11}$$

The vectors $k_{T,i}^{\mu}$ are orthogonal to P, $\tilde{P}$ and η

$$k_{T,i} \cdot \tilde{P} = k_{T,i} \cdot P = k_{T,i} \cdot \eta = 0. \tag{5.2.12}$$

Momentum conservation implies that:

$$\sum_{i=1}^{m} z_i = 1 \tag{5.2.13}$$

$$\sum_{i=1}^{m} k_{T,i}^{\mu} = 0^{\mu} \tag{5.2.14}$$

$$-\delta^2 \sum_{i=1}^{m} \frac{k_{T,i}^2}{z_i} = P^2. \tag{5.2.15}$$

The function K_i^{μ} is a generic map that keeps the factorized momenta $m+1, \ldots, n$ on-shell as well as absorbing the recoil $P^2/(2P \cdot \eta)\eta^{\mu}$, and it satisfies $K_i^{\mu} \to p_i^{\mu}$ as $\delta \to 0$. The exact form is not important for our purpose of explicitly taking the limit and various mappings have been considered in the literature (for example in the Catani-Seymour subtraction [41] or Kosower's antenna [83]). When implementing the collinear phase-space numerically we employed the Catani-Seymour map as described in Appendix F.1.

Since we are working at the amplitude level, we would like to have a parametrisation of the limit valid for the spinors of p_i as well. This can be achieved using an appropriate choice of the transverse vectors $k_{T,i}$,

$$2\,\delta\,k_{T,i}^{\mu} = \langle z_i \rangle [\omega_i] \langle \tilde{P} \gamma^{\mu} \eta] + [z_i] \langle \omega_i \rangle \langle \eta \gamma^{\mu} \tilde{P}]. \tag{5.2.16}$$

In the above we use the notation

$$\langle z_i \rangle = \frac{\langle i\eta \rangle}{\langle \tilde{P}\eta \rangle}, \qquad [z_i] = \frac{[i\eta]}{[\tilde{P}\eta]}, \qquad \langle \omega_i \rangle = \frac{\langle i\tilde{P} \rangle}{\langle \eta\tilde{P} \rangle}, \qquad [\omega_i] = \frac{[i\tilde{P}]}{[\eta\tilde{P}]}, \tag{5.2.17}$$

where the spinor variables $\langle z_i \rangle$ and $[z_i]$ differ by a phase from the usual parametrisation which uses $\sqrt{z_i}$. It is worth to notice that both $\langle \omega_i \rangle$ and $[\omega_i]$ are $\mathcal{O}(\delta)$ in the

collinear limit. The spinor parametrisation then reads,

$$|i\rangle = \langle z_i \rangle |\tilde{P}\rangle + \langle \omega_i \rangle |\eta\rangle \qquad\qquad |i] = [z_i]|\tilde{P}] + [\omega_i]|\eta]. \qquad (5.2.18)$$

We find that this is a convenient way to take the limit at the amplitude level since the spinor variables $\langle z_i \rangle$ obey Schouten identities:

$$\sum_{ijk\,\text{cyclic}} \langle z_i \rangle \langle jk \rangle = 0, \qquad (5.2.19)$$

as well as momentum conservation,

$$\sum_i p_i^\mu - \tilde{P}^\mu - \frac{P^2}{2P \cdot \eta}\eta^\mu = 0^\mu. \qquad (5.2.20)$$

For the triple collinear splitting amplitudes this means we have the kinematics of a five-point function event though the colour space is that of a four-point function.

5.3 One-loop basis functions for $pp \to H{+}2j$ in the triple collinear limit

The analytic $H + 4$ parton amplitudes have been computed using unitarity cuts and expressed in terms of the universal infrared poles plus finite logarithmic and di-logarithmic functions as well as rational terms [84]. Taking the triple collinear limit of the infrared poles, rational terms and logarithms as above presents no difficulties. Dealing with the di-logarithmic parts requires some minor effort to ensure the arguments are in the appropriate region so the limit will converge. Polylogarithmic identities are well known and understood in huge detail (see[85] for a review) - way beyond the simple structures appearing here. Nevertheless we collect some

potentially useful identities here to aid the reader,

$$\text{Li}_2 (1 - x) + \text{Li}_2 (x) + \log(x) \log(1 - x) - \frac{\pi^2}{6} = 0 \qquad x \in [0, 1] \quad (5.3.21)$$

$$\text{Li}_2 (x) + \text{Li}_2 \left(\frac{1}{x}\right) + \frac{1}{2} \log(-x)^2 + \frac{\pi^2}{6} = 0 \qquad x < 0 \quad (5.3.22)$$

$$\text{Li}_2 \left(\frac{xy}{(1-x)(1-y)}\right) - \text{Li}_2 \left(-\frac{x}{1-x}\right) - \text{Li}_2 \left(-\frac{y}{1-y}\right) +$$
$$- \text{Li}_2 \left(\frac{x}{1-y}\right) - \text{Li}_2 \left(\frac{y}{1-x}\right) - \log^2 \left(\frac{1-x}{1-y}\right) = 0 \qquad x, y \in [0, 1] \quad (5.3.23)$$

One function requiring a bit more thought is the three mass triangle which has square roots appearing in the arguments of the di-logarithms [73, 86, 87, 88, 89]:

$$I_3^{3m} \left(s_{ij}, s_{kl}, m_H^2\right) \xrightarrow{i||j||k} \frac{1}{(1 - z_k) m_H^2} \left(\text{Li}_2 (1 - z_k) - \text{Li}_2 \left(1 - \frac{1}{z_k}\right)\right.$$
$$\left. - \frac{1}{2} \log^2 (z_k) - \log \left(\frac{m_H^2}{s_{ij}}\right) \log (z_k)\right) \qquad (5.3.24)$$

5.4 $g \to ggg$ **splitting amplitudes**

In this section we present the colour structure and the primitive decomposition for the $g \to ggg$ channel. Then we compute the set of independent primitive amplitudes. We will suppress all helicity superscripts and the function arguments are taken to represent both momenta and helicity. The tree-level colour decomposition can be written as,

$$\mathcal{S}p^{(0)}(\{a_P, a_1, a_2, a_3\}, -P; 1, 2, 3)$$
$$= \sum_{\sigma \in S_3} \text{tr}(a_P, a_{\sigma(1)}, a_{\sigma(2)}, a_{\sigma(3)}) \text{Sp}^{(0)}(-P; \sigma(1), \sigma(2), \sigma(3)) \qquad (5.4.25)$$
$$= \sum_{\sigma \in S_2} \tilde{f}^{a_1 a_{\sigma(2)} b} \tilde{f}^{b a_{\sigma(3)} a_P} \text{Sp}^{(0)}(-P; 1, \sigma(2), \sigma(3)) \qquad (5.4.26)$$

where $\text{tr}(a_1, \ldots, a_n) = T_{ji_1}^{a_1} T_{i_1 i_2}^{a_2} \ldots T_{i_{n-1} j}^{a_n}$ in terms of the fundamental generators of $SU(N_c)$ and $\tilde{f}^{abc} = i\sqrt{2} f^{abc}$ in terms of the adjoint structure constants. The relation between the two representations can be shown to hold using the Kleiss-Kuijf relations

[90] for the splitting amplitudes,

$$\mathrm{Sp}^{(0)}(-P; 3, 2, 1) = \mathrm{Sp}^{(0)}(-P; 1, 2, 3) \tag{5.4.27}$$

$$\mathrm{Sp}^{(0)}(-P; 1, 3, 2) = -\mathrm{Sp}^{(0)}(-P; 1, 2, 3) - \mathrm{Sp}^{(0)}(-P; 1, 3, 2) \tag{5.4.28}$$

The one-loop colour decomposition is[1],

$$
\begin{aligned}
\mathcal{S}p^{(1)}(\{a_P, a_1, a_2, a_3\}, &-P; 1, 2, 3) \\
&= \sum_{\sigma \in S_3} \mathrm{tr}(a_P, a_{\sigma(1)}, a_{\sigma(2)}, a_{\sigma(3)}) \mathrm{Sp}_1^{(1)}(-P; \sigma(1), \sigma(2), \sigma(3)) \\
&+ \sum_{\sigma \in S_3/Z_2} \mathrm{tr}(a_P, a_{\sigma(1)} \mathrm{tr}(a_{\sigma(2)}, a_{\sigma(3)}) \mathrm{Sp}_3^{(1)}(-P; \sigma(1), \sigma(2), \sigma(3))
\end{aligned} \tag{5.4.29}
$$

where the partial amplitudes are composed of primitive amplitudes as follows:

$$
\begin{aligned}
\mathrm{Sp}_1^{(1)}&(-P; 1, 2, 3) \\
&= N_c \mathrm{Sp}^{[g]}(-P; 1, 2, 3) - N_f \mathrm{Sp}^{[f]}(-P; 1, 2, 3), \tag{5.4.30} \\
\mathrm{Sp}_3^{(1)}&(-P; 1, 2, 3) \\
&= 2 \left(\mathrm{Sp}^{[g]}(-P; 1, 2, 3) + \mathrm{Sp}^{[g]}(-P; 1, 3, 2) + \mathrm{Sp}^{[g]}(-P; 3, 1, 2) \right). \tag{5.4.31}
\end{aligned}
$$

The primitive amplitudes for the gluon and fermion loops obey line-reversal symmetry,

$$\mathrm{Sp}^{[X]}(-P; 1, 2, 3) = \mathrm{Sp}^{[X]}(-P; 3, 2, 1) \tag{5.4.32}$$

and so in all we have three independent gluon loop primitive amplitudes, three fermion loop primitive amplitudes and two tree-level primitive amplitudes. The colour summed Born and virtual corrections can then be written according to (5.1.6)

---

[1]We write the one-loop decomposition in the standard trace basis rather than the slightly more compact 'F-basis' representation of Del Duca-Maltoni-Dixon [53]. Since we express the colour summed squared matrix element in terms of the minimal basis of primitive amplitudes the final expressions are equivalent to the DDM forms.

using:

$$\vec{\mathrm{Sp}}^{[0]} = \begin{pmatrix} \mathrm{Sp}^{[0]}(-P; 1, 2, 3) \\ \mathrm{Sp}^{[0]}(-P; 1, 3, 2) \end{pmatrix} \tag{5.4.33}$$

$$\mathcal{C}_{\mathrm{Sp}}^{[0,0]} = N_c^2 \begin{pmatrix} 4 & 2 \\ 2 & 4 \end{pmatrix} \tag{5.4.34}$$

$$\vec{\mathrm{Sp}}^{[1]} = \begin{pmatrix} N_c \, \mathrm{Sp}^{[g]}(-P; 1, 2, 3) \\ N_c \, \mathrm{Sp}^{[g]}(-P; 2, 1, 3) \\ N_c \, \mathrm{Sp}^{[g]}(-P; 2, 3, 1) \\ N_f \, \mathrm{Sp}^{[f]}(-P; 1, 2, 3) \\ N_f \, \mathrm{Sp}^{[f]}(-P; 2, 1, 3) \\ N_f \, \mathrm{Sp}^{[f]}(-P; 2, 3, 1) \end{pmatrix} \tag{5.4.35}$$

$$\mathcal{C}_{\mathrm{Sp}}^{[0,1]} = 2 N_c^2 \begin{pmatrix} 2 & -2 & 0 & -2 & 2 & 0 \\ 0 & -2 & 2 & 0 & 2 & -2 \end{pmatrix} \tag{5.4.36}$$

We also choose to present the results using the super-symmetric decomposition:

$$\begin{aligned} &\mathrm{Sp}^{[g]}(-P; 1, 2, 3) \\ &= \mathrm{Sp}^{[\mathcal{N}=4]}(-P; 1, 2, 3) + 4\mathrm{Sp}^{[\mathcal{N}=1]}(-P; 1, 2, 3) + (1 - \epsilon \delta_R)\mathrm{Sp}^{[\mathcal{N}=0]}(-P; 1, 2, 3) \end{aligned}$$

$$\tag{5.4.37}$$

$$\begin{aligned} &\mathrm{Sp}^{[f]}(-P; 1, 2, 3) \\ &= \mathrm{Sp}^{[\mathcal{N}=1]}(-P; 1, 2, 3) + \mathrm{Sp}^{[\mathcal{N}=0]}(-P; 1, 2, 3) \end{aligned} \tag{5.4.38}$$

since this yields particularly compact expressions. We also include the scheme dependence for both the FDH ($\delta_R = 0$) and CDR ($\delta_R = 1$) schemes. The full result for the set of primitive amplitudes is given in Appendix F.3.

5.5 $g \to \bar{q}qg$ splitting amplitudes

The colour structure of the tree-level splitting amplitudes is

$$\mathcal{S}p^{(0)}(\{a_P, \bar{\imath}_1, i_2, a_3\}, -P, 1_{\bar{q}}, 2_q, 3) =$$
$$T(a_P, a_3)^{\bar{\imath}_1}_{i_2} \mathrm{Sp}^{(0)}(-P; 1_{\bar{q}}, 2_q, 3) \; + \; T(a_3, a_P)^{\bar{\imath}_1}_{i_2} \mathrm{Sp}^{(0)}(-P; 2_q, 1_{\bar{q}}, 3) \qquad (5.5.39)$$

where $T(a_1, \ldots, a_n)^{\bar{\jmath}}_i = T^{a_1}_{\bar{\jmath}k_1} T^{a_1}_{k_1 k_2} \ldots T^{a_n}_{k_{n-1} i}$. Note that charge conjugation symmetry allows us to write $\mathrm{Sp}^{(0)}(-P; 2_q, 1_{\bar{q}}, 3) = \mathrm{Sp}^{(0)}(-P; 2_{\bar{q}}, 1_q, 3)$. At one-loop we have three colour structures,

$$\mathcal{S}p^{(1)}(\{a_P, \bar{\imath}_1, i_2, a_3\}, -P; 1_{\bar{q}}, 2_q, 3) = N_c \left[T(a_P, a_3)^{\bar{\imath}_1}_{i_2} \; \mathrm{Sp}^{(1)}_{4;1}(-P; 1_{\bar{q}}, 2_q, 3) \right.$$
$$\left. + T(a_3, a_P)^{\bar{\imath}_1}_{i_2} \; \mathrm{Sp}^{(1)}_{4;1}(-P; 2_q, 1_{\bar{q}}, 3) \right]$$
$$+ \delta^{a_P a_3} \delta^{\bar{\imath}_1}_{i_2} \; \mathrm{Sp}^{(1)}_{4;3}(-P; 1_{\bar{q}}, 2_q, 3). \qquad (5.5.40)$$

The partial amplitudes $\mathrm{Sp}_{4;1}$ and $\mathrm{Sp}_{4;3}$ are given in terms of the primitive amplitudes

$$\mathrm{Sp}_{4;1}(-P; 1_{\bar{q}}, 2_q, 3) = \mathrm{Sp}^{[L]}(-P; 1_{\bar{q}}, 2_q, 3) - \frac{1}{N_c^2} \mathrm{Sp}^{[R]}(-P; 1_{\bar{q}}, 2_q, 3)$$
$$+ \frac{n_f}{N_c} \mathrm{Sp}^{[f]}(-P; 1_{\bar{q}}, 2_q, 3) \qquad (5.5.41)$$

$$\mathrm{Sp}_{4;3}(-P; 1_{\bar{q}}, 2_q, 3) = \mathrm{Sp}^{[L]}(-P; 1_{\bar{q}}, 2_q, 3) + \mathrm{Sp}^{[L]}(-P; 2_{\bar{q}}, 1_q, 3) + \mathrm{Sp}^{[L+R]}(-P; 1_{\bar{q}}, 3, 2_q)$$
$$+ \mathrm{Sp}^{[R]}(-P; 1_{\bar{q}}, 2_q, 3) + \mathrm{Sp}^{[R]}(-P; 2_{\bar{q}}, 1_q, 3) \qquad (5.5.42)$$

where the indices $[L]$ and $[R]$ label the primitive amplitudes corresponding to fermion lines turning left or right upon entering the loop and $[f]$ denotes the primitive amplitudes with fermion-loop contribute. The label $[L+R]$ in the sub-leading colour amplitude corresponds to the sum of the left and right primitive amplitudes for the non-adjacent fermion configuration. Some representative diagrams of the primitive amplitudes are depicted in fig. 5.2.

The colour summed Born and virtual corrections can be written as in Eq. (5.1.4),

$$\mathrm{Sp}^{[L]}(-P; 1_{\bar{q}}, 2_q, 3) = \quad \text{[diagram]} \quad + \dots$$

$$\mathrm{Sp}^{[R]}(-P; 1_{\bar{q}}, 2_q, 3) = \quad \text{[diagram]} \quad + \dots$$

$$\mathrm{Sp}^{[f]}(-P; 1_{\bar{q}}, 2_q, 3) = \quad \text{[diagram]} \quad + \dots$$

$$\mathrm{Sp}^{[L+R]}(-P; 1_{\bar{q}}, 2, 3_q) = \quad \text{[diagram]}^2 + \quad \text{[diagram]}^2 + \dots$$

Figure 5.2: Sample diagrams corresponding to primitive amplitudes for $\mathrm{Sp}^{(1)}(-P; 1_{\bar{q}}, 2_q, 3_g)$

where the vectors $\vec{\mathrm{Sp}}^{(L)}$ and the colour matrices $\mathcal{C}_{\mathrm{Sp}}^{(L,L')}$ are now given by

$$\vec{\mathrm{Sp}}^{(0)} = \begin{pmatrix} \mathrm{Sp}^{(0)}(-P; 1, 2, 3) \\ -\mathrm{Sp}^{(0)}(-P; 2, 1, 3) \end{pmatrix} \tag{5.5.43}$$

$$\mathcal{C}_{\mathrm{Sp}}^{(0,0)} = \frac{1}{N_c} \begin{pmatrix} N_c^2 - 1 & -1 \\ -1 & N_c^2 - 1 \end{pmatrix} \tag{5.5.44}$$

$$\vec{\mathrm{Sp}}^{(1)} = \begin{pmatrix} N_c \, \mathrm{Sp}_{4;1}(-P; 1, 2, 3) \\ -N_c \, \mathrm{Sp}_{4;1}(-P; 2, 1, 3) \\ \mathrm{Sp}_{4;3}(-P; 1, 2, 3) \end{pmatrix} \tag{5.5.45}$$

$$\mathcal{C}_{\mathrm{Sp}}^{(0,1)} = \frac{1}{N_c} \begin{pmatrix} N_c^2 - 1 & -1 & N_c \\ -1 & N_c^2 - 1 & N_c \end{pmatrix} \tag{5.5.46}$$

$$\tag{5.5.47}$$

The quark primitive splitting amplitudes also have a useful super-symmetric decomposition [91]. In this case we can write the complicated "left-moving" amplitudes

Figure 5.3: Sample diagrams corresponding to scalar contribution for $\mathrm{Sp}^{(1)}(-P; 1_{\bar{q}}, 2_q, 3_g)$ in $\mathcal{N} = 4$ super-symmetric Yang-Mills theory.

in terms of simpler ones built using the $\mathcal{N} = 4$ super-multiplet,

$$\mathrm{Sp}^{[L]}(-P; 1_{\bar{q}}, 2_q, 3) = \mathrm{Sp}^{[\mathcal{N}=4]}(-P; 1_{\bar{q}}, 2_q, 3) - \mathrm{Sp}^{[R]}(-P; 1_{\bar{q}}, 2_q, 3)$$
$$- \mathrm{Sp}^{[f]}(-P; 1_{\bar{q}}, 2_q, 3) - \mathrm{Sp}^{[\mathrm{scalar}]}(-P; 1_{\bar{q}}, 2_q, 3) \quad (5.5.48)$$
$$\mathrm{Sp}^{[L+R]}(-P; 1_{\bar{q}}, 2, 3_q) = \mathrm{Sp}^{[\mathcal{N}=4]}(-P; 1_{\bar{q}}, 2, 3_q) - \mathrm{Sp}^{[\mathrm{scalar}]}(-P; 1_{\bar{q}}, 2, 3_q) \quad (5.5.49)$$

where the $\mathrm{Sp}^{[\mathrm{scalar}]}$ function indicates the contribution from the complete scalar sector of $\mathcal{N} = 4$. This includes a scalar-fermion-fermion vertex as well as the scalar-gluon-gluon vertex which contributes to the function $\mathrm{Sp}^{[\mathcal{N}=0]}$ in the pure gluonic case. Representative diagrams contributing to $\mathrm{Sp}^{[\mathrm{scalar}]}$ are shown in fig. 5.3. Using these relations we find a compact form for the colour dressed splitting amplitudes in terms of $\mathrm{Sp}^{[\mathcal{N}=4]}(-P; 1_{\bar{q}}, 2_q, 3)$, $\mathrm{Sp}^{[R]}(-P; 1_{\bar{q}}, 2_q, 3)$, $\mathrm{Sp}^{[f]}(-P; 1_{\bar{q}}, 2_q, 3)$, $\mathrm{Sp}^{[\mathrm{scalar}]}(-P; 1_{\bar{q}}, 2_q, 3)$, $\mathrm{Sp}^{[\mathcal{N}=4]}(-P; 1_{\bar{q}}, 2_q, 3)$ and $\mathrm{Sp}^{[\mathrm{scalar}]}(-P; 1_{\bar{q}}, 2, 3_q)$. The full result is given in Appendix F.4.

5.6 Cross checks and discussion

We check the universality of the splitting functions derived in the previous section numerically against the six parton amplitudes available in NJET [19]. In order to make sure we could evaluate as close to the precise limit as possible, we implemented the checks in octuple precision using the QD and ONELOOP [92] packages.

We check the validity of Eq. (5.1.2) by computing the ratio between the two sides of the equation summed over the external helicities

$$
r_{\text{collinear123}} =
$$

$$
\frac{\sum_{\lambda_i} \mathcal{M}_n^{(L,L')}(\{p_i^{\lambda_i}\})}{\sum_{k=0}^{L} \sum_{k'=0}^{L'} \sum_{\lambda_P,\lambda_P'} \mathcal{P}_{m,s;-\lambda_P,-\lambda_P'}^{(L-k,L'-k')}(-P;\{p_i\}_{i=1}^m) \, \mathcal{M}_{n-m+1,s;\lambda_P,\lambda_P'}^{(k,k')}(\{P,\{p_i\}_{i=m+1}^n\})}
$$

$$(5.6.50)$$

where $\mathcal{M}_{n,s}$ and $\mathcal{P}_{n,s}$ in the denominator are defined from $\mathcal{M}_n$ and $\mathcal{P}_n$ by summing over the external helicities:

$$
\mathcal{M}_{n-m+1;\lambda_P,\lambda_P'}^{(L,L')}(P,\{p_i\}) = \sum_{\lambda_{m+1},\dots,\lambda_n} \mathcal{M}_{n-m+1,s;\lambda_P,\lambda_P'}^{(L,L')}(P,\{p_i^{\lambda_i}\})
$$

$$
\mathcal{P}_{m;\lambda_P,\lambda_P'}^{(L,L')}(-P;\{p_i\}) = \sum_{\lambda_1,\dots,\lambda_m} \mathcal{P}_{m,s;\lambda_P,\lambda_P'}^{(L,L')}(-P;\{p_i^{\lambda_i}\}).
$$

Eq. (5.1.2) obviously implies

$$
r_{\text{collinear123}} \xrightarrow{1||2||3} 1. \tag{5.6.51}
$$

It is worth observing that the finite one-loop all-plus and all-minus four-gluon helicity amplitudes, while giving no contribution to the NLO squared matrix element, they give instead a finite contribution to $r_{\text{collinear123}}$ because of spin correlations.

In Fig. 5.4 we plot $r_{\text{collinear123}} - 1$ as a function of the invariant mass s_{123} of the three collinear partons. More in detail we verify the validity of Eq. (5.6.51) in double, double-double and double-quadruple precision for both gluon (on the left) and quark (on the right) splitting functions. As one can see, going to higher precision allowed us to make stronger checks on phase-space space points which are closer to the limit, where the numerical evaluation is highly unstable at lower floating-point precision.

Similarly, we also numerically verified Eq. (5.1.1) for each primitive amplitude and all the helicity configurations, although all of these already contribute to the check described above.
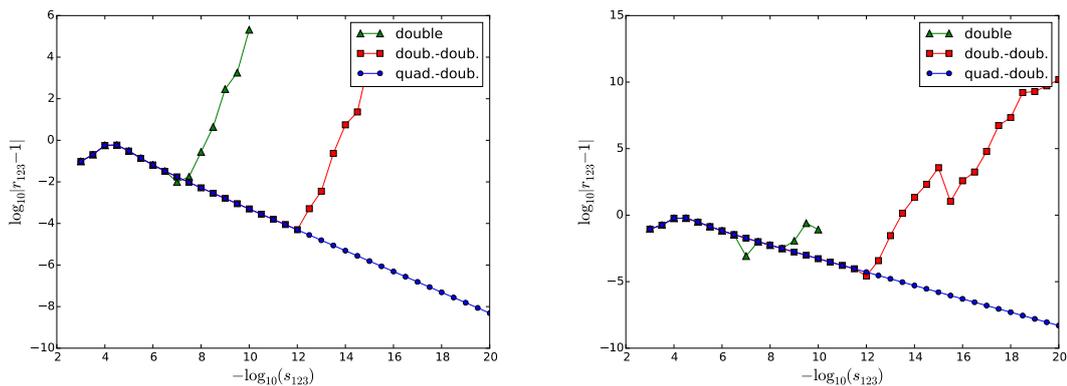
Figure 5.4: Numerical check of the collinear limit of $r_{\text{collinear123}} - 1$, with $r_{\text{collinear123}}$ defined by Eq. (5.6.50), as a function of the invariant mass s_{123}, from $s_{123} = 10^{-3}$ to $s_{123} = 10^{-20}$. For this check we set $n_f = 5$, $\sqrt{s} = 10^3$ and $\mu_R = 10^3/7$. The plot on the left shows the all-gluon case, while the one on the right shows the quark case. In the latter it was not possible to obtain numerical results in double precision for $s_{123} \leq 10^{-10}$.

As well as the numerical checks we have also verified that all splitting functions factorise correctly in the iterated collinear limit,

$$
\lim_{1||2} \text{Sp}^{(L)}(-P_{123}^{-\lambda_P}, 1^{\lambda_1}, 2^{\lambda_2}, 3^{\lambda_3})
$$
$$
= \sum_{\lambda=\pm} \sum_{k=0}^{L} \text{Sp}^{(L-k)}(-P_{\widetilde{123}}^{-\lambda_P}, \tilde{P}_{12}^{\lambda}, 3^{\lambda_3}) \text{Sp}^{(k)}(-P_{12}^{-\lambda}, 1^{\lambda_1}, 2^{\lambda_2}), \qquad (5.6.52)
$$

where the scale $s_{12} \ll s_{123}$ and $P_{\widetilde{123}} = \tilde{P}_{12} + p_3$. All di-logarithms drop out in this limit though some care should be taken to ensure the hierarchy of scales is imposed correctly.

In conclusion, we have computed the one-loop triple collinear splitting amplitudes in QCD initiated by a gluon. These functions are one of the last remaining ingredients to complete the classification of universal infrared limits relevant at N^{3}LO.

Some effort has been taken to ensure the splitting amplitudes have compact analytic forms. We made use of the spinor-helicity formalism and super-symmetric decompositions and related the pure gluonic amplitudes to the ones containing a

quark anti-quark pair. The primitive amplitude colour decomposition was also a useful tool to express full colour and helicity summed splitting functions which were all checked explicitly against the numerical matrix elements for $2 \to 4$ scattering in NJET. In the course of these checks we made use of the high precision numerical evaluation available with up to 64 digits via the QD package. This allowed us to probe deep into the collinear limit and verify that all parts of the computation behaved correctly. This was particularly important for the spin correlated and sub-leading colour corrections which are significantly suppressed.

There are still some missing ingredients needed for the constructions of a fully differential N^{3}LO subtraction scheme. Firstly, the quark initiated channels are still unavailable - they are not directly accessible from the $H + 2j$ amplitudes since they have been computed in the effective theory where the Higgs couples only to gluons. The necessary splitting amplitudes could be extracted from the vector boson plus four parton one-loop amplitudes [93].

Secondly when integrating the splitting functions over the unresolved phase space the expansion of the limit may be required to higher order in the dimensional regularisation parameter ϵ. This would require a new computation of the one-loop matrix elements valid in $D = 4 - 2\epsilon$ dimensions which is quite feasible using modern unitarity methods. The appearance of the one-loop pentagon function in the full d-dimensional amplitude may complicate this part of the computation even if it is only required in the triple collinear limit.

We hope that the expressions presented here will be of use in future high precision QCD computations.

Chapter 6

One-loop amplitudes for Higgs + five-gluon scattering in the large mass top limit

In this chapter we discuss the calculation of the one-loop amplitudes for Higgs + five-gluon scattering in the large mass top limit. The main aim is to study how the generalised unitarity method, combined with the six-dimensional spinor helicity formalism and the momentum twistor parametrisation, provides a framework suitable for the analytic calculation of high multiplicity one-loop amplitudes. Also, this process is involved in the calculation of the $pp \to H + 2\mathrm{j}$ cross section at NNLO, since the virtual-real subtraction terms get contributions from $2 \to 4$ one-loop amplitudes. We expect that such one-loop analytic expressions, which are unknown at the moment, may provide faster and stable evaluations than numerical implementations for this challenging high precision calculation.

6.1   The large top mass limit

Gluon fusion is the most relevant channel for the Higgs production at LHC. Since the SM Higgs boson does not couple to massless particles at tree-level, the processes such as $gg \to H$, at lowest order in perturbation theory, are mediated by the interaction via a closed fermion loop. The top quark is the most relevant fermion that
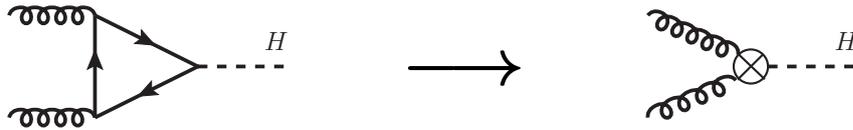
Figure 6.1: ggH effective interaction in the $m_t \to \infty$ limit.

contributes to this interaction because of its large Yukawa coupling [94]. Therefore, one can consider the approximation where the mass of the top is much larger than the mass of the Higgs and the top loop can be integrated out. The operation is schematically showed in picture 6.1. In this framework, called Higgs Effective Field Theory (HEFT), the Higgs field couples directly to the gluons while the interaction with the fermions is negligible. The HEFT has the advantage of effectively reducing the number of loops in any calculation by one. In addition, this approach is justified by the fact that, in the total inclusive cross section for the Higgs boson production, finite top quark mass effects remain very moderate at NLO accuracy. Indeed, this approximation has been used with great success to calculate a wide variety of processes. The one-loop amplitudes for Higgs plus three partons were first computed in 1997 [95], followed in the next decade by the analytic calculation of the one-loop amplitudes for Higgs plus four partons [84, 96, 97, 98, 99, 100, 101]. Such results, in addition with the numerical implementation of automated techniques for one-loop matrix elements, allowed us the study of Higgs production in association with up to three jets at NLO [102, 103, 104, 105]. Moreover, the two-loop amplitudes for Higgs plus three partons [106] were computed, enabling the calculation of the differential H+jet production at NNLO [107, 108, 109]. Also, in 2015 the inclusive Higgs production at N³LO [26, 110] was computed. A comprehensive review of the theoretical studies of the Higgs goes beyond the scope of this thesis and further details can be found in [111].

Neglecting higher mass-dimension operators, the effective Lagrangian can be written as [112],

$$\mathcal{L}_H = \frac{C}{2} H \operatorname{tr} G_{\mu\nu} G^{\mu\nu}, \tag{6.1.1}$$

where the trace is performed over the $SU(N_c)$ colour indices. The Wilson coefficient C can be computed by considering the perturbative corrections to the vertex in the l.h.s. of Fig.6.1. For one-loop applications, the Wilson coefficient is required up to order $\mathcal{O}(\alpha_s^2)$ [1] [94, 114],

$$C = \frac{\alpha_s}{6\pi v} \left(1 + \frac{11}{4\pi}\alpha_s\right) + \mathcal{O}(\alpha_s^3), \tag{6.1.2}$$

where v is the vacuum expectation value of the Higgs field.

A useful simplification can be obtained by splitting the effective Lagrangian into two terms, containing purely self-dual and purely anti-self-dual gluon field strengths, such that the amplitudes separately have a simpler structure than full one.

Following reference [115], the self-dual and anti-self-dual gluon field strength tensors are defined as,

$$G^{SD\,\mu\nu} = \frac{1}{2}\left(G^{\mu\nu} + \tilde{G}^{\mu\nu}\right), \quad G^{ASD\,\mu\nu} = \frac{1}{2}\left(G^{\mu\nu} - \tilde{G}^{\mu\nu}\right), \quad \tilde{G}_{\mu\nu} = \frac{i}{2}\epsilon^{\mu\nu\rho\sigma}G_{\rho\sigma}. \tag{6.1.3}$$

We therefore introduce a complex field ϕ, such that the Higgs represents its real component,

$$\phi = \frac{1}{2}(H + iA), \qquad \phi^\dagger = \frac{1}{2}(H - iA) \tag{6.1.4}$$

where A is an auxiliary scalar field. The effective Lagrangian splits into two pieces, one where ϕ couples with the self-dual gluon strength tensor and another where $\phi^\dagger$ couples with the anti-self-dual gluon field strength tensor,

$$\mathcal{L}_{H,A} = \frac{C}{2}\left(H\,\mathrm{tr}\,G_{\mu\nu}G^{\mu\nu} + iA\,\mathrm{tr}\,G_{\mu\nu}\tilde{G}^{\mu\nu}\right) = \tag{6.1.5}$$

$$= C\left(\phi\,\mathrm{tr}\,G_{SD\,\mu\nu}G^{SD\,\mu\nu} + \phi^\dagger\,\mathrm{tr}\,G_{ASD\,\mu\nu}G^{ASD\,\mu\nu}\right). \tag{6.1.6}$$

The Feynman rules obtained from the effective Lagrangian are given in Appendix A.

---

[1] The Wilson coefficient is known up to four-loop accuracy [113].

The advantage given by this effective Lagrangian is that the amplitudes for ϕ and $\phi^\dagger$ are simpler than the amplitudes for the H, which can be reconstructed at the end using the relation,

$$A^{(L)}(H, \{p_n\}) = A^{(L)}(\phi, \{p_n\}) + A^{(L)}(\phi^\dagger, \{p_n\}), \qquad (6.1.7)$$

because $H = \phi + \phi^\dagger$ from Eq. (6.1.4). Moreover the amplitudes for the $\phi^\dagger$ and n gluons are related with the amplitudes for ϕ by parity,

$$A^{(L)}(\phi^\dagger, 1_g^{\lambda_1}, 2_g^{\lambda_2}, \ldots, n_g^{\lambda_n}) = \left(A^{(L)}(\phi, 1_g^{-\lambda_1}, 2_g^{-\lambda_2}, \ldots, n_g^{-\lambda_n}) \right)^*. \qquad (6.1.8)$$

For this reason we will focus on the calculation of the ϕ amplitudes only.

6.2 Parametrisation of the kinematics and colour decomposition

We now introduce the kinematic parametrisation used to represent the process involving the ϕ field and five gluons. All the momenta are considered outgoing,

$$p_\phi + \sum_{i=1}^{5} p_i = 0, \qquad (6.2.9)$$

where the p_i are massless $p_i^2 = 0$. Since the Higgs particle is massive, we use the massless decomposition discussed in Section 3.2,

$$p_\phi^\mu = p_\phi^{\flat\,\mu} + \frac{m_H^2}{2 p_\phi^\flat \cdot \eta} \eta^\mu \qquad (6.2.10)$$

with $p_\phi^\flat$ and η massless vectors. The massless decomposition turns out to be useful in order to embed p_ϕ into the momentum twistor representation [2]. The momentum twistor parametrisation of Section 3.3 is employed to parametrise the amplitudes.

---

[2] The two massless momenta $p_\phi^\flat$ and η can be also interpreted as the decay products of the Higgs. However we will not discuss this connection, since it is irrelevant for our calculation. A

We generate a phase-space point including the massless decomposition of the Higgs which involves 7 particles. This parametrisation contains 11 variables but is reduced to 9, since we can fix the direction of the momentum of the Higgs. We fix the direction of p_ϕ by imposing $\eta = p_2$ and the momentum twistor parametrisation takes the form,

$$
Z = \begin{pmatrix}
1 & 0 & q_1 & q_2 & q_3 & q_4 & 0 \\
0 & 1 & 1 & 1 & 1 & 1 & 1 \\
0 & 0 & 0 & \frac{z_5}{z_2} & 1 - \frac{m_H^2 z_5}{z_1 z_2 z_3 z_4 (-z_5 + z_8 + z_5 z_7)} & 1 & 1 \\
0 & 0 & 1 & 1 & z_6 & z_7 & 1 - \frac{z_8}{z_5}
\end{pmatrix}
\tag{6.2.11}
$$

which is given in terms of the nine parameters $z_1, \ldots, z_8$ and m_H^2 and $q_k = \sum_{i=1}^{k} \left(\Pi_{j=1}^{i} z_j \right)^{-1}$. The columns of the Z matrix correspond to the momenta $p_1, \ldots, p_5, p_\phi^\flat, \eta$. The momentum twistor variables z can be written in terms of the external momenta as,,

$$
z_1 = s_{12}, \qquad\qquad z_2 = \frac{\langle 23 \rangle \langle 14 \rangle}{\langle 12 \rangle \langle 34 \rangle}, \qquad z_3 = \frac{\langle 34 \rangle \langle 15 \rangle}{\langle 13 \rangle \langle 45 \rangle},
$$

$$
z_4 = \frac{\langle 45 \rangle \langle 16 \rangle}{\langle 14 \rangle \langle 56 \rangle}, \qquad\qquad z_5 = \frac{s_{23}}{s_{12}}, \qquad z_6 = \frac{\langle 1(2+3)(2+3+4)51]}{s_{23} s_{15}},
$$

$$
z_7 = \frac{\langle 1(2+3)(2+3+4+5)p_\phi 2]}{s_{23} \langle 1 p_\phi 2]}, \qquad z_8 = \frac{s_{123}}{s_{12}}, \qquad m_H^2 = s_{12345}.
\tag{6.2.12}
$$

We use the parametrisation discussed above to compute all the independent one-loop helicity amplitudes in dimensional regularisation. Firstly, we consider the colour decomposition of such amplitudes. Since the Higgs is colourless, the colour dressed amplitudes $\mathcal{A}_6^{(L)}(\phi, 1_g^{\lambda_1}, 2_g^{\lambda_2}, 3_g^{\lambda_3}, 4_g^{\lambda_4}, 5_g^{\lambda_5})$ have the same colour decomposition of pure gluons amplitudes [97, 115]. Therefore, we can focus on computing the colour ordered amplitudes, considering a set of independent helicity configurations.

---

similar and more interesting case is studied in Section 8.1.
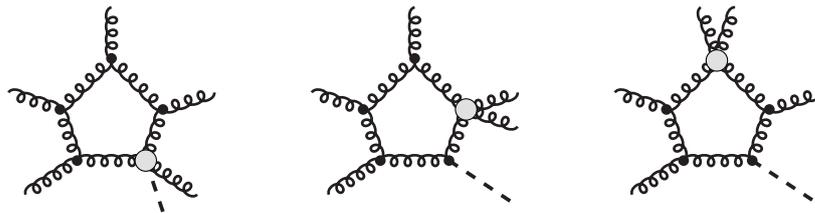
Figure 6.2: Example of pentagon topologies for the Higgs plus five-gluon one-loop amplitudes.

6.3   Results and discussion

We computed the un-renormalised one-loop helicity amplitudes using the generalised unitarity method described in Section 4.3.4. The momenta are embedded in six dimensions and are represented using the six dimensional spinor-helicity formalism. The six dimensional spinors are parametrised using the momentum twistor parametrisation described in the previous section. The tree-level building-blocks are generated using the six dimensional BCFW of Section 4.1. Indeed, since the Higgs enters as an external off-shell scalar particle, the BCFW recursion relation can be easily implemented in analogy with the pure gluon amplitudes.

The algorithm of the integrand reduction consist of the same steps described in the example of Section 4.3.4. We compute all the coefficients of the d-dimensional integrand decomposition (4.3.56), starting from the 25 different pentagon maximal cuts. Examples of them are shown in Figure 6.2. Finally, we keep arbitrary the spin dimension d_s in the dimensional reduction of (4.3.68) in order to cover different regularisation schemes.

After expanding in ϵ the integral basis of Eq. (4.3.57), one can confirm the universal infrared pole structure of the un-renormalized amplitudes, which is given by [97],

$$I_6(\phi, 1_g^{\lambda_1}, 2_g^{\lambda_2}, 3_g^{\lambda_3}, 4_g^{\lambda_4}, 5_g^{\lambda_5}) = -A_6^{(0)}(\phi, 1_g^{\lambda_1}, 2_g^{\lambda_2}, 3_g^{\lambda_3}, 4_g^{\lambda_4}, 5_g^{\lambda_5})\frac{1}{\epsilon^2}\left(\sum_{i=1}^{5}\left(\frac{\mu^2}{-s_{i(i+1)}}\right)^{\epsilon}\right).$$

$$(6.3.13)$$

The same expression is also valid for the $\phi^\dagger$ and the H amplitudes, considering the appropriate tree-level. Due to the Wilson coefficient (6.1.2) of the effective Lagrangian, in the universal pole structure [116], the ultraviolet divergent term cancel against the gluon anomalous dimension, then no overall $1/\epsilon$ poles appear in addition to the one of (6.3.13). As a consequence a relation among the bubble coefficients [84] exists,

$$\sum_{1 \le i_1 < i_2 \le 6} c_{i_1, i_2} = 0, \tag{6.3.14}$$

which is useful in order to avoid the direct calculation of the bubble with the eight gluon tree-level building-block, reducing the degree of complexity of the calculation.

The six dimensional cuts discussed so far have been used to compute the primitive amplitudes for exact numerical kinematics. While this method could be extended to analytic calculations using the finite field reconstruction technique [30], at the present time our MATHEMATICA algorithm produced large algebraic functions of the nine variables that were too difficult to factorise. We therefore leave the complete analytic reconstruction for future work.

As benchmark, we provide numerical values for the physical Higgs and the self-dual Higgs helicity amplitudes at a given phase-space point. We generate the phase-space point by using the momentum twistor parametrisation in Eq. (6.2.11). We choose the following rational values for the momentum twistor variables,

$$
\begin{aligned}
z_1 &= 1, & z_2 &= 50/43, \\
z_3 &= 32/43, & z_4 &= 10/13, \\
z_5 &= 13/46, & z_6 &= 19/28, \\
z_7 &= 26/17, & z_8 &= 29/48, \\
m_H^2 &= 1/64 &
\end{aligned}
\tag{6.3.15}
$$

In Table 6.1 we present the result for the ratio of one-loop helicity amplitudes

to the corresponding tree-level. We define the ratio as,

$$r^{(1)} = \frac{1}{c_\Gamma} \frac{A^{(1)}}{A^{(0)}} = \frac{r_2}{\epsilon^2} + \frac{r_1}{\epsilon} + r_0 + \mathcal{O}(\epsilon) \qquad (6.3.16)$$

The ϵ pole matches with the one in Eq. (6.3.13). We also split the finite piece distinguishing the term proportional to $d_s - 2$,

$$r_0 = r_{0;0} + (d_s - 2) \, r_{0;d_s}. \qquad (6.3.17)$$

We write the results rounding the rational numbers up to the eighth decimal digit. The scalar integrals have been evaluated with the public QCDLoop fortran package based on [73].

$A(\phi, 1, 2, 3, 4, 5)$	$A^{(0)}$	r_2	r_1	$r_{0;0}$	$r_{0;d_s}$
$+ + + + +$	$-$	$-$	$-$	0.00073696	-0.000122827
$- + + + +$	$-$	$-$	$-$	$-0.63024404 - 0.32277279i$	$0.093616354 + 0.16138639i$
$- - + + +$	$-0.00024565i$	5	$9.42477796 + 10.59771489i$	$66.71557778 - 33.07680365i$	$0.10944284 + 0.84344350i$
$- + - + +$	$-0.00024565i$	5	$9.42477796 + 10.59771489i$	$79.45268537 - 1.108544465i$	$3.17009873 + 2.6701051i$
$- - - - -$	$-0.00024565i$	5	$9.42477796 + 10.59771489i$	$80.47749789 - 34.95658021i$	$4299.599244i$
$+ - - - -$	$-0.00024565i$	5	$9.42477796 + 10.59771489i$	$29.37474449 - 30.11559451i$	$0.23234002 - 0.63732483i$
$+ + - - -$	$-0.00024565i$	5	$9.42477796 + 10.59771489i$	$91.59756458 - 25.41850817i$	$7.33913140 + 3.05921981i$
$+ - + - -$	$-0.00024565i$	5	$9.42477796 + 10.59771489i$	$62.3022456 - 49.74619103i$	$0.060812228 - 0.095965525i$
$A(H, 1, 2, 3, 4, 5)$	$A^{(0)}$	r_2	r_1	$r_{0;0}$	$r_{0;d_s}$
$+ + + + +$	$-0.00024565i$	5	$9.42477796 + 10.59771489i$	$80.47749789 - 31.95658021i$	$324.8576271i$
$- + + + +$	$0.21670076i$	5	$9.42477796 + 10.59771489i$	$15.39354755 - 5.15456235i$	$0.69230813 + 1.9806648i$
$- - + + +$	$-1.13445397i$	5	$9.42477796 + 10.59771489i$	$71.73522074 - 30.52078016i$	$0.28723277 - 0.55810797i$
$- + - + +$	$-7.78522163i$	5	$9.42477796 + 10.59771489i$	$69.25972153 - 28.23463144i$	$0.3740289 + 0.45413157i$

Table 6.1: Numerical results for the tree-level and one loop helicity amplitudes. The one-loop amplitudes are evaluated at the phase-space point in Eq. (6.3.15) and at the renormalisation scale $\mu_R^2 = 2m_H^2$. We do not include closed fermion loop contributions. For the helicity configurations with zero tree-level, the ratio is replaced by the value of the corresponding one-loop amplitude.

In conclusion, we have implemented an algebraic framework for the calculation of analytic one-loop scattering amplitudes in dimensional regularisation, based on six dimensional generalised unitarity cuts. We tested it on a high multiplicity process with non-trivial kinematic such as Higgs plus five gluons in the large top mass

effective theory. We combined the momentum twistor representation of Eq. (6.2.11) with the six dimensional spinor-helicity formalism and implemented an algorithm suitable for evaluations with rational numerics.

Chapter 7

A unitarity compatible approach to one-loop amplitudes with massive fermions

In this chapter we explain how one-loop amplitudes with massive fermions can be computed using only on-shell information. We first use the spinor-helicity formalism in six dimensions to perform generalised unitarity cuts in d dimensions. We then show that divergent wavefunction cuts can be avoided, and the remaining ambiguities in the renormalised amplitudes can be fixed, by matching to universal infrared poles in $4 - 2\epsilon$ dimensions and ultraviolet poles in $6 - 2\epsilon$ dimensions. In the latter case we construct an effective Lagrangian in six dimensions and reduce the additional constraint to an on-shell tree-level computation. The main results are based on reference [2].

7.1 Amplitudes with massive fermions

The current precision level of predictions is in relatively good shape in matching the experimental uncertainties, with top quark pair production now known differentially at NNLO in QCD [117, 118] and a full range of off-shell decays known at NLO in QCD with an additional jet [119]. Modern one-loop techniques are also able to explore high multiplicity final states where the current state-of-the-art is

top quark pair production in association with three jets [120]. The GoSam collaboration has also been able to produce NLO predictions for the challenging $t\bar{t}H + j$ final state [121]. A more complete overview of the current status can be found in reference [50].

On the other hand, these processes are often overlooked by more formal studies of amplitudes in gauge theory which can uncover hidden simplicity and structure. While it is well known that on-shell techniques like unitarity (see Section 4.2), spinor integration [122, 123] and BCFW recursion apply equally well to massive amplitudes, explicit computations are relatively few [60, 124, 125]. Nevertheless some computations using these approaches have produced compact analytic results useful for phenomenological applications [125, 126]. While elements of these computations use unitarity cuts and on-shell trees, Feynman diagrams techniques were also employed to compute the UV counterterms necessary for mass and wavefunction renormalisation. To the best of our knowledge the only computations not to do this are those with a massive internal loop where a UV matching prescription was used [78, 124].

The obstacle is that the traditional approach to renormalisation requires the amputation of wavefunction graphs, and the addition of counterterm diagrams. This procedure breaks gauge invariance during intermediate steps and therefore causes problems for methods based on (generalised) unitarity [10, 11, 127], which construct amplitudes from on-shell tree-level building blocks. Naive attempts to amputate wavefunction graphs in generalised unitarity are precluded by the presence of an on-shell propagator, leading to a factor $1/0$: this is depicted explicitly in figure 7.1, where the on-shell tree amplitude appearing on the right hand side of a two-particle cut is expanded to reveal a divergent propagator inside. Consequently, the favoured method is still to follow an approach based on Feynman diagrams; then the amputation of wavefunction graphs is straightforward.

Two solutions to this problem have been proposed. Ellis, Giele, Kunszt and Melnikov showed that modifying the tree-level input entering the double cuts of the wavefunction graphs allowed a simple implementation of the on-shell renormalisation scheme [31]. All cuts can then be performed but gauge invariance is only

restored at the end of the computation. Since the removal of the unwanted graphs is extremely easy to implement within a Berends-Giele construction of the tree-level amplitudes in the cuts this method is quite efficient numerically. A second solution, proposed by Britto and Mirabella [32], is to regulate the divergent tree by introducing a momentum shift. This procedure allows us to preserve gauge invariance but introduces an additional variable into the calculation which will cancel when combined with the mass-renormalisation counterterms. In either case a set of extra two- and single-particle cuts is necessary together with the counterterms to fully determine the amplitude in comparison to the massless case.

Despite both of these solutions there is still an open question: is it possible to compute amplitudes with masses using only on-shell gauge invariant building blocks and without introducing additional regulators. Both of the approaches mentioned above follow the on-shell renormalisation scheme where divergences can be absorbed into additional terms in the Lagrangian. In this chapter we will explore an alternative way to absorb the divergences by appealing to an effective six dimensional version of QCD.

This procedure relies on first computing a full set of finite d-dimensional unitarity cuts. We show how this can be done efficiently in the six-dimensional spinor-helicity formalism by embedding the additional mass into the higher dimensions and performing cuts in six dimensions. In particular we show how these results can be dimensionally reduced to d-dimensional amplitudes keeping the spin dimension of the gluon d_s arbitrary.[1] This generalises the previous approaches used for massless

---

[1]The distinction between the spin dimension, d_s, and spacetime dimension, d, is motivated by different regularisation schemes. We find it to be very convenient to maintain the distinction
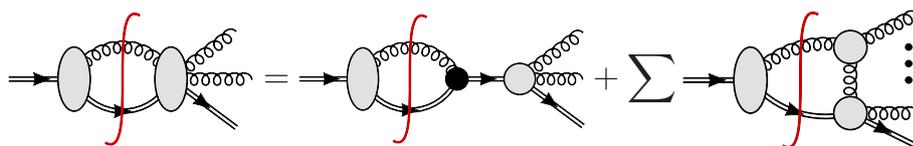
Figure 7.1: Decomposing the tree amplitude appearing on the left hand side the equation reveals a divergent graph.

cuts in six-dimensions [68, 81].

7.2 QCD one-loop amplitudes and integrands with massive fermions

In this section we discuss the one-loop integrand parametrisations in d dimensions for QCD one-loop amplitudes with one massive fermion flavour. In this case there are only two possible basis integrals which go beyond those appearing in the massless case,

$$A_n^{(1)} = B_n^{(1)} + c_{2;m^2} I_{2,m^2} + c_1 I_1. \tag{7.2.1}$$

The amplitude labelled $B_n^{(1)}$ is the part that can be constructed from finite d-dimensional unitarity cuts. The additional basis integrals depend only on the fermion mass and in dimensional regularisation are,

$$I_{2,m^2} = \mu_R^{2\epsilon} \int \frac{d^d k}{(2\pi)^d} \frac{1}{k^2((k-p)^2 - m^2)} \overset{d=4-2\epsilon}{=} ic_\Gamma \left(\frac{1}{\epsilon} + \log\left(\frac{\mu_R^2}{m^2}\right) + 2 \right) + \mathcal{O}(\epsilon),$$
$$\tag{7.2.2}$$

$$I_1 = \mu_R^{2\epsilon} \int \frac{d^d k}{(2\pi)^d} \frac{1}{k^2 - m^2} \overset{d=4-2\epsilon}{=} ic_\Gamma m^2 \left(\frac{1}{\epsilon} + \log\left(\frac{\mu_R^2}{m^2}\right) + 1 \right) + \mathcal{O}(\epsilon), \tag{7.2.3}$$

where $c_\Gamma = \frac{\Gamma(1+\epsilon)\Gamma(1-\epsilon)^2}{(4\pi)^{2-\epsilon}\Gamma(1-2\epsilon)}$.

The amplitudes $B_n^{(1)}$ can be written in the usual integrand basis of irreducible scalar products including extra dimensional terms following the constructions in

---

throughout our calculations. To be clear, we define the spin dimension such that the gluon has $d_s - 2$ physical polarization states.

Eq. (4.3.48),

$$B_n^{(1)} = \mu_R^{2\epsilon} \int \frac{d^d k}{(2\pi)^d} \Biggl\{$$

$$\sum_{1 \le i_1 < i_2 < i_3 < i_4 < i_5 \le n} \frac{\Delta_{\{i_1, i_2, i_3, i_4, i_5\}}}{D_{i_1} D_{i_2} D_{i_3} D_{i_4} D_{i_5}} + \sum_{1 \le i_1 < i_2 < i_3 < i_4 \le n} \frac{\Delta_{\{i_1, i_2, i_3, i_4\}}}{D_{i_1} D_{i_2} D_{i_3} D_{i_4}}$$

$$+ \sum_{1 \le i_1 < i_2 < i_3 \le n} \frac{\Delta_{\{i_1, i_2, i_3\}}}{D_{i_1} D_{i_2} D_{i_3}} + \sum_{\substack{1 \le i_1 < i_2 \le n \\ i_2 - i_1 \bmod n > 1}} \frac{\Delta_{\{i_1, i_2\}}}{D_{i_1} D_{i_2}} \Biggr\}. \tag{7.2.4}$$

For renormalisable gauge theories a complete parametrisation of the numerators is given in Eq. (4.3.56). After elimination of vanishing integrals over the spurious directions, the d-dimensional representation of the amplitude is,

$$B_n^{(1)}(d, d_s) = \sum_{1 \le i_1 < i_2 < i_3 < i_4 < i_5 \le n} c_{i_1, i_2, i_3, i_4, i_5}^{(0)} I_{i_1, i_2, i_3, i_4, i_5}^d[\mu^2]$$

$$+ \sum_{1 \le i_1 < i_2 < i_3 < i_4 \le n} c_{i_1, i_2, i_3, i_4}^{(0)} I_{i_1, i_2, i_3, i_4}^d[1] + c_{i_1, i_2, i_3, i_4}^{(2)} I_{i_1, i_2, i_3, i_4}^d[\mu^2] + c_{i_1, i_2, i_3, i_4}^{(4)} I_{i_1, i_2, i_3, i_4}^d[\mu^4]$$

$$+ \sum_{1 \le i_1 < i_2 < i_3 \le n} c_{i_1, i_2, i_3}^{(0)} I_{i_1, i_2, i_3}^d[1] + c_{i_1, i_2, i_3}^{(9)} I_{i_1, i_2, i_3}^d[\mu^2]$$

$$+ \sum_{\substack{1 \le i_1 < i_2 \le n \\ i_2 - i_1 \bmod n > 1}} c_{i_1, i_2}^{(0)} I_{i_1, i_2}^d[1] + c_{i_1, i_2}^{(9)} I_{i_1, i_2}^d[\mu^2], \tag{7.2.5}$$

where we use the same notation as in Eq. (4.3.58).

7.3   Generalised unitarity cuts in six dimensions

To illustrate our method we consider two gauge invariant primitive amplitudes relevant for the $gg \to t\bar{t}$ one-loop scattering amplitude. Helicity amplitudes for this process have been previously presented in reference [60]. Using the usual colour decomposition [91] we define the ordered partial amplitudes $A_{4;1}^{(1)}$ and $A_{4;3}^{(1)}$ by,

$$\mathcal{A}^{(1)}\left(1_t, 2, 3, 4_{\bar{t}}\right) = \sum_{P(2,3)} (T^{a_2} T^{a_3})_{i_1}^{\bar{i}_4} A_{4;1}^{(1)}\left(1_t, 2, 3, 4_{\bar{t}}\right) + \mathrm{tr}\,(T^{a_2} T^{a_3})\, \delta_{i_1}^{\bar{i}_4} A_{4;3}^{(1)}\left(1_t, 4_{\bar{t}}; 2, 3\right),$$

$$\tag{7.3.6}$$

where $P(2,3)$ is the permutations over the order of gluons. These partial amplitudes can be further decomposed into gauge invariant primitive amplitudes,

$$A_{4;1}^{(1)}\left(1_t, 2, 3, 4_{\bar{t}}\right) = N_c A^{[L]}\left(1_t, 2, 3, 4_{\bar{t}}\right) - \frac{1}{N_c} A^{[R]}\left(1_t, 2, 3, 4_{\bar{t}}\right)$$
$$- N_f A^{[f]}\left(1_t, 2, 3, 4_{\bar{t}}\right) - N_H A^{[H]}\left(1_t, 2, 3, 4_{\bar{t}}\right), \tag{7.3.7}$$
$$A_{4;3}^{(1)}\left(1_t 4_{\bar{t}}; 2, 3\right) = \sum_{P(2,3)} \left(A^{[L]}\left(1_t, 2, 3, 4_{\bar{t}}\right) + A^{[L]}\left(1_t, 2, 4_{\bar{t}}, 3\right) + A^{[R]}\left(1_t, 2, 3, 4_{\bar{t}}\right)\right),$$
$$\tag{7.3.8}$$

where N_c is the number of colours, while N_f and N_H are the number of light and heavy fermion flavours, respectively. The left-moving $A^{[L]}$ and right-moving $A^{[R]}$ primitive amplitudes are labelled according to the direction of the fermion current as it enters the loop, following the convention of reference [91]. Representative diagrams for these amplitudes are shown in figure 7.2. We will not consider the fermion loop contributions $A^{[f]}$ and $A^{[H]}$ in this discussion as they do not present any further technical difficulties.

Each primitive amplitude can be decomposed at the integrand level into the basis of integrals described in Section 7.2. To capture the full d-dimensional dependence, we first compute generalised cuts in six dimensions using the spinor-helicity formalism described in Section 3.2. We then compute the two additional scalar loop contributions and perform the state sum reduction onto a general dimension d. The complete set of generalised cuts needed for the amputated primitives $B^{[L]}$ and $B^{[R]}$, c.f. $B_n^{(1)}$ in equation 7.2.1, are shown in Fig. 7.3 and 7.4, in which the divergent two-particle and one-particle cuts are removed.

Figure 7.2: Configurations for left- and right-moving primitive amplitudes contributing to $gg \to t\bar{t}$ scattering.
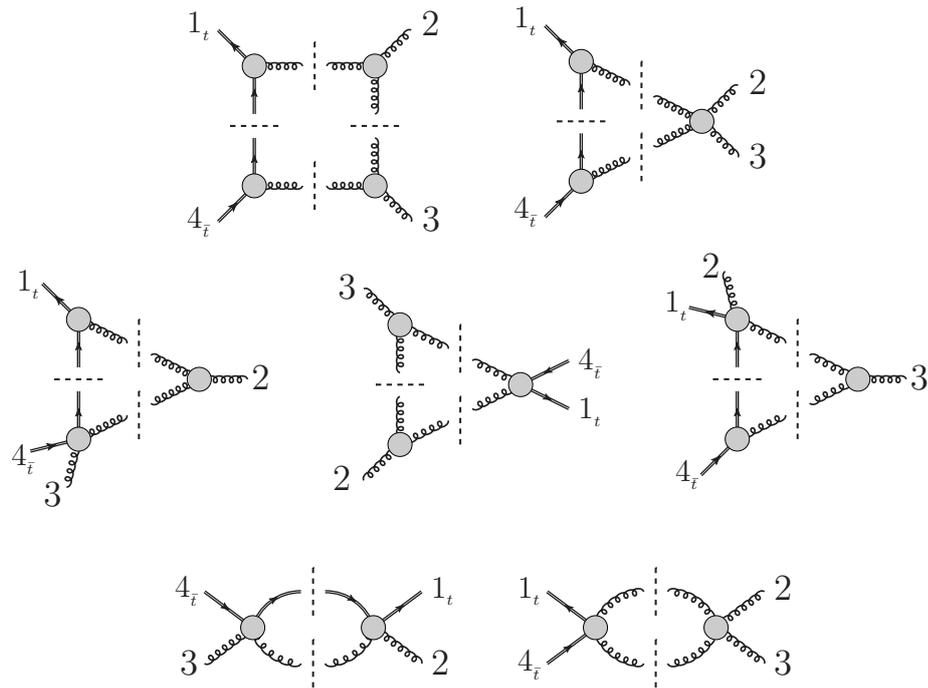
Figure 7.3: The complete set of cuts for $B^{[L]}(1_t, 2, 3, 4_{\bar{t}})$. Double lines represent massive fermions.
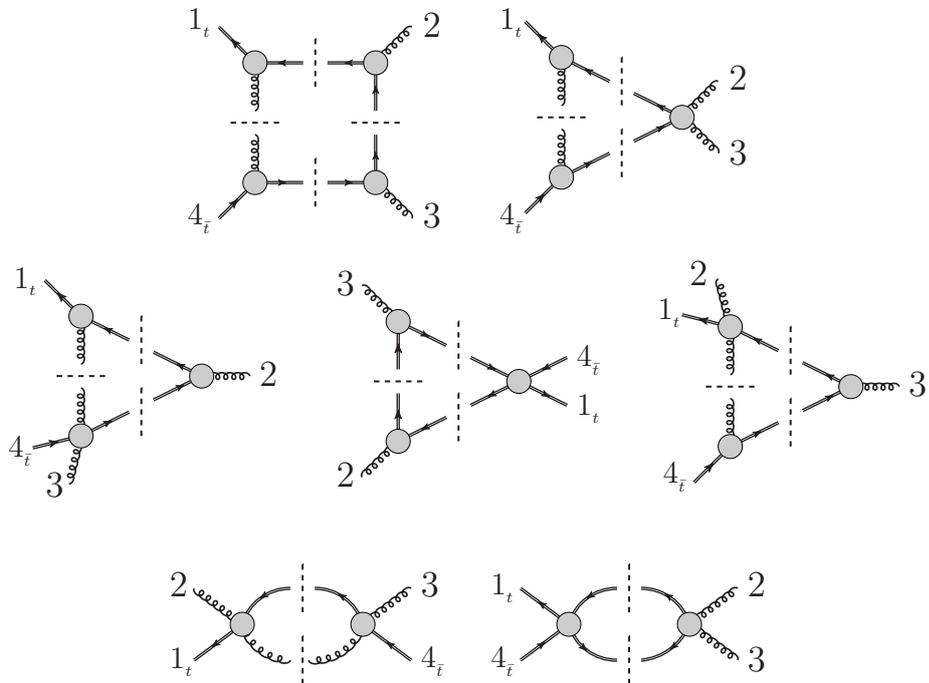
Figure 7.4: The complete set of cuts for $B^{[R]}(1_t, 2, 3, 4_{\bar{t}})$. Double lines represent massive fermions.

Each six-dimensional cut is associated with a set of loop momenta ℓ_i which enter the tree-level amplitudes. These momenta are determined by solving the system of on-shell equations $\{\ell_i^2 = 0, i \in S\}$. The complete set of loop momenta for our ordered amplitudes are labelled as,

$$\ell_i^\mu \equiv \ell_0^\mu - P_i^\mu, \qquad P_i^\mu = \sum_{n=1}^{i} p_n^\mu,$$

$$\ell_0^\mu \equiv k^\mu, \tag{7.3.9}$$

where p_n^μ are the external momenta and k is the loop integration momentum.

The internal particles are embedded into six dimensions by allowing the mass to flow in the sixth component, following our convention in eq. (3.2.52), and the $(d-4)$ part of the loop momentum to flow in the fifth component,

$$\text{gluon loop momentum:} \quad \ell = \{\bar{\ell}, \mu, 0\},$$

$$\text{fermion loop momentum:} \quad \ell = \{\bar{\ell}, \mu, m\}. \tag{7.3.10}$$

The gluon and fermion loop propagators can then be expanded into a four-dimensional part and an effective mass term μ^2,

$$\text{gluon propagator:} \quad \ell^2 = \bar{\ell}^2 - \mu^2, \tag{7.3.11}$$

$$\text{fermion propagator:} \quad \ell^2 = \bar{\ell}^2 - \mu^2 - m^2. \tag{7.3.12}$$

This choice is particularly convenient when requiring momentum conservation and orthogonality of the -2ϵ component with respect to the external massive fermion momenta expressed in the six dimensional representation, as shown in figure 7.5.

As an explicit example we will describe the computation of the quadruple cuts. The on-shell equations for these cuts in the left- and right-moving configurations

$(\bar{p}_1, 0, m)$ $(\bar{\ell}_1, \mu, -m)$ $(\bar{\ell}_0, \mu, 0)$
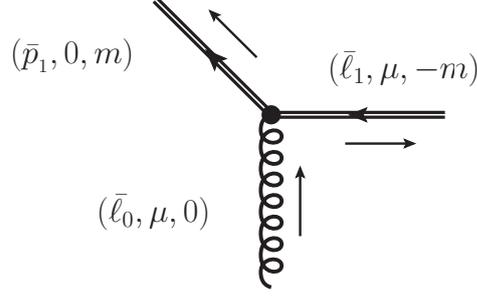
Figure 7.5: To perform the unitarity cuts of the six dimensional propagators involving internal fermions, we allow the $(d - 4)$ part, μ, of the loop momentum to flow in the fifth component and the mass term to flow in the sixth component, in order to easily impose momentum conservation.

are,

$$
S^L_{4;0123} = \begin{cases} \ell_0^2 = \ell_1^2 = \ell_2^2 = \ell_3^2 = 0 \\ \ell_0^{(5)} = m \end{cases} \qquad , \qquad S^R_{4;0123} = \begin{cases} \ell_0^2 = \ell_1^2 = \ell_2^2 = \ell_3^2 = 0 \\ \ell_0^{(5)} = 0 \end{cases} .
$$

$$(7.3.13)$$

The constraint on the sixth component of the loop momentum ℓ_0 distinguishes between the two different configurations. The explicit solutions for the six-dimensional spinors of ℓ_i are given in Appendix E.

On the quadruple cut the amplitudes factorise into products of four tree-level amplitudes,

$$
C^L_{4;0123} = A(-\ell_{0a}, 1_t^\alpha, \ell_1^{b\dot{b}}) A(-\ell_{1b\dot{b}}, 2^{\beta\dot{\beta}}, \ell_2^{c\dot{c}}) A(-\ell_{2c\dot{c}}, 3^{\gamma\dot{\gamma}}, \ell_3^{d\dot{d}}) A(-\ell_{3d\dot{d}}, 4_t^\delta, \ell_0^a),
$$

$$(7.3.14)$$

and

$$
C^R_{4;0123} = A(-\ell_{0a\dot{a}}, 1_t^\alpha, \ell_1^b) A(-\ell_{1b}, 2^{\beta\dot{\beta}}, \ell_2^c) A(-\ell_{2c}, 3^{\gamma\dot{\gamma}}, \ell_3^d) A(-\ell_{3d}, 4_t^\delta, \ell_0^{a\dot{a}}),
$$

$$(7.3.15)$$

where in both cases the repeated $SU(2)$ spinor indices are summed over the six dimensional polarisation states.

The integrand reduction method then proceeds to extract the five independent coefficients in the integrand parametrisation from eq. (4.3.57) by evaluating both the product of trees and the irreducible scalar products μ^2 and $k \cdot w_{1;123}$, as described in Section 4.3.3. We encounter an interesting subtlety when following this procedure since the six-dimensional cut contains additional terms which are linear in the extra-dimensional component of the loop momentum μ. These terms are spurious and integrate to zero, but require additional coefficients to be added at the integrand level if this direct approach is taken. A slightly simpler approach is to cancel the linear part of the cut by averaging over the two different flows of the momentum in the fifth component,

$$\frac{1}{2} \left(C_{4;0123}\big|_{S_{4;0123}^+} + C_{4;0123}\big|_{S_{4;0123}^-} \right) = \Delta_{\{0,1,2,3\}}\big|_{S_{4;0123}}, \qquad (7.3.16)$$

where

$$S^+ = \left\{ \ell_i^2 = 0, \ell_i = \{\ldots, \mu, \ldots\} \right\}, \quad S^- = \left\{ \ell_i^2 = 0, \ell_i = \{\ldots, -\mu, \ldots\} \right\}. \qquad (7.3.17)$$

The triangle and bubble coefficients follow using the OPP method to systematically remove all singularities from the cut amplitude using the previously computed irreducible numerators. The mass dependence of the propagators is now dictated by six dimensional momentum conservation applied to the loop momenta, so all propagators are simply ℓ_i^2. To remove the terms linear in μ, we average over the two

directions for the extra-dimensional component, as described above. Thus,

$$\frac{1}{2}\sum_{\sigma=\pm} C_{4;0123}\Big|_{S^{\sigma}_{4;0123}} = \Delta_{\{0,1,2,3\}}\Big|_{S_{4;0123}},$$

$$(7.3.18a)$$

$$\frac{1}{2}\sum_{\sigma=\pm} C_{3;012}\Bigg|_{S^{\sigma}_{3;012}} - \frac{\Delta_{\{0,1,2,3\}}}{\ell_3^2}\Bigg|_{S_{3;012}} = \Delta_{\{0,1,2\}}\Big|_{S_{3;012}},$$

$$(7.3.18b)$$

$$\frac{1}{2}\sum_{\sigma=\pm} C_{2;02}\Bigg|_{S^{\sigma}_{3;02}} - \left(\frac{\Delta_{\{0,1,2\}}}{\ell_1^2} + \frac{\Delta_{\{0,2,3\}}}{\ell_3^2} + \frac{\Delta_{\{0,1,2,3\}}}{\ell_1^2\ell_3^2}\right)\Bigg|_{S_{2;02}} = \Delta_{\{0,2\}}\Big|_{S_{2;02}}, \quad (7.3.18c)$$

where the parametrisations for each irreducible numerator are those of equation (4.3.56). The remaining triple and double cuts follow by permuting the equations (7.3.18). Further details on the on-shell cut solutions are given in Appendix E.

The final step to dimensionally reduce the coefficients from 6 to a general dimension d is to remove the extra degrees of freedom contained in the six dimensional loop momentum. However, the dimension reduction formula in Eq. (4.3.68) needs to be modified, given our convention in Eq. (7.3.10). Indeed, according to [72, 81] and Section 4.3.4, gluons in six dimensions have $6 - 2 = 4$ polarisation states, so for each extra dimension introduced we get one more state. Each of these states corresponds to the contribution from replacing gluons in the loop by a scalar. In our set-up for massive fermions, the scalar associated with the mass direction should be subtracted separately and we arrive at the state-sum reduction prescription,

$$\boldsymbol{c} = \boldsymbol{c}^{6d} - (5 - d_s)\boldsymbol{c}_{\phi_1} - \boldsymbol{c}_{\phi_2}, \tag{7.3.19}$$

where ϕ_1 and ϕ_2 are associated to the last two entries of the six dimensional gauge field. The complete derivation of Eq. (7.3.19) is given in Appendix C.

The computation of these extra cuts is done using the same procedure as above, but the internal gluon lines in figures 7.3 and 7.4 are replaced with scalar lines. For

example, the quadruple cuts are given by the following expressions

$$C_{4;0123}^{L,\phi_{(1,2)}} = A(-\ell_{0\dot{a}}, 1_t^\alpha, \ell_1) A(-\ell_1, 2^{\beta\dot{\beta}}, \ell_2) A(-\ell_2, 3^{\gamma\dot{\gamma}}, \ell_3) A(-\ell_3, 4_{\dot{t}}^\delta, \ell_0^{\dot{a}}), \qquad (7.3.20)$$

$$C_{4;0123}^{R,\phi_{(1,2)}} = A(-\ell_0, 1_t^\alpha, \ell_1^{\dot{b}}) A(-\ell_{1\dot{b}}, 2^{\beta\dot{\beta}}, \ell_2^{\dot{c}}) A(-\ell_{2\dot{c}}, 3^{\gamma\dot{\gamma}}, \ell_3^{\dot{d}}) A(-\ell_{3\dot{d}}, 4_{\dot{t}}^\delta, \ell_0). \qquad (7.3.21)$$

The relevant six dimensional trees are given in appendix B.1.

7.4 Determining the remaining integral coefficients

At this point, let us pause to take stock of what has been achieved, and what remains to be done. To do so, we return to equation (7.2.1), the standard expression for a one-loop amplitude, expanded in a basis of scalar integrals:

$$A_n^{(1)} = B_n^{(1)} + c_{2;m^2} I_{2,m^2} + c_1 I_1. \qquad (7.4.22)$$

By definition, $B_n^{(1)}$ is the part of the amplitude which can be computed using finite d-dimensional unitarity cuts; its expansion in terms of an integral basis was explicitly given in equation (4.3.48). We have therefore computed $B_n^{(1)}$ explicitly in section 7.3. A complete construction of the amplitude requires us to find the integral coefficients $c_{2;m^2}$ and c_1. This is the task of the present section.

7.4.1 Fixing c_{2,m^2} by matching the poles in $4-2\epsilon$ dimensions

Our first source of additional information is the universal pole structure of four dimensional amplitudes. The poles of general one-loop QCD amplitudes in four dimensions were inferred from the corresponding real-radiation contributions to the NLO cross-section in full generality by Catani, Dittmaier and Trocsanyi [116],

$$A^{(1),4-2\epsilon} = c_\Gamma \, I^{(1)}(\epsilon) A^{(0)} + \text{finite}. \qquad (7.4.23)$$

The integrals I_{2,m^2} and I_1 appearing in equation (7.4.22) are divergent, and therefore the coefficients $c_{2;m^2}$ and c_1 contribute to the pole structure of our amplitude. This will allow us to constrain them.

For the simplified case of $t\bar{t} + n(g)$ with n_f light quark flavours and one heavy flavour of mass m, the function $I^{(1)}(\epsilon)$ appearing in the universal pole formula is, explicitly,

$$I^{(1)}(\epsilon) = \frac{n_g \beta_0 (n_f + 1)}{2\epsilon} + \sum_{i,j} \left(\frac{\mu_R^2}{s_{ij}} \right)^\epsilon \mathcal{V}_{ij} - n_g \Gamma_g - 2\Gamma_t + \text{finite}. \tag{7.4.24}$$

Following Catani et al. [116], this formula corresponds to partially renormalised amplitudes. The first term contains UV poles related to charge renormalisation, the second term corresponds to soft-collinear poles and takes the familiar dipole form in colour space. The last terms contain poles given by the anomalous dimensions,

$$\Gamma_g = \frac{\beta_0(n_f)}{2\epsilon} + \frac{2T_R}{3} \log \left(\frac{\mu_R^2}{m_t^2} \right), \tag{7.4.25}$$

$$\Gamma_t = C_F \left(\frac{1}{\epsilon} - \frac{1}{2} \log \left(\frac{\mu_R^2}{m_t^2} \right) - 2 \right). \tag{7.4.26}$$

The QCD β function appears as a function of the active fermion flavours $\beta_0(n_f) = (11 C_A - 4 T_R n_f)/3$. For the purposes of this method we will not require the finite parts of $I^{(1)}$ which depend on the dimensional regularisation scheme, e.g. CDR or FDH/DR. The exact form of the function $\mathcal{V}$ is a little more complicated and not of direct relevance here. Clearly there is an enormous amount of information contained in this result and further details can be found by consulting the original reference [116].

The simple observation relevant for our approach is that this universal information can be compared to the integral basis in equation (7.4.22), enabling a partial determination of the unknown coefficients of wavefunction bubble and tadpole integrals. These integrals give rise to single poles in ϵ and single logarithms in the mass m. This comparison is however insufficient to constrain both c_{2,m^2} and c_1.

It is convenient to modify the integral basis slightly, introducing finite bubble

and tadpole functions defined by

$$F_{2;i_1,i_2} = I_{2,i_1,i_2} - I_{2,m^2}, \tag{7.4.27}$$

$$F_1 = I_1 - m^2 I_{2,m^2}. \tag{7.4.28}$$

The result of this modification is that only the finite bubble integrals and the wave-function integral contribute to the $\log(\mu_R^2/m_t^2)$ dependence of the universal pole structure (7.4.24). Upon matching the amplitude with the universal pole structure, we find that the amplitude takes the explicit expression

$$A^{(1)} = A^{6D,(1)}\Big|_{I_2 \to F_2} + \frac{d_s - 2}{4} A^{(0)} I_{2,m^2} + c_1 F_1, \tag{7.4.29}$$

where the only missing information now lies in the tadpole coefficient c_1.

7.4.2   Counterterms for QCD in six dimensions

Because of our exploitation of the universal four-dimensional pole structure, the one-loop amplitude, in the form given in equation (7.4.29), has the property that its infrared and ultraviolet poles have been correctly determined. In addition, all logs in the mass m_t are correctly reproduced. Indeed, the unknown coefficient c_1 now multiplies an integral F_1 which we may explicitly compute:

$$F_1 \overset{d=4-2\epsilon}{=} -ic_\Gamma m^2 + \mathcal{O}(\epsilon) = -\frac{im^2}{(4\pi)^2} + \mathcal{O}(\epsilon). \tag{7.4.30}$$

Since c_1 is also a rational function, the part of the amplitude which remains to be determined is simply a rational function of the external momenta and masses.

Having made heavy use of higher dimensional methods so far in our computation, it is natural to regard the four-dimensional result we wish to determine as a specialisation of an amplitude that exists in higher dimensions. Indeed, a quantum field theory which is an analogue of QCD exists in six dimensions. Moreover, in six dimensions the integral F_1 is no longer simply a finite rational function. It has an

epsilon-pole given by

$$F_1 \stackrel{d=6-2\epsilon}{=} -\frac{im^4}{(4\pi)^3}\frac{1}{6\epsilon} + \mathcal{O}(\epsilon). \tag{7.4.31}$$

We may therefore find c_1 by comparison with the universal epsilon-pole structure of the amplitude in six dimensions.

Thus, we are motivated to consider QCD in six dimensions. Above four dimensions QCD ceases to be renormalisable, so to determine the universal epsilon-pole structure in six dimensions we must include higher (mass-)dimension operators[2] and treat the theory as an effective theory. By power counting, these operators have one or two powers of momentum more than in the usual QCD Lagrangian, so that they have mass-dimension five or six. The point of view we adopt is that the role of the additional operators is simply to provide counterterms, subtracting the infinities from any one-loop amplitude in the theory. Once all the counterterms have been determined, the epsilon-pole structure of any one-loop amplitude is known.

We therefore begin by constructing a basis of the dimension five and six operators which are required for renormalising QCD amplitudes in six dimensions. These operators contain either two quark fields and three derivatives, such as $\mathcal{O}_1 \equiv i\bar{\psi}\slashed{D}\slashed{D}\slashed{D}\psi$, or are purely bosonic operators such as $\text{tr}\, F^{\mu\nu}F_{\nu\rho}F^{\rho}{}_{\mu}$.[3] A full list of potential operators appears in table 7.1.

Since we are only concerned with poles of on-shell amplitudes, rather than of off-shell correlation functions, we need only study operators which lead to independent contributions to the S matrix. It is a well known fact that operators which are related by the classical equations of motion of the theory lead to the same contribution to the S matrix, to all orders of perturbation theory [128, 129, 130, 131, 132]. Thus

---

[2]It is linguistically unfortunate that we are now dealing with operators of mass-dimension five and six (using the usual four-dimensional classification of operator dimension) in a theory defined in six spacetime dimensions. We hope that context will make the meaning of the word "dimension" clear.

[3]Recall that a field strength F counts as two derivatives since $[D_\mu, D_\nu] = -igF_{\mu\nu}$.

we may simplify the list of operators in table 7.1 using the equations of motion

$$i\not{D}\psi = m\psi, \tag{7.4.32}$$

$$D^\mu F^a_{\mu\nu} = -g\bar{\psi}\gamma^\nu T^a\psi. \tag{7.4.33}$$

It is straightforward to see that many operators in table 7.1 are related to other operators in our Lagrangian. For example,

$$\mathcal{O}_1 \equiv i\bar{\psi}\not{D}\not{D}\not{D}\psi = -im^2\bar{\psi}\not{D}\psi, \tag{7.4.34}$$

so that $\mathcal{O}_1$ does not lead to a new, independent counterterm. It may therefore be omitted.

Our task now is to construct a basis of operators which are independent under the use of the equations of motion, integration by parts etc. To construct such a basis, we consider several categories of operators. Firstly, we will focus on operators containing two quark fields. We classify these operators further according to the powers of derivatives, or of derivatives and field strength insertions as shown in detail in table 7.1. We will begin by examining operators containing the largest number of derivatives or field strengths, as the use of the equations of motion may reduce these operators to simpler operators containing fewer derivatives (or field strengths.)

Each of the derivatives contained in operators of type $[\bar{\psi}D^3\psi]$ has one Lorentz index which we must contract using either metric tensors or gamma matrices. By making use of the equations of motion, we may ignore the options of contracting the left-most or right-most D index against a gamma matrix—such a contraction would reduce to an operator with fewer derivatives which we will analyze below. We are left with the unique possibility $\bar{\psi}D^\mu\not{D}D_\mu\psi$. However, this operator is equivalent to a linear combination of operators of class $[\bar{\psi}DF\psi]$ and $[\bar{\psi}D^2\psi]$ upon use of the equations of motion, since

$$\bar{\psi}D^\mu\not{D}D_\mu\psi = \bar{\psi}\left(-imD^\mu D_\mu - igD^\mu\gamma^\nu F_{\mu\nu}\right)\psi. \tag{7.4.35}$$

Quark fields	Operator	Operator class name
Two quarks	$i\bar{\psi}\slashed{D}\slashed{D}\slashed{D}\psi$	
	$i\bar{\psi}\slashed{D}D^2\psi$	$[\bar{\psi}D^3\psi]$
	$i\bar{\psi}D^\mu\slashed{D}D_\mu\psi$	
	$\bar{\psi}\gamma^\mu\gamma^\nu F_{\mu\nu}\slashed{D}\psi$	
	$\bar{\psi}D^\mu F_{\mu\nu}\gamma^\nu\psi$	$[\bar{\psi}DF\psi]$
	$\bar{\psi}F_{\mu\nu}\gamma^\mu D^\nu\psi$	
	$\bar{\psi}\slashed{D}\slashed{D}\psi$	
	$\bar{\psi}D^2\psi$	$[\bar{\psi}D^2\psi]$
	$i\bar{\psi}\gamma^\mu\gamma^\nu F_{\mu\nu}\psi$	$[\bar{\psi}F\psi]$
Zero quarks	$i\operatorname{tr}F^{\mu\nu}F_{\nu\rho}F^\rho{}_\mu$	
	$\operatorname{tr}F^{\mu\nu}D^2 F_{\mu\nu}$	
	$\operatorname{tr}(D^\mu F_{\mu\nu})(D^\rho F_\rho{}^\nu)$	

Table 7.1: Table of potential higher dimension operators in the 6 dimensional QCD effective Lagrangian. We have ignored four quark operators, which are not relevant for $t\bar{t}$ + gluons scattering at this order, and operators related to those in our table by integration-by-parts or Hermitian conjugation. We have also imposed the parity symmetry of QCD.

Therefore, the class $[\bar{\psi}D^3\psi]$ can be completely reduced to simpler operators.

Next, consider the class $[\bar{\psi}DF\psi]$. In this case we again have three possible Lorentz indices which must be contracted against gamma matrices or metric tensors. We may ignore the possibility of contracting the Lorentz index of the covariant derivative against a gamma matrix because of the equations of motion. We are left with two potential operator structures: $\bar{\psi}D^\mu F_{\mu\nu}\gamma^\nu\psi$ and $\bar{\psi}F_{\mu\nu}D^\mu\gamma^\nu\psi$. But

$$\bar{\psi}D^\mu F_{\mu\nu}\gamma^\nu\psi = \bar{\psi}(-g\bar{\psi}\gamma_\nu\psi)\gamma^\nu\psi + \bar{\psi}F_{\mu\nu}D^\mu\gamma^\nu\psi, \tag{7.4.36}$$

using the Yang-Mills equation. Since we are only interested in processes with two quarks, we will systematically ignore four quark operators. Therefore, we may replace the operator $\bar{\psi}D^\mu F_{\mu\nu}\gamma^\nu\psi$ with $\bar{\psi}F_{\mu\nu}D^\mu\gamma^\nu\psi$. This is the only member of the class $[\bar{\psi}DF\psi]$ which is of interest to us.

We now turn to operator structures containing two quark fields but only one extra power of derivatives or gauge fields. Thus the available operator structures are $[\bar{\psi}DD\psi]$ and $[\bar{\psi}F\psi]$. Up to equations of motion, there is only one operator of the first type: $\bar{\psi}D^\mu D_\mu\psi$. However, this is a reducible operator:

$$\bar{\psi}D^\mu D_\mu\psi = \bar{\psi}\slashed{D}\slashed{D}\psi - \frac{ig}{2}\bar{\psi}F_{\mu\nu}\gamma^\nu\gamma^\mu\psi. \tag{7.4.37}$$

Thus, up to equations of motion, we may reduce the $[\bar{\psi}DD\psi]$ class to the $[\bar{\psi}F\psi]$ class. Because of the antisymmetry of the field strength tensor, there is only one operator in the $[\bar{\psi}F\psi]$ class, namely $\bar{\psi}F_{\mu\nu}\gamma^\nu\gamma^\mu\psi$.

Finally, we must consider operators containing no quark fields. There are three gauge invariant possibilities: $\operatorname{tr}F^{\mu\nu}F_{\nu\rho}F^\rho{}_\mu$, $\operatorname{tr}F_{\mu\nu}D^2F^{\mu\nu}$, and $\operatorname{tr}(D^\mu F_{\mu\nu})(D^\rho F_\rho{}^\nu)$. The last of these three operators is equivalent to a four quark operator using the Yang-Mills equation, and is therefore of no interest to us. Meanwhile, the second of the three is equivalent to the other two:

$$\operatorname{tr}F_{\mu\nu}D^2F^{\mu\nu} = -2\operatorname{tr}(D^\mu F_{\mu\nu})D_\alpha F^{\alpha\nu} - 2ig\operatorname{tr}F_{\nu\mu}F^\mu{}_\alpha F^{\alpha\nu}. \tag{7.4.38}$$

As a result, we may also ignore this operator, leaving only $\operatorname{tr}F^{\mu\nu}F_{\nu\rho}F^\rho{}_\mu$.

In summary, there are only three higher dimension operators that contribute to the on-shell amplitudes. We may therefore take the full QCD Lagrangian in six dimensions, at one loop order, to be

$$
\mathcal{L}_{QCD}^6 = \bar{\psi}(i\slashed{D} - m)\psi - \frac{1}{2}\operatorname{tr} F_{\mu\nu}F^{\mu\nu} + \frac{i}{2}\sigma_1\, g_s^3 m_t\, \bar{\psi}\gamma^\mu\gamma^\nu F_{\mu\nu}\psi
$$
$$
+ i\sigma_2\, g_s^3\, \bar{\psi}F_{\mu\nu}\gamma^\mu D^\nu\psi + \frac{i}{6}\gamma\, g_s^3 \operatorname{tr}\left(F^{\mu\nu}[F_{\mu\lambda}, F_\nu{}^\lambda]\right). \quad (7.4.39)
$$

A selection of the resulting Feynman rules are listed in Appendix A.

We adopt the point of view that σ_1, σ_2 and γ are couterterms which remove the divergences in loop amplitudes. In addition there are the usual counterterms from the dimension four vertices $t\bar{t}g$ and ggg. We can compute the constants $\delta_{t\bar{t}g}, \delta_{ggg}, \sigma_1, \sigma_2$ and γ from simple one-loop vertex graphs. For example, expanding the $t\bar{t}g$ vertex to $\mathcal{O}(g_s^3)$ leads to,

$$
+\mathcal{O}(g_s^5). \quad (7.4.40)
$$

Renormalising this correlation function off-shell would require the inclusion of all possible counterterms (before use of the equations of motion.) For us, it is simpler to compute the on-shell three point vertex, in which case all infinities can be absorbed in our effective Lagrangian, equation (7.4.39). This presents a minor problem since the three point vertex is not well defined for real momenta. The computation may be performed using complex external kinematics or alternatively performed with the gluon taken off-shell and the constants extracted by taking the on-shell limit $p^2 \to 0$ at the end of the computation. We find this amplitude is UV finite in $6 - 2\epsilon$

dimensions for the values:

$$\delta_{t\bar{t}g} = \frac{m_t^2}{24(4\pi)^3\epsilon} C_F(3d_s + 2), \tag{7.4.41}$$

$$\sigma_1 = -\frac{1}{12(4\pi)^3\epsilon} \left(C_A(d_s - 5) - \frac{C_F}{2}(3d_s - 14) \right), \tag{7.4.42}$$

where $C_F = \frac{N_c^2 - 1}{2N_c}$ and $C_A = N_c$. A similar computation for the three gluon vertex,
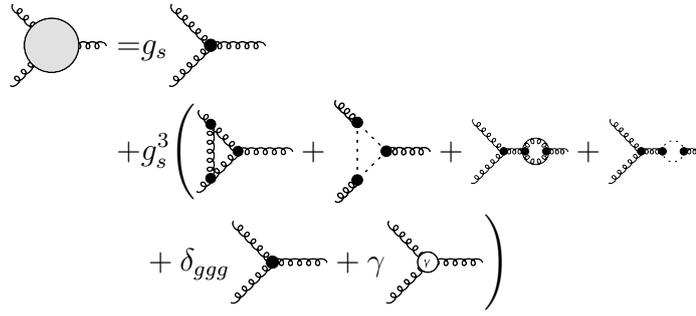
$$+\mathcal{O}(g_s^5), \tag{7.4.43}$$

results in

$$\delta_{ggg} = 0, \tag{7.4.44}$$

$$\gamma = \frac{1}{12(4\pi)^3\epsilon} C_A \frac{(d_s - 2)}{5}. \tag{7.4.45}$$

7.4.3 Fixing c_1 by matching poles in $6 - 2\epsilon$ dimensions

We finally apply this knowledge of the universal epsilon poles in six dimensions to determine the remaining unknown coefficient, c_1 in equation (7.4.29). The six-dimensional leading colour partial amplitude $A_{4;1}^{(1),6-2\epsilon}(1_t, 2, 3, 4_{\bar{t}})$ can be decomposed into gauge invariant primitives

$$A_{4;1}^{(1),6-2\epsilon}(1_t, 2, 3, 4_{\bar{t}}) = N_c A^{[L],6-2\epsilon}(1_t, 2, 3, 4_{\bar{t}}) - \frac{1}{N_c} A^{[R],6-2\epsilon}(1_t, 2, 3, 4_{\bar{t}}), \tag{7.4.46}$$

precisely as in four dimensions (we ignore fermion loops as they present no technical difficulties.) Because the epsilon-poles are universal, we know that the poles of this

amplitude are

$$A_{4;1}^{(1),6-2\epsilon}(1_t, 2, 3, 4_{\bar{t}}) = g_s^4 \left(2\delta_{t\bar{t}g} A^{(0)}(1_t, 2, 3, 4_{\bar{t}}) + \sigma_1 A^{[\sigma_1]}(1_t, 2, 3, 4_{\bar{t}}) \right.$$

$$\left. + \sigma_2 A^{[\sigma_2]}(1_t, 2, 3, 4_{\bar{t}}) + \gamma A^{[\gamma]}(1_t, 2, 3, 4_{\bar{t}}) \right) + \mathcal{O}(\epsilon^0), \quad (7.4.47)$$

where the tree-type amplitudes $A^{[\sigma_1]}(1_t, 2, 3, 4_{\bar{t}})$, $A^{[\sigma_2]}(1_t, 2, 3, 4_{\bar{t}})$ and $A^{[\gamma]}(1_t, 2, 3, 4_{\bar{t}})$ are associated with the three higher dimension operators in the effective 6d QCD Lagrangian, equation (7.4.39). They are explicitly defined by the diagrams shown in figure 7.6. In a similar fashion to the vertex computation we find that $A^{[\sigma_2]}(1_t, 2, 3, 4_{\bar{t}}) = 0$. By collecting in powers of N_c, and inserting the known expressions for $\delta_{t\bar{t}g}$, σ_1 and γ given in equations (7.4.41), (7.4.42) and (7.4.45) we find,

$$A^{[L],6-2\epsilon}(1_t, 2, 3, 4_{\bar{t}}) = \frac{g_s^4}{48(4\pi)^3\epsilon} \left(2(3d_s + 2)m_t^2 A^{(0)}(1_t, 2, 3, 4_{\bar{t}}) + \frac{4(d_s - 2)}{5} A^{[\gamma]}(1_t, 2, 3, 4_{\bar{t}}) \right.$$

$$\left. - (d_s - 6)A^{[\sigma_1]}(1_t, 2, 3, 4_{\bar{t}}) \right) + \mathcal{O}(\epsilon^0) \quad (7.4.48)$$

for the left-moving ordering and

$$A^{[R],6-2\epsilon}(1_t, 2, 3, 4_{\bar{t}}) = \frac{g_s^4}{48(4\pi)^3\epsilon} \left(2(3d_s + 2)m_t^2 A^{(0)}(1_t, 2, 3, 4_{\bar{t}}) \right.$$

$$\left. + (3d_s - 14)A^{[\sigma_1]}(1_t, 2, 3, 4_{\bar{t}}) \right) + \mathcal{O}(\epsilon^0) \quad (7.4.49)$$

for the right-moving case.

The tree amplitudes $A^{[\sigma_1]}(1_t, 2, 3, 4_{\bar{t}})$ and $A^{[\gamma]}(1_t, 2, 3, 4_{\bar{t}})$ are easily determined by calculating the diagrams in figure 7.6. The explicit expressions are listed in Appendix B.2.

The final step necessary to determine the tadpole coefficient is to evaluate the

$$A^{[\sigma_1]}(1_t, 2, 3, 4_{\bar{t}}) =$$

$$A^{[\gamma]}(1_t, 2, 3, 4_{\bar{t}}) =$$

Figure 7.6: The Feynman diagrams contributing to the tree-level amplitudes appearing the pole structure of the one-loop $t\bar{t}gg$ amplitudes in $6 - 2\epsilon$ dimensions. Solid vertices correspond to the usual QCD interactions while the open vertices are those resulting from the corresponding dimension six operators in $\mathcal{L}^6_{QCD}$ of eq. (7.4.39).

poles of the basis integrals of the one-loop amplitude in $6 - 2\epsilon$ dimensions. We find

$$I_1^{6-2\epsilon}[1](m^2) = \frac{-im^4}{2(4\pi)^3\epsilon} + \mathcal{O}(\epsilon^0) \tag{7.4.50}$$

$$I_2^{6-2\epsilon}[1](P^2, m_1^2, m_2^2) = i\frac{P^2 - 3(m_1^2 + m_2^2)}{6(4\pi)^3\epsilon} + \mathcal{O}(\epsilon^0) \tag{7.4.51}$$

$$I_2^{6-2\epsilon}[\mu^2](P^2, m_1^2, m_2^2) = i\frac{P^4 - 5P^2(m_1^2 + m_2^2) + 10\left((m_1^2 + m_2^2)^2 - m_1^2 m_2^2\right)}{60(4\pi)^3\epsilon} + \mathcal{O}(\epsilon^0), \tag{7.4.52}$$

$$I_3^{6-2\epsilon}[1] = \frac{-i}{2(4\pi)^3\epsilon} + \mathcal{O}(\epsilon^0) \tag{7.4.53}$$

$$I_3^{6-2\epsilon}[\mu^2](P_1^2, P_2^2, P_3^2, m_1^2, m_2^2, m_3^2) = -i\frac{P_1^2 + P_2^2 + P_3^2 - 4(m_1^2 + m_2^2 + m_3^2)}{24(4\pi)^3\epsilon} + \mathcal{O}(\epsilon^0), \tag{7.4.54}$$

$$I_4^{6-2\epsilon}[1] = \mathcal{O}(\epsilon^0), \tag{7.4.55}$$

$$I_4^{6-2\epsilon}[\mu^2] = \frac{i}{6(4\pi)^3\epsilon} + \mathcal{O}(\epsilon^0), \tag{7.4.56}$$

$$I_4^{6-2\epsilon}[\mu^4](P_1^2, P_2^2, P_3^2, P_4^2, s, t, m_1^2, m_2^2, m_3^2, m^4) = \tag{7.4.57}$$

$$i\frac{P_1^2 + P_2^2 + P_3^2 + P_4^2 + s + t - 5(m_1^2 + m_2^2 + m_3^2 + m_4^2)}{60(4\pi)^3\epsilon} + \mathcal{O}(\epsilon^0). \tag{7.4.58}$$

The formulae are easy to derive using the dimensional recurrence relation implemented in LiteRed [133] in any case.

The only unknowns in equations (7.4.48) and (7.4.49) are then the left- and right-moving tadpole coefficients c_1, allowing a direct determination of these rational functions. The results are somewhat lengthy formulae which are not presented here explicitly We have checked that this procedure matches the expected result by comparing with the previous computation of reference [60].

7.5 Discussion

In this chapter we have explored a new technique for the computation of one-loop amplitudes with massive fermions. Our methods are designed to be compatible with on-shell generalised unitarity.

The six-dimensional spinor-helicity scheme proved to be an efficient way to describe the tree-level input into the d-dimensional generalised unitarity method. Divergent wavefunction cuts were avoided, and the remaining ambiguities in the amplitudes were fixed by matching to the universal physical pole structure. The $4 - 2\epsilon$ pole structure of Catani et al. [116] is sufficient to constrain all remaining logarithms in the fermion mass while additional information is needed to fix the remaining finite corrections connected to tadpole integrals. We obtained this second constraint by allowing the loop momenta in our integrals to be defined in a higher dimension spacetime, and imposing the universality of ultraviolet divergences in this higher dimensional quantum field theory. Since six is the next even dimension above four it was natural to study QCD as an effective theory in $6 - 2\epsilon$ dimensions. We used the on-shell equations of motion to find a minimal set of additional dimension six operators in this theory, and computed the required counterterms essentially following the textbooks. We applied our method to a variety of simple cases and validated it on helicity amplitudes for top quark pair production (see Section 8).

The methods we used in this chapter are flexible, and it is clear that they apply more generally than to $gg \to t\bar{t}$ scattering. It would be interesting to work out the extension to more general cases with multiple fermions and multiple masses, as well

as to higher loops. In the presence of more fermions, four quark operators would need to be included in the effective Lagrangian, while at higher loops one would need to consider operators of mass-dimension greater than six.

Since this method can compute amplitudes with fewer cuts than other known approaches it has the potential to optimise existing numerical and analytical approaches. However, since the main computational bottleneck in most phenomenological collider studies at NLO lies in the integration over the unresolved phase-space, the technique is probably best suited to find compact analytic expressions where the improvement in stability and speed over existing numerical approaches is particularly beneficial.

Perhaps a more interesting direction would be to look into the implications of the higher dimensional pole structure on the spurious singularities appearing in integral reductions. As a result of matching to a tree-level computation with an effective Lagrangian, we find non-trivial relations between the d-dimensional integral coefficients in which all spurious poles cancel. These cancellations had to occur, since the effective theory contains only local operators. This information could be useful in finding compact and stable representations of one-loop amplitudes.

Chapter 8

Analytic $t\bar{t}$ plus three partons one-loop amplitudes

In this chapter we present the analytic calculation of the one-loop helicity amplitudes involving a $t\bar{t}$ pair and three gluons, based on the techniques explored in Chapter 3, 4 and 7.

As we have already discussed in this thesis, analytic expressions have several advantages over numerical implementations. In this case, they may provide more stable evaluations of virtual-real subtraction terms required for the calculation of the $pp \to t\bar{t}$ cross section at NNLO, as well of virtual corrections to $pp \to t\bar{t} + \mathrm{j}$ at NLO.

Moreover, they also give us the opportunity to test the practicality of the method introduced in Chapter 7, when the kinematics are more complicated.

Finally, we also study how introducing a spin basis for the $t\bar{t}$ pair may simplify the calculation of the corresponding helicity amplitudes.

8.1 Including top quark decays in the narrow width approximation

The top quarks are unstable and will decay via weak interaction before hadronisation occurs. To construct a realistic observable, the decay products of the $t\bar{t}$ pair have to be taken into account. We consider the SM semi-leptonic decay of the top(antitop),

$$t \to bW^+ \to b\ell^+\nu_\ell \qquad (8.1.1)$$

where $\ell = e, \mu, \tau$. The decay of a $t\bar{t}$ pair produced in the collision of partons a and b can be written as,

$$ab \to t\bar{t} + X \to (b\ell^+\nu_\ell)(\bar{b}\ell^-\bar{\nu}_\ell) + X, \qquad (8.1.2)$$

where X represents additional final states. The tree-level amplitude for this process can be written as [134, 135],

$$A = \bar{\Psi}_\alpha(t^* \to \ell^+\nu_\ell) \, \tilde{A}_{\alpha\beta}(ab \to t^*\bar{t}^* + X) \, \Xi_\beta(\bar{t}^* \to \bar{b}\ell^-\bar{\nu}_\ell) \qquad (8.1.3)$$

where Ψ and Ξ are off-shell fermion currents, which take into account the decays of the off-shell top (t^*) and antitop ($\bar{t}^*$), and $\tilde{A}_{\alpha\beta}$ are sub-amplitudes associated with the top pair production. The fermion currents contain the top(antitop) propagators and the sub-amplitudes that describe the off-shell decay,

$$\bar{\Psi}_\alpha(t^* \to \ell^+\nu_\ell) = \tilde{A}^{(0)}(t^* \to \ell^+\nu_\ell)_\gamma \frac{i(\not{p}_t + m_t)_{\gamma\alpha}}{p_t^2 - m_t^2 + i\Gamma_t m_t} \qquad (8.1.4)$$

$$\Xi_\beta(\bar{t}^* \to \bar{b}\ell^-\bar{\nu}_\ell) = \frac{i(\not{p}_{\bar{t}} - m_t)_{\beta\gamma}}{p_{\bar{t}}^2 - m_t^2 + i\Gamma_t m_t} \tilde{A}_\gamma(\bar{t}^* \to \bar{b}\ell^-\bar{\nu}_\ell) \qquad (8.1.5)$$

For the majority of studies we can use the narrow width approximation $\Gamma_t/m_t \to 0$, since $\Gamma_t/m_t = \mathcal{O}(1\%)$ [1]. When we consider the squared amplitude in this approx-

---

[1]Studies of the off-shell $t\bar{t}$ decay can be found in [136, 137]

imation, the propagators become,

$$\left. \frac{1}{(p_t^2 - m_t^2)^2 + \Gamma_t^2 m_t^2} \right|_{\Gamma_t/m_t \to 0} = \frac{2\pi}{2\Gamma_t m_t} \delta(p_t^2 - m_t^2), \qquad (8.1.6)$$

therefore the top and antitop turn into on-shell particles. The narrow width approximation allows us to factorise the production of the $t\bar{t}$ pair and its decay. Using the Eq. (8.1.6) at the amplitude level, the fermion currents (8.1.4)-(8.1.5) can be seen as effective spinors,

$$\left. \bar{\Psi}_\alpha(t^* \to \ell^+ \nu_\ell) \right|_{\Gamma_t/m_t \to 0} \quad \to \quad \bar{U}_\alpha(p_t) = \tilde{A}^{(0)}(t \to \ell^+ \nu_\ell)_\gamma \frac{i(\not{p}_t + m_t)_{\gamma\alpha}}{\sqrt{2m_t \Gamma_t}} \qquad (8.1.7)$$

$$\left. \Xi_\beta(\bar{t}^* \to \bar{b}\ell^- \bar{\nu}_\ell) \right|_{\Gamma_t/m_t \to 0} \quad \to \quad V_\beta(p_t) = \frac{i(\not{p}_{\bar{t}} - m_t)_{\beta\gamma}}{\sqrt{2m_t \Gamma_t}} \tilde{A}_\gamma(\bar{t} \to \bar{b}\ell^- \bar{\nu}_\ell) \qquad (8.1.8)$$

and the amplitude simplifies to,

$$A = \bar{U}_\alpha(p_t) \; \tilde{A}_{\alpha\beta}(ab \to t\bar{t} + X) \; V_\beta(p_t) + \mathcal{O}\left(\frac{\Gamma_t}{m_t}\right). \qquad (8.1.9)$$

The advantage of this form is that including the decays of the $t\bar{t}$ does not increase the complexity of the amplitudes, since they are expressed in terms of on-shell spinors. Also, because all the decay products are treated as massless, the weak interaction uniquely defines the polarisation of the U and V spinors and no helicity sum for t and $\bar{t}$ is required in the cross-section calculation.

As a result, one can compute the helicity amplitudes for the partonic process and link the decays to the $t\bar{t}$ spinors afterwards. To find the connection between the helicity amplitudes and the amplitudes in the narrow width approximation, we look in detail at the tree-level associated with the top decay $t \to \ell^+ \nu_\ell$ shown in Fig.
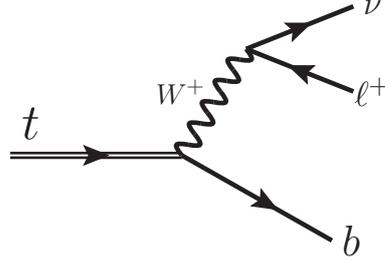
Figure 8.1: Tree-level diagram associated to the semi-leptonic decay of the top quark. The b quark and the leptons are considered massless.

8.1. The amplitude is written as,

$$A^{(0)}(t \to \ell^+ \nu_\ell) =$$

$$\left(\frac{-ig_W}{\sqrt{2}} \bar{u}(p_\nu) \gamma^\rho \frac{1}{2}(1-\gamma^5) v(p_{\ell^+}) \right) \frac{g^{\rho\sigma}}{p_W^2 - M_W^2} \left(\frac{-ig_W V_{tb}}{\sqrt{2}} \bar{u}(p_b) \gamma^\sigma \frac{1}{2}(1-\gamma^5) u(p_t) \right) =$$

$$\frac{g_W^2 V_{tb}}{2} \frac{-1}{p_W^2 - M_W^2} \left(\bar{u}_L(p_\nu) \gamma^\rho v_R(p_{\ell^+}) \bar{u}_L(p_b) \gamma_\rho u_L(p_t) \right) =$$

$$\frac{g_W^2 V_{tb}}{2} \frac{1}{p_W^2 - M_W^2} \left(\bar{u}_L(p_\nu) u_R(p_b) \bar{v}_L(p_{\ell^+}) u_L(p_t) \right) \tag{8.1.10}$$

where in the second line we have highlighted how the $V - A$ structure of the weak interaction fixes the helicities of the final states. To recast this amplitude in the spinor form of Eq. (8.1.8) one has to replace the on-shell spinor $u(p_t)$ with the top propagator, then the effective spinor can be written as,

$$\bar{U}(p_t) = \frac{ig_W^2 V_{tb}}{2\sqrt{2m_t \Gamma_t}} \frac{\langle p_\nu p_b \rangle}{p_W^2 - M_W^2} [p_{\ell^+}|(\not{p}_t + m_t) \tag{8.1.11}$$

where we have used the compact notation of the spinor-helicity formalism since the b and the leptons are massless. Excluding the prefactor associated with the decay, we can notice the analogy between Eq. (8.1.11) and Eq. (3.2.48), where in the former the reference momentum is chosen to be that of ℓ^+. The same approach can be used to obtain the $V(p_{\bar{t}})$, considering the antitop decay.

Therefore we can focus on the calculation of the helicity amplitudes involving

the $t\bar{t}$ production only,

$$A(ab \to t\bar{t} + X) = \frac{[p_{\ell+}|(\not{p}_t + m_t)_\alpha}{[p_t^\flat p_{\ell+}]} \tilde{A}_{\alpha\beta}(ab \to t\bar{t} + X)\frac{(\not{p}_{\bar{t}} - m_t)_\beta|p_{\ell-}\rangle}{\langle p_{\bar{t}}^\flat p_{\ell-}\rangle}, \quad (8.1.12)$$

using the massless projection of Section 3.2 for the massive spinors, normalised as in Eq. (3.2.48). The helicity amplitudes in the remainder of this chapter are quoted for arbitrary reference directions but the decays are simple to include using the argument above. Also, because of the relations in Eq. (3.2.50), we can compute our favourite set of independent helicity amplitudes and then obtain the ones that are relevant for the decays.

8.2 Spin structure and kinematic variables

We consider amplitudes with the following particle content,

$$A_5(\bar{t}^{\lambda_1}, t^{\lambda_2}, 3^{\lambda_3}, 4^{\lambda_4}, 5^{\lambda_5}), \quad (8.2.13)$$

where all the momenta are outgoing and

$$p_1^2 = p_2^2 = m_t^2, \qquad p_3^2 = p_4^2 = p_5^2 = 0. \quad (8.2.14)$$

The massive momenta can be decomposed with respect to massless reference vectors η_i, recalling the construction given Section 3.2,

$$p_1^\flat = p_1 - \frac{m_t^2}{2p_1 \cdot \eta_1}\eta_1, \qquad p_2^\flat = p_2 - \frac{m_t^2}{2p_2 \cdot \eta_2}\eta_2, \quad (8.2.15)$$

such that $(p_1^\flat)^2 = (p_2^\flat)^2 = 0$. The massive spinors can be expressed in terms of the reference spinors as in Eq. (3.2.48).

We find it convenient to decompose the amplitudes in a spin basis of the top and the anti-top. The spin correlation structure of the $t\bar{t}$ production has been studied in [138, 139]. A general helicity amplitude involving on-shell $t\bar{t}$, in the spin correlation

basis, can be written as a sum of four terms,

$$A_n(\bar{t}^{\lambda_1}(p_1^\flat, \eta_1), t^{\lambda_2}(p_2^\flat, \eta_2), 3^{\lambda_3}, 4^{\lambda_4}, \ldots, n^{\lambda_n}) =$$

$$\sum_{i=1}^{4} \rho_i^{\lambda_1 \lambda_2}(\eta_1, \eta_2, p_1^\flat, p_2^\flat) A_{n;\rho_i}(\bar{t}, t, 3^{\lambda_3}, 4^{\lambda_4}, \ldots, n^{\lambda_n}) \quad (8.2.16)$$

where the ρ_i are the elements of the $t\bar{t}$ spin correlation basis and the $A_{n;\rho_i}$ are independent sub-amplitudes.

We can notice that the sub-amplitudes are functions of the $t\bar{t}$ momenta only and the explicit dependence on η_1 and η_2 is contained in the ρ_i. As a result, the sub-amplitudes are simpler objects than the whole amplitude and can be computed in terms of projections with respect to the spin basis. Also, the relation between amplitudes with different $t\bar{t}$ helicities is obtained just by acting on the spin basis whereas the sub-amplitudes remain unchanged.

For the process discussed in this chapter, we look at the decomposition for the following helicity amplitudes,

$$A_5(\bar{t}^+(p_1^\flat, \eta_1), t^+(p_2^\flat, \eta_2), 3^{\lambda_3}, 4^{\lambda_4}, 5^{\lambda_5}) =$$

$$\sum_{i=1}^{4} \rho_i^{++}(\eta_1, \eta_2, p_1^\flat, p_2^\flat) A_{5;\rho_i}(\bar{t}, t, 3^{\lambda_3}, 4^{\lambda_4}, 5^{\lambda_5}), \quad (8.2.17)$$

where we choose the following spin basis,

$$\rho_1^{++} = \frac{\langle 45 \rangle}{\langle 34 \rangle \langle 35 \rangle} \frac{\langle \eta_1 3 \rangle \langle \eta_2 3 \rangle}{\langle \eta_1 p_1^\flat \rangle \langle \eta_2 p_2^\flat \rangle}, \qquad \rho_2^{++} = \frac{\langle 35 \rangle}{\langle 34 \rangle \langle 45 \rangle} \frac{\langle \eta_1 4 \rangle \langle \eta_2 4 \rangle}{\langle \eta_1 p_1^\flat \rangle \langle \eta_2 p_2^\flat \rangle}, \qquad (8.2.18)$$

$$\rho_3^{++} = \frac{1}{\langle 34 \rangle} \frac{\langle \eta_1 4 \rangle \langle \eta_2 3 \rangle}{\langle \eta_1 p_1^\flat \rangle \langle \eta_2 p_2^\flat \rangle}, \qquad \rho_4^{++} = \frac{\langle \eta_1 \eta_2 \rangle}{\langle \eta_1 p_1^\flat \rangle \langle \eta_2 p_2^\flat \rangle}. \qquad (8.2.19)$$

The sub-amplitudes can be computed by projecting out the coefficients of the spin

basis, for example obtaining the solutions,

$$A_{5;\rho_2} = \frac{A_5(\bar{t}^+(p_1^\flat, p_3), t^+(p_2^\flat, p_3), \cdots)}{\rho_2^{++}(p_3, p_3, p_1^\flat, p_2^\flat)} \tag{8.2.20}$$

$$A_{5;\rho_1} = \frac{A_5(\bar{t}^+(p_1^\flat, p_4), t^+(p_2^\flat, p_4), \cdots)}{\rho_1^{++}(p_4, p_4, p_1^\flat, p_2^\flat)} \tag{8.2.21}$$

$$A_{5;\rho_4} = \frac{A_5(\bar{t}^+(p_1^\flat, p_4), t^+(p_2^\flat, p_3), \cdots)}{\rho_4^{++}(p_4, p_3, p_1^\flat, p_2^\flat)} \tag{8.2.22}$$

$$A_{5;\rho_3} = \frac{A_5(\bar{t}^+(p_1^\flat, p_3), t^+(p_2^\flat, p_4), \cdots) - \rho_4^{++}(p_3, p_4, p_1^\flat, p_2^\flat)A_{5;\rho_4}}{\rho_3^{++}(p_3, p_4, p_1^\flat, p_2^\flat)} \tag{8.2.23}$$

where the full amplitudes are evaluated on certain values of η_1 and η_2.

In order to perform the computations at fixed values of η_1 and η_2 we set up a rational parametrisation in terms of momentum twistors as described in Section 3.3. We begin by generating a phase-space point including the massless decay momenta which involves 7 particles. This parametrisation contains 11 variables but is reduced to 10 after imposing the condition that $m_t = m_{\bar{t}}$. For each computation of $A_{5;\rho_i}$ we fix 4 additional parameters and set the overall scale $s_{34} = 1$. The dependence on s_{34} can then be restored at the end of the computation using dimensional analysis. Therefore each sub-amplitude $A_{5;\rho_i}$ is a function of five variables.

As an example, we show the case of $\eta_1 = p_4$ and $\eta_2 = p_3$, which is realised by imposing,

$$|\eta_1\rangle = |3\rangle, \qquad |\eta_1] = |3], \qquad |\eta_2\rangle = |4\rangle, \qquad |\eta_2] = |4]. \tag{8.2.24}$$

A momentum twistor parametrisation in terms of the five parameters $z_1, \ldots, z_5$ is

then,

$$|3\rangle = (1,0)\,, \qquad\qquad |3] = \begin{pmatrix} -\frac{z_4-z_5}{z_4} \\ 1 \end{pmatrix} \qquad\qquad (8.2.25)$$

$$|4\rangle = (0,1)\,, \qquad\qquad |4] = \begin{pmatrix} -1 \\ 0 \end{pmatrix} \qquad\qquad (8.2.26)$$

$$|5\rangle = (1,1)\,, \qquad\qquad |5] = \begin{pmatrix} 1 \\ z_4 \end{pmatrix} \qquad\qquad (8.2.27)$$

$$|p_1^\flat\rangle = \left(-\frac{z_1-z_2+z_4}{z_2-z_3-z_4},1\right)\,, \qquad |p_1^\flat] = \begin{pmatrix} \frac{(-z_2+z_3+z_4)(z_4z_3-z_5z_3+z_3+z_2z_5)}{z_4(z_1-z_2+z_4)} \\ z_2-z_3-z_4 \end{pmatrix} \qquad (8.2.28)$$

$$|p_2^\flat\rangle = \left(\frac{-z_1+z_2+1}{z_2-z_3},1\right)\,, \qquad |p_2^\flat] = \begin{pmatrix} \frac{(z_2-z_3)(z_4z_3-z_5z_3+z_3+z_2z_5+z_5)}{(z_1-z_2-1)z_4} \\ z_3-z_2 \end{pmatrix}\,, \qquad (8.2.29)$$

where the variables z can be written in terms of the external momenta as,

$$z_1 = \frac{2p_1\cdot p_5}{s_{34}}, \quad z_2 = \frac{2p_2\cdot p_3}{s_{34}}, \quad z_3 = \frac{\langle 32(3+4)5\rangle}{\langle 35\rangle s_{34}}, \quad z_4 = \frac{s_{45}}{s_{34}}, \quad z_5 = \frac{s_{12}}{s_{34}}. \quad (8.2.30)$$

Similar phase-space parametrisations are used for the different choices of η_1 and η_2 in the projection of Eq. (8.2.23). Also, in this framework, the sub-amplitudes are suitable for a finite field fitting reconstruction in order to obtain analytic expressions.

8.3   Colour decomposition

We write down explicitly the colour decomposition of the $t\bar{t}ggg$ partonic sub process, at tree-level and one-loop.

The colour decomposition for the tree-level amplitudes is [91]

$$\mathcal{A}_5^{(0)}(1_{\bar{t}},2_t,3,4,5) = g_s^3 \sum_{P(3,4,5)} (T^{a_3}T^{a_4}T^{a_5})_{i_1}^{\bar{i}_2} A_5^{(0)}(1_{\bar{t}},2_t,3,4,5) \qquad (8.3.31)$$

The one-loop colour decomposition in terms of partial amplitudes is [53, 91, 140],

$$\mathcal{A}^{(1)}(1_{\bar{t}}, 2_t, 3, 4, 5) = g_s^5 \sum_{p=2}^{5} \sum_{\sigma \in S_3} (T^{x_1} T^{a_{\sigma_3}} \ldots T^{a_{\sigma_p}} T^{x_2})_{i_2}^{\bar{i}_1} (f^{a_{\sigma_{p+1}}} \ldots f^{a_{\sigma_5}})_{x_1 x_2}$$

$$\times A^{[L]}(1_{\bar{t}}, \sigma(p), \ldots, \sigma(3), 2_t, \sigma(n), \ldots, \sigma(p+1)) +$$

$$-\frac{1}{N_c} \sum_{j=1}^{n-1} \sum_{\sigma \in S_3/S_{5;j}} \mathrm{Gr}_{5;j}(\sigma_3, \sigma_4, \sigma_5) \tag{8.3.32}$$

$$\times \Big(n_f A^{[f]}(1_{\bar{t}}, 2_t, \sigma(3), \sigma(4), \sigma(5)) + \tag{8.3.33}$$

$$n_H A^{[H]}(1_{\bar{t}}, 2_t, \sigma(3), \sigma(4), \sigma(5)) \Big) \tag{8.3.34}$$

In this formula $(f^a \ldots f^b)_{x_1 x_2} = f^{x_1 a y} \ldots f^{y b x_2}$ and, for $p = 5$, it evaluates to $(f^a \ldots f^b)_{x_1 x_2} = \delta_{x_1 x_2}$. Primitive amplitudes $A^{[f]}$ and $A^{[H]}$ contain one closed loop of massless and massive fermions, respectively. The colour factors $\mathrm{Gr}_{5;j}$ take the explicit form,

$$\mathrm{Gr}_{5;1}(\sigma_3, \sigma_4, \sigma_5) = N_c (T^{a_{\sigma_3}} T^{a_{\sigma_4}} T^{a_{\sigma_5}})_{i_2}^{\bar{i}_1}, \tag{8.3.35}$$

$$\mathrm{Gr}_{5;2}(\sigma_3, \sigma_4, \sigma_5) = 0, \tag{8.3.36}$$

$$\mathrm{Gr}_{5;3}(\sigma_3, \sigma_4, \sigma_5) = \mathrm{tr}(T^{a_{\sigma_3}} T^{a_{\sigma_4}})(T^{a_{\sigma_5}})_{i_2}^{\bar{i}_1} \tag{8.3.37}$$

$$\mathrm{Gr}_{5;4}(\sigma_3, \sigma_4, \sigma_5) = \mathrm{tr}(T^{a_{\sigma_3}} T^{a_{\sigma_4}} T^{a_{\sigma_5}}) \delta_{i_2}^{\bar{i}_1} \tag{8.3.38}$$

Considering this decomposition, we need to compute the helicity primitive amplitudes $A^{[L]}(1_{\bar{t}}, 2_t, 3, 4, 5)$, $A^{[R]}(1_{\bar{t}}, 2_t, 3, 4, 5) \equiv A^{[L]}(1_{\bar{t}}, 3, 4, 5, 2_t)$, $A^{[L]}(1_{\bar{t}}, 5, 2_t, 3, 4)$, $A^{[L]}(1_{\bar{t}}, 3, 4, 2_t, 5)$ and $A^{[H]}(1_{\bar{t}}, 2_t, 3, 4, 5)$.

An example of maximal topology diagrams contributing to the primitive amplitudes are shown in Fig. 8.2.

8.4 Analytic integrand reduction of Feynman diagrams

The six dimensional cuts discussed in Section 7 have been used to compute the primitive amplitudes for exact numerical kinematics. While this method could be

$$A_5^{[L]}(1_{\bar{t}}, 2_t, 3, 4, 5) \qquad A_5^{[R]}(1_{\bar{t}}, 2_t, 3, 4, 5) \qquad A_5^{[L]}(1_{\bar{t}}, 5, 2_t, 3, 4) \qquad A_5^{[L]}(1_{\bar{t}}, 3, 4, 2_t, 5)$$
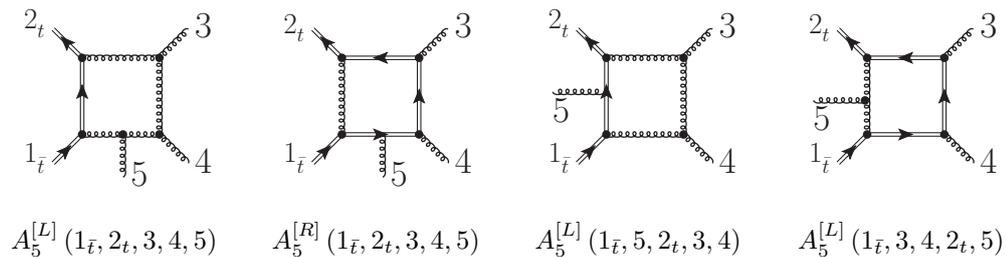
Figure 8.2: Example of maximal topology diagrams belonging to the primitive amplitudes $A_5^{[L]}$. Double lines represent massive fermions.

extended to analytic calculations using the finite field reconstruction technique, at the present time our MATHEMATICA algorithm produced large algebraic functions of the five variables z_i that were too difficult to factorise.

Instead we combined an integrand reduction of Feynman diagrams with the momentum twistor representation of the kinematics to obtain analytic results. The method allows us to obtain the d-dimensional integral representation of Eq. (4.3.57) by parametrising the Feynman diagrams in terms of components of the loop momentum. This approach is conceptually similar to the integrand reduction discussed in Section 4.3. Here we present the main steps of the modifications used in the implementation of a diagram based reduction. We just recall the decomposition of the loop momentum given in Eq. (4.3.46),

$$k^\mu = \bar{k}^{[4]} + \tilde{k}^{[-2\epsilon]} \tag{8.4.39}$$

$$k^2 = \bar{k}^2 - \mu^2, \qquad \tilde{k}^2 = -\mu^2, \qquad \bar{k} \cdot \tilde{k} = 0.$$

The procedure used for the diagram reduction is the following:

1. We consider the integrand of a diagram having a general form
   $N(\{p\}, k) / \prod_i D_i$

2. We span $\bar{k}^\mu$ in a four dimensional basis $\vec{v}$ which is a function of external momenta and spurious vectors w. The coefficients of the basis can be written in terms of propagators and irreducible scalar products according with the

given topology,

$$\bar{k}^{\mu} = \vec{a}(D_i, \text{ISP}) \cdot \vec{v}. \tag{8.4.40}$$

This allows us to express the numerator as a combination of propagators and ISP. In particular, because the external momenta are living in four dimensions, any scalar product like $k_{\mu} J^{\mu}$, where J^{μ} is an external momentum or a current, can be expanded using the basis $\vec{v}$.

3. We reduce the integrand by partial fractioning the numerator with respect to the propagators. Terms with no dependence of the loop momentum give rise to scalar integrals. Elements containing propagators can be reduced to an integrand belonging to a lower topology, which can be further processed repeating the procedure from step 1. Combinations of ISP containing spurious terms vanish according with (4.3.56) (see also Appendix D).

4. For the calculation of the amplitude, we consider the set of Feynman diagrams contributing to the amplitude and apply the reduction procedure until all the diagrams are written in the basis of the scalar integrals according with (4.3.57).

To clarify this procedure we consider a simple example of the application to a triangle topology:

1. Consider an integrand of the form

$$\frac{N(\{p\}, k)}{D_1 D_2 D_3} \tag{8.4.41}$$

$$D_1 = k^2, \quad D_2 = (k - p_1)^2 - m^2, \quad D_3 = (k - p_1 - p_2)^2 - m^2, \tag{8.4.42}$$

$$p_1^2 = m^2, \quad p_2^2 = 0. \tag{8.4.43}$$

2. The four dimensional basis can be chosen to be,

$$\vec{v} = \{p_1, p_2, w_1, w_2\}, \tag{8.4.44}$$

with,

$$w_1^\mu = \frac{1}{2}([21\sigma^\mu 2] + \langle 21\sigma^\mu 2 \rangle), \quad w_2^\mu = \frac{1}{2}([21\sigma^\mu 2] - \langle 21\sigma^\mu 2 \rangle) \tag{8.4.45}$$

and we have the following sets of reducible and irreducible scalar products,

$$\text{RSP} = \begin{cases} k \cdot k = D_1, \\[2mm] k \cdot p_1 = \frac{1}{2}(D_1 - D_2), \\[2mm] k \cdot p_2 = \frac{1}{2}(D_3 - D_2 + s_{12} - m^2) \end{cases} \tag{8.4.46}$$

$$\text{ISP} = \{k \cdot w_1, k \cdot w_2, \mu^2\}. \tag{8.4.47}$$

Therefore the parametrisation of $\bar{k}$ with respect to $\vec{v}$ is,

$$\bar{k} = \sum_{i=1}^{4} a_i v_i, \tag{8.4.48}$$

$$a_1 = 1 + \frac{D_2 - D_3}{s_{12} - m^2} \tag{8.4.49}$$

$$a_2 = \frac{D_1 - 2m^2}{s_{12} - m^2} + \frac{2m^2 D_3 - (s_{12} + m^2) D_2}{(s_{12} - m^2)^2} \tag{8.4.50}$$

$$a_3 = -\frac{k \cdot w_1}{(s_{12} - m^2)^2} \tag{8.4.51}$$

$$a_4 = \frac{k \cdot w_2}{(s_{12} - m^2)^2}, \tag{8.4.52}$$

3. Finally we can expand the numerator using the parametrisation of the loop momentum and partial fractioning it with respect to the propagators, thus the reduction follows as discussed in the general description.

After the reduction, one obtains the un-renormalised amplitude. To compute the renormalised amplitude $A^{(1)}$, we add the appropriate counter-terms following the standard renormalisation procedure in the on-shell scheme. We use the counter-

terms written in their integral representation,

$$\text{———}\otimes\text{———} = 4I_2[1][m^2, 0, m^2] + \frac{d_s - 2}{m^2}I_1[1][m^2] \tag{8.4.53}$$

$$\text{OOO}\otimes\text{OOO} = 4m^2 I_2[1][m^2, 0, m^2] + 4I_2[\mu^2][m^2, 0, m^2] - 4I_1[1][m^2] \tag{8.4.54}$$

which are of particular advantage in order to obtain a d-dimensional representation of the amplitudes.

We have validated this setup on simpler cases such as the $gg \to t\bar{t}$ primitive amplitudes. Moreover, one can perform a gauge invariant test at integrand level, where the coefficients of the scalar integral basis are checked to satisfy the Ward identity.

Alternatively to the standard renormalisation, one can use the method proposed in Chapter 7. In this case, the contribution of wavefunction bubbles and tadpole obtained from the reduction can be discarded and the full amplitude can be reconstructed by matching the universal pole structure in $4 - 2\epsilon$ and $6 - 2\epsilon$ dimensions. We remark that this procedure can be applied since the reduction delivers the d-dimensional representation of the amplitude, which is suitable for evaluations in different dimensions. Also, this approach is more efficient than considering the counterterms of Eq. 8.4.54. In fact, this method allows us to obtain directly the gauge invariant coefficients for wavefunction bubbles and tadpoles, avoiding having to combine together all the different contributions coming from Feynman diagrams and counterterms.

8.5 Results and discussion

We computed the $t\bar{t}$ plus three gluons helicity primitive amplitudes at tree-level and one-loop, obtaining analytic expressions. We consider four independent helicity configurations, choosing the cases with $t^+\bar{t}^+$.

Firstly, we set up the parametrisation of the kinematics as described in Section 8.2. Therefore, we compute the primitive amplitudes using both the six dimensional generalised unitarity approach of Chapter 7 and the integrand reduction of

Feynman diagrams of Section 8.4.

As mentioned in the previous section, the six dimensional cuts have been used to compute the amplitudes in a rational numerics phase space, obtained by choosing rational numbers for the momentum twistor variables. The coefficients of wavefunction bubbles and tadpole are fixed by matching the pole structures in $4 - 2\epsilon$ and $6 - 2\epsilon$, following the prescriptions given in Chapter 7. We generate the required six dimensional tree-level building-blocks by implementing the BCFW recursion relation of Section 4.1.

We employ the integrand reduction of Feynman diagrams, where the renormalized amplitudes are computed using the d-dimensional counterterms of Eq.(8.4.54), as an independent method to check the results obtained with the unitarity-based approach. Moreover, the diagram reduction provides an algorithm which allows us to address the calculation of the analytic amplitudes, whereas we rely on future implementation of the unitarity method with a finite field reconstruction. The analytic computation of the coefficients of wavefunction bubble and tadpole is performed by matching the pole structures in $4 - 2\epsilon$ and $6 - 2\epsilon$, which is a more efficient operation than combining together terms from the reduction and counterterms.

For the sake of completeness, we need to mention further details about the method of pole matching. In particular, the calculation of primitive amplitudes with closed fermion loop and non-adjacent $t\bar{t}$ are not discussed in Chapter 7, where we focused on $A^{[L]}(t, \bar{t}, \dots)$ and $A^{[R]}(t, \bar{t}, \dots)$ only.

The heavy fermion loop primitive amplitudes can be computed as follows. We rewrite the amplitude in Eq. (7.2.1) as,

$$A_n^{(1)} = B_n^{(1)} + c_{2;m^2} I_{2,m^2}^{m^2} + c_1 I_1 \tag{8.5.55}$$

where the new bubble integral is,

$$I_{2,m^2}^{m^2} = \mu_R^{2\epsilon} \int \frac{d^d k}{(2\pi)^d} \frac{1}{(k^2 - m^2)((k-p)^2 - m^2)} \stackrel{d=4-2\epsilon}{=} i c_\Gamma \left(\frac{1}{\epsilon} + \log \left(\frac{\mu_R^2}{m^2} \right) \right) + \mathcal{O}(\epsilon). \tag{8.5.56}$$

The integral basis is modified through introducing finite bubble and tadpole functions defined by

$$F^{m^2}_{2;i_1,i_2} = I_{2,i_1,i_2} - I^{m^2}_{2,m^2}, \tag{8.5.57}$$

$$F^{m^2}_1 = I_1 - m^2 I^{m^2}_{2,m^2}. \tag{8.5.58}$$

Upon matching the amplitude with the universal pole structure in $4-2\epsilon$ dimensions, we find that the amplitude takes the explicit expression,

$$A^{(1)} = A^{6D,(1)}\bigg|_{I_2 \to F^{m^2}_2} + c_1 F^{m^2}_1 \tag{8.5.59}$$

Now we rely on the matching with the universal pole structure in $6-2\epsilon$ dimensions to fix c_1. The six dimensional integral $F^{m_2}_1$ has an epsilon-pole given by,

$$F_1 \overset{d=6-2\epsilon}{=} \frac{im^4}{(4\pi)^3} \frac{1}{2\epsilon} + \mathcal{O}(\epsilon). \tag{8.5.60}$$

From the six dimensional effective Lagrangian of Eq. (7.4.39)

$$A^{[H],6-2\epsilon}(t,\bar{t},3,4,5) = \frac{g^4_s}{48(4\pi)^3\epsilon}\left(-\frac{2d_s}{5} A^{[\gamma]}(t,\bar{t},3,4,5) \right) + \mathcal{O}(\epsilon^0)$$

The primitive amplitudes $A^{[L]}_5(1_{\bar{t}},5,2_t,3,4)$ and $A^{[L]}_5(1_{\bar{t}},3,4,2_t,5)$, which have a configuration with non-adjacent $t\bar{t}$ can be computed with the same procedure used for the left and right moving adjacent cases. We only need to introduce the appropriate counterterms which are required to remove the epsilon pole in $6-2\epsilon$ dimensions. The match with the six dimensional amplitude obtained from the $6d$

Lagrangian is,

$$A^{[L],6-2\epsilon}(1_{\bar{t}}, 5, 2_t, 3, 4) = \frac{g_s^4}{48(4\pi)^3\epsilon}\Bigg(2(3d_s + 2)m_t^2 A^{(0)}(1_{\bar{t}}, 5, 2_t, 3, 4)+$$

$$\frac{4(d_s - 2)}{5}A^{[\gamma]}(1_{\bar{t}}, 5, 2_t, 3, 4) + 2(d_s - 4)A^{[\sigma_1]}(1_{\bar{t}}, 5, 2_t, 3, 4)\Bigg) + \mathcal{O}(\epsilon^0)$$

$$(8.5.61)$$

A similar relation is valid for the $A_5^{[L]}(1_{\bar{t}}, 3, 4, 2_t, 5)$ partial amplitude,

$$A^{[L],6-2\epsilon}(1_{\bar{t}}, 3, 4, 2_t, 5) = \frac{g_s^4}{48(4\pi)^3\epsilon}\Bigg(2(3d_s + 2)m_t^2 A^{(0)}(1_{\bar{t}}, 3, 4, 2_t, 5)+$$

$$+ 2(d_s - 4)A^{[\sigma_1]}(1_{\bar{t}}, 3, 4, 2_t, 5)\Bigg) + \mathcal{O}(\epsilon^0) \qquad (8.5.62)$$

We validated these counterterms computing the corresponding $gg \to t\bar{t}$ primitive amplitudes.

The results of the $t\bar{t}ggg$ have been validated against the numerical results in [31].

Despite the amplitudes have been divided in four pieces according with the spin basis decomposition, the analytic expressions are still quite large to be written explicitly on a paper. Only the $A_5^{[L]}(1_{\bar{t}}^+, 2_t^+, 3^+, 4^+, 5^+)$ has a compact expression and it is shown in Appendix G.

In Table 8.1, numerical results for the primitive amplitudes are presented in the FDH scheme. We evaluate the ratio,

$$r^{(1)} = \frac{1}{c_\Gamma}\frac{A^{(1)}}{A^{(0)}} = \frac{r_2}{\epsilon^2} + \frac{r_1}{\epsilon} + r_0 + \mathcal{O}(\epsilon) \qquad (8.5.63)$$

at the following phase space point,

$$p_1 = \{1.2327, 0, 0, 1.22021\}, \tag{8.5.64}$$

$$p_2 = \{1.2327, 0, 0, -1.22021\}, \tag{8.5.65}$$

$$p_3 = \{-0.59461, 0.59461, 0, 0\}, \tag{8.5.66}$$

$$p_4 = \{-0.84090, 0, 0.59461, 0.59461\}, \tag{8.5.67}$$

$$p_5 = \{-1.02989, -0.59461, -0.59461, -0.59461\}, \tag{8.5.68}$$

$$\eta_1 = \{-2.09405, 2.09405, 0, 0\}, \tag{8.5.69}$$

$$\eta_2 = \{1.20416, 0.9, 0.8, 0\}, \tag{8.5.70}$$

$$p_1^\flat = \{1.22028, 0.0124, 0, 1.22021\}, \tag{8.5.71}$$

$$p_2^\flat = \{1.22028, -0.00928, -0.00825, -1.22021\} \tag{8.5.72}$$

$$m_t = m_H = \mu_R = 0.175 \tag{8.5.73}$$

We have tackled the calculation of the analytic helicity amplitudes for $t\bar{t}$ plus three-gluon scattering at one-loop order, although several aspects are left for future studies. Firstly, we have not tested the performance of the evaluation of the analytic expressions against numerical methods, for example by plugging them in existing frameworks such as NJET [19].

Moreover, some expressions are still quite large and further simplifications may be necessary. The implementation of the six dimensional unitarity framework with a finite field reconstruction algorithm may overcome this problem. Also, we are interested in looking for different integrand basis in order to make manifest the singular behaviour of the amplitudes at integrand level, which may deliver more compact and well performing expressions.

For phenomenological applications the amplitudes with two massless quarks and gluon are also required. These could be computed using the same methods used in this chapter though the dimension six operators in the effective Lagrangian would need to be extended. We therefore leave these amplitudes for future work.

Primitive Amplitude	$A_{5;\rho_1}$	$A_{5;\rho_2}$	$A_{5;\rho_3}$	$A_{5;\rho_4}$	A_5
$A^{(0)}(1_{\bar{t}}^+,2_t^+,3^+,4^+,5^+)$	0	0	0	0.005062+0.002969 i	-0.004388-0.000741 i
$r_0^{[L]}(1_{\bar{t}}^+,2_t^+,3^+,4^+,5^+)$	-0.229546+0.123809 i	-0.186892+0.200238 i	0.418535-0.128430 i	70.630700-19.147600 i	20.655100-4.072640 i
$A^{(0)}(1_{\bar{t}}^+,2_t^+,3^+,4^+,5^-)$	0.193099+0.341251 i	0.193099+0.341251 i	-0.386198-0.682502 i	-0.125837-0.454723 i	-0.020980+0.026896 i
$r_0^{[L]}(1_{\bar{t}}^+,2_t^+,3^+,4^+,5^-)$	26.118900-3.064520 i	26.560400-3.606450 i	26.362200-3.711340 i	26.077000-3.979200 i	23.352500-3.187260 i
$A^{(0)}(1_{\bar{t}}^+,2_t^+,3^+,4^-,5^-)$	-0.110631-0.033478 i	-0.013874-0.042370 i	0.018284+0.055837 i	-0.062308+0.089417 i	0.025647-0.063735 i
$r_0^{[L]}(1_{\bar{t}}^+,2_t^+,3^+,4^-,5^-)$	22.936900+2.118290 i	20.651900+18.221400 i	24.907800+18.375200 i	28.854200+5.332130 i	26.872500+3.874860 i
$A^{(0)}(1_{\bar{t}}^+,2_t^+,3^+,4^-,5^+)$	0	-0.073514+0.122982 i	0	0.056180+0.034812 i	0.005062+0.002969 i
$r_0^{[L]}(1_{\bar{t}}^+,2_t^+,3^+,4^-,5^+)$	10.087700-5.351580 i	-0.681923-144.240000 i	-23.140300-8.361680 i	-319.344000-77.504300 i	5.909830-61.528600 i
$A^{(0)}(1_{\bar{t}}^+,2_t^+,3^+,4^+,5^+)$	0	0	0	0.005062+0.002969 i	-0.004388-0.000741 i
$r_0^{[R]}(1_{\bar{t}}^+,2_t^+,3^+,4^+,5^+)$	-0.248365+0.078236 i	-0.055921+0.243956 i	0.515859-0.012842 i	63.240600-23.786400 i	-29.385900-9.163350 i
$A^{(0)}(1_{\bar{t}}^+,2_t^+,3^+,4^+,5^-)$	0.193099+0.341251 i	0.193099+0.341251 i	-0.386198-0.682502 i	-0.125837-0.454723 i	-0.020980+0.026896 i
$r_0^{[R]}(1_{\bar{t}}^+,2_t^+,3^+,4^+,5^-)$	-21.307600+26.582700 i	-22.669000+23.472800 i	-21.830300+24.628500 i	-22.701800+23.870500 i	-39.325700+38.944100 i
$A^{(0)}(1_{\bar{t}}^+,2_t^+,3^+,4^-,5^-)$	-0.110631-0.033478 i	-0.013874-0.042370 i	0.018284+0.055837 i	-0.062308+0.089417 i	0.025647-0.063735 i
$r_0^{[R]}(1_{\bar{t}}^+,2_t^+,3^+,4^-,5^-)$	105.670000+266.765000 i	375.921000-14.885500 i	545.197000+156.983000 i	180.437000+27.790600 i	-0.777453+109.779000 i
$A^{(0)}(1_{\bar{t}}^+,2_t^+,3^+,4^-,5^+)$	0	-0.073514+0.122982 i	0	0.056180+0.034812 i	0.005062+0.002969 i
$r_0^{[R]}(1_{\bar{t}}^+,2_t^+,3^+,4^-,5^+)$	-36.696100+19.910800 i	-35.279000+16.986800 i	-36.371200+18.394700 i	-35.912900+17.535900 i	-29.534200+34.297900 i
$A^{(0)}(1_{\bar{t}}^+,5^+,2_t^+,3^+,4^+)$	0	0	0	0.001573+0.000663 i	-0.001293-0.000046 i
$r_0^{[L]}(1_{\bar{t}}^+,5^+,2_t^+,3^+,4^+)$	-12.563413 + 1.282216i	-0.186892+0.200238 i	5.817966 - 14.616696i	-31.626850 - 3.310587i	70.630754 - 19.147667 i
$A^{(0)}(1_{\bar{t}}^+,5^-,2_t^+,3^+,4^+)$	0.068653+0.090918 i	0.068653+0.090918 i	-0.137306-0.181836i	-0.053641-0.126134i	-0.005006+0.008514 i
$r_0^{[L]}(1_{\bar{t}}^+,5^-,2_t^+,3^+,4^+)$	4.500739 + 0.902133i	-0.666992 - 0.645430i	3.067734 + 8.039904i	-3.644197 - 15.3278150*i	3.257287 - 7.031204 i
$A^{(0)}(1_{\bar{t}}^+,5^+,2_t^+,3^+,4^-)$	0	-0.016498+0.038159 i	0	0.017384+0.007892i	-0.010049+0.025670 i
$r_0^{[L]}(1_{\bar{t}}^+,5^+,2_t^+,3^+,4^-)$	24.880735 - 0.875213i	-9.555913 - 9.134219 i	-7.991341 + 27.812801i	43.40379 - 1.0529877 i	22.936943+ 2.118295 i
$A^{(0)}(1_{\bar{t}}^+,5^+,2_t^+,3^-,4^+)$	-0.009273-0.024050 i	0	0	-0.018058-0.008257 i	0.015024+0.000986 i
$r_0^{[L]}(1_{\bar{t}}^+,5^+,2_t^+,3^-,4^+)$	15.89683 + 1.028210i	-7.827587 - 4.18071423 i	-1.646687 + 17.486103 i	19.909854 - 5.854061 i	5.909830-61.528600 i
$A^{(0)}(1_{\bar{t}}^+,3^+,4^+,2_t^+,5^+)$	0	0	0	0.001573+0.000663 i	-0.001293-0.000046 i
$r_0^{[L]}(1_{\bar{t}}^+,3^+,4^+,2_t^+,5^+)$	0.616934 + 0.607897 i	0.007854+ 0.0279197i	1.040824 - 0.920014i	2.482324 + 0.31750 i	3.240645 - 3.786422 i
$A^{(0)}(1_{\bar{t}}^+,3^+,4^+,2_t^+,5^-)$	0.068653+0.090918 i	0.068653+0.090918 i	-0.137306-0.181836i	-0.053641-0.126134i	-0.005006+0.008514 i
$r_0^{[L]}(1_{\bar{t}}^+,3^+,4^+,2_t^+,5^-)$	0.009435 + 0.1845446i	.292554 + 0.059403i	0.635912 + 0.474917i	0.4132203 + 1.4536603 i	-1.35112 + 2.17252 i
$A^{(0)}(1_{\bar{t}}^+,3^+,4^-,2_t^+,5^+)$	0	-0.016498+0.038159 i	0	0.017384+0.007892i	-0.010049+0.025670 i
$r_0^{[L]}(1_{\bar{t}}^+,3^+,4^-,2_t^+,5^+)$	0.588002 - 0.221334 i	0.127825 + 0.27604i	0.933226 - 0.113822 i	2.523587+ 2.255809i	-0.777453+1.779000 i
$A^{(0)}(1_{\bar{t}}^+,3^-,4^+,2_t^+,5^+)$	-0.009273-0.024050 i	0	0	-0.018058-0.008257 i	0.015024+0.000986 i
$r_0^{[L]}(1_{\bar{t}}^+,3^-,4^+,2_t^+,5^+)$	0.339424 + 1.174763 i	0.087087 - 0.09957265i	0.159224 - 0.253058 i	0.449392 - 0.439997 i	6.118954 - 3.064524 i
$A^{(0)}(1_{\bar{t}}^+,2_t^+,3^+,4^+,5^+)$	0	0	0	0.005062+0.002969 i	-0.004388-0.000741 i
$r_0^{[H]}(1_{\bar{t}}^+,2_t^+,3^+,4^+,5^+)$	-0.011558+0.017952 i	-0.034144-0.003384 i	0.009685+0.001295 i	4.133880+3.352110 i	6.604910+1.010880 i
$A^{(0)}(1_{\bar{t}}^+,2_t^+,3^+,4^+,5^-)$	0.193099+0.341251 i	0.193099+0.341251 i	-0.386198-0.682502 i	-0.125837-0.454723 i	-0.020980+0.026896 i
$r_0^{[H]}(1_{\bar{t}}^+,2_t^+,3^+,4^+,5^-)$	-0.069945-0.024710 i	-0.084733-0.175454 i	-0.034493-0.106540 i	-0.046054-0.177834 i	-1.225720+0.266619 i
$A^{(0)}(1_{\bar{t}}^+,2_t^+,3^+,4^-,5^-)$	-0.110631-0.033478 i	-0.013874-0.042370 i	0.018284+0.055837 i	-0.062308+0.089417 i	0.025647-0.063735 i
$r_0^{[H]}(1_{\bar{t}}^+,2_t^+,3^+,4^-,5^-)$	-0.155949-0.200315 i	-1.226840+0.504261 i	-1.356790+0.365411 i	-0.275387+0.433699 i	0.014927+0.233753 i
$A^{(0)}(1_{\bar{t}}^+,2_t^+,3^+,4^-,5^+)$	0	-0.073514+0.122982 i	0	0.056180+0.034812 i	0.005062+0.002969 i
$r_0^{[H]}(1_{\bar{t}}^+,2_t^+,3^+,4^-,5^+)$	-0.012308-0.073154 i	0.112356-0.159185 i	0.052755-0.145486 i	0.113662-0.157610 i	0.013365-0.079955 i

Table 8.1: Numerical evaluation of tree-level amplitudes and finite part of ratio of primitive amplitudes. We give numerical values of sub-amplitudes and total amplitudes. When the tree-level is zero, the ratio is replaced by the corresponding one-loop amplitude.

Chapter 9

Conclusions

Scattering amplitudes play a fundamental role in precise studies of the Standard Model. In order to make the best use of data gathered at hadron colliders we need to keep theoretical uncertainties in line with experimental errors. The remarkable progress in experimental measurements makes it necessary to have predictions beyond leading order accuracy. For this reason, the development of new methods for the calculation of scattering amplitudes at higher-order in perturbation theory has been particularly important in recent years.

In this thesis, we discussed new on-shell methods for the analytic calculation of one-loop amplitudes in QCD. Despite the fact that many automated frameworks for obtaining one-loop numerical results are known, the problem of computing high multiplicity analytic amplitudes is still not well established. Moreover, analytic expressions are expected to perform better than numerical tools. This may contribute to avoid some of the bottlenecks which typical appear in higher order simulations, where one-loop matrix elements need to be integrated over an unresolved phase-space.

In our approach, we relied on the simplifications given by working with physical degrees of freedom, which is more efficient than traditional Feynman diagram computations. We used dedicated techniques such as the spinor-helicity formalism, momentum twistor parametrisation, generalised unitarity and integrand reduction, providing a complete algebraic framework where only rational functions appear into intermediate steps. We computed the universal one-loop triple collinear

splitting functions in QCD, which contribute to N³LO subtraction terms for differential observables. We obtained compact analytic expressions by introducing a new parametrisation of the kinematics in the collinear limit based on spinor-helicity and presenting the result in terms of a supersymmetric decomposition.

We explored how a loop amplitude in dimensional regularisation can be computed efficiently by looking at its higher dimensional representation. In particular we worked in a six dimensional space, parametrising the on-shell building-blocks of generalised unitarity by invoking the six dimensional spinor-helicity formalism. We discussed the setup for the calculation of the one-loop amplitudes for Higgs plus five gluon scattering in the large top mass effective theory. The analytic expressions for this high multiplicity process may overcome potential bottlenecks in the calculation of the $H + 2j$ cross section at NNLO. We have provided a benchmark for a rational phase-space point, proving that our method is suitable for a finite field fitting reconstruction.

Then we discussed how one-loop amplitudes with massive fermions can be computed in a unitarity compatible approach, answering the formal question if loop massive amplitudes can be computed with on-shell information only. We showed that the part of the amplitude not captured by unitarity can be fixed by considering the universal pole structure in four and six dimensions. In particular the match with poles in six dimensions is realised by constructing an effective QCD Lagrangian with operators of mass-dimension six. Finally, we computed the $t\bar{t}$ plus three partons one-loop helicity amplitudes using the new method proposed, also showing how the introduction of a spin basis reduce the degree of complexity of the calculation.

The one-loop techniques presented in this thesis have been shown to be successful for obtaining analytic expressions, which can be used for flexible phenomenological studies. Furthermore, we look forward for the developments of these methods for applications in multi-loop scattering amplitude calculations.

The thesis has been organised as follows. In Chapter 2 we reviewed same basic and well known concepts about the Standard Model, focusing in particular on QCD. In Chapter 3 we introduced the properties of QCD scattering amplitudes and the frameworks of spinor-helicity and momentum-twistors for their representation. In

Chapter 4 we discussed some of the modern methods for scattering amplitude calculations such as generalised unitarity and integrand reduction, also in combination with the six-dimensional spinor-helicity formalism. In Chapter 5 we computed the universal one-loop triple collinear splitting functions in QCD. In Chapter 6 we discussed the calculation of the one-loop amplitudes for Higgs plus 5 gluons scattering in the large mass top limit. In Chapter 7 we discussed a unitarity compatible approach to one-loop amplitudes with massive fermions. In Chapter 8 we showed the calculation of the one-loop amplitudes for the $t\bar{t}$ plus three parton scattering, based on the new method described in the previous chapter.

Appendix A

Feynman rules

In this appendix we list the set of Feynman rules that are relevant for the scope of this thesis. Because we have alway dealt with the calculation of colour ordered amplitudes, we will present colour ordered Feynman rules only. Some of the rules were derived with the help of FeynCalc [141, 142] and FeynRules [143, 144]. We also adopt the convention where all the momenta entering in the vertices are outgoing.

QCD

The rules for the propagators are:

$$\mu \;\text{\scriptsize{k}}\; \nu \quad = \frac{-ig^{\mu\nu}}{k^2 + i\epsilon} \quad \text{(gluon propagator)} \tag{A.0.1}$$

$$\xrightarrow{\;k\;} \quad = \frac{i\slashed{k} + m}{k^2 - m^2 + i\epsilon} \quad \text{(fermion propagator)} \tag{A.0.2}$$

$$\cdots\;\text{\scriptsize{k}}\;\cdots \quad = \frac{i}{k^2 + i\epsilon} \quad \text{(scalar propagator)} \tag{A.0.3}$$

The rules for the vertices are:

 $= \dfrac{ig_s}{\sqrt{2}}\left(g^{\mu\nu}(p_1 - p_2)^\rho + g^{\nu\rho}(p_2 - p_3)^\mu + g^{\rho\mu}(p_3 - p_1)^\nu\right)$ (A.0.4)

 $= ig_s^2\left(g^{\mu\rho}g^{\nu\sigma} - \dfrac{1}{2}(g^{\mu\nu}g^{\rho\sigma} + g^{\nu\rho}g^{\sigma\mu})\right)$ (A.0.5)

 $= \dfrac{ig_s}{\sqrt{2}}\gamma^\mu$ (A.0.6)

 $= \dfrac{ig_s}{\sqrt{2}}(p_1 - p_2)^\mu$ (A.0.7)

 $= \dfrac{ig_s^2}{2}g^{\mu\nu}$ (A.0.8)

(A.0.9)

HEFT

We list the set of Feynman rules for the Higgs interaction in the HEFT introduced in Section 6. They are obtained from the Lagrangian in Eq. (6.1.1) and Eq. (6.1.6).

$$\cancel{p}_H = -2ig_s\left(g^{\mu\nu}p_1\cdot p_2 - p_1^\mu p_2^\nu\right) \qquad (A.0.10)$$

$$\cancel{p}_\phi = -ig_s\left(g^{\mu\nu}p_1\cdot p_2 - p_1^\mu p_2^\nu + i\epsilon^{\mu\nu\rho\sigma}p_{1\rho}p_{2\sigma}\right) \qquad (A.0.11)$$

$$\cancel{p}_{H/\phi} = -2ig_s p_1\cdot p_2 \qquad (A.0.12)$$

Six dimensional QCD effective Lagrangian

In this appendix we present selected Feynman rules for the six dimensional effective theory of interest to us, defined by the Lagrangian

$$\mathcal{L}_{QCD}^6 = \bar\psi(i\cancel{D} - m)\psi - \frac{1}{2}\operatorname{tr} F_{\mu\nu}F^{\mu\nu} + \frac{i}{2}\sigma_1\, g_s^3 m_t\, \bar\psi\gamma^\mu\gamma^\nu F_{\mu\nu}\psi$$
$$+ i\sigma_2\, g_s^3\, \bar\psi F_{\mu\nu}\gamma^\mu D^\nu\psi + \frac{i}{6}\gamma\, g_s^3\operatorname{tr}\left(F^{\mu\nu}[F_{\mu\lambda}, F_\nu{}^\lambda]\right). \qquad (A.0.13)$$

We further define

$$F_{\mu\nu}^a = \partial_\mu A_\nu^a - \partial_\nu A_\mu^a + g_s f^{abc} A_\mu^b A_\nu^c, \qquad (A.0.14)$$

$$\sigma^{\mu\nu} = \frac{i}{2}\left(\gamma^\mu\gamma^\nu - \gamma^\nu\gamma^\mu\right). \qquad (A.0.15)$$

These rules were derived with the help of FeynCalc [141, 142] and FeynRules [143, 144]. The vertices are colour ordered and all momenta are considered to be outgoing. We include the coupling constants here for clarity though in the main text they are stripped off.

$$\begin{array}{r}\includegraphics{fig}\end{array} = -g_s^3 \sigma_1 \, m_t \sigma^{\mu_3 \nu} p_{3\nu} \tag{A.0.16}$$

$$\begin{array}{r}\includegraphics{fig}\end{array} = -ig_s^3 \sigma_2 \left(p_2^{\mu_3} \slashed{p}_3 - p_2 \cdot p_3 \gamma^{\mu_3} \right) \tag{A.0.17}$$

$$\begin{array}{r}\includegraphics{fig}\end{array} = g_s^4 \sigma_1 \, m_t \sigma^{\mu_3 \mu_4} \tag{A.0.18}$$

$$\begin{array}{r}\includegraphics{fig}\end{array} = -ig_s^4 \sigma_2 \left(g^{\mu_3 \mu_4} \slashed{p}_3 - \gamma^{\mu_4} p_1^{\mu_3} + \gamma^{\mu_3} (p_1^{\mu_4} - p_3^{\mu_4}) \right) \tag{A.0.19}$$

$$\begin{array}{r}\includegraphics{fig}\end{array} = -\frac{i}{2} g_s^3 \gamma \left(\vphantom{\int} \right.$$
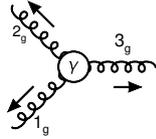
$$g^{\mu_1 \mu_2} \left(p_1 \cdot p_3 \, p_2^{\mu_3} - p_2 \cdot p_3 \, p_1^{\mu_3} \right)$$

$$+ \, g^{\mu_2 \mu_3} \left(p_2 \cdot p_1 \, p_3^{\mu_1} - p_3 \cdot p_1 \, p_2^{\mu_1} \right)$$

$$+ \, g^{\mu_3 \mu_1} \left(p_3 \cdot p_2 \, p_1^{\mu_2} - p_1 \cdot p_2 \, p_3^{\mu_2} \right)$$

$$\left. - \, p_3^{\mu_1} p_1^{\mu_2} p_2^{\mu_3} + p_2^{\mu_1} p_3^{\mu_2} p_1^{\mu_3} \right). \tag{A.0.20}$$
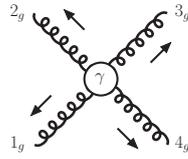
$$= -\frac{i}{2}g_s^4\gamma \Bigg($$

$$(A.0.21)$$

$$g^{\mu_1\mu_2}g^{\mu_3\mu_4}\left(p_1\cdot p_4 + p_2\cdot p_3\right) +$$

$$g^{\mu_1\mu_4}g^{\mu_2\mu_3}\left(p_1\cdot p_2 + p_3\cdot p_4\right) +$$

$$g^{\mu_1\mu_3}g^{\mu_2\mu_4}\left(-p_1\cdot p_2 - p_1\cdot p_4 - p_2\cdot p_3 - p_3\cdot p_4\right) +$$

$$g^{\mu_2\mu_3}\left(-p_1^{\mu_4}p_2^{\mu_1} + p_3^{\mu_4}p_2^{\mu_1} - p_3^{\mu_1}p_2^{\mu_4} - p_3^{\mu_4}p_4^{\mu_1}\right) +$$

$$g^{\mu_3\mu_4}\left(-p_3^{\mu_2}p_2^{\mu_1} - p_1^{\mu_2}p_4^{\mu_1} + p_3^{\mu_2}p_4^{\mu_1} - p_3^{\mu_1}p_4^{\mu_2}\right) +$$

$$g^{\mu_1\mu_3}\left(p_2^{\mu_4}p_1^{\mu_2} + p_4^{\mu_2}p_1^{\mu_4} + p_2^{\mu_4}p_3^{\mu_2} + p_3^{\mu_4}p_4^{\mu_2}\right) +$$

$$g^{\mu_1\mu_2}\left(-p_2^{\mu_4}p_1^{\mu_3} + p_2^{\mu_3}p_1^{\mu_4} - p_4^{\mu_3}p_1^{\mu_4} - p_2^{\mu_3}p_3^{\mu_4}\right) +$$

$$g^{\mu_2\mu_4}\left(p_1^{\mu_3}p_2^{\mu_1} + p_3^{\mu_1}p_2^{\mu_3} + p_1^{\mu_3}p_4^{\mu_1} + p_3^{\mu_1}p_4^{\mu_3}\right) +$$

$$g^{\mu_1\mu_4}\left(-p_2^{\mu_3}p_1^{\mu_2} + p_4^{\mu_3}p_1^{\mu_2} - p_4^{\mu_2}p_1^{\mu_3} - p_3^{\mu_2}p_4^{\mu_3}\right) \Bigg)$$
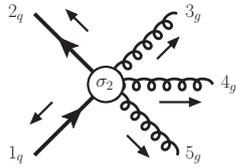
$$= -ig_s^5\sigma_2\left(\gamma^{\mu_3}g^{\mu_4\mu_5} - \gamma^{\mu_4}g^{\mu_3\mu_5}\right) \qquad (A.0.22)$$

Appendix B

Analytic expressions for tree-level amplitudes

B.1 Tree-level amplitudes using six dimensional spinor-helicity

In this section we list some QCD tree-level amplitudes in the six dimensional spinor-helicity formalism.

Three-point amplitudes

- $A^{(0)}(1_q, 2_{\bar{q}}, 3_g)$

$$A^{(0)}(1_q^a, 2_{\bar{q}}^b, 3_g^{c\dot{c}}) = \frac{i}{s_{r3}}\langle 1^a 2^b 3^c \rangle r^x \langle r_x | 3^{\dot{c}}] \tag{B.1.1}$$

where r is a massless reference vector satisfying $s_{r3} \neq 0$.

- $A^{(0)}(1_g, 2_g, 3_g)$

$$A^{(0)}(1_{a\dot{a}}, 2_{b\dot{b}}, 3_{c\dot{c}}) = i\Gamma_{abc}\tilde{\Gamma}_{\dot{a}\dot{b}\dot{c}} \qquad \Gamma_{abc} = u_{1a}u_{2b}w_{3c} + u_{1a}w_{2b}u_{3c} + w_{1a}u_{2b}u_{3c}$$

$$\text{(B.1.2)}$$

$$\tilde{\Gamma}_{\dot{a}\dot{b}\dot{c}} = \tilde{u}_{1\dot{a}}\tilde{u}_{2\dot{a}}\tilde{w}_{3\dot{c}} + \tilde{u}_{1\dot{a}}\tilde{w}_{2\dot{a}}\tilde{u}_{3\dot{c}} + \tilde{w}_{1\dot{a}}\tilde{u}_{2\dot{a}}\tilde{u}_{3\dot{c}},$$

$$\text{(B.1.3)}$$

where the tensors Γ and $\tilde{\Gamma}$ are written in terms of the $SU(2)$ spinors $u, \tilde{u}$ satisfying the following properties, defined on a cyclic order $\{ijk\}$,

$$u_{ia}\tilde{u}_{j\dot{b}} = \langle i_a | j_{\dot{b}}], \qquad\qquad u_{ja}\tilde{u}_{i\dot{b}} = -\langle j_a | i_{\dot{b}}], \qquad \text{(B.1.4)}$$

and $w, \tilde{w}$ are the inverse of the $u, \tilde{u}$

$$\epsilon_{ab} = u_a w_b - u_b w_a, \qquad\qquad \epsilon_{\dot{a}\dot{b}} = \tilde{u}_{\dot{a}}\tilde{w}_{\dot{b}} - \tilde{u}_{\dot{b}}\tilde{w}_{\dot{a}}, \qquad \text{(B.1.5)}$$

for which we impose momentum conservation

$$0 = \tilde{w}_{1\dot{a}}\tilde{\lambda}^{\dot{a}}_{1A} + \tilde{w}_{2\dot{a}}\tilde{\lambda}^{\dot{a}}_{2A} + \tilde{w}_{3\dot{a}}\tilde{\lambda}^{\dot{a}}_{3A}. \qquad \text{(B.1.6)}$$

- $A^{(0)}(1_{\phi_{1,2}}, 2_{\phi_{1,2}}, 3_g)$

$$A^{(0)}(1_{\phi_{1,2}}, 2_{\phi_{1,2}}, 3_g^{a\dot{a}}) = \frac{-i}{2s_{r3}}\langle 3^a | (1-2) | r | 3^{\dot{a}}] \qquad \text{(B.1.7)}$$

where r is a massless reference vector satisfying $s_{r3} \neq 0$.

- $A^{(0)}(1_{\phi_1}, 2_{\bar{q}}, 3_q)$

$$A^{(0)}(1_{\phi_1}, 2_{\bar{q}}^a, 3_q^{\dot{b}}) = \frac{i}{\sqrt{2}}\langle 1^a | 2^{\dot{b}}]. \qquad \text{(B.1.8)}$$

- $A^{(0)}(1_{\phi_2}, 2_{\bar{q}}, 3_q)$

$$A^{(0)}(1_{\phi_1}, 2_{\bar{q}}^a, 3_q^{\dot{b}}) = \frac{i}{\sqrt{2}}\langle 1^a \gamma^5 2^{\dot{b}}].$$
(B.1.9)

Four-point amplitudes

- $A^{(0)}(1_g, 2_g, 3_g, 4_g)$

$$A^{(0)}(1_{a\dot{a}}, 2_{b\dot{b}}, 3_{c\dot{c}}, 4_{d\dot{d}}) = \frac{-i}{s_{12}s_{23}}\langle 1_a 2_b 3_c\rangle 4_d [1_{\dot{a}} 2_{\dot{b}} 3_{\dot{c}} 4_{\dot{d}}]$$
(B.1.10)

- $A(1_q, 2_g, 3_g, 4_{\bar{q}})$

$$A^{(0)}(1_{q,a}, 2_{b\dot{b}}, 3_{c\dot{c}}, 4_{\bar{q},d}) = \frac{i}{2s_{12}s_{23}}\langle 1_a 2_b 3_c 4_d\rangle [1_{\dot{x}} 2_{\dot{b}} 3_{\dot{c}} 1^{\dot{x}}].$$
(B.1.11)

- $A^{(0)}(1_g, 2_g, 3_{\phi_{1,2}}, 4_{\phi_{1,2}})$

$$A^{(0)}(1_{a\dot{a}}, 2_{b\dot{b}}, 3, 4) = \frac{i}{4s_{12}s_{23}}\langle 1_a 2_b 3_x\rangle 3^x [1_{\dot{a}} 2_{\dot{b}} 3_{\dot{x}} 3^{\dot{x}}]$$
(B.1.12)

B.2   Tree-level amplitudes from the QCD effective Lagrangian

Written in terms of four dimensional spinor products, the independent helicity amplitudes are [2],

$$
\begin{aligned}
-i\langle\eta_1 1^\flat\rangle\langle\eta_4 4^\flat\rangle A^{[\sigma_1]}(1_t^+, 2^+, 3^+, 4_{\bar t}^+) = \\
\frac{-2m_t(2m_t^2 - 4p_1\cdot p_2 - s_{23})s_{23}\langle\eta_1 2\rangle\langle\eta_4 3\rangle}{\langle 23\rangle^3} + \frac{2m_t(m_t^2 - 2p_1\cdot p_2)s_{23}\langle\eta_1\eta_4\rangle}{m_t\langle 23\rangle^2} \\
- \frac{m_t(m_t^2 - 2p_1\cdot p_2)s_{23}\langle\eta_1 3\rangle\langle\eta_4 3\rangle\langle 213]}{p_1\cdot p_2\langle 23\rangle^3} + \frac{m_t(m_t^2 - 2p_1\cdot p_2)s_{23}\langle\eta_1 2\rangle\langle\eta_4 2\rangle\langle 312]}{p_1\cdot p_2\langle 23\rangle^3},
\end{aligned}
$$

$$(\text{B.2.13})$$

$$
\begin{aligned}
-i\langle\eta_1 1^\flat\rangle\langle\eta_4 4^\flat\rangle A^{[\sigma_1]}(1_t^+, 2^+, 3^-, 4_{\bar t}^+) = \\
\frac{(-4m_t(p_1\cdot p_2)^2 + m_t^2 s_{23} - 2p_1\cdot p_2 s_{23})\langle\eta_1 3\rangle\langle\eta_4 3\rangle\langle 312]}{p_1\cdot p_2 s_{23}\langle 23\rangle} \\
- \frac{2m_t\langle\eta_1\eta_4\rangle\langle 312]^2}{m_t s_{23}} + \frac{m_t(4p_1\cdot p_2 + s_{23})\langle\eta_1 2\rangle\langle\eta_4 3\rangle\langle 312]^2}{p_1\cdot p_2 s_{23}\langle 23\rangle} - \frac{m_t\langle\eta_1 2\rangle\langle\eta_4 2\rangle\langle 312]^3}{p_1\cdot p_2 s_{23}\langle 23\rangle},
\end{aligned}
$$

$$(\text{B.2.14})$$

$$
-i\langle\eta_1 1^\flat\rangle\langle\eta_4 4^\flat\rangle A^{[\gamma]}(1_t^+, 2^+, 3^+, 4_{\bar t}^+) = \frac{m_t s_{23}^2\langle\eta_1 2\rangle\langle\eta_4 3\rangle}{2\langle 23\rangle^3} + \frac{m_t p_1\cdot p_2 s_{23}\langle\eta_1\eta_4\rangle}{\langle 23\rangle^2},
$$

$$(\text{B.2.15})$$

$$
-i\langle\eta_1 1^\flat\rangle\langle\eta_4 4^\flat\rangle A^{[\gamma]}(1_t^+, 2^+, 3^-, 4_{\bar t}^+) = 0, \tag{B.2.16}
$$

$$
-i\langle\eta_1 1^\flat\rangle\langle\eta_4 4^\flat\rangle A^{[\sigma_2]}(1_t^+, 2^+, 3^+, 4_{\bar t}^+) = 0, \tag{B.2.17}
$$

$$
-i\langle\eta_1 1^\flat\rangle\langle\eta_4 4^\flat\rangle A^{[\sigma_2]}(1_t^+, 2^+, 3^-, 4_{\bar t}^+) = 0. \tag{B.2.18}
$$

We note that the amplitudes of the σ_2 operator vanish in the cases we have considered. We have used the massless decomposition as in Eq. (8.2.15).

Appendix C

Interactions and state-sum reduction for six dimensional spinors

C.1   Derivation of the state-sum reduction

We begin our discussion by looking at a free massive fermion field in four dimensions,

$$\mathcal{L}^{4d} = \overline{\psi}(x)(i\gamma^\mu \partial_\mu - m)\psi(x), \tag{C.1.1}$$

using the Weyl representation of the Dirac γ. For the spinors associated with external fermions we seek solutions to the massive Dirac equation

$$(\gamma \cdot \bar{p} - m)u_s(\bar{p}) = 0 \text{ and } \bar{u}_s(\bar{p})(\gamma \cdot \bar{p} - m) = 0, \tag{C.1.2}$$

where the bar on the momentum $\bar{p}$ denotes that the vector is in four dimensions.

Alternatively we can consider a massless fermion field in six dimensions, with Lagrangian

$$\mathcal{L}^{6d} = \overline{\Psi}(x)(i\Gamma^M \partial_M)\Psi(x). \tag{C.1.3}$$

Note that, in this case, for six dimensions we use capital Greek letters M, which runs from 0 to 5. In six spacetime dimensions the Dirac matrices are 8×8 objects, which we choose to be

$$
\Gamma^M = \begin{pmatrix} 0 & \tilde{\Sigma}^M \\ \Sigma^M & 0 \end{pmatrix}, \tag{C.1.4}
$$

where the Σ matrices are defined by taking outer products of Pauli matrices and are listed explicitly in Eq. (3.2.31).

This representation of the Γ matrices is simply related to the four dimensional γ-matrices. The relation for the first four Σ matrices is

$$
-\tilde{\Sigma}^{5,AX}\Sigma^\mu_{XB} = (\gamma^\mu)^A{}_B = \tilde{\Sigma}^{\mu,AX}\Sigma^5_{XB}, \tag{C.1.5}
$$

where we have adopted the convention that Σ^M carry lower spinor indices while $\tilde{\Sigma}^M$ carry upper indices. For the remaining two Σ matrices we have

$$
-\tilde{\Sigma}^{5,AX}\Sigma^4_{XB} = (-\gamma^0\gamma^1\gamma^2\gamma^3)^A{}_B = i(\gamma^5)^A{}_B, \tag{C.1.6}
$$

$$
-\tilde{\Sigma}^{5,AX}\Sigma^5_{XB} = \mathbf{1}^A{}_B. \tag{C.1.7}
$$

In the present case, there is no six dimensional mass term. Moreover, in our Weyl basis for the Γ matrices (C.1.4) we can decompose $\Psi = (\Psi_1, \Psi_2)$ and see that the two fields decouple:

$$
\mathcal{L}^{6d} = \overline{\Psi}_1(x)(i\Sigma^M\partial_M)\Psi_1(x) + \overline{\Psi}_2(x)(i\tilde{\Sigma}^M\partial_M)\Psi_2(x). \tag{C.1.8}
$$

Hence the two Ψ_i are essentially copies of each other. The relations among the four dimensional massive spinors and the six dimensional massless spinors are given in Eq. (3.2.59) and (3.2.61) (see Section 3.2).

We introduce interactions as always by replacing the derivative with the covariant

derivative. In six dimensions

$$\partial_M \to D_M = \partial_M - ig A_M^i(x) t^i, \tag{C.1.9}$$

where $A_M^i(x)$ are the gauge fields and t^i are the generators of the gauge group. We dimensionally reduce the six-dimensional gauge field to four dimensions by treating its last two entries as scalar fields,

$$A_M(x) = A_M^i(x) t^i = (A_\mu(x), \phi_1(x), \phi_2(x)), \tag{C.1.10}$$

leading to the following interaction terms for Ψ_1 (dropping dependence on position for simplicity):

$$
\begin{aligned}
\mathcal{L}^{6d}_{\text{int}, \Psi_1} &= -ig \overline{\Psi}_1 \Sigma^M A_M \Psi_1 \\
&= -ig \overline{\Psi}_1 \left(\Sigma^\mu A_\mu - \Sigma^4 \phi_1 - \Sigma^5 \phi_2 \right) \Psi_1 \\
&= -ig \overline{\Psi}_1 \Sigma^\mu A_\mu \Psi_1 + g \overline{\Psi}_1 \phi_1 \Psi_2 - ig \overline{\Psi}_1 \phi_2 \gamma_5 \Psi_2,
\end{aligned} \tag{C.1.11}
$$

where, in the last line, we have used the relation between chiral and anti-chiral spinors $\lambda^A = i \tilde{\Sigma}^{4,AB} \tilde{\lambda}_B$, which for the fields reads $\Psi_1 = i \tilde{\Sigma}^4 \Psi_2$. The last two terms give rise to the three-point amplitudes given in (B.1.8) and (B.1.9). While the first term resembles the four dimensional interaction term the two last terms are additional contributions arising from the extra momentum components. For internal lines these contributions correspond to additional gluon polarisation states that should be subtracted to obtain the four-dimensional result. This procedure is known as state-sum reduction.

The contraction of Lorentz indices over internal propagators leads to explicit dependence on the spin dimension d_s. Working explicitly in six dimensions this dependence will be lost but can be recovered through state-sum reduction. The general procedure is described in [72, 81]. Gluons in six dimensions have $6 - 2 = 4$ polarisation states, so for each extra dimension introduced we get one more state. Each of these states correspond to the contribution from replacing gluons in the loop
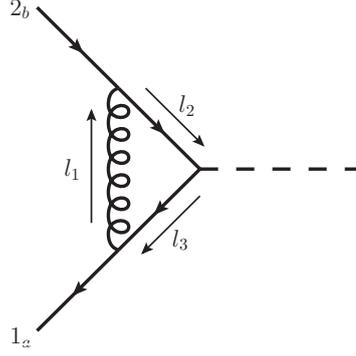
Figure C.1: Feynman diagram for one-loop contribution to the coupling between a massive fermion pair and an off-shell scalar. All external momenta are outgoing.

by a scalar. By subtracting these scalars the number of polarisation states can be reduced to $d_s - 2$. In our set-up, the scalar associated with the mass direction should be subtracted separately and we arrive at the state-sum reduction prescription

$$\boldsymbol{c} = \boldsymbol{c}^{6d} - (5 - d_s)\boldsymbol{c}_{\phi_1} - \boldsymbol{c}_{\phi_2}. \tag{C.1.12}$$

C.2 A one-loop example

Let us now illuminate this higher dimensional formalism with a worked example: the one-loop amplitude for a massive fermion pair coupling to an off-shell scalar, $A^{(1)}$. This calculation involves only one Feynman diagram (figure C.1), which, using the colour-ordered four dimensional Feynman rules, is given by

$$A^{(1),4d} = \int \frac{d^d \ell_1}{(2\pi)^d} \, \bar{u}_1 \gamma^\mu \frac{(\gamma \cdot \ell_3 + m)}{\ell_3^2 - m^2} \frac{(\gamma \cdot \ell_2 + m)}{\ell_2^2 - m^2} \gamma^\nu v_2 \frac{\eta_{\mu\nu}}{\ell_1^2} \equiv \int \frac{d^d \ell_1}{(2\pi)^d} \frac{N^{4d}}{D_1 D_2 D_3}, \tag{C.2.13}$$

where $\ell_2 = \ell_1 - p_2$, $\ell_3 = \ell_1 + p_1$, $D_i = \ell_i^2 - m_i^2$, and N^{4d} is the numerator. We will write the result in terms of the scalar integrals using the notation of [73]

$$\boldsymbol{I} = \left\{ I_3(m^2, s, m^2; 0, m^2, m^2), F_2(s, m^2), I_2(m^2; 0, m^2) \right\}, \tag{C.2.14}$$

where $F_2(s, m^2) = I_2(s; m^2, m^2) - I_2(m^2; 0, m^2)$. The result is $A^{(1),4d} = \boldsymbol{c}^{(d_s)} \cdot \boldsymbol{I} A^{(0),4d}$ where the integral coefficients are given by

$$\boldsymbol{c}^{(d_s)} = \left\{ -2(s - 2m^2), (d_s - 4) - \frac{8m^2}{s\beta^2}, d_s \right\}. \tag{C.2.15}$$

We have set $\beta^2 = 1 - \frac{4m^2}{s}$ and d_s, as usual, is the polarisation state dimension. Using the relation between γ^μ and the Σ- and $\tilde{\Sigma}$-matrices (C.1.5) we may simplify the numerator by insertion of $\boldsymbol{1}^A_{\ B} = -\tilde{\Sigma}^{5,AX} \Sigma^5_{XB}$ in (C.2.13):

$$
\begin{aligned}
N^{4d} &= \bar{u}_1 \gamma^\mu (\gamma \cdot \bar{\ell}_3 + m)(\gamma \cdot \bar{\ell}_2 + m) \gamma_\mu v_2 \\
&= \bar{u}_1 \boldsymbol{1} \gamma^\mu (\gamma \cdot \bar{\ell}_3 + m) \boldsymbol{1} (\gamma \cdot \bar{\ell}_2 + m) \boldsymbol{1} \gamma_\mu v_2 \\
&= -\bar{u}_1 \tilde{\Sigma}^5 \Sigma^\mu (\tilde{\Sigma}^\nu \bar{\ell}_{3\nu} - \tilde{\Sigma}^5 m) \Sigma^5 (\tilde{\Sigma}^\rho \bar{\ell}_{2\rho} - \tilde{\Sigma}^5 m) \Sigma_\mu v_2 \\
&= \lambda_1 \Sigma^\mu (\tilde{\Sigma} \cdot \ell_3) \Sigma^5 (\tilde{\Sigma} \cdot \ell_2) \Sigma_\mu \lambda_2.
\end{aligned} \tag{C.2.16}
$$

Note the leftover Σ^5 which is associated with the scalar interaction. Hence the tree level amplitude in six dimensions is given by

$$A^{(0),6d} = \lambda_1 \Sigma^5 \lambda_2. \tag{C.2.17}$$

As we discussed in section C, the contraction of the six-dimensional Lorentz indices of internal gluon lines includes contributions from the extra dimensions. The procedure of reducing the sum over internal states allows us to obtain the explicit dependence on spacetime dimensionality. In the case at hand, the numerator in the six dimensional calculation is:

$$N^{6d} = \lambda_1 \Sigma^M (\tilde{\Sigma} \cdot \ell_3) \Sigma^5 (\tilde{\Sigma} \cdot \ell_2) \Sigma_M \lambda_2. \tag{C.2.18}$$

Comparing with N^{4d} in equation (C.2.16), the extra contributions in six dimensions

are evidently

$$N_{\phi_1}^{6d} = -\lambda_1 \Sigma^4 (\tilde{\Sigma} \cdot \ell_3) \Sigma^5 (\tilde{\Sigma} \cdot \ell_2) \Sigma^4 \lambda_2, \tag{C.2.19}$$

$$N_{\phi_2}^{6d} = -\lambda_1 \Sigma^5 (\tilde{\Sigma} \cdot \ell_3) \Sigma^5 (\tilde{\Sigma} \cdot \ell_2) \Sigma^5 \lambda_2.$$

It follows from (C.1.11) that contributions from the scalars can equivalently by obtained with

$$N_{\phi_1}^{6d} = -\lambda_1 (\Sigma \cdot \ell_3) \tilde{\Sigma}^5 (\Sigma \cdot \ell_2) \lambda_2, \tag{C.2.20}$$

$$N_{\phi_2}^{6d} = \lambda_1 \gamma_5 (\Sigma \cdot \ell_3) \tilde{\Sigma}^5 (\Sigma \cdot \ell_2) \tilde{\gamma}_5 \lambda_2,$$

where $(\tilde{\gamma}_5)^A{}_B = -i \tilde{\Sigma}^{4,AX} \Sigma^5_{XB}$. Using the integral basis in (C.2.14) the result is

$$A^{(1),6d} = \boldsymbol{c}^{6d} \cdot \boldsymbol{I} A^{(0),6d}$$

$$= \left\{ -2s, -\frac{16m^2}{s\beta^2}, 4 \right\} \cdot \boldsymbol{I} A^{(0),6d}, \tag{C.2.21}$$

$$A_{\phi_1}^{(1)} = \boldsymbol{c}_{\phi_1} \cdot \boldsymbol{I} A^{(0),6d}$$

$$= \{0, 1, 1\} \cdot \boldsymbol{I} A^{(0),6d}, \tag{C.2.22}$$

$$A_{\phi_2}^{(1)} = \boldsymbol{c}_{\phi_2} \cdot \boldsymbol{I} A^{(0),6d}$$

$$= \left\{ -4m^2, -1 - \frac{8m^2}{s\beta^2}, -1 \right\} \cdot \boldsymbol{I} A^{(0),6d}. \tag{C.2.23}$$

The coefficients above are the ingredients needed to perform the state-sum reduction and reproduce (C.2.15).

Appendix D

Spurious directions

In this appendix we give more details about the spurious vectors introduced in Section 4.3. In the integrand decomposition (4.3.56), we introduced some spurious directions in order to define a basis for the four-dimensional space spanning the loop momentum. The advantage of having spurious directions is that their contribution vanishes at integral level. The spurious directions were first introduced in [80].

D.1   Definition of spurious directions

A key idea of the integrand decomposition is to write the integrand of a loop scattering amplitude in terms of the components of the loop momentum. The four-dimensional part of the loop momentum can be spanned into a basis β defined by the external momenta. The basis can be chosen depending on the set of loop denominators, thus for each cut we can use an appropriate basis.

For pentagon topologies, one can pick four external momenta which define the propagators. Indeed, as a consequence, the parametrisation of the pentagon has no four-dimensional components, since such terms reduce to lower topologies. An example of a basis for a pentagon topology is shown in Fig. D.1

For lower topologies, because of momentum conservation, the basis made of the external momenta needs to be completed with additional (spurious) vectors. We require these vectors be orthogonal to the other elements of the basis.
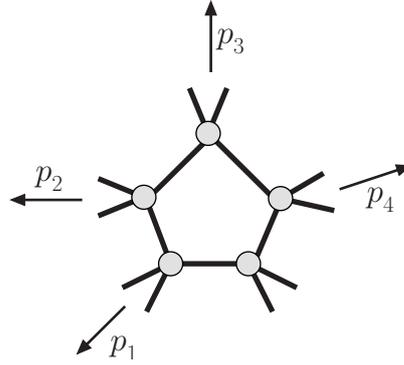
Figure D.1: Example of a four-dimensional basis which can be choosen for the pentagon parametrisation.

Boxes

For the box topologies only one spurious vector is needed, which can be written in general as,

$$w^\mu = \epsilon^{\mu\nu_1\nu_2\nu_3} p_{1\nu_1} p_{2\nu_2} p_{3\nu_3} \tag{D.1.1}$$

which is clearly orthogonal to the momenta p_1, p_2, p_3. In the case where the three momenta are massless, this expression simplifies to,

$$w^\mu = \frac{\langle 231]}{s_{12}} \frac{\langle 1\sigma^\mu 2]}{2} - \frac{\langle 132]}{s_{12}} \frac{\langle 2\sigma^\mu 1]}{2}. \tag{D.1.2}$$

Triangles

In the triangle cases, two spurious vectors are required. The general expression for these vectors can be complicated and will not be written explicitly here. They can be found by imposing the following conditions,

$$\beta = \{p_1, p_2, w_1, w_2\} \tag{D.1.3}$$

$$\begin{cases} w_i \cdot p_j = 0 \\ w_i \cdot w_j \propto \delta_{ij} \end{cases} \quad i, j = 1, 2 \tag{D.1.4}$$

If p_2 is massless, the system has solutions,

$$w_1^\mu = \frac{1}{2}([21\sigma^\mu 2] + \langle 21\sigma^\mu 2\rangle), \quad w_2^\mu = \frac{1}{2}([21\sigma^\mu 2] - \langle 21\sigma^\mu 2\rangle) \tag{D.1.5}$$

Bubbles

The parametrisation of bubble topologies requires three spurious vectors, which can be found by solving the following system,

$$\beta = \{p_1, w_1, w_2, w_3\} \tag{D.1.6}$$

$$\begin{cases} w_i \cdot p_1 = 0 \\ w_i \cdot w_j \propto \delta_{ij} \end{cases} \quad i, j = 1, 2, 3 \tag{D.1.7}$$

The tadpole case can be, in general, parametrised in the same way, using four spurious momenta. However, for QCD applications, such a parametrisation is not appropriate and different methods must be used to compute the tadpole contribution (see Section 7).

D.2 Spurious integrals

A term in the integrand parametrisation is said to be spurious when it vanishes after integration. Two kinds of spurious terms appear in the one-loop parametrisation (4.3.56).

One term is represented by the monomial $k \cdot w$. We consider a basis β with at least one spurious vector and define the basis β' as the subset of the external momenta of β. The spurious integral is written as,

$$I = \int \frac{d^d k}{(2\pi)^d} \frac{k \cdot w}{\prod_i D_i(k, \beta')} = w_\mu \int \frac{d^d k}{(2\pi)^d} \frac{k^\mu}{\prod_i D_i(k, \beta')} \tag{D.2.8}$$

where the denominators are functions of the loop momentum and the set of the external momenta β'. The tensor integral evaluates to a linear combination of the momenta which are members of β' and then, by the definition of spurious vectors,

the integral vanishes,

$$w_\mu \int \frac{d^d k}{(2\pi)^d} \frac{k^\mu}{\prod_i D_i(k, \beta')} = w_\mu \sum_{i \in \beta'} B_i p_i^\mu = 0, \qquad \text{(D.2.9)}$$

where B_i are the appropriate form factors. The same relation is valid for any integral with an odd power of $k \cdot w$.

The other spurious terms appearing in the integrand parametrisation have the form,

$$I = \int \frac{d^d k}{(2\pi)^d} \frac{(w_i \cdot k)^2 - (w_j \cdot k)^2}{\prod_i D_i(k, \beta')}. \qquad \text{(D.2.10)}$$

The single terms $(k \cdot w_i)^2$ do not vanish since the tensor integral contains a term proportional to $g^{\mu\nu}$,

$$\int \frac{d^d k}{(2\pi)^d} \frac{(w_i \cdot k)^2}{\prod_i D_i(k, \beta')} = w_{i\mu} w_{i\nu} \left(A g^{\mu\nu} + \sum_{i \leq j} B_{ij} p_i^\mu p_j^\nu \right) = A w_i^2. \qquad \text{(D.2.11)}$$

As a result, the linear combination in (D.2.10) vanishes as long as the two spurious vectors have the same modulus $w_i^2 = w_j^2$. In the original formulation appearing in [80] the spurious vectors are built imposing these conditions. In the construction discussed in the previous section we do not impose this constraint, since it may cause the appearance of undesired square roots. Alternatively, we prefer to define the spurious terms as,

$$(w_i \cdot k)^2 - (w_j \cdot k)^2 \quad \rightarrow \quad \frac{(w_i \cdot k)^2}{w_i^2} - \frac{(w_j \cdot k)^2}{w_j^2}, \qquad \text{(D.2.12)}$$

which is ensured to integrate to zero.

Appendix E

Cut solutions in six dimensions

In this section we give details on the solutions for the cut solutions in six dimensions. We will describe the parametrisation used to get the solutions without writing down any explicit expression for them. Notice that all the cut solutions are rational functions of the kinematics and the free parameters and contain no square roots.

Quintuple cut

We write the loop momentum ℓ_i^μ in the following basis,

$$\beta = \left\{ v^\mu, w^\mu, \langle v^1 \Sigma^\mu w_1, \rangle \langle v^1 \Sigma^\mu w_2, \rangle \langle v^2 \Sigma^\mu w_1, \rangle \langle v^2 \Sigma^\mu w_2 \rangle \right\}, \qquad \text{(E.0.1)}$$

where v and w are six dimensional massless momenta and use the parametrisation

$$\ell_i = \beta \cdot \left\{ y_1, y_2, y_3, y_4, y_5, y_6 \right\}. \qquad \text{(E.0.2)}$$

$$S_{ijkln} = \begin{cases} \ell_i^2 = \ell_j^2 = \ell_k^2 = \ell_l^2 = \ell_n^2 = 0 \\[2mm] \ell_i^{(5)} = \begin{cases} 0 & \text{if } i \text{ gluon} \\[2mm] \pm m & \text{if } i \text{ fermion} \end{cases} \end{cases}, \qquad \text{(E.0.3)}$$

where $\{ijkln\}$ is the set of the five cut propagators and the sign of the mass component depends on the kinematic configuration. This system of equations for ℓ_i constrains the y_i.

Quadruple cut

We construct explicit solutions for the six-dimensional spinors of ℓ_i by introducing arbitrary two-component reference spinors x_a and $\tilde{x}_{\dot{a}}$. These solutions, which have a similar form to those presented in refs. [13, 145], take a simple form [2],

$$\ell_0^M = \frac{\langle x.4|\Sigma^M\,1\,2\,3|4.\tilde{x}]}{\langle x.4|2\,3|4.\tilde{x}]}, \qquad \ell_1^M = \frac{\langle x.4|1\,\tilde{\Sigma}^M\,2\,3|4.\tilde{x}]}{\langle x.4|2\,3|4.\tilde{x}]},$$

$$\ell_2^M = \frac{\langle x.4|1\,2\,\Sigma^M\,3|4.\tilde{x}]}{\langle x.4|2\,3|4.\tilde{x}]}, \qquad \ell_3^M = \frac{\langle x.4|1\,2\,3\,\tilde{\Sigma}^M|4.\tilde{x}]}{\langle x.4|2\,3|4.\tilde{x}]}, \qquad \text{(E.0.4)}$$

where $\langle x.4| = x^a\langle 4_a|$, $|4.\tilde{x}] = |4^{\dot{a}}]\tilde{x}_{\dot{a}}$ and the spinor product strings have the following expression (for n even)

$$\langle 1_a|2\,3\dots(n-1)|n^{\dot{b}}] = \lambda_a^A(p_1)(\Sigma\cdot p_2)_{AB}\,(\tilde{\Sigma}\cdot p_3)^{BC}\dots(\tilde{\Sigma}\cdot p_{n-1})^{CA}\tilde{\lambda}_A^{\dot{b}}(p_n).$$

$$\text{(E.0.5)}$$

The expressions for the two reference spinors can generically be chosen to be

$$x_a = (1, \tau_1), \qquad\qquad \tilde{x}_{\dot{a}} = (1, y), \qquad\qquad \text{(E.0.6)}$$

where y is fixed, for left and right, by the mass constraint for $\ell_0^{(5)}$ specified in (7.3.13). Because we have a system of 5 equations for 6 dimensional momenta, the parameter τ_1 is left unconstrained.

Triple cut

We write the loop momentum ℓ_i^μ in the following basis of Eq. (E.0.1),

$$S_{ijk} = \begin{cases} \ell_i^2 = \ell_j^2 = \ell_k^2 = 0 \\ \ell_i^{(5)} = \begin{cases} 0 & \text{if } i \text{ gluon} \\ \pm m & \text{if } i \text{ fermion} \end{cases} \end{cases}, \qquad (E.0.7)$$

where $\{ijk\}$ is the set of the three cut propagators and the sign of the mass component depends on the kinematic configuration. This system of equations for ℓ_i only constrains 4 parameters so solving for the y_i's, τ_1, τ_2 are left as free parameters.

Double cut

For the double cut solutions we use the basis in (E.0.1) and use the following parametrisation

$$\ell_i = \beta \cdot \{y_1, \tau_1, y_2, \tau_2, y_3, \tau_3\}. \qquad (E.0.8)$$

The y_i's are fixed by the double cut constraints

$$S_{ij} = \begin{cases} \ell_i^2 = \ell_j^2 = 0 \\ \ell_i^{(5)} = \begin{cases} 0 & \text{if } i \text{ gluon} \\ \pm m & \text{if } i \text{ fermion} \end{cases} \end{cases}, \qquad (E.0.9)$$

where $\{ij\}$ is the set of the two cut propagators and the sign of the mass component depends on the kinematic configuration. The parameters τ_1, τ_2, τ_3 are unconstrained.

Appendix F

Results and further details of one-loop splitting amplitudes

F.1   Generation of collinear phase space points

In this Appedix we illustrate a practical way to generate a set of on-shell n-particle phase-space points where the first m particles approach the collinear limit $1||\cdots||m$. The limit is approached by varying a single free parameter δ as $\delta \to 0$ and it is based on the parametrisation presented in Section 5.2. This has been used for the numerical checks we discussed in Section 5.6.

As a first step we generate an on-shell $(n - m + 1)$-particle phase space point defining the set of momenta

$$\{\tilde{P}, \, p_{m+1}(0), \, p_{m+2}(0), \ldots, \, p_n(0)\} \tag{F.1.1}$$

where, as suggested by the notation, $p_i(0)$ for $i \geq m + 1$ are the momenta of the non-collinear particles at $\delta = 0$, while $\tilde{P}$ is the sum of the collinear momenta in the limit. We then define the *exact* collinear limit as the set of momenta

$$\{z_1\tilde{P}, \, z_2\tilde{P}, \ldots, \, z_m\tilde{P}, \, p_{m+1}(0), \ldots, \, p_n(0)\}, \tag{F.1.2}$$

where z_i are randomly generated real numbers satisfying Eq. (5.2.13). In order to

162

avoid regions with soft kinematics (which would introduce other kinds of singularities) one can generate a set of random numbers between, for example, 1 and 3 and divide them by their sum.

In order to define the orthogonal direction we must specify the reference vector η appearing in Eq. (5.2.9). A particular convenient choice is one of the non-collinear vectors, i.e.

$$\eta^\mu = p^\mu_{m+1}(0). \tag{F.1.3}$$

The orthogonal direction is thus spanned by the two complex vectors

$$\frac{\langle \tilde{P} \gamma^\mu \eta]}{2}, \quad \frac{\langle \eta \gamma^\mu \tilde{P}]}{2}. \tag{F.1.4}$$

While these are particularly convenient when working with the spinor-helicity formalism, for numerical checks with real kinematics it is convenient to define two real linear combinations

$$v^\mu_{1,\perp} = \frac{1}{2} \left(\frac{\langle \tilde{P} \gamma^\mu \eta]}{2} + \frac{\langle \eta \gamma^\mu \tilde{P}]}{2} \right), \quad v^\mu_{2,\perp} = \frac{1}{2i} \left(\frac{\langle \tilde{P} \gamma^\mu \eta]}{2} - \frac{\langle \eta \gamma^\mu \tilde{P}]}{2} \right). \tag{F.1.5}$$

Hence the orthogonal vectors $k^\mu_{T,i}$ are defined as

$$k^\mu_{T,i} = y_{1,i}\, v^\mu_{1,\perp} + y_{2,i}\, v^\mu_{2,\perp} \tag{F.1.6}$$

where $y_{1,i}$ and $y_{2,i}$ are randomly generated real numbers satisfying

$$\sum_i y_{1,i} = \sum_i y_{2,i} = 0. \tag{F.1.7}$$

The variables $y_{1,i}$ and $y_{2,i}$ are related to the spinor variables $\langle z_i \rangle$, $[z_i]$, $\langle \omega_i \rangle$ and $[\omega_i]$ introduced in Section 5.2 by

$$y_{1,i} = \langle z_i \rangle [\omega_i] + \langle \omega_i \rangle [z_i], \quad y_{2,i} = i\left(\langle z_i \rangle [\omega_i] - \langle \omega_i \rangle [z_i] \right), \tag{F.1.8}$$

as one can check by requiring consistency with Eq. (5.2.16). As already stated, these

spinor variables differ by a phase from the usual parametrisation in terms of $\sqrt{z_i}$. If

$$\langle z_i \rangle = [z_i]^* = \sqrt{z_i}\, e^{i\,\theta}, \qquad \langle \omega_i \rangle = [\omega_i]^* = \sqrt{\omega_i}\, e^{i\,\phi} \qquad \text{(F.1.9)}$$

then

$$y_{1,i} = 2\,\sqrt{z_i\,\omega_i}\cos(\phi - \theta), \quad y_{2,i} = 2\,\sqrt{z_i\,\omega_i}\sin(\phi - \theta). \qquad \text{(F.1.10)}$$

From here it is easy to see that while the parametrisation in terms of $\langle z_i \rangle$ and $[z_i]$ has the advantage of producing results that are analytic functions of the spinor variables in the complex plane, the parametrisation in terms of $\sqrt{z_i}$ is in fact entirely equivalent in the physical region.

Using $k_{T,i}^\mu$ as in Eq. (F.1.6), one can simply define the momenta $p_1, \ldots, p_m$ for any value of the free parameter δ using Eq. (5.2.9). With our choice of η we can absorb the recoil by defining

$$p_{m+1}^\mu(\delta) = \left(1 + \sum_{i=0}^{m} \frac{\delta^2\, k_{T,i}^2}{2\, z_i\, (\tilde{P} \cdot \eta)}\right) p_{m+1}^\mu(0) \qquad \text{(F.1.11)}$$

$$p_i^\mu(\delta) = p_i^\mu(0), \qquad m + 2 \leq i \leq n. \qquad \text{(F.1.12)}$$

F.2 Example: the tree-level MHV multi-collinear splitting amplitude

The result for the multi-collinear limit of the maximal-helicity-violating (MHV) amplitude has been known for a long time. More recently the general helicity cases were also examined through use of the MHV rules [146, 147]. This case is incredibly straightforward and serves as a useful example of the general treatment introduced in the previous section.

We start with the Parke-Taylor MHV amplitude with particles 1 and $r > m$ having negative helicities and all others positive helicity,

$$A_n^{(0)}(1^-, 2^+, 3^+, \ldots, r^-, \ldots, n^+) = \frac{\langle 1r \rangle^4}{\prod_{i=1}^{n}\langle ii + 1 \rangle}, \qquad \text{(F.2.13)}$$

where the product in the denominator is considered modulo n. The limit is simply taken by applying eq. (5.2.18)

$$A_n^{(0)}(1^-, 2^+, 3^+, \ldots, r^-, \ldots, n^+) =$$

$$\frac{\left(\langle z_1 \rangle \langle \tilde{P}_{1,m} r \rangle + \langle \omega_1 \rangle \langle \eta r \rangle\right)^4}{\prod_{j=1}^{m-1} \langle jj+1 \rangle \left(\langle z_1 \rangle \langle n\tilde{P}_{1,m} \rangle + \langle \omega_1 \rangle \langle n\eta \rangle\right) \left(\langle z_m \rangle \langle \tilde{P}_{1,m} m+1 \rangle + \langle \omega_m \rangle \langle \eta m+1 \rangle\right) \prod_{i=r}^{n-1} \langle ii+1 \rangle}$$

$$\xrightarrow{\delta \to 0} \frac{\langle z_1 \rangle^3}{\langle z_m \rangle \prod_{j=1}^{m-1} \langle jj+1 \rangle} \frac{\langle \tilde{P}_{1,m} r \rangle^4}{\langle n\tilde{P}_{1,m} \rangle \langle \tilde{P}_{1,m} m+1 \rangle \prod_{i=m+1}^{n-1} \langle ii+1 \rangle} + \mathcal{O}(\delta^{3-m})$$

$$= \mathrm{Sp}^{(0)}(-\tilde{P}_{1,m}^+; 1^-, 2^+, \ldots, m^+) \, A_{n-m+1}^{(0)}(\tilde{P}_{1,m}^-, (m+1)^+, \ldots, r^-, \ldots, n^+) + \mathcal{O}(\delta^{3-m})$$

$$(\text{F.2.14})$$

where we have used eq. (5.2.16) to perform the power counting. For $i, j \in [1, m]$ this can be seen explicitly,

$$\langle \omega_i \rangle = -\delta \frac{\langle \tilde{P}_{1,m} k_T \eta]}{2(P_{1,m} \cdot \eta)[z_j]} = \mathcal{O}(\delta)$$

$$\Rightarrow \langle ij \rangle = (\langle z_i \rangle \langle \omega_j \rangle - \langle z_j \rangle \langle \omega_i \rangle) \langle \tilde{P}_{1,m} \eta \rangle = \mathcal{O}(\delta). \qquad (\text{F.2.15})$$

One can clearly arrive at this final result without being so explicit about the parametrisation, yet it is convenient to have one in a generic implementation.

F.3 $g \to ggg$ **splitting amplitudes: results**

We define the following phase-free quantities,

$$\alpha_{ij} \equiv \alpha_{ijk} = \frac{\langle ij \rangle \langle z_k \rangle}{\langle jk \rangle \langle z_i \rangle}, \qquad \beta_{ij} \equiv \beta_{ijk} = \frac{[ij][\omega_k]}{[jk][\omega_i]}, \qquad \gamma_{ij} = \frac{\langle z_i \rangle [ij]}{[j\tilde{P}]}. \qquad (\text{F.3.16})$$

Since there can be no repeated index in either α_{ijk} and β_{ijk} each can be uniquely specified by the two first labels.

The integral functions are defined using the following basis,

$$F^{\text{MHV}} = \frac{1}{2}\left(\log^2(z_1) + \log^2(z_3) + \frac{\pi^2}{3}\right) - \log\left(\frac{s_{12}}{s_{123}}\right)\log\left(\frac{s_{23}}{s_{123}}\right)$$
$$+ \log\left(\frac{1-z_3}{z_1}\right)\log\left(\frac{s_{12}}{s_{123}}\right) + \log\left(\frac{1-z_1}{z_3}\right)\log\left(\frac{s_{23}}{s_{123}}\right)$$
$$+ \text{Li}_2\left(-\frac{z_2}{z_1}\right) + \text{Li}_2\left(-\frac{z_2}{z_3}\right) + \text{Li}_2\left(-\frac{z_3}{1-z_3}\right) + \text{Li}_2\left(-\frac{z_1}{1-z_1}\right)$$
$$- \text{Li}_2\left(1 - \frac{s_{12}}{(1-z_3)\,s_{123}}\right) - \text{Li}_2\left(1 - \frac{s_{23}}{(1-z_1)\,s_{123}}\right) \tag{F.3.17}$$

$$F_1^{\text{NMHV}} = -\log(1-z_3)\left(\log\left(\frac{z_1 z_3}{1-z_3}\right) + \log\left(\frac{s_{12}}{s_{23}}\right)\right) + \log(z_1 z_3)\log\left(\frac{s_{12}}{s_{123}}\right)$$
$$- \frac{1}{2}\left(\log(z_3)\log\left(\frac{s_{12}}{s_{123}}\right) + \log(z_1)\log\left(\frac{s_{23}}{s_{123}}\right) - \frac{\pi^2}{3}\right) \tag{F.3.18}$$

$$F_2^{\text{NMHV}} = F_1^{\text{NMHV}}\big|_{1 \leftrightarrow 3} \tag{F.3.19}$$

$$F_3^{\text{NMHV}} = \frac{1}{2}\left(\log(z_3)\log\left(\frac{s_{12}}{s_{123}}\right) + \log(z_1)\log\left(\frac{s_{23}}{s_{123}}\right) - \frac{\pi^2}{3}\right)$$
$$- \log\left(\frac{s_{12}}{s_{123}}\right)\log\left(\frac{s_{23}}{s_{123}}\right) \tag{F.3.20}$$

$$F_{\text{box}}^{1\text{m}} = -\frac{\pi^2}{3} - \log^2\left(\frac{s_{12}}{s_{23}}\right) - 2\left(\text{Li}_2\left(1 - \frac{s_{123}}{s_{12}}\right) + \text{Li}_2\left(1 - \frac{s_{123}}{s_{23}}\right)\right) \tag{F.3.21}$$

$$\hat{L}_0(s_1, s_2) = \log\left(\frac{s_1}{s_2}\right) \tag{F.3.22}$$

$$\hat{L}_1(s_1, s_2) = \frac{1}{s_1 - s_2}\log\left(\frac{s_1}{s_2}\right) \tag{F.3.23}$$

$$\hat{L}_2(s_1, s_2) = \frac{1}{(s_1 - s_2)^2}\log\left(\frac{s_1}{s_2}\right) - \frac{1}{2}\frac{1}{s_1 - s_2}\left(\frac{1}{s_1} + \frac{1}{s_2}\right) \tag{F.3.24}$$

$$\hat{L}_3(s_1, s_2) = \frac{1}{(s_1 - s_2)^3}\log\left(\frac{s_1}{s_2}\right) - \frac{1}{2}\frac{1}{(s_1 - s_2)^2}\left(\frac{1}{s_1} + \frac{1}{s_2}\right) \tag{F.3.25}$$

We express the infrared poles and associated logarithms as described by Catani's formula [148],

$$V_g = -\frac{1}{\epsilon^2}\left(\left(\frac{\mu_R}{-s_{12}}\right)^\epsilon + \left(\frac{\mu_R}{-s_{23}}\right)^\epsilon + \left(\frac{\mu_R}{-s_{123}}\right)^\epsilon \left(z_1^{-\epsilon} + z_3^{-\epsilon} - 2\right)\right) \tag{F.3.26}$$

All results in this section are presented unrenormalized.

The tree-level splitting amplitudes are,

$$\text{Sp}^{(0)}\left(-P^+; 1^+, 2^+, 3^+\right) = 0 \tag{F.3.27}$$

$$\text{Sp}^{(0)}\left(-P^+; 1^-, 2^-, 3^-\right) = \frac{1}{[z_1]\,[z_3]\,[12][23]} \tag{F.3.28}$$

$$\text{Sp}^{(0)}\left(-P^+; 1^+, 2^+, 3^-\right) = \frac{\langle z_3\rangle^3}{\langle z_1\rangle\langle 12\rangle\langle 23\rangle} \tag{F.3.29}$$

$$\text{Sp}^{(0)}\left(-P^+; 1^+, 2^-, 3^+\right) = \frac{\langle z_2\rangle^4}{\langle z_1\rangle\langle z_3\rangle\langle 12\rangle\langle 23\rangle} \tag{F.3.30}$$

$$\text{Sp}^{(0)}\left(-P^+; 1^+, 2^-, 3^-\right) = -\frac{[1P]^2}{[23]^2}\left(\frac{\beta_{32}}{s_{123}} + \frac{\gamma_{23}^3 \alpha_{12}\beta_{12}^2 s_{23}}{(1-z_3)\,z_3 s_{12}^2}\right) \tag{F.3.31}$$

$$\text{Sp}^{(0)}\left(-P^+; 1^-, 2^+, 3^-\right) = -\frac{[2P]^2}{[13]^2 s_{1P}s_{3P}}\Bigg($$

$$\frac{\beta_{21}\beta_{23}s_{13}^4}{s_{12}s_{123}s_{23}} + \frac{\gamma_{32}^2 z_2 z_3 s_{1P}\,(\alpha_{13}\alpha_{31})^\dagger}{\gamma_{23}\,(1-z_3)} + \frac{\gamma_{12}^2 z_1 z_2 s_{3P}\,(\alpha_{13}\alpha_{31})^\dagger}{\gamma_{21}\,(1-z_1)}\Bigg) \tag{F.3.32}$$

All other helicity configurations are given via parity or the line-reversal symmetry

of eq. (5.4.32). The one-loop splitting primitive amplitudes are,

$$\mathrm{Sp}^{[\mathcal{N}=4]}\left(-P^+; 1^+, 2^+, 3^+\right) = 0 \tag{F.3.33}$$

$$\mathrm{Sp}^{[\mathcal{N}=4]}\left(-P^+; 1^-, 2^-, 3^-\right) = \mathrm{Sp}^{(0)}\left(-P^+; 1^-, 2^-, 3^-\right)\left(V_g + F^{\mathrm{MHV}}\right) \tag{F.3.34}$$

$$\mathrm{Sp}^{[\mathcal{N}=4]}\left(-P^+; 1^+, 2^+, 3^-\right) = \mathrm{Sp}^{(0)}\left(-P^+; 1^+, 2^+, 3^-\right)\left(V_g + F^{\mathrm{MHV}}\right) \tag{F.3.35}$$

$$\mathrm{Sp}^{[\mathcal{N}=4]}\left(-P^+; 1^+, 2^-, 3^+\right) = \mathrm{Sp}^{(0)}\left(-P^+; 1^+, 2^-, 3^+\right)\left(V_g + F^{\mathrm{MHV}}\right) \tag{F.3.36}$$

$$\mathrm{Sp}^{[\mathcal{N}=4]}\left(-P^+; 1^+, 2^-, 3^-\right) = \mathrm{Sp}^{(0)}\left(-P^+; 1^+, 2^-, 3^-\right)\left(V_g\right) - \frac{[1P]^2}{[23]^2}\left(\right.$$

$$+ \left(\frac{\gamma_{23}\alpha_{12}\beta_{12}s_{23}}{z_3 s_{12}^2}\left(\frac{s_{12}\left(z_1 - 1\right)^3}{z_2 s_{1P}} + \frac{2\gamma_{23}^2\beta_{12}}{z_3 - 1}\right) + \frac{1}{s_{123}}\left(\frac{\beta_{12}s_{23}^3}{s_{12}s_{1P}s_{3P}} - \beta_{32}\right)\right) F_1^{\mathrm{NMHV}}$$

$$- \frac{\gamma_{23}\alpha_{12}\beta_{12}s_{23}\left(z_1 - 1\right)^3}{z_2 z_3 s_{12}s_{1P}} F_2^{\mathrm{NMHV}}$$

$$+ \frac{1}{s_{123}}\left(\frac{\beta_{12}s_{23}^3}{s_{12}s_{1P}s_{3P}} + \beta_{32}\right) F_3^{\mathrm{NMHV}}\left.\right) \tag{F.3.37}$$

$$\mathrm{Sp}^{[\mathcal{N}=4]}\left(-P^+; 1^-, 2^+, 3^-\right) = \mathrm{Sp}^{(0)}\left(-P^+; 1^-, 2^+, 3^-\right)\left(V_g\right) - \frac{[2P]^2}{[13]^2}\left(\right.$$

$$+ \left(\frac{\gamma_{32}\beta_{31}s_{13}\gamma_{12}^2}{\gamma_{23}z_3 s_{12}s_{3P}} + \frac{z_2 z_3\left(\alpha_{13}\alpha_{31}\right)^\dagger\gamma_{32}^2}{\gamma_{23}s_{3P}(z_3 - 1)} + \frac{\gamma_{12}^2 z_2 \beta_{31}^2\gamma_{32}^2}{\gamma_{23}^2 z_3 s_{3P}(z_3 - 1)}\right) F_1^{\mathrm{NMHV}}$$

$$+ \left(\frac{z_1\left(\alpha_{13}\alpha_{31}\right)^\dagger\gamma_{12}^2}{s_{1P}} + \frac{\gamma_{12}\beta_{13}\beta_{31}\gamma_{32}^3}{\gamma_{23}z_1 s_{23}(z_1 - 1)} + \frac{\gamma_{12}z_1^2\left(\alpha_{13}\alpha_{31}\right)^\dagger\gamma_{32}}{s_{1P}(z_1 - 1)}\right) F_2^{\mathrm{NMHV}}$$

$$+ \frac{1}{s_{123}}\left(\frac{\beta_{21}\beta_{23}s_{13}^4}{s_{12}s_{23}s_{1P}s_{3P}} + \beta_{13}\beta_{31}\right) F_3^{\mathrm{NMHV}}\left.\right) \tag{F.3.38}$$

$$\mathrm{Sp}^{[\mathcal{N}=1]}\left(-P^+; 1^+, 2^+, 3^+\right) = 0 \tag{F.3.39}$$

$$\mathrm{Sp}^{[\mathcal{N}=1]}\left(-P^+; 1^-, 2^-, 3^-\right) = 0 \tag{F.3.40}$$

$$\mathrm{Sp}^{[\mathcal{N}=1]}\left(-P^+; 1^+, 2^+, 3^-\right) = \mathrm{Sp}^{(0)}\left(-P^+; 1^+, 2^+, 3^-\right) \alpha_{32} s_{12} \hat{L}_1\left(s_{23}, s_{123}\right) \tag{F.3.41}$$

$$\mathrm{Sp}^{[\mathcal{N}=1]}\left(-P^+; 1^+, 2^-, 3^+\right) = \mathrm{Sp}^{(0)}\left(-P^+; 1^+, 2^-, 3^+\right) \frac{\alpha_{23}}{\alpha_{31}} \Bigg($$

$$\frac{F_{\mathrm{box}}^{1\mathrm{m}}}{2} - \left(\hat{L}_1\left(s_{12}, s_{123}\right) + \hat{L}_1\left(s_{23}, s_{123}\right)\right) s_{13}\Bigg) \tag{F.3.42}$$

$$\mathrm{Sp}^{[\mathcal{N}=1]}\left(-P^+; 1^+, 2^-, 3^-\right) = -\frac{[1P]^2 s_{23}}{[23]^2 s_{123}} \hat{L}_1\left(s_{12}, s_{123}\right) \tag{F.3.43}$$

$$\mathrm{Sp}^{[\mathcal{N}=1]}\left(-P^+; 1^-, 2^+, 3^-\right) = -\frac{[2P]^2}{[13]^2 s_{123}} \Bigg($$

$$\frac{F_{\mathrm{box}}^{1\mathrm{m}}}{2} - \left(\hat{L}_1\left(s_{12}, s_{123}\right) + \hat{L}_1\left(s_{23}, s_{123}\right)\right) s_{13}\Bigg) \tag{F.3.44}$$

$$\text{Sp}^{[\mathcal{N}=0]}\left(-P^+;1^+,2^+,3^+\right) = -\frac{[1P][3P]}{3\langle 12\rangle\langle 23\rangle}\left(\frac{1}{s_{123}} - \frac{\gamma_{23}^2\beta_{13}\left(\alpha_{32}s_{12}+\alpha_{12}s_{23}\right)}{\beta_{31}s_{12}s_{23}}\right)$$

(F.3.45)

$$\text{Sp}^{[\mathcal{N}=0]}\left(-P^+;1^-,2^-,3^-\right) = \frac{1}{3}\text{Sp}^{(0)}\left(-P^+;1^-,2^-,3^-\right)\Bigg($$

$$z_1 z_2 + \frac{z_1\left(1-z_2{}^2\right)z_3 z_2}{\left(1-z_1\right)\left(1-z_2\right)\left(1-z_3\right)} + z_3 z_2 + z_1 z_3 - \frac{z_1 z_3}{\gamma_{12}\gamma_{32}}\left(\frac{\gamma_{32}z_1}{1-z_3} + \frac{\gamma_{12}z_3}{1-z_1} + \frac{s_{13}}{s_{123}}\right)\Bigg)$$

(F.3.46)

$$\text{Sp}^{[\mathcal{N}=0]}\left(-P^+;1^+,2^+,3^-\right) = \text{Sp}^{(0)}\left(-P^+;1^+,2^+,3^-\right)\frac{\gamma_{12}s_{23}}{3\gamma_{32}^3}\Bigg($$

$$\frac{\gamma_{32}z_2}{s_{12}}\left(\frac{\gamma_{12}}{z_3} + \frac{\gamma_{32}}{z_3-1}\right) - \gamma_{12}\gamma_{32}\hat{L}_2\left(s_{23},s_{123}\right)s_{23} + 2\gamma_{12}\beta_{23}\hat{L}_3\left(s_{23},s_{123}\right)s_{13}s_{23}$$

$$+\frac{1}{s_{123}}\left(\frac{s_{23}}{s_{12}} - \frac{1}{2}\left(\gamma_{12}+2\right)\gamma_{32}\right)\Bigg)$$

(F.3.47)

$$\text{Sp}^{[\mathcal{N}=0]}\left(-P^+;1^+,2^-,3^+\right) = \text{Sp}^{(0)}\left(-P^+;1^+,2^-,3^+\right)\frac{\alpha_{23}^2 s_{13}}{3\alpha_{31}^2}\Bigg($$

$$-\frac{2\hat{L}_3\left(s_{12},s_{123}\right)s_{13}^2}{\alpha_{32}} - 2\alpha_{32}\hat{L}_3\left(s_{23},s_{123}\right)s_{13}^2 - 3\hat{L}_2\left(s_{23},s_{123}\right)\left(2s_{12}+3s_{13}\right)$$

$$+\frac{5}{2}\left(\frac{2}{s_{123}} + \frac{1}{s_{23}} + \frac{1}{s_{12}}\right) - 3\hat{L}_2\left(s_{12},s_{123}\right)\left(3s_{13}+2s_{23}\right) - \frac{1}{2s_{123}}\left(\frac{s_{12}}{s_{23}} + \frac{s_{23}}{s_{12}}\right)$$

$$+\frac{s_{123}}{s_{12}s_{23}} - \frac{3F_{\text{box}}^{1m}}{s_{13}}\Bigg)$$

(F.3.48)

$$\mathrm{Sp}^{[\mathcal{N}=0]}\left(-P^+; 1^+, 2^-, 3^-\right) = \frac{[1P]^2}{3[23]^2}\Bigg($$

$$\frac{2\gamma_{23}^2\alpha_{21}^2 s_{13}^2 s_{23}\beta_{12}^2}{s_{12}}\hat{L}_3\left(s_{12}, s_{123}\right) + \frac{\gamma_{23}^2\alpha_{21}s_{13}\left(-s_{12}-\alpha_{21}s_{13}\right)s_{23}\beta_{12}^2}{s_{12}s_{123}}\hat{L}_2\left(s_{12}, s_{123}\right)$$

$$+ \frac{\gamma_{23}^2\left(3\alpha_{21}s_{13}-s_{12}\right)s_{23}\beta_{12}^2}{s_{12}s_{123}}\hat{L}_1\left(s_{12}, s_{123}\right) - \frac{\gamma_{23}^2\alpha_{12}s_{23}\beta_{12}^2}{s_{12}^2} - \frac{\gamma_{23}^2\alpha_{21}s_{13}s_{23}\beta_{12}^2}{s_{12}^2 s_{123}}$$

$$+ \frac{1}{s_{123}^2}\frac{\gamma_{23}\alpha_{21}\beta_{12}^2\beta_{32}s_{13}s_{23}}{2s_{12}} - \frac{\gamma_{23}^2\alpha_{21}\beta_{12}^2 s_{13}s_{23}}{s_{12}}\Bigg) \tag{F.3.49}$$

$$\mathrm{Sp}^{[\mathcal{N}=0]}\left(-P^+; 1^-, 2^+, 3^-\right) = \frac{[2P]^2}{3[13]^2}\Bigg($$

$$- 2\hat{L}_3\left(s_{23}, s_{123}\right)s_{123}s_{13}\gamma_{12}^2 + \hat{L}_2\left(s_{23}, s_{123}\right)\left(3\gamma_{12}s_{123}+s_{13}\right)\gamma_{12}$$

$$- 2\gamma_{32}^2\hat{L}_3\left(s_{12}, s_{123}\right)s_{123}s_{13} + \frac{3\left(2s_{12}+4\gamma_{12}s_{123}+s_{13}\right)}{s_{123}s_{13}}\hat{L}_0\left(s_{23}, s_{123}\right)$$

$$+ \gamma_{32}\hat{L}_2\left(s_{12}, s_{123}\right)\left(3\gamma_{32}s_{123}+s_{13}\right) + \hat{L}_1\left(s_{23}, s_{123}\right)\left(\frac{s_{13}}{s_{123}}-\frac{6\gamma_{12}^2 s_{123}}{s_{13}}\right)$$

$$+ \hat{L}_1\left(s_{12}, s_{123}\right)\left(\frac{s_{13}}{s_{123}}-\frac{6\gamma_{32}^2 s_{123}}{s_{13}}\right) + \frac{3\left(4\gamma_{32}s_{123}+s_{13}+2s_{23}\right)}{s_{123}s_{13}}\hat{L}_0\left(s_{12}, s_{123}\right)$$

$$+ \frac{1}{2s_{12}s_{123}s_{23}}\Big(- 4s_{123}s_{23}\gamma_{32}^2 + \left(\gamma_{12}s_{123}\left(-3s_{12}+2s_{123}-3s_{23}\right)+\left(5s_{12}-s_{23}\right)s_{23}\right)\gamma_{32}$$

$$- \gamma_{12}s_{12}\left(s_{12}+4\gamma_{12}s_{123}-5s_{23}\right)\Big) - \frac{3\beta_{21}\beta_{23}}{s_{123}}F_{\mathrm{box}}^{\mathrm{1m}}\Bigg) \tag{F.3.50}$$

F.4 $g \rightarrow \bar{q}qg$ splitting amplitudes: results

As before all results in this section are presented unrenormalized. The non-vanishing independent tree-level splitting amplitudes $g \rightarrow \bar{q}qg$ are

$$\mathrm{Sp}^{(0)} \left(-P^+; 1_{\bar{q}}^+, 2_q^-, 3^- \right) = -\frac{\langle z_2 \rangle \langle z_3 \rangle}{\beta_{12}[23]\langle 12 \rangle} \left(\frac{\gamma_{21}}{(1 - z_3) z_3} + \frac{s_{12}}{\gamma_{32} s_{123} \gamma_{21}} \right) \qquad \text{(F.4.51)}$$

$$\mathrm{Sp}^{(0)} \left(-P^+; 1_{\bar{q}}^-, 2_q^+, 3^- \right) = -\frac{\langle z_3 \rangle (\beta_{31})^\dagger}{[13]\langle 2P \rangle} \Bigg($$
$$\frac{s_{23} \left(\alpha_{13}^2 \beta_{13} \right)^\dagger z_1^2}{z_3 s_{13} (\beta_{31})^\dagger} + \frac{s_{13} \left(\gamma_{31} \right)^\dagger}{z_3 s_{123}} + \frac{z_3^2 s_{12} \left(\alpha_{31}^2 \right)^\dagger}{(1 - z_3) s_{13}} \Bigg) \qquad \text{(F.4.52)}$$

$$\mathrm{Sp}^{(0)} \left(-P^+; 1_{\bar{q}}^+, 2_q^-, 3^+ \right) = \frac{\langle z_2 \rangle^3}{\langle z_3 \rangle \langle 12 \rangle \langle 23 \rangle} \qquad \text{(F.4.53)}$$

$$\mathrm{Sp}^{(0)} \left(-P^+; 1_{\bar{q}}^-, 2_q^+, 3^+ \right) = -\frac{\langle z_1 \rangle^2 \langle z_2 \rangle}{\langle z_3 \rangle \langle 12 \rangle \langle 23 \rangle} \qquad \text{(F.4.54)}$$

and the others are obtained by conjugation using the relation

$$\mathrm{Sp} \left(-P^+; 1_{\bar{q}}^{h_1}, 2_q^{h_2}, 3^{h_3} \right) = \mathrm{Sp} \left(-P^-; 1_{\bar{q}}^{-h_1}, 2_q^{-h_2}, 3^{-h_3} \right) \Big|_{\langle ij \rangle \leftrightarrow [ij]}. \qquad \text{(F.4.55)}$$

The sub-leading colour tree-level splitting amplitudes $g \rightarrow \bar{q}gq$ are not independent because they can be expressed in terms of (F.4.54) using the KK relation (5.4.28) re-written with the quark labels,

$$\mathrm{Sp}^{(0)} \left(-P^+; 1_{\bar{q}}^{h_1}, 2^{h_2}, 3_q^{h_3} \right) =$$
$$- \mathrm{Sp}^{(0)} \left(-P^+; 1_{\bar{q}}^{h_1}, 3_q^{h_3}, 2^{h_2} \right) + \mathrm{Sp}^{(0)} \left(-P^+; 3_{\bar{q}}^{h_3}, 1_q^{h_1}, 2^{h_2} \right) \qquad \text{(F.4.56)}$$

A sample of two representative tree-level splitting amplitudes $g \to \bar{q}gq$ is

$$\text{Sp}^{(0)}\left(-P^+; 1_{\bar{q}}^+, 2^-, 3_q^-\right) = \frac{[1P]^2}{[12][23]s_{123}} \tag{F.4.57}$$

$$\text{Sp}^{(0)}\left(-P^+; 1_{\bar{q}}^-, 2^+, 3_q^+\right) = -\frac{\langle z_1 \rangle^2}{\langle 12 \rangle \langle 23 \rangle} \tag{F.4.58}$$

The non-zero independent one-loop splitting amplitudes $g \to \bar{q}qg$ are

$$\text{Sp}^{[\mathcal{N}=4]}\left(-P^+; 1_{\bar{q}}^+, 2_q^-, 3^-\right) = \text{Sp}^{(0)}\left(-P^+; 1_{\bar{q}}^+, 2_q^-, 3^-\right) V_g$$

$$- \frac{\langle z_2 \rangle \langle z_3 \rangle}{[23]\langle 12 \rangle} \left(\frac{(1-z_1)^2 s_{12}}{\gamma_{21} z_3 s_{1P}} \text{F}_2^{\text{NMHV}} - \left(\frac{\gamma_{32}^2 s_{2P}^2 (\gamma_{12}^2)^\dagger}{(1-z_3)\gamma_{23} s_{12} s_{3P}} - \frac{\gamma_{23}}{(1-z_3) z_3} \right) \text{F}_1^{\text{NMHV}} \right.$$

$$- \frac{z_3 s_{12} s_{13}^3}{\gamma_{21}\gamma_{23}\gamma_{31}^2 s_{123} s_{1P}^2 s_{3P}(\gamma_{31})^\dagger} \left(\frac{z_1 \beta_{12} s_{23}^3}{s_{12} s_{13} s_{3P}(\gamma_{13})^\dagger} - \frac{\gamma_{31}^2 s_{1P}(\gamma_{31})^\dagger s_{23}^2}{z_3 s_{13}^3} \right.$$

$$\left. \left. + \frac{z_1 \beta_{32} s_{1P}}{s_{13}(\gamma_{13})^\dagger} + \frac{\gamma_{23} z_3 s_{3P}}{\gamma_{21} s_{13}(\gamma_{31})^\dagger} \right) \text{F}_3^{\text{NMHV}} \right) \tag{F.4.59}$$

$$\text{Sp}^{[\mathcal{N}=4]}\left(-P^+; 1_{\bar{q}}^-, 2_q^+, 3^-\right) = \text{Sp}^{(0)}\left(-P^+; 1_{\bar{q}}^-, 2_q^+, 3^-\right) V_g$$

$$- \frac{\langle z_3 \rangle [2P]}{[13]} \left(-\frac{\gamma_{32} z_2 s_{3P}(\gamma_{23})^\dagger (\gamma_{31})^\dagger \gamma_{13}^2}{\gamma_{23} z_3^2 s_{13} s_{23}} \text{F}_2^{\text{NMHV}} \right.$$

$$+ \frac{\gamma_{32}}{(1-z_3)\gamma_{23} s_{3P}} \left(\frac{\gamma_{31} z_2^2}{\gamma_{21}} - \frac{\gamma_{13}\gamma_{21} z_1 s_{13}}{\gamma_{31} z_3 s_{12}(\gamma_{13})^\dagger} \right) \text{F}_1^{\text{NMHV}}$$

$$\left. - \left(\frac{\gamma_{12} s_{13}(\gamma_{31})^\dagger}{z_3 s_{12} s_{3P}} + \frac{s_{13}(\gamma_{31})^\dagger}{z_3 s_{123} s_{3P}} + \frac{z_1 s_{13}}{\gamma_{12}\gamma_{32} s_{123} s_{3P}(\gamma_{13})^\dagger} \right) \text{F}_3^{\text{NMHV}} \right) \tag{F.4.60}$$

$$\text{Sp}^{[\mathcal{N}=4]}\left(-P^+; 1_{\bar{q}}^+, 2_q^-, 3^+\right) = \text{Sp}^{(0)}\left(-P^+; 1_{\bar{q}}^+, 2_q^-, 3^+\right) \left(V_g + F^{\text{MHV}}\right) \tag{F.4.61}$$

$$\text{Sp}^{[\mathcal{N}=4]}\left(-P^+; 1_{\bar{q}}^-, 2_q^+, 3^+\right) = \text{Sp}^{(0)}\left(-P^+; 1_{\bar{q}}^-, 2_q^+, 3^+\right) \left(V_g + F^{\text{MHV}}\right) \tag{F.4.62}$$

$$\mathrm{Sp}^{[\mathrm{R}]}\left(-P^+;1_{\bar{q}}^+,2_q^-,3^-\right) = \mathrm{Sp}^{(0)}\left(-P^+;1_{\bar{q}}^+,2_q^-,3^-\right)\left(-\frac{1}{\epsilon^2}\left(\frac{\mu_R}{-s_{12}}\right)^\epsilon - \frac{3}{2\epsilon}\left(\frac{\mu_R}{-s_{12}}\right)^\epsilon\right.$$

$$-\frac{7}{2}-\frac{\delta_{\mathrm{R}}}{2}\right) - \frac{\alpha_{21}\langle z_2\rangle\langle z_3\rangle}{[23]\langle 12\rangle}\left(-\frac{s_{12}}{2\gamma_{21}\gamma_{31}\alpha_{21}s_{123}}\mathrm{F}_{\mathrm{box}}^{1m} - \frac{1}{2}s_{123}s_{23}\hat{L}_2\left(s_{12},s_{123}\right)\right.$$

$$+\frac{1}{2}\left(-3s_{123}-\frac{2s_{23}}{\gamma_{32}}\right)\hat{L}_1\left(s_{12},s_{123}\right)+\frac{1}{2}+\frac{s_{23}}{4s_{12}}\right) \tag{F.4.63}$$

$$\mathrm{Sp}^{[\mathrm{R}]}\left(-P^+;1_{\bar{q}}^-,2_q^+,3^-\right) = \mathrm{Sp}^{(0)}\left(-P^+;1_{\bar{q}}^-,2_q^+,3^-\right)\left(-\frac{1}{\epsilon^2}\left(\frac{\mu_R}{-s_{12}}\right)^\epsilon - \frac{3}{2\epsilon}\left(\frac{\mu_R}{-s_{12}}\right)^\epsilon\right.$$

$$-\frac{7}{2}-\frac{\delta_{\mathrm{R}}}{2}\right) + \frac{\langle z_3\rangle[2P]}{[13]s_{13}}\left(\frac{\beta_{12}\beta_{21}s_{13}}{2\gamma_{31}s_{123}}\mathrm{F}_{\mathrm{box}}^{1m} - \frac{\beta_{12}\beta_{21}s_{13}^2s_{23}}{2\gamma_{31}s_{123}}\hat{L}_2\left(s_{12},s_{123}\right)\right.$$

$$-\frac{3\beta_{12}\beta_{21}s_{13}^2}{2\gamma_{31}s_{123}}\hat{L}_1\left(s_{12},s_{123}\right)+\frac{s_{12}s_{23}\gamma_{12}^2}{2\gamma_{32}}\hat{L}_2\left(s_{23},s_{123}\right)$$

$$+\frac{s_{12}\gamma_{12}}{\gamma_{32}}\left(\frac{\gamma_{12}\left(2s_{12}s_{123}+3s_{23}s_{123}-3s_{12}s_{23}\right)}{2s_{12}s_{123}}+1\right)\hat{L}_1\left(s_{23},s_{123}\right)$$

$$+\frac{1}{2}\left(3\gamma_{12}-\frac{s_{23}}{\gamma_{32}s_{123}}-\frac{3\left(\gamma_{12}-1\right)s_{12}}{s_{123}}-1\right)\hat{L}_0\left(s_{23},s_{123}\right)$$

$$-\frac{\gamma_{12}^2s_{23}}{4\gamma_{32}s_{12}}+\frac{\gamma_{12}s_{23}}{2\gamma_{32}s_{123}}+\gamma_{12}+\frac{\left(1-\gamma_{12}\right)s_{12}}{4s_{123}}-\frac{\left(s_{123}-s_{23}\right)s_{12}}{4\gamma_{32}s_{123}^2}\right) \tag{F.4.64}$$

$$\mathrm{Sp}^{[\mathrm{R}]}\left(-P^+;1_{\bar{q}}^+,2_q^-,3^+\right) = \mathrm{Sp}^{(0)}\left(-P^+;1_{\bar{q}}^+,2_q^-,3^+\right)\left(-\frac{1}{\epsilon^2}\left(\frac{\mu_R}{-s_{12}}\right)^\epsilon - \frac{3}{2\epsilon}\left(\frac{\mu_R}{-s_{12}}\right)^\epsilon\right.$$

$$-\frac{7}{2}-\frac{\delta_{\mathrm{R}}}{2}-\frac{\alpha_{12}^3}{\alpha_{13}^3}\left(-\frac{\mathrm{F}_{\mathrm{box}}^{1m}}{2}-\frac{1}{2}\left(6s_{12}^2+s_{23}^2-6s_{12}s_{123}\right)\hat{L}_2\left(s_{12},s_{123}\right)\right.$$

$$+\left(3s_{123}-2s_{23}\right)\hat{L}_1\left(s_{12},s_{123}\right)+\frac{3}{2}\hat{L}_0\left(s_{12},s_{123}\right)$$

$$+\frac{\left(s_{123}^2-s_{12}^2-s_{23}^2\right)}{2\alpha_{12}^2}\hat{L}_2\left(s_{23},s_{123}\right)+\left(\frac{s_{23}}{\alpha_{12}^2}-\frac{2s_{13}}{\alpha_{12}}\right)\hat{L}_1\left(s_{23},s_{123}\right)$$

$$-\frac{\left(s_{123}+s_{23}\right)^2-s_{12}^2-2s_{23}s_{12}}{4\alpha_{12}^2s_{123}s_{23}}-\frac{6s_{12}^2-s_{23}^2-2s_{23}s_{12}}{4s_{123}s_{12}}+\frac{s_{13}}{\alpha_{12}s_{123}}-\frac{3}{2}\right)\right) \tag{F.4.65}$$

$$\mathrm{Sp}^{[\mathrm{R}]}\left(-P^+;1_{\bar{q}}^-,2_q^+,3^+\right) = \mathrm{Sp}^{(0)}\left(-P^+;1_{\bar{q}}^-,2_q^+,3^+\right)\left(-\frac{1}{\epsilon^2}\left(\frac{\mu_R}{-s_{12}}\right)^\epsilon - \frac{3}{2\epsilon}\left(\frac{\mu_R}{-s_{12}}\right)^\epsilon\right.$$

$$-\frac{7}{2}-\frac{\delta_{\mathrm{R}}}{2}+\frac{\alpha_{12}}{\alpha_{13}}\left(\frac{\mathrm{F}_{\mathrm{box}}^{1m}}{2}+\frac{\alpha_{12}^2s_{23}^2}{2}\hat{L}_2\left(s_{12},s_{123}\right)-2\alpha_{12}s_{23}\hat{L}_1\left(s_{12},s_{123}\right)\right.$$

$$+\frac{3}{2}\hat{L}_0\left(s_{12},s_{123}\right)+\frac{\left(s_{123}-s_{12}\right)}{2s_{123}}+\frac{\alpha_{12}s_{23}}{s_{123}}-\frac{\alpha_{12}^2s_{23}^2}{4s_{12}s_{123}}\right)\right) \tag{F.4.66}$$

$$\mathrm{Sp}^{[\mathrm{f}]}\left(-P^+; 1_{\bar{q}}^+, 2_q^-, 3^-\right) = \mathrm{Sp}^{(0)}\left(-P^+; 1_{\bar{q}}^+, 2_q^-, 3^-\right)\left(-\frac{2}{3\epsilon}\left(\frac{\mu_R}{-s_{12}}\right)^\epsilon - \frac{10}{9}\right)$$

$$-\frac{\langle z_2 \rangle \langle z_3 \rangle}{3[12]\langle 23 \rangle}\left(-\frac{2s_{23}}{\gamma_{23}}\hat{L}_3\left(s_{12}, s_{123}\right) - \frac{1}{\gamma_{21}}\hat{L}_2\left(s_{12}, s_{123}\right)\right.$$

$$\left.-\frac{2}{\gamma_{21}\gamma_{31}s_{123}}\hat{L}_1\left(s_{12}, s_{123}\right) - \frac{2}{\gamma_{21}\gamma_{31}s_{123}s_{23}}\hat{L}_0\left(s_{12}, s_{123}\right) + \frac{1}{2\gamma_{21}s_{12}s_{123}}\right) \quad \text{(F.4.67)}$$

$$\mathrm{Sp}^{[\mathrm{f}]}\left(-P^+; 1_{\bar{q}}^-, 2_q^+, 3^-\right) = \mathrm{Sp}^{(0)}\left(-P^+; 1_{\bar{q}}^-, 2_q^+, 3^-\right)\left(-\frac{2}{3\epsilon}\left(\frac{\mu_R}{-s_{12}}\right)^\epsilon - \frac{10}{9}\right)$$

$$+\frac{\langle z_3 \rangle s_{13}[2P]}{3[13]}\left(2\gamma_{32}s_{123}\hat{L}_3\left(s_{12}, s_{123}\right) - \hat{L}_2\left(s_{12}, s_{123}\right)\right.$$

$$+\left(\frac{2\gamma_{12}^2}{\gamma_{32}s_{123}} + \frac{2s_{123}\gamma_{12}}{s_{12}^2} - \frac{2}{s_{12}}\right)\hat{L}_1\left(s_{12}, s_{123}\right)$$

$$\left.+\left(\frac{2\gamma_{12}\left(s_{12} + s_{123}\right)}{s_{12}^2 s_{123}} - \frac{2}{s_{12}s_{123}}\right)\hat{L}_0\left(s_{12}, s_{123}\right) - \frac{1}{2s_{12}s_{123}}\right) \quad \text{(F.4.68)}$$

$$\mathrm{Sp}^{[\mathrm{f}]}\left(-P^+; 1_{\bar{q}}^+, 2_q^-, 3^+\right) = \mathrm{Sp}^{(0)}\left(-P^+; 1_{\bar{q}}^+, 2_q^-, 3^+\right)\left(-\frac{2}{3\epsilon}\left(\frac{\mu_R}{-s_{12}}\right)^\epsilon - \frac{10}{9}\right)$$

$$-\frac{\alpha_{12}^3}{3\alpha_{13}^3}\left(\left(s_{13}^3 - s_{23}^3\right)\hat{L}_3\left(s_{12}, s_{123}\right) - \frac{3\left(s_{13}^2 + 2s_{23}s_{13}\right)}{\alpha_{12}}\hat{L}_2\left(s_{12}, s_{123}\right)\right.$$

$$+\frac{3s_{13}}{\alpha_{12}^2}\hat{L}_1\left(s_{12}, s_{123}\right) - \hat{L}_0\left(s_{12}, s_{123}\right) - \frac{1}{2}\frac{\left(s_{123} - s_{13}\right)^2 - s_{13}s_{123} - s_{12}(s_{123} - s_{23})}{s_{12}s_{123}}$$

$$\left.-\frac{s_{13}}{\alpha_{12}^2 s_{123}} + \frac{s_{13}\left(3s_{12} + 5s_{123} + s_{23}\right)}{2\alpha_{12}s_{12}s_{123}}\right)\right) \quad \text{(F.4.69)}$$

$$\mathrm{Sp}^{[\mathrm{f}]}\left(-P^+; 1_{\bar{q}}^-, 2_q^+, 3^+\right) = \mathrm{Sp}^{(0)}\left(-P^+; 1_{\bar{q}}^-, 2_q^+, 3^+\right)\left(-\frac{2}{3\epsilon}\left(\frac{\mu_R}{-s_{12}}\right)^\epsilon - \frac{10}{9}\right)$$

$$-\frac{\alpha_{12}}{3\alpha_{13}}\left(-2\alpha_{12}^2 s_{23}^3 \hat{L}_3\left(s_{12}, s_{123}\right) + 3\alpha_{12}s_{23}^2\hat{L}_2\left(s_{12}, s_{123}\right) + 2s_{13}\hat{L}_1\left(s_{12}, s_{123}\right)\right.$$

$$\left.-\frac{s_{23}}{s_{12} - s_{123}}\hat{L}_0\left(s_{12}, s_{123}\right) + \frac{s_{23}}{s_{123}} - \frac{\alpha_{12}s_{23}^2}{2s_{12}s_{123}}\right)\right) \quad \text{(F.4.70)}$$

$$\mathrm{Sp}^{[\mathrm{scalar}]}\left(-P^+; 1_{\bar{q}}^+, 2_q^-, 3^-\right) = \mathrm{Sp}^{(0)}\left(-P^+; 1_{\bar{q}}^+, 2_q^-, 3^-\right)\left(\frac{2}{3}\delta_{\mathrm{R}}\right)$$

$$+ \frac{3\langle z_2\rangle\langle z_3\rangle}{\gamma_{21}\gamma_{32}[12]\langle 23\rangle s_{123}}\hat{L}_1\left(s_{12}, s_{123}\right) \tag{F.4.71}$$

$$\mathrm{Sp}^{[\mathrm{scalar}]}\left(-P^+; 1_{\bar{q}}^-, 2_q^+, 3^-\right) = \mathrm{Sp}^{(0)}\left(-P^+; 1_{\bar{q}}^-, 2_q^+, 3^-\right)\left(\frac{2}{3}\delta_{\mathrm{R}} - 2\right)$$

$$\frac{\langle z_3\rangle}{[13]\langle 2P\rangle}\left(+\frac{3s_{2P}}{2\gamma_{31}s_{123}}\mathrm{F}_{\mathrm{box}}^{1m} - \frac{3s_{13}s_{2P}}{\gamma_{31}s_{123}}\hat{L}_1\left(s_{12}, s_{123}\right) - \frac{3s_{13}s_{2P}}{\gamma_{31}s_{123}}\hat{L}_1\left(s_{23}, s_{123}\right)\right.$$

$$\left. + \frac{2s_{13}s_{2P}}{\gamma_{32}s_{12}s_{123}} - \frac{2\gamma_{13}\gamma_{32}z_2 s_{2P}}{\gamma_{23}\left(1-z_3\right)s_{12}} + \frac{2\gamma_{12}\gamma_{13}z_2 s_{2P}}{\gamma_{23}z_3 s_{12}}\right) \tag{F.4.72}$$

$$\mathrm{Sp}^{[\mathrm{scalar}]}\left(-P^+; 1_{\bar{q}}^+, 2_q^-, 3^+\right) = \mathrm{Sp}^{(0)}\left(-P^+; 1_{\bar{q}}^+, 2_q^-, 3^+\right)\left(\frac{2}{3}\delta_{\mathrm{R}} - \frac{3\alpha_{12}}{\alpha_{13}^2}\left(\frac{1}{2}\mathrm{F}_{\mathrm{box}}^{1m}\right.\right.$$

$$\left.\left. + s_{12}\hat{L}_1\left(s_{23}, s_{123}\right) + s_{23}\hat{L}_1\left(s_{12}, s_{123}\right) + \hat{L}_0\left(s_{12}, s_{123}\right) + \hat{L}_0\left(s_{23}, s_{123}\right)\right)\right) \tag{F.4.73}$$

$$\mathrm{Sp}^{[\mathrm{scalar}]}\left(-P^+; 1_{\bar{q}}^-, 2_q^+, 3^+\right) = \mathrm{Sp}^{(0)}\left(-P^+; 1_{\bar{q}}^-, 2_q^+, 3^+\right)\left(\frac{2}{3}\delta_{\mathrm{R}} - 3\alpha_{12}s_{23}\hat{L}_1\left(s_{12}, s_{123}\right)\right) \tag{F.4.74}$$

The expressions for the non-zero independent one loop splitting amplitudes $g \to \bar{q}gq$ are

$$\mathrm{Sp}^{[\mathcal{N}=4]}\left(-P^+; 1_{\bar{q}}^+, 2^-, 3_q^-\right) = \mathrm{Sp}^{(0)}\left(-P^+; 1_{\bar{q}}^+, 2^-, 3_q^-\right)\left(V_g + \frac{\gamma_{21}\left(1-z_1\right)^2 s_{123}}{z_2 s_{1P}}\mathrm{F}_2^{\mathrm{NMHV}}\right.$$

$$\left. + \left(\frac{\gamma_{21}\alpha_{23}s_{23}(\gamma_{13})^\dagger}{z_1 s_{1P}} + 1\right)\mathrm{F}_3^{\mathrm{NMHV}} - \frac{\gamma_{31}^2 s_{123}\left(\gamma_{13}\alpha_{23}\right)^\dagger}{s_{13}}\mathrm{F}_1^{\mathrm{NMHV}}\right) \tag{F.4.75}$$

$$\mathrm{Sp}^{[\mathcal{N}=4]}\left(-P^+; 1_{\bar{q}}^-, 2^+, 3_q^+\right) = \mathrm{Sp}^{(0)}\left(-P^+; 1_{\bar{q}}^-, 2^+, 3_q^+\right)\left(V_g + F^{\mathrm{MHV}}\right) \tag{F.4.76}$$

$$\mathrm{Sp}^{[\mathrm{scalar}]}\left(-P^+; 1_{\bar{q}}^+, 2^-, 3_q^-\right) = \mathrm{Sp}^{(0)}\left(-P^+; 1_{\bar{q}}^+, 2^-, 3_q^-\right)\left(-\frac{2}{3\epsilon}\left(\frac{\mu_R}{-s_{13}}\right)^\epsilon - \frac{10}{9}\right.$$

$$\left. + \frac{2\delta_{\mathrm{R}}}{3} + \frac{3\gamma_{21}s_{23}}{\gamma_{23}}\hat{L}_1\left(s_{12}, s_{123}\right) - \frac{2}{3}\hat{L}_0\left(s_{13}, s_{123}\right)\right) \tag{F.4.77}$$

$$\mathrm{Sp}^{[\mathrm{scalar}]}\left(-P^+; 1_{\bar{q}}^-, 2^+, 3_q^+\right) = \mathrm{Sp}^{(0)}\left(-P^+; 1_{\bar{q}}^-, 2^+, 3_q^+\right)\left(-\frac{2}{3\epsilon}\left(\frac{\mu_R}{-s_{123}}\right)^\epsilon - \frac{29}{18}\right.$$

$$+ \frac{2\delta_{\mathrm{R}}}{3} + \left(\frac{\gamma_{32}^2 s_{12}^2}{2\gamma_{12}^2} - \frac{s_{13}^2}{2\gamma_{13}^2}\right)\hat{L}_2\left(s_{12}, s_{123}\right) - 4\alpha_{12}s_{23}\hat{L}_1\left(s_{12}, s_{123}\right)$$

$$\left. + \frac{1}{2}\hat{L}_0\left(s_{12}, s_{123}\right) + \frac{\gamma_{32}^2 s_{12}}{4\gamma_{12}^2 s_{123}} - \frac{\gamma_{32}}{\gamma_{12}} - \frac{s_{13}^2}{4\gamma_{13}^2 s_{12}s_{123}} + \frac{s_{123}}{2s_{12}}\right) \tag{F.4.78}$$

The expressions for the other helicity configurations are obtained by conjugation operation or by reversing the fermion line, namely $\mathrm{Sp}\left(-P; 1_{\bar{q}}^h, 2, 3_q^{-h}\right) = \mathrm{Sp}\left(-P; 3_{\bar{q}}^{-h}, 2, 1_q^h\right)$.

Appendix G

All plus one-loop $t\bar{t}$ + 3-gluon scattering amplitudes

In this appendix we present the analytic formulae for the $t\bar{t}$ + 3 gluons scattering amplitudes in the 'all-plus' helicity configuration.

G.0.1 Tree-level

Recalling the decomposition given in Eq. (8.2.17), the tree level amplitude for the all-plus case can be written as

$$
A_5^{(0)}(\bar{t}^+(p_1^\flat, \eta_1), t^+(p_2^\flat, \eta_2), 3^+, 4^+, 5^+) =
$$

$$
\sum_{i=1}^{4} \rho_i^{++}(\eta_1, \eta_2, p_1^\flat, p_2^\flat) A_{5;\rho_i}^{(0)}(\bar{t}, t, 3^+, 4^+, 5^+), \qquad \text{(G.0.1)}
$$

where the sub amplitudes take the explicit form,

$$
A_{5;\rho_1}^{(0)} = A_{5;\rho_2}^{(0)} = A_{5;\rho_3}^{(0)} = 0, \qquad \text{(G.0.2)}
$$

$$
A_{5;\rho_4}^{(0)} = 16 m_t^3 \frac{A_4^{(0)}}{\langle 34 \rangle \langle 45 \rangle \langle 35 \rangle} \qquad \text{(G.0.3)}
$$

with

$$s_{35} = s_{12} - s_{34} - s_{45} \tag{G.0.4}$$

$$A_4^{(0)} = \frac{P_{15}(s_{12} - s_{45}) + P_{23}(s_{12} - s_{34}) - s_{35}\Delta + s_{34}s_{45}}{P_{15}P_{23}s_{34}} \tag{G.0.5}$$

G.0.2   One-loop

The one-loop amplitude is decomposed as,

$$A_5^{(1)}(\bar{t}^+(p_1^\flat, \eta_1), t^+(p_2^\flat, \eta_2), 3^+, 4^+, 5^+) =$$

$$\sum_{i=1}^{4} \rho_i^{++}(\eta_1, \eta_2, p_1^\flat, p_2^\flat) A_{5;\rho_i}^{(1)}(\bar{t}, t, 3^+, 4^+, 5^+), \tag{G.0.6}$$

The analytic expressions for the sub amplitudes are presented in the following, where we use the QCDLoop [73] notation for the integrals.

$$A^{(1)}_{5;\rho_1} = -\,\mathrm{F}_2[s_{15}; 0\; m_t^2]16m_t^3 A_4^{(0)}\left(A_4^{(0)}P_{23} - \frac{s_{35}}{s_{34}}\right)$$

$$-\,\mathrm{F}_2[s_{23}; 0\; m_t^2]16m_t^3 A_4^{(0)}\left(A_4^{(0)}\frac{P_{15}s_{34}}{s_{45}} - \frac{s_{35}}{s_{45}}\right)$$

$$+\,(D_s - 2)4m_t\left(A_4^{(0)2}\left(P_{15}P_{23} + \frac{P_{15}P_{23}s_{34}}{s_{45}}\right)\right.$$

$$\left.+\,A_4^{(0)}\left(-\frac{P_{15}s_{35}}{s_{34}} - \frac{P_{23}s_{35}}{s_{45}}\right) - \frac{2s_{35}^2}{3s_{12}s_{34}}\right)$$

$$A^{(1)}_{5;\rho_2} = \mathrm{F}_2[s_{23}; 0\; m_t^2]16m_t^3 A_4^{(0)}\frac{P_{23} - \Delta}{P_{15} - P_{23}} -$$

$$\mathrm{F}_2[s_{15}; 0\; m_t^2]16m_t^3 A_4^{(0)}\left(A_4^{(0)}P_{23} - \frac{P_{15}(s_{34} + s_{35}) - P_{23}(2s_{34} + s_{35}) + s_{34}\Delta}{(P_{15} - P_{23})s_{34}}\right) +$$

$$(D_s - 2)4m_t\left(A_4^{(0)2}P_{15}P_{23} - A_4^{(0)}\frac{P_{15}s_{34} - 3P_{23}s_{34} + 3P_{15}s_{35} + 3s_{34}\Delta}{3s_{34}}\right.$$

$$\left.-\,2\frac{s_{35}^2 + s_{34}(s_{35} - s_{45})}{3s_{12}s_{34}^2}\right)$$

$$A^{(1)}_{5;\rho_3} = 2\mathrm{F}_2[s_{23}; 0\; m_t^2]16m_t^3 A_4^{(0)} +$$

$$2\mathrm{F}_2[s_{15}; 0\; m_t^2]16m_t^3 A_4^{(0)}\left(A_4^{(0)}P_{23} - \frac{s_{12} - s_{45}}{s_{34}}\right) +$$

$$(D_s - 2)\left(\frac{8m_t(s_{12} - 2s_{45})s_{35}}{3s_{12}s_{34}} - 8m_tP_{15}P_{23}A_4^{(0)2} -\right.$$

$$\left.A_4^{(0)}\frac{8m_t(2P_{23}s_{34} + P_{15}(-3s_{12} + s_{34} + 3s_{45}))}{3s_{34}}\right)$$

$$
\begin{aligned}
A_{5;\rho_4}^{(1)} = \ &\mathrm{I}_4\left[m_t^2 0 0 s_{15}; s_{23}s_{34}; 0 0 0 m_t^2\right]\left(-A_4^{(0)}\frac{16m_t^3 P_{23}}{s_{34}} + \frac{8m_t^3 P_{23}s_{12}}{s_{34}^2\Delta}\right) - \\
&\mathrm{I}_4\left[m_t^2 m_t^2 0 s_{45}; s_{12}s_{23}; m_t^2 0 0 0\right]\frac{8m_t^3 P_{23}s_{12}^2}{s_{34}^3\Delta} - \\
&\mathrm{I}_4\left[m_t^2 m_t^2 s_{34}0; s_{12}s_{15}; m_t^2 0 0 0\right]\frac{8m_t^3 P_{15}s_{12}^2}{s_{34}^3\Delta} + \\
&\mathrm{I}_4\left[m_t^2 s_{23}0 0; s_{15}s_{45}; m_t^2 0 0 0\right]\left(-A_4^{(0)}\frac{16m_t^3 P_{15}s_{45}}{s_{34}^2} + \frac{8m_t^3 P_{15}s_{12}s_{45}}{s_{34}^3\Delta}\right) - \\
&\mathrm{I}_4\left[0 0 0 s_{12}; s_{34}s_{45}; 0 0 0 0\right]\frac{8m_t^3 s_{12}s_{45}}{s_{34}^2\Delta} + \\
&\mathrm{I}_2[m_t^2; m_t^2\ 0](D_s - 2)m_t^3 4 A_4^{(0)} + \\
&\mathrm{F}_2[s_{15}; 0\ m_t^2]\Bigg(\\
&\qquad A_4^{(0)\,2}\frac{16m_t^3 P_{23}(2P_{15}P_{23} + P_{15}s_{45} - P_{23}s_{45} + 2P_{15}\Delta)}{(P_{15} - P_{23})s_{45}} - \\
&\qquad A_4^{(0)}\frac{16m_t^3}{(P_{15} - P_{23})s_{34}s_{45}}\Big(4P_{15}P_{23}s_{12} + 2P_{23}^2 s_{12} - 2P_{23}^2 s_{34} - 2P_{15}P_{23}s_{45} + \\
&\qquad\qquad P_{15}s_{12}s_{45} - P_{23}s_{12}s_{45} + 2P_{15}s_{34}s_{45} + 2P_{23}s_{34}s_{45} - P_{15}s_{45}^2 + P_{23}s_{45}^2\Big) + \\
&\qquad \frac{32m_t^3 s_{35}(P_{23}s_{12} + s_{34}s_{45})}{(P_{15} - P_{23})s_{34}^3 s_{45}}\Bigg) - \\
&\mathrm{F}_2[s_{23}; 0\ m_t^2]\Bigg(\\
&\qquad A_4^{(0)\,2}\frac{32m_t^3 P_{15}P_{23}(P_{15} + \Delta)}{(P_{15} - P_{23})s_{45}} + \\
&\qquad A_4^{(0)}\frac{16m_t^3\left(-2P_{15}^2 s_{12} - 4P_{15}P_{23}s_{12} + 2P_{15}P_{23}s_{34} + 2P_{15}^2 s_{45} - 3P_{15}s_{34}s_{45} - P_{23}s_{34}s_{45}\right)}{(P_{15} - P_{23})s_{34}s_{45}} + \\
&\qquad \frac{32m_t^3 s_{35}(P_{15}s_{12} + s_{34}s_{45})}{(P_{15} - P_{23})s_{34}^3 s_{45}}\Bigg) + \\
&\mathrm{F}_1(D_s - 2)4m_t A_4^{(0)} + \\
&(D_s - 2)4m_t\Bigg(\\
&\qquad -A_4^{(0)\,2}P_{15}P_{23} + \\
&\qquad A_4^{(0)}\frac{1}{3s_{12}s_{34}s_{45}}\Big(-2P_{15}^2 s_{12}s_{34} + 2P_{15}P_{23}s_{12}s_{34} - 2P_{15}P_{23}s_{34}^2 - \\
&\qquad\qquad 2P_{23}^2 s_{12}s_{45} + 3P_{15}s_{12}^2 s_{45} - 6P_{15}P_{23}s_{34}s_{45} - 5P_{15}s_{12}s_{34}s_{45} - \\
&\qquad\qquad 6P_{23}s_{12}s_{34}s_{45} - 2P_{15}P_{23}s_{45}^2 - 3P_{15}s_{12}s_{45}^2\Big) + \\
&\qquad \frac{s_{35}}{3s_{12}s_{34}^2 s_{45}}\Big(2P_{15}s_{12}s_{34} - 2P_{23}s_{12}s_{34} + 2P_{23}s_{34}^2 - 2P_{15}s_{12}s_{45} + 2P_{23}s_{12}s_{45} + \\
&\qquad\qquad 2P_{15}s_{34}s_{45} + 2P_{23}s_{34}s_{45} + 5s_{12}s_{34}s_{45} - 2s_{34}^2 s_{45} + 2P_{15}s_{45}^2 - 4s_{34}s_{45}^2\Big)\Bigg)
\end{aligned}
$$

Bibliography

[1] S. Badger, F. Buciuni and T. Peraro, *One-loop triple collinear splitting amplitudes in QCD*, *JHEP* **09** (2015) 188, [`1507.05070`].

[2] S. Badger, C. Brønnum-Hansen, F. Buciuni and D. O'Connell, *A unitarity compatible approach to one-loop amplitudes with massive fermions*, *JHEP* **06** (2017) 141, [`1703.05734`].

[3] S. L. Glashow, *Partial Symmetries of Weak Interactions*, *Nucl. Phys.* **22** (1961) 579–588.

[4] S. Weinberg, *A Model of Leptons*, *Phys. Rev. Lett.* **19** (1967) 1264–1266.

[5] ATLAS collaboration, G. Aad et al., *Observation of a new particle in the search for the Standard Model Higgs boson with the ATLAS detector at the LHC*, *Phys. Lett.* **B716** (2012) 1–29, [`1207.7214`].

[6] CMS collaboration, S. Chatrchyan et al., *Observation of a new boson at a mass of 125 GeV with the CMS experiment at the LHC*, *Phys. Lett.* **B716** (2012) 30–61, [`1207.7235`].

[7] F. A. Berends and W. Giele, *The Six Gluon Process as an Example of Weyl-Van Der Waerden Spinor Calculus*, *Nucl. Phys.* **B294** (1987) 700–732.

[8] R. Britto, F. Cachazo and B. Feng, *New Recursion Relations for Tree Amplitudes of Gluons*, *Nucl. Phys.* **B715** (2005) 499–522, [`hep-th/0412308`].

[9] G. Passarino and M. J. G. Veltman, *One Loop Corrections for e+ e- Annihilation Into mu+ mu- in the Weinberg Model*, *Nucl. Phys.* **B160** (1979) 151–207.

[10] Z. Bern, L. J. Dixon, D. C. Dunbar and D. A. Kosower, *One loop n point gauge theory amplitudes, unitarity and collinear limits*, *Nucl. Phys.* **B425** (1994) 217–260, [`hep-ph/9403226`].

[11] R. Britto, F. Cachazo and B. Feng, *Generalized unitarity and one-loop amplitudes in N=4 super-Yang-Mills*, *Nucl. Phys.* **B725** (2005) 275–305, [`hep-th/0412103`].

[12] G. Ossola, C. G. Papadopoulos and R. Pittau, *Reducing full one-loop amplitudes to scalar integrals at the integrand level*, *Nucl. Phys.* **B763** (2007) 147–169, [`hep-ph/0609007`].

[13] C. F. Berger, Z. Bern, L. J. Dixon, F. Febres Cordero, D. Forde, H. Ita et al., *An Automated Implementation of On-Shell Methods for One-Loop Amplitudes*, *Phys. Rev.* **D78** (2008) 036003, [`0803.4180`].

[14] G. Bevilacqua, M. Czakon, M. V. Garzelli, A. van Hameren, A. Kardos, C. G. Papadopoulos et al., *HELAC-NLO*, *Comput. Phys. Commun.* **184** (2013) 986–997, [`1110.1499`].

[15] V. Hirschi, R. Frederix, S. Frixione, M. V. Garzelli, F. Maltoni et al., *Automation of one-loop QCD corrections*, *JHEP* **1105** (2011) 044, [`1103.0621`].

[16] G. Cullen, N. Greiner, G. Heinrich, G. Luisoni, P. Mastrolia, G. Ossola et al., *Automated One-Loop Calculations with GoSam*, *Eur. Phys. J.* **C72** (2012) 1889, [`1111.2034`].

[17] F. Cascioli, P. Maierhofer and S. Pozzorini, *Scattering Amplitudes with Open Loops*, `1111.5206`.

[18] S. Badger, B. Biedermann and P. Uwer, *NGluon: A Package to Calculate One-loop Multi-gluon Amplitudes*, *Comput.Phys.Commun.* **182** (2011) 1674–1692, [`1011.2900`].

[19] S. Badger, B. Biedermann, P. Uwer and V. Yundin, *Numerical evaluation of virtual corrections to multi-jet production in massless QCD*, *Comput.Phys.Commun.* **184** (2013) 1981–1998, [`1209.0100`].

[20] K. G. Chetyrkin and F. V. Tkachov, *Integration by Parts: The Algorithm to Calculate beta Functions in 4 Loops*, *Nucl. Phys.* **B192** (1981) 159–204.

[21] S. Laporta, *High precision calculation of multiloop Feynman integrals by difference equations*, *Int. J. Mod. Phys.* **A15** (2000) 5087–5159, [`hep-ph/0102033`].

[22] A. V. Kotikov, *Differential equation method: The Calculation of N point Feynman diagrams*, *Phys. Lett.* **B267** (1991) 123–127.

[23] E. Remiddi, *Differential equations for Feynman graph amplitudes*, *Nuovo Cim.* **A110** (1997) 1435–1452, [`hep-th/9711188`].

[24] M. Beneke and V. A. Smirnov, *Asymptotic expansion of Feynman integrals near threshold*, *Nucl. Phys.* **B522** (1998) 321–344, [`hep-ph/9711391`].

[25] C. Anastasiou, S. Beerli and A. Daleo, *Evaluating multi-loop Feynman diagrams with infrared and threshold singularities numerically*, *JHEP* **05** (2007) 071, [`hep-ph/0703282`].

[26] C. Anastasiou, C. Duhr, F. Dulat, F. Herzog and B. Mistlberger, *Higgs Boson Gluon-Fusion Production in QCD at Three Loops*, *Phys. Rev. Lett.* **114** (2015) 212001, [`1503.06056`].

[27] C. Anastasiou, C. Duhr, F. Dulat, F. Herzog and B. Mistlberger, *Higgs Boson Gluon-Fusion Production in QCD at Three Loops*, *Phys.Rev.Lett.* **114** (2015) 212001, [`1503.06056`].

[28] A. Hodges, *Eliminating spurious poles from gauge-theoretic amplitudes*, *JHEP* **05** (2013) 135, [`0905.1473`].

[29] C. Cheung and D. O'Connell, *Amplitudes and Spinor-Helicity in Six Dimensions*, *JHEP* **07** (2009) 075, [`0902.0981`].

[30] T. Peraro, *Scattering amplitudes over finite fields and multivariate functional reconstruction*, *JHEP* **12** (2016) 030, [1608.01902].

[31] R. K. Ellis, W. T. Giele, Z. Kunszt and K. Melnikov, *Masses, fermions and generalized D-dimensional unitarity*, *Nucl. Phys.* **B822** (2009) 270–282, [0806.3467].

[32] R. Britto and E. Mirabella, *External leg corrections in the unitarity method*, *JHEP* **01** (2012) 045, [1109.5106].

[33] M. E. Peskin and D. V. Schroeder, *An Introduction to quantum field theory*, .

[34] R. K. Ellis, W. J. Stirling and B. R. Webber, *QCD and Collider Physics*. Cambridge Monographs on Particle Physics, Nuclear Physics and Cosmology. Cambridge University Press, 1996, 10.1017/CBO9780511628788.

[35] G. Altarelli and G. Parisi, *Asymptotic Freedom in Parton Language*, *Nucl. Phys.* **B126** (1977) 298–318.

[36] V. N. Gribov and L. N. Lipatov, *Deep inelastic e p scattering in perturbation theory*, *Sov. J. Nucl. Phys.* **15** (1972) 438–450.

[37] Y. L. Dokshitzer, *Calculation of the Structure Functions for Deep Inelastic Scattering and e+ e- Annihilation by Perturbation Theory in Quantum Chromodynamics.*, *Sov. Phys. JETP* **46** (1977) 641–653.

[38] G. 't Hooft and M. J. G. Veltman, *Regularization and Renormalization of Gauge Fields*, *Nucl. Phys.* **B44** (1972) 189–213.

[39] T. Kinoshita, *Mass singularities of Feynman amplitudes*, *J. Math. Phys.* **3** (1962) 650–677.

[40] T. D. Lee and M. Nauenberg, *Degenerate Systems and Mass Singularities*, *Phys. Rev.* **133** (1964) B1549–B1562.

[41] S. Catani and M. H. Seymour, *A General algorithm for calculating jet cross-sections in NLO QCD*, *Nucl. Phys.* **B485** (1997) 291–419, [hep-ph/9605323].

[42] S. Frixione, Z. Kunszt and A. Signer, *Three jet cross-sections to next-to-leading order, Nucl. Phys.* **B467** (1996) 399–442, [`hep-ph/9512328`].

[43] S. Frixione, *A General approach to jet cross-sections in QCD, Nucl. Phys.* **B507** (1997) 295–314, [`hep-ph/9706545`].

[44] W. T. Giele and E. W. N. Glover, *Higher-order corrections to jet cross sections in e^+e^- annihilation, Phys. Rev. D* **46** (Sep, 1992) 1980–2010.

[45] R. Ellis, W. Stirling and B. Webber, *QCD and Collider Physics, Camb.Monogr.Part.Phys.Nucl.Phys.Cosmol.* **8** (1996) 1–435.

[46] S. Catani, Y. L. Dokshitzer, M. Olsson, G. Turnock and B. R. Webber, *New clustering algorithm for multi - jet cross-sections in e+ e- annihilation, Phys. Lett.* **B269** (1991) 432–438.

[47] Y. L. Dokshitzer, G. D. Leder, S. Moretti and B. R. Webber, *Better jet clustering algorithms, JHEP* **08** (1997) 001, [`hep-ph/9707323`].

[48] G. P. Salam and G. Soyez, *A Practical Seedless Infrared-Safe Cone jet algorithm, JHEP* **05** (2007) 086, [`0704.0292`].

[49] M. Cacciari, G. P. Salam and G. Soyez, *The Anti-k(t) jet clustering algorithm, JHEP* **04** (2008) 063, [`0802.1189`].

[50] J. R. Andersen et al., *Les Houches 2015: Physics at TeV Colliders Standard Model Working Group Report*, in *9th Les Houches Workshop on Physics at TeV Colliders (PhysTeV 2015) Les Houches, France, June 1-19, 2015*, 2016, `1605.04692`, http://lss.fnal.gov/archive/2016/conf/fermilab-conf-16-175-ppd-t.pdf.

[51] H. Elvang and Y.-t. Huang, *Scattering Amplitudes*, `1308.1697`.

[52] M. L. Mangano, S. J. Parke and Z. Xu, *Duality and Multi - Gluon Scattering, Nucl. Phys.* **B298** (1988) 653–672.

[53] V. Del Duca, L. J. Dixon and F. Maltoni, *New color decompositions for gauge amplitudes at tree and loop level, Nucl. Phys.* **B571** (2000) 51–70, [hep-ph/9910563].

[54] L. J. Dixon, *Calculating scattering amplitudes efficiently*, in *QCD and beyond. Proceedings, Theoretical Advanced Study Institute in Elementary Particle Physics, TASI-95, Boulder, USA, June 4-30, 1995*, pp. 539–584, 1996, hep-ph/9601359, http://www-public.slac.stanford.edu/sciDoc/docMeta.aspx?slacPubNumber=SLAC-PUB-7106.

[55] R. Kleiss and W. J. Stirling, *Spinor Techniques for Calculating p anti-p $\rightarrow W^{\pm}/Z^0$ + Jets, Nucl. Phys.* **B262** (1985) 235–262.

[56] K. Hagiwara and D. Zeppenfeld, *Helicity Amplitudes for Heavy Lepton Production in e+ e- Annihilation, Nucl. Phys.* **B274** (1986) 1–32.

[57] C. Schwinn and S. Weinzierl, *Scalar diagrammatic rules for Born amplitudes in QCD, JHEP* **05** (2005) 006, [hep-th/0503015].

[58] G. Rodrigo, *Multigluonic scattering amplitudes of heavy quarks, JHEP* **09** (2005) 079, [hep-ph/0508138].

[59] D. Maitre and P. Mastrolia, *S@M, a Mathematica Implementation of the Spinor-Helicity Formalism, Comput. Phys. Commun.* **179** (2008) 501–574, [0710.5559].

[60] S. Badger, R. Sattler and V. Yundin, *One-Loop Helicity Amplitudes for $t\bar{t}$ Production at Hadron Colliders, Phys. Rev.* **D83** (2011) 074020, [1101.5947].

[61] R. Cutkosky, *Singularities and discontinuities of Feynman amplitudes, J.Math.Phys.* **1** (1960) 429–433.

[62] E. Witten, *Perturbative gauge theory as a string theory in twistor space, Commun. Math. Phys.* **252** (2004) 189–258, [hep-th/0312171].

[63] G. Ossola, C. G. Papadopoulos and R. Pittau, *Numerical evaluation of six-photon amplitudes*, *JHEP* **0707** (2007) 085, [`0704.1271`].

[64] F. A. Berends and W. T. Giele, *Recursive Calculations for Processes with n Gluons*, *Nucl. Phys.* **B306** (1988) 759–808.

[65] R. Britto, F. Cachazo, B. Feng and E. Witten, *Direct proof of tree-level recursion relation in Yang-Mills theory*, *Phys.Rev.Lett.* **94** (2005) 181602, [`hep-th/0501052`].

[66] N. Arkani-Hamed and J. Kaplan, *On Tree Amplitudes in Gauge Theory and Gravity*, *JHEP* **04** (2008) 076, [`0801.2385`].

[67] S. J. Parke and T. R. Taylor, *Amplitude for n-gluon scattering*, *Phys. Rev. Lett.* **56** (Jun, 1986) 2459–2460.

[68] Z. Bern, J. J. Carrasco, T. Dennen, Y.-t. Huang and H. Ita, *Generalized Unitarity and Six-Dimensional Helicity*, *Phys. Rev.* **D83** (2011) 085022, [`1010.0494`].

[69] Z.-G. Xiao, G. Yang and C.-J. Zhu, *The rational parts of one-loop QCD amplitudes I: The general formalism*, *Nucl. Phys.* **B758** (2006) 1–34, [`hep-ph/0607015`].

[70] D. Forde, *Direct extraction of one-loop integral coefficients*, *Phys. Rev.* **D75** (2007) 125019, [`0704.1835`].

[71] R. K. Ellis, W. T. Giele and Z. Kunszt, *A Numerical Unitarity Formalism for Evaluating One-Loop Amplitudes*, *JHEP* **03** (2008) 003, [`0708.2398`].

[72] W. T. Giele, Z. Kunszt and K. Melnikov, *Full one-loop amplitudes from tree amplitudes*, *JHEP* **04** (2008) 049, [`0801.2237`].

[73] R. K. Ellis and G. Zanderighi, *Scalar one-loop integrals for QCD*, *JHEP* **02** (2008) 002, [`0712.1851`].

[74] P. Mastrolia and G. Ossola, *On the Integrand-Reduction Method for Two-Loop Scattering Amplitudes*, *JHEP* **11** (2011) 014, [`1107.6041`].

[75] S. Badger, H. Frellesvig and Y. Zhang, *Hepta-Cuts of Two-Loop Scattering Amplitudes*, *JHEP* **04** (2012) 055, [`1202.2019`].

[76] Y. Zhang, *Integrand-Level Reduction of Loop Amplitudes by Computational Algebraic Geometry Methods*, *JHEP* **09** (2012) 042, [`1205.5707`].

[77] P. Mastrolia, E. Mirabella, G. Ossola and T. Peraro, *Scattering Amplitudes from Multivariate Polynomial Division*, *Phys. Lett.* **B718** (2012) 173–177, [`1205.7087`].

[78] Z. Bern and A. G. Morgan, *Massive loop amplitudes from unitarity*, *Nucl. Phys.* **B467** (1996) 479–509, [`hep-ph/9511336`].

[79] P. Mastrolia, E. Mirabella, G. Ossola and T. Peraro, *Integrand-Reduction for Two-Loop Scattering Amplitudes through Multivariate Polynomial Division*, *Phys.Rev.* **D87** (2012) 085026, [`1209.4319`].

[80] W. L. van Neerven and J. A. M. Vermaseren, *Large Loop Integrals*, *Phys. Lett.* **B137** (1984) 241–244.

[81] S. Davies, *One-Loop QCD and Higgs to Partons Processes Using Six-Dimensional Helicity and Generalized Unitarity*, *Phys. Rev.* **D84** (2011) 094016, [`1108.0398`].

[82] S. Badger, G. Mogull and T. Peraro, *Local integrands for two-loop all-plus Yang-Mills amplitudes*, *JHEP* **08** (2016) 063, [`1606.02244`].

[83] D. A. Kosower, *Antenna factorization of gauge theory amplitudes*, *Phys. Rev.* **D57** (1998) 5410–5416, [`hep-ph/9710213`].

[84] S. Badger, E. Nigel Glover, P. Mastrolia and C. Williams, *One-loop Higgs plus four gluon amplitudes: Full analytic results*, *JHEP* **1001** (2010) 036, [`0909.4475`].

[85] C. Duhr, *Mathematical aspects of scattering amplitudes*, in *Proceedings, Theoretical Advanced Study Institute in Elementary Particle Physics: Journeys Through the Precision Frontier: Amplitudes for Colliders (TASI*

2014): Boulder, Colorado, June 2-27, 2014, pp. 419–476, 2015, `1411.7538`, DOI.

[86] H. J. Lu and C. A. Perez, *Massless one loop scalar three point integral and associated Clausen, Glaisher and L functions*, .

[87] Z. Bern, L. J. Dixon and D. A. Kosower, *Dimensionally regulated pentagon integrals*, *Nucl. Phys.* **B412** (1994) 751–816, [`hep-ph/9306240`].

[88] T. Binoth, J. P. Guillet, G. Heinrich and C. Schubert, *Calculation of one loop hexagon amplitudes in the Yukawa model*, *Nucl. Phys.* **B615** (2001) 385–401, [`hep-ph/0106243`].

[89] A. van Hameren, J. Vollinga and S. Weinzierl, *Automated computation of one-loop integrals in massless theories*, *Eur. Phys. J.* **C41** (2005) 361–375, [`hep-ph/0502165`].

[90] R. Kleiss and H. Kuijf, *Multi - Gluon Cross-sections and Five Jet Production at Hadron Colliders*, *Nucl. Phys.* **B312** (1989) 616.

[91] Z. Bern, L. J. Dixon and D. A. Kosower, *One loop corrections to two quark three gluon amplitudes*, *Nucl. Phys.* **B437** (1995) 259–304, [`hep-ph/9409393`].

[92] A. van Hameren, *OneLOop: For the evaluation of one-loop scalar functions*, *Comput.Phys.Commun.* **182** (2011) 2427–2438, [`1007.4716`].

[93] Z. Bern, L. J. Dixon and D. A. Kosower, *One loop amplitudes for e+ e- to four partons*, *Nucl. Phys.* **B513** (1998) 3–86, [`hep-ph/9708239`].

[94] A. Djouadi, M. Spira and P. M. Zerwas, *Production of Higgs bosons in proton colliders: QCD corrections*, *Phys. Lett.* **B264** (1991) 440–446.

[95] C. R. Schmidt, *H —gt; g g g (g q anti-q) at two loops in the large M(t) limit*, *Phys.Lett.* **B413** (1997) 391–395, [`hep-ph/9707448`].

[96] C. F. Berger, V. Del Duca and L. J. Dixon, *Recursive Construction of Higgs-Plus-Multiparton Loop Amplitudes: The Last of the Phi-nite Loop Amplitudes*, *Phys. Rev.* **D74** (2006) 094021, [`hep-ph/0608180`].

[97] S. D. Badger and E. W. N. Glover, *One-loop helicity amplitudes for H —¿ gluons: The All-minus configuration*, Nucl. Phys. Proc. Suppl. **160** (2006) 71–75, [`hep-ph/0607139`].

[98] S. Badger, E. N. Glover and K. Risager, *One-loop phi-MHV amplitudes using the unitarity bootstrap*, JHEP **0707** (2007) 066, [`0704.3914`].

[99] E. N. Glover, P. Mastrolia and C. Williams, *One-loop phi-MHV amplitudes using the unitarity bootstrap: The General helicity case*, JHEP **0808** (2008) 017, [`0804.4149`].

[100] S. Badger, J. M. Campbell, R. K. Ellis and C. Williams, *Analytic results for the one-loop NMHV Hqqgg amplitude*, JHEP **0912** (2009) 035, [`0910.4481`].

[101] L. J. Dixon and Y. Sofianatos, *Analytic one-loop amplitudes for a Higgs boson plus four partons*, JHEP **08** (2009) 058, [`0906.0008`].

[102] J. M. Campbell, R. K. Ellis and G. Zanderighi, *Next-to-Leading order Higgs + 2 jet production via gluon fusion*, JHEP **0610** (2006) 028, [`hep-ph/0608194`].

[103] J. M. Campbell, R. K. Ellis and C. Williams, *Hadronic production of a Higgs boson and two jets at next-to-leading order*, Phys. Rev. **D81** (2010) 074023, [`1001.4495`].

[104] H. van Deurzen, N. Greiner, G. Luisoni, P. Mastrolia, E. Mirabella, G. Ossola et al., *NLO QCD corrections to the production of Higgs plus two jets at the LHC*, Phys. Lett. **B721** (2013) 74–81, [`1301.0493`].

[105] G. Cullen, H. van Deurzen, N. Greiner, G. Luisoni, P. Mastrolia, E. Mirabella et al., *Next-to-Leading-Order QCD Corrections to Higgs Boson Production Plus Three Jets in Gluon Fusion*, Phys. Rev. Lett. **111** (2013) 131801, [`1307.4737`].

[106] T. Gehrmann, M. Jaquier, E. W. N. Glover and A. Koukoutsakis, *Two-Loop QCD Corrections to the Helicity Amplitudes for H → 3 partons*, JHEP **02** (2012) 056, [`1112.3554`].

[107] R. Boughezal, F. Caola, K. Melnikov, F. Petriello and M. Schulze, *Higgs boson production in association with a jet at next-to-next-to-leading order in perturbative QCD*, *JHEP* **06** (2013) 072, [1302.6216].

[108] X. Chen, T. Gehrmann, E. W. N. Glover and M. Jaquier, *Precise QCD predictions for the production of Higgs + jet final states*, *Phys. Lett.* **B740** (2015) 147–150, [1408.5325].

[109] R. Boughezal, F. Caola, K. Melnikov, F. Petriello and M. Schulze, *Higgs boson production in association with a jet at next-to-next-to-leading order*, *Phys. Rev. Lett.* **115** (2015) 082003, [1504.07922].

[110] B. Mistlberger, *Higgs Boson Production at Hadron Colliders at N^3LO in QCD*, 1802.00833.

[111] LHC HIGGS CROSS SECTION WORKING GROUP collaboration, D. de Florian et al., *Handbook of LHC Higgs Cross Sections: 4. Deciphering the Nature of the Higgs Sector*, 1610.07922.

[112] F. Wilczek, *Decays of heavy vector mesons into higgs particles*, *Phys. Rev. Lett.* **39** (Nov, 1977) 1304–1306.

[113] K. G. Chetyrkin, B. A. Kniehl and M. Steinhauser, *Hadronic higgs boson decay to order α_s^4*, *Phys. Rev. Lett.* **79** (Jul, 1997) 353–356.

[114] S. Dawson, *Radiative corrections to Higgs boson production*, *Nucl. Phys.* **B359** (1991) 283–300.

[115] L. J. Dixon, E. W. N. Glover and V. V. Khoze, *MHV rules for Higgs plus multi-gluon amplitudes*, *JHEP* **12** (2004) 015, [hep-th/0411092].

[116] S. Catani, S. Dittmaier and Z. Trocsanyi, *One loop singular behavior of QCD and SUSY QCD amplitudes with massive partons*, *Phys. Lett.* **B500** (2001) 149–160, [hep-ph/0011222].

[117] M. Czakon, P. Fiedler and A. Mitov, *Total Top-Quark Pair-Production Cross Section at Hadron Colliders Through $O(\alpha_S^4)$, Phys. Rev. Lett.* **110** (2013) 252004, [1303.6254].

[118] M. Czakon, D. Heymes and A. Mitov, *High-precision differential predictions for top-quark pairs at the LHC, Phys. Rev. Lett.* **116** (2016) 082003, [1511.00549].

[119] G. Bevilacqua, H. B. Hartanto, M. Kraus and M. Worek, *Top Quark Pair Production in Association with a Jet with Next-to-Leading-Order QCD Off-Shell Effects at the Large Hadron Collider, Phys. Rev. Lett.* **116** (2016) 052003, [1509.09242].

[120] S. Höche, P. Maierhoefer, N. Moretti, S. Pozzorini and F. Siegert, *Next-to-leading order QCD predictions for top-quark pair production with up to three jets*, 1607.06934.

[121] H. van Deurzen, G. Luisoni, P. Mastrolia, E. Mirabella, G. Ossola and T. Peraro, *Next-to-Leading-Order QCD Corrections to Higgs Boson Production in Association with a Top Quark Pair and a Jet, Phys. Rev. Lett.* **111** (2013) 171801, [1307.8437].

[122] R. Britto and B. Feng, *Unitarity cuts with massive propagators and algebraic expressions for coefficients, Phys. Rev.* **D75** (2007) 105006, [hep-ph/0612089].

[123] R. Britto, B. Feng and P. Mastrolia, *Closed-Form Decomposition of One-Loop Massive Amplitudes, Phys. Rev.* **D78** (2008) 025031, [0803.1989].

[124] J. S. Rozowsky, *Feynman diagrams and cutting rules*, hep-ph/9709423.

[125] S. Badger, J. M. Campbell and R. K. Ellis, *QCD corrections to the hadronic production of a heavy quark pair and a W-boson including decay correlations, JHEP* **03** (2011) 027, [1011.6647].

[126] J. M. Campbell and R. K. Ellis, *Top-quark processes at NLO in production and decay, J. Phys.* **G42** (2015) 015005, [1204.1513].

[127] Z. Bern, L. J. Dixon, D. C. Dunbar and D. A. Kosower, *Fusing gauge theory tree amplitudes into loop amplitudes*, Nucl. Phys. **B435** (1995) 59–101, [`hep-ph/9409265`].

[128] M. B. Wise and E. Witten, *A Diagrammatic Analysis of Some Contributions to the $\Delta I = 1/2$ Rule*, Phys. Rev. **D20** (1979) 1216.

[129] H. D. Politzer, *Power Corrections at Short Distances*, Nucl. Phys. **B172** (1980) 349–382.

[130] C. Arzt, *Reduced effective Lagrangians*, Phys. Lett. **B342** (1995) 189–195, [`hep-ph/9304230`].

[131] C. Grosse-Knetter, *Effective Lagrangians with higher derivatives and equations of motion*, Phys. Rev. **D49** (1994) 6709–6719, [`hep-ph/9306321`].

[132] H. Simma, *Equations of motion for effective Lagrangians and penguins in rare B decays*, Z. Phys. **C61** (1994) 67–82, [`hep-ph/9307274`].

[133] R. N. Lee, *Presenting LiteRed: a tool for the Loop InTEgrals REDuction*, `1212.2685`.

[134] K. Melnikov and M. Schulze, *NLO QCD corrections to top quark pair production and decay at hadron colliders*, JHEP **08** (2009) 049, [`0907.3090`].

[135] K. Melnikov and M. Schulze, *NLO QCD corrections to top quark pair production in association with one hard jet at hadron colliders*, Nucl.Phys. **B840** (2010) 129–159, [`1004.3284`].

[136] A. Denner, S. Dittmaier, S. Kallweit and S. Pozzorini, *NLO QCD corrections to off-shell top-antitop production with leptonic decays at hadron colliders*, JHEP **10** (2012) 110, [`1207.5018`].

[137] G. Bevilacqua, H. B. Hartanto, M. Kraus, M. Schulze and M. Worek, *Top quark mass studies with $t\bar{t}j$ at the LHC*, `1710.07515`.

[138] W. Bernreuther, A. Brandenburg, Z. G. Si and P. Uwer, *Top quark pair production and decay at hadron colliders*, *Nucl. Phys.* **B690** (2004) 81–137, [hep-ph/0403035].

[139] W. Bernreuther, A. Brandenburg, Z. G. Si and P. Uwer, *Next-to-leading order QCD corrections to top quark spin correlations at hadron colliders: The Reactions gg → t anti-t(g) and gq(anti-q) → t anti-tq(anti-q)*, *Phys. Lett.* **B509** (2001) 53–58, [hep-ph/0104096].

[140] R. K. Ellis, Z. Kunszt, K. Melnikov and G. Zanderighi, *One-loop calculations in quantum field theory: from Feynman diagrams to unitarity cuts*, *Phys. Rept.* **518** (2012) 141–250, [1105.4319].

[141] R. Mertig, M. Bohm and A. Denner, *FEYN CALC: Computer algebraic calculation of Feynman amplitudes*, *Comput. Phys. Commun.* **64** (1991) 345–359.

[142] V. Shtabovenko, R. Mertig and F. Orellana, *New Developments in FeynCalc 9.0*, *Comput. Phys. Commun.* **207** (2016) 432–444, [1601.01167].

[143] N. D. Christensen and C. Duhr, *FeynRules - Feynman rules made easy*, *Comput. Phys. Commun.* **180** (2009) 1614–1641, [0806.4194].

[144] A. Alloul, N. D. Christensen, C. Degrande, C. Duhr and B. Fuks, *FeynRules 2.0 - A complete toolbox for tree-level phenomenology*, *Comput. Phys. Commun.* **185** (2014) 2250–2300, [1310.1921].

[145] K. Risager Larsen, *Unitarity and On-Shell Recursion Methods for Scattering Amplitudes*, Ph.D. thesis, Bohr Inst., 2007. 0804.3310.

[146] T. Birthwright, E. N. Glover, V. Khoze and P. Marquard, *Multi-gluon collinear limits from MHV diagrams*, *JHEP* **0505** (2005) 013, [hep-ph/0503063].

[147] T. Birthwright, E. N. Glover, V. Khoze and P. Marquard, *Collinear limits in QCD from MHV rules*, *JHEP* **0507** (2005) 068, [hep-ph/0505219].

[148] S. Catani, D. de Florian and G. Rodrigo, *The Triple collinear limit of one loop QCD amplitudes*, *Phys.Lett.* **B586** (2004) 323–331, [hep-ph/0312067].